INTEGRATED REGIONAL SALT TECTONIC ANALYSIS AND LOCAL MINIBASIN SEQUENCE STRATIGRAPHIC ANALYSIS ADJACENT TO MULTI-STAGE DIAPIRS IN THE WEST MEDITERRANEAN MESSINIAN SALT BASINS

Submitted for the degree of Doctor of Philosophy

Project By

Victoria N. Mianaekere

Department of Earth Sciences

Royal Holloway, University of London

Supervisor: Professor Jürgen Adam

Declaration of Authorship

I Victoria N. Mianaekere hereby declare that this thesis and the work presented in it is entirely my own. Where I have consulted the work of others, this is always clearly stated.

Signed: VNM

Date: 11/10/2019

ACKNOWLEDGEMENTS

My immense gratitude goes to my supervisor Professor Jürgen Adam for his tireless support, motivation and incredible knowledge that made this project possible. I would also like to thank TGS for providing the data used in this project. I like to also thank my financial sponsors PTDF, Nigeria and finally to my beloved family, my husband Pierre, daughter Carmen and unborn baby, big thank you for the entire love and moral support that weathered the storm.

ABSTRACT

Wide coverage 2D PSTM data in west Mediterranean enabled detailed study of Cenozoic gravity driven thin-skinned salt tectonic processes including progradational loading by deltaic and pelagic sedimentation in the deepwater basins overlying oceanic crust. Results uncovered convergent regional salt tectonic linked extension-contraction trends along 3 basin segment along dip of the Valencia Trough, the Balearic and along dip of the Gulf of Lion.

Seismic interpretation of unique depositional patterns within minibasins in the contractional province in the deepwater Provencal basin allow inferences to kinematic growth histories of salt diapirs as a direct result from the reciprocal interactions of net salt rise rates and sedimentation rates. As a new approach, the local depositional processes controlling the formation of the minibasin halo-kinematic sequences are visualised by minibasin scale sedimentary Wheeler diagrams and structural Wheeler diagrams. Sequentially restored 2D Minibasin depositional sequences and derived sedimentary wheeler diagrams and structural Wheeler diagrams show the syn-kinematic cycle of events consisting of ponding, flap folding and erosion within halo-kinematic sequences.

New methods and concepts developed in this study may be integrated into an approach for hydrocarbon prospectivity analysis, e.g. reservoir mapping within minibasin sequences and dynamics of trap formation around multi-stage salt structures

Contents

A. Introduction

The aim of this project is the development of a robust halokinetic sequence-stratigraphy method for an improved kinematic analysis of salt structures and tectono-depositional analysis of the salt-related depocentres in passive margin salt basins.

The presented workflows, methods and analyses in this project aim to integrate the regional tectono-stratigraphic and kinematic analysis of salt basins with the halokinetic sequence-stratigraphic analysis of salt-related depocentres which record the variable kinematic stages and growth phases of salt structures.

Data-driven analytical aspects of this project include the following:

1. Structural and depositional analysis of stratigraphic packages proximal to diapirs which formed in different kinematic growth phases. (Sensu Stricto: Halokinetic Sequence-Stratigraphy, HKSS).
2. Minibasin-scale geometric and depositional analysis of syn-kinematic depocentres including their characteristic stratal geometries and kinematic stacking pattern.
3. Correlation of regional sequence-stratigraphic sequences and halokinetic sequence-stratigraphic sequences from the regional salt basin scale to sub-basins, and salt withdrawal basins/minibasin scales.
4. Case study investigates the tectono-depositional patterns and tectono-stratigraphic control factors of deepwater environments.
5. Case study also includes halokinetic, contractional, extensional and multi-phase salt systems.

Motivational statement

An integrated sequence-stratigraphic approach will enable an improved understanding of salt-sediment dynamics and their local and regional controls based on characteristic tectono-depositional patterns in salt-controlled depocentres adjacent to salt structures and diapirs. Concepts and models derived from the West-Mediterranean salt basins will be applicable to passive margin salt basins world-wide. Additionally, for future applications beyond the scope of this project, the derived work flows, concepts and robust methods will provide a better understanding of the dynamic depositional systems around salt structures which will improve hydrocarbon prospectivity analysis, e.g. reservoir mapping within minibasin sequences and dynamics of trap formation around multi-stage salt structures.

Problem statement

Existing models in halokinetic sequence stratigraphy (Giles and Rowan 2012) are defined as *'Packages of genetically related thinned and upturned beds adjacent to passive diapirs bound by local angular unconformities proximal to the diapir flanks and correlative conformities towards minibasin centre'*. Hence, passive diapirism due to downbuilding being the pivotal point of their

model, the derived concepts of formation of halokinetic sequences do not address other kinematic phases of salt growth. Also structural conformance of syn-kinematic sediments are proximal i.e. within 3km of the diapir flank and do not extend comprehensively throughout and between salt-withdrawal depocentres and minibasins making it impossible to distinguish structural and sedimentary patterns resulting from regional tectonic, basin tectonic and local salt tectonic processes. Furthermore, the structural styles and depositional geometries resulting from the advancement of passive salt diapirs described in the current model of Giles & Rowan (2012) have not been sufficiently tested in depositional settings other than in shallow marine settings and shelf settings. Structural and depositional patterns from syn-kinematic salt rise in other depositional environments (e.g. deepwater hemi-pelagic depositional settings), is therefore still poorly understood.

New Research Elements

This project further develops existing halokinetic sequence-stratigraphic concepts by Giles and Rowan 2012 by expanding interpretations of structural and depositional and stratal geometries from diapir proximal scale to minibasin scale. The derived concepts form the basis (Holser et al. 1988) for a robust analysis of the kinematic evolution of salt structures and salt-related depocentres., and (2) for further integration of the derived halokinetic sequence-stratigraphic results with regional salt tectonic concepts and regional sequence-stratigraphic analysis.

In addition, this project tests the new concepts for the analyses of salt-structural and depositional patterns through all salt-kinematic phases of diapir growth from single-phase to multi-phase salt diapirs in varied kinematic domains of gravity-driven passive margin salt basins, i.e. halokinetic, extensional, and contractional. The approach includes the identification, redefinition, and detailed analysis of characteristic seismic-stratigraphic sequences in salt related depocentres to aid the investigation of the regional and local salt sediment dynamics.

General Overarching Project Goals

1. Development of an expanded terminology for halokinetic sequence-stratigraphy for a minibasin-scale salt-kinematic analysis.
2. New conceptual models for halokinetic sequence development taking into account interpretational elements observed on the regional, minibasin and near-diapir scale.

Case study rationale: West Mediterranean, Provencal Basin

The young Cenozoic Provencal Basin formed as a back-arc basin in the Mid Miocene (16-21Ma) and further developed into a post-rift passive margin salt basin (Warren 2010b) since the Messinian (5.3Ma). The sedimentary succession includes a Messinian megahalite sequence and is characterised by extensive gravity-driven salt tectonics forming a salt-detached, linked extensional-contractional salt system stretching from the slope into the deepwater basin (dos Reis et al. 2005b; Leroux et al. 2015a). The contractional kinematic domain hosts mature contractional salt structures and minibasins. Multi-stage diapirs in active and passive growth phases are

present. In regards to petroleum geology, pre-salt plays have been discovered proximal to the Gulf of Lion basin margin (Roberts and Christoffersen 2013).

The expected outcomes are therefore to analyse basin-scale controls specifically down-slope/localized shortening on the development of halokinetic sequences in the deepwater salt diapir province of the Liguro-Provencal basin, to analyse the related halokinetic processes, salt tectonic processes and the development of halokinetic sequences in deep marine conditions. The results derived from regional 2D seismic data will be applied to investigate the complexity of the deepwater Messinian salt basin province. Its relatively young age allows for seismic correlations between regional depositional sequences and minibasin halokinetic sequences. This case study of a Cenozoic passive margin salt basin is a well-preserved analogue for an early post-rift linked thin-skinned, extensional – contractional gravity driven processes of Mesozoic Atlantic passive margin salt basins, which in modern days are strongly over-printed by extensive outboard propagation of Cenozoic sediment wedges during the drift stage of passive margin evolution (see Fig. 1). Figure 1 highlights the study area (the West- Mediterranean Messinian Salt Basin) and comparable examples of mature Atlantic margin salt basins.

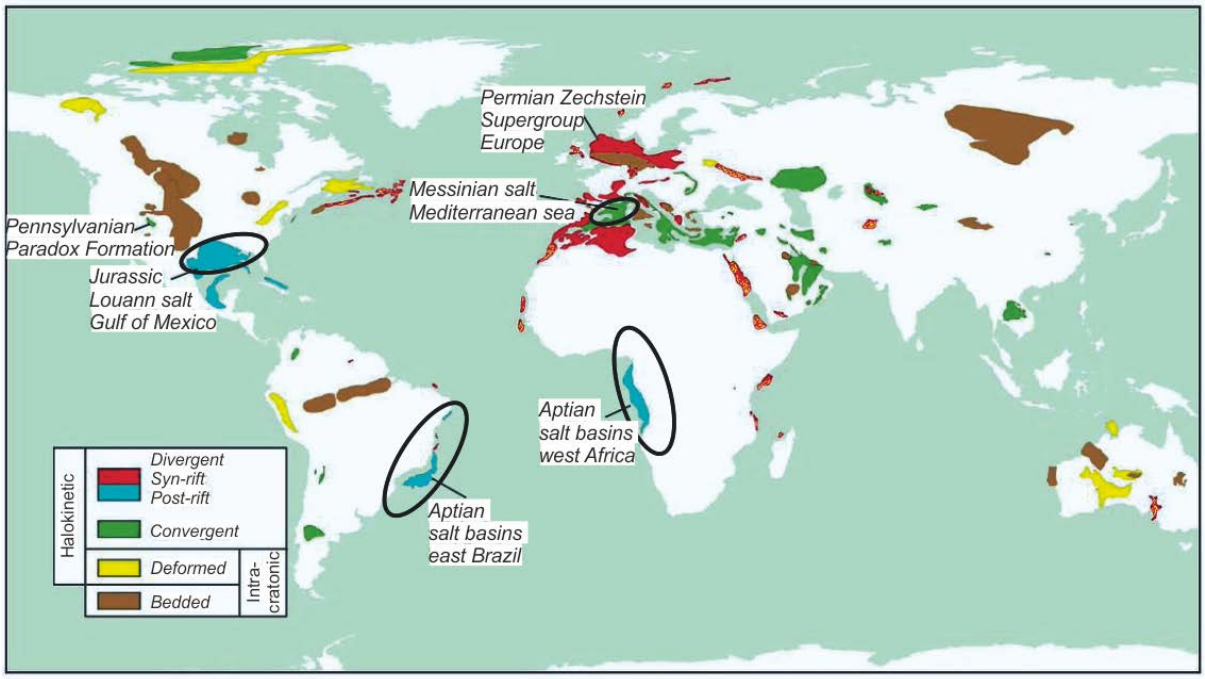

Figure, 1: Global map showing the distribution of salt basins and their tectonic settings (Warren 2010b). Highlighted areas show analogue Mesozoic salt basins that host passive margin post-rift salt tectonic structures.

Outline of Methods

1. Regional salt tectonic structural and kinematic analysis carried out on multiple 2D seismic section view of regional sections and local sections. Produces salt structural domains and salt kinematic domains.
2. 2D whole survey seismic interpretation with derivative 2D surface and time-structure maps using Kingdom geo-physical interpretational software.
3. Detailed halokinetic sequence stratigraphy and minibasin sequence stratigraphy mapping. Specifically Halokinetic sequence (HKS) horizons around key diapir structures and minibasin with ties to the regional stratigraphic framework.
4. 2D kinematic reconstruction of salt structures and salt controlled depocentres from flattening key seismic horizons using Kingdom geo-physical interpretational software.
5. Correlation of halokinetic sequence stratigraphy and minibasin sequence stratigraphy analysis to basin-scale stratigraphic framework with a simple regional correlation exercise incorporating horizon maps, regional sequence stratigraphic/ seismic stratigraphic interpretations, chronostratigraphic diagrams, isopach/isochron maps.
6. Conceptual salt-kinematic process model.

Thesis outline

Chapter 1: Introduction
Chapter 2: Salt tectonics overview (Background)
Chapter 3: Convergent salt tectonics in the Balearic and Liguro-Provencal deepwater basins of the Western Mediterranean Messinian salt Basin (Manuscript)
Chapter 4: 'Halo-kinematic' sequence stratigraphic analysis of minibasins in the deepwater contractional province, Liguro-Provencal Basin, Western Mediterranean. (Manuscript)
Chapter 5: 'Halo-kinematic sequence stratigraphic analysis of minibasin in the deepwater contractional province, Liguro-Provencal Basin, Western Mediterranean: An amalgamation of Halokinetic Sequence Stratigraphy, Megaflap and minibasin stratigraphy concepts. (Manuscript)
Chapter 6: Discussion

B. Salt Tectonics Overview (Background)

This chapter is an overview of the analytical workflow for an integrated salt tectonic analysis. It covers systematically the various scales of interpretation, methods applied for each of the different scales of interpretation and relevant models and concepts applied. Salt tectonics analysis are carried out on regional scale and local (diapir proximal –minibasin) scale.

Regional scale salt tectonics

Salt tectonics on regional scale is analysed with respect to interactions with **basin-scale tectonics** (Jackson and Hudec 2017). These interactions include the timing of evaporite accumulation on divergent passive margins and rift basins and geometries of the regional salt **detachment** i.e. basement involved or detached salt tectonics (thick or thin-skinned). Hence, the key interpretation on regional scale is the timing of the salt deposition, e.g. pre-rift salt, syn-rift salt and post-rift salt (Rowan 2014a; Warren 2010b) and classification of the salt tectonic styles into thin-skinned i.e. basement detached or thick-skinned i.e. basement-involved salt tectonics (Jackson 1995) (workflow1).

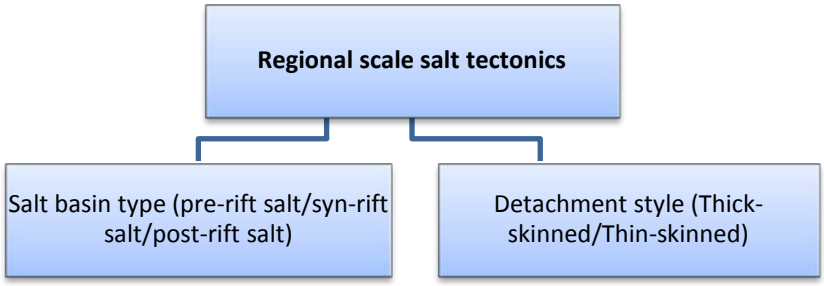

Workflow 1: 1st order interpretational elements of regional scale salt tectonics

Pre-rift salt is initially distributed extensively throughout the margin prior to rifting. During rifting, pre-rift salt becomes decoupled from substrate and stays in connection with the largest faults detached on salt that in tandem propagates throughout the margin. A classic example of pre-rift salt is the Triassic Keuper in the Western Spanish Pyrenees. Syn-rift salt is deposited during early rifting and is concentrated in proximal areas with variable thickness and extent 10's km controlled by graben edges. Syn-rift salt in segmented salt basins is observed in the UK, Central North Sea rift basin , Gabon (Hudec and Jackson 2004; Jackson et al. 2004) and the Iberian and Newfoundland margins (Rowan 2014a). Geological cross sections from Gabon (Fig. 1) show the discontinuity of the syn-rift salt detachment will control different gravity units along the margin. On the other hand, post-rift salt on passive margins show laterally extensive detachment and dècollements enabling linked kinematic systems accommodating lengthy seaward translation (Jackson and Hudec 2017), an up-dip extension and a down-dip contraction domain. The Messinian mega-halite is a post-rift salt deposit as observed in the West-

Mediterranean passive margin. By definition, post-rift salt basins generally have basin widths >100 km and can extend from the oceanic ridge to the continental margin overlying extensional grabens in continental crust (Warren 2010b). In post-rift thin-skinned salt tectonics, detachment dip or topographic slope make up mechanical configurations enabling gravity driven salt tectonics (Marton et al. 2000). Thin-skinned gravity driven salt tectonics in post-rift salt basins is analysed from the post-salt sedimentary overburden succession above autochthonous salt. Discussed in following sections, gravity driven deformation in post salt sedimentary overburden occurs as characteristic structural domains in the up-dip extension, transition and down-dip contraction domain (workflow 2). Lateral extents of these salt structural domains and intensity of salt kinematic deformation with host sediments are crucial analytical elements.

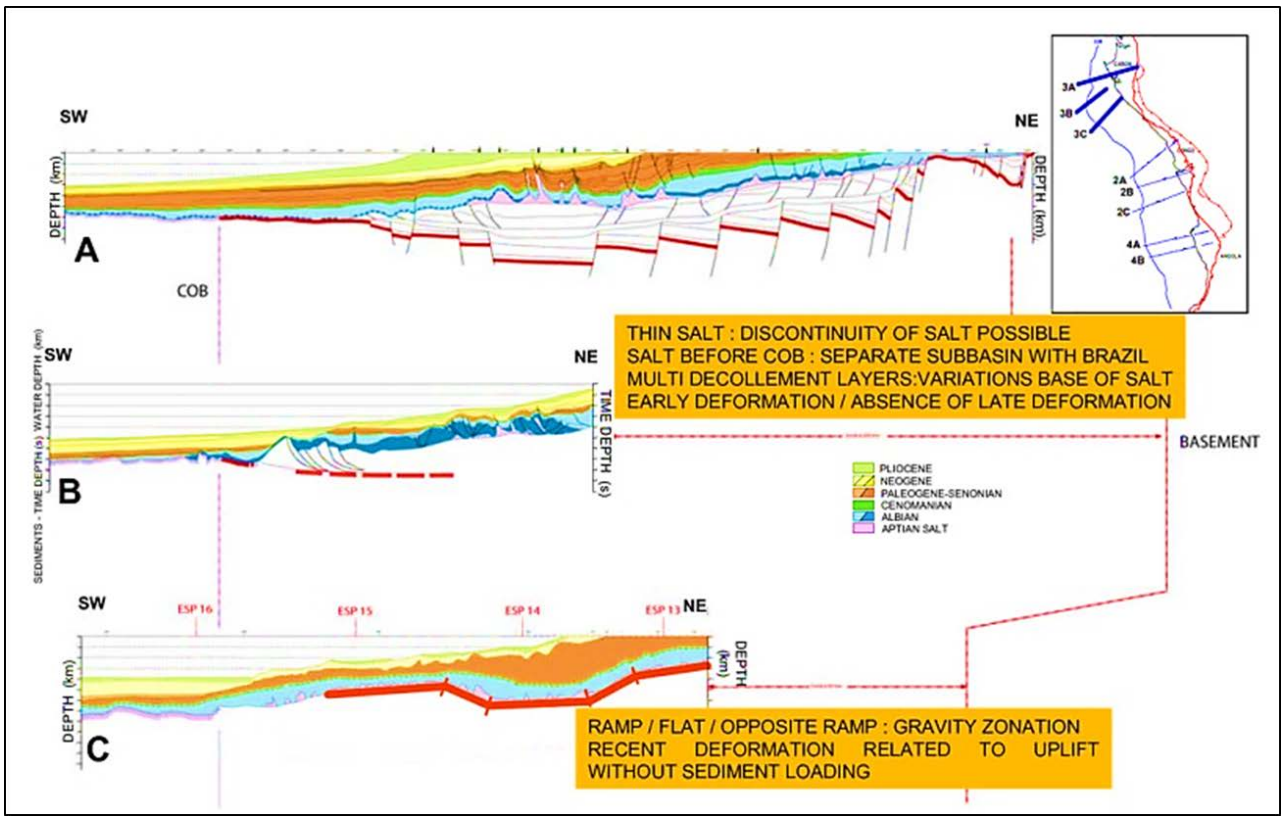

Figure 1: Geological cross sections from Gabon. The discontinuity of the salt detachment will control different gravity units along the margin. These may be both normal and parallel to the margin. Locations of cross-sections are given in index map (Marton et al. 2000).

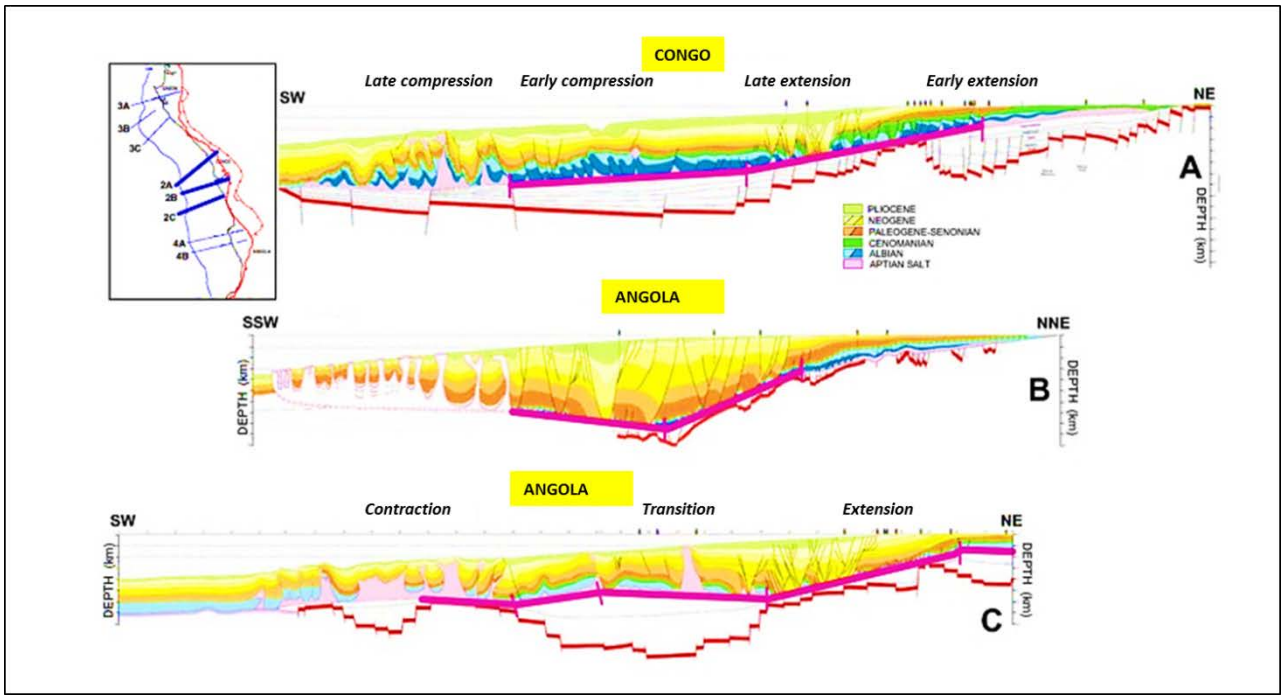

Figure 2: Zonation of the gravity driven tectonics and the geological cross sections from Congo/Angola. Locations of cross-sections are given in index map. Note that there are different flat/ramp geometries at the base of salt (thick purple line) that act as breaks in the continuity of the salt detachment (Marton et al. 2000).

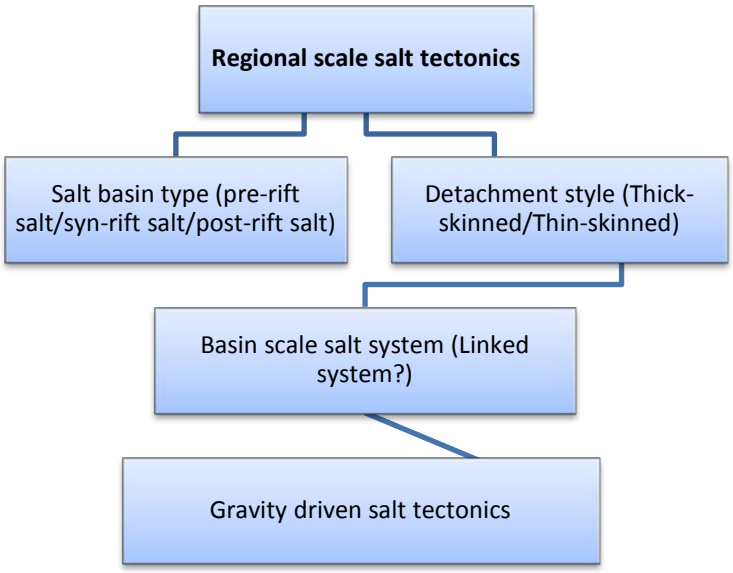

Workflow 2: Interpretational elements of regional scale salt tectonics

Gravity-driven salt tectonics in passive margin sedimentary basins

In general, salt tectonics is strongly controlled by the **mechanical behaviour of salt**. Because salt behaves as a viscous material at geological timescales with negligible strength under high stresses, salt deformation can be initiated by minimal deviatoric gravity-induced stress already immediately after deposition (Hudec and Jackson 2007; Jackson 1995). This minimal deviatoric stress is caused by early postrift basinward tilting of the margin as a result of differential thermal subsidence or late postrift differential loading due to prograding sedimentary wedges (Gaullier and Vendeville 2005; Gemmer et al. 2005; Hudec and Jackson 2007; Jackson and Hudec 2009; Vendeville 2005).

Many sedimentary basins on continental passive margins contain a regional continuous layer of late syn-rift or early post-rift evaporites that facilitated thin-skinned gravity-driven salt tectonic deformation of the post-salt over burden during post-rift sediment loading. The post-rift evolution of these sedimentary basins is characterized by complex basin architectures and variable salt tectonic structures with varying complexity due to the thin-skinned deformation of the sedimentary overburden detached on the viscous salt substratum. e.g. Morocco (Tari and Molnar 2005), Angolan Margin (Brun and Fort 2004; Duval et al. 1992; Fort et al. 2004a, b), Gulf of Mexico (Diegel et al. 1995), Scotia Margin (Adam and Krezsek 2012b; Kendell 2005; Wade et al. 1995) and Brazil Margin (Adam et al. 2012a; Mohriak et al. 1995; Quirk et al. 2012). Examples of passive margin salt tectonics (Fig. 1) show that gravity-driven deformation detached on salt is characterized by linked an extensional-contractional kinematic systems with up-slope extension and coeval down-slope contraction (Adam 2008; Adam et al. 2011, 2012b; Brun and Fort 2004; Brun and Fort 2011b; Brun and Fort 2010; Warren 2010b). Figure 1 illustrates that regional salt tectonic styles are influenced by original salt thickness, number of successive salt layers, geological age and time spans of the salt basins causing varying complexity in basin geodynamic evolution and salt tectonic evolution.

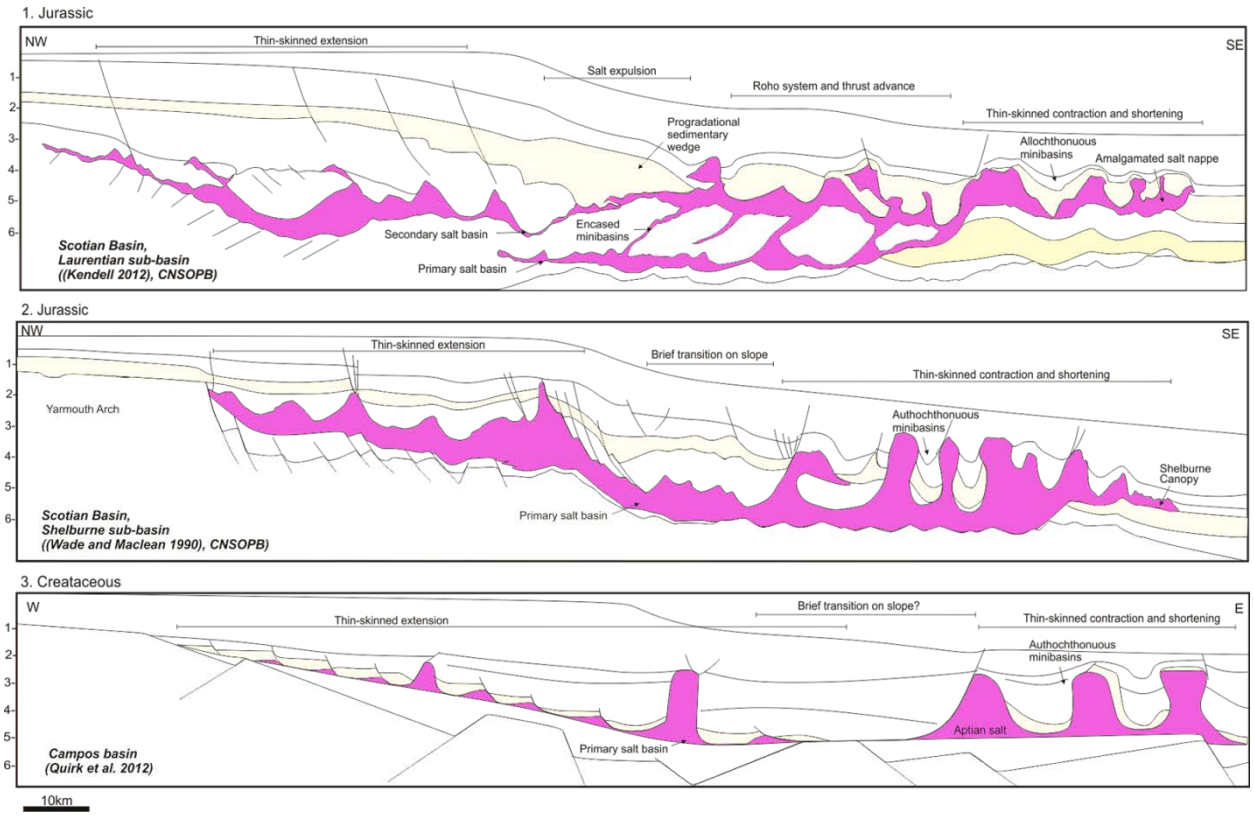

Figure 3: Regional section views of passive margin salt basins showing varying complexity

The early Cretaceous Campos salt basin (Quirk et al. 2012) containing a thinner Aptian salt layer shows minimal kinematic deformation in conforming overburden of Albian and Cenomanian age. In addition, an undeformed transitional kinematic domain links an up-dip extensional domain with salt rollers (e.g. reactive diapirs) exhibiting low amplitude to wavelength ratios to a down-dip contractional domain with vertical diapirs exhibiting low intensity shortening. The Jurassic Scotian margin along the Shelburne sub-basin (Wade and MacLean 1990) with thicker original Argos salt shows a deformed transition domain linking a moderately deformed up-dip extensional domain with reactive diapirism affecting thick overburden to a down-dip contractional domain with shortened diapirs, extrusive salt tongue and extensive canopies. Salt structures in the Shelburne sub-basin have been reactivated and continually squeezed till Cenozoic times (Wade and MacLean 1990). The Laurentian sub-basin (Adam and Krezsek 2012b; Kendell 2005; Shimeld 2004) contains successive stacked salt detachments and shows salt tectonics affected by a thick progradational sedimentary wedge displaying a highly complex salt system with an amalgamated salt nappe. Salt tectonics in the Laurentian sub-basin spans 190 Ma (Adam and Krezsek 2012b; Kendell 2005; Shimeld 2004).

Local salt systems

Local salt systems refer to segmented kinematic provinces. **Kinematic provinces** host characteristic salt structural styles, salt kinematic styles and salt-related depocentre types (workflow 3). See example (Fig. 4) from composite regional-scale cross-section of the north Angolan margin showing the extensional and contractional deformation domains and the type of individual structures (Brun and Fort 2011b).

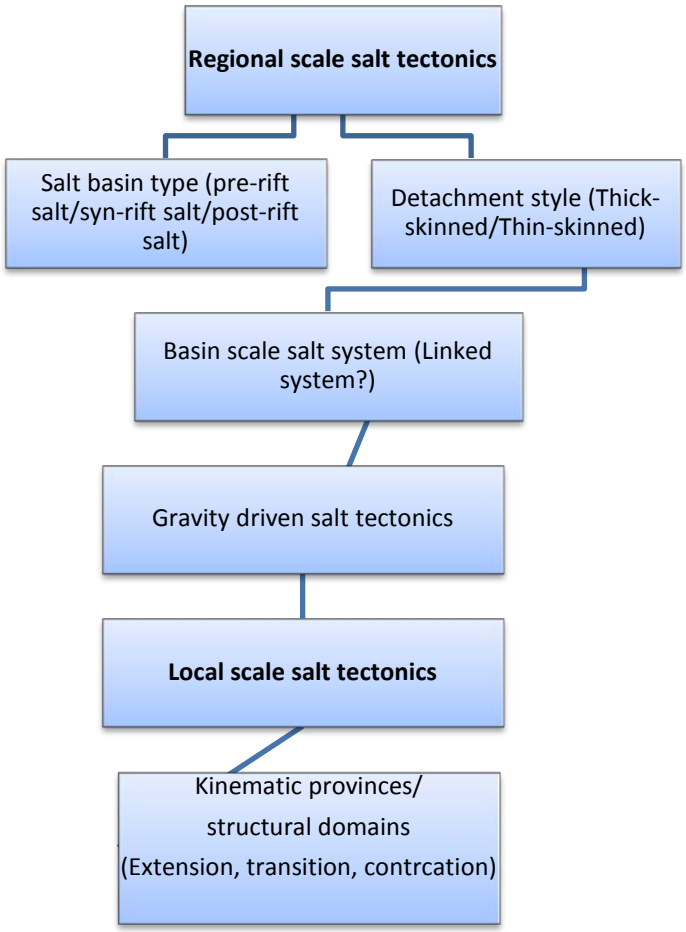

Workflow 3: Interpretational elements of regional scale salt tectonics to local scale salt tectonics

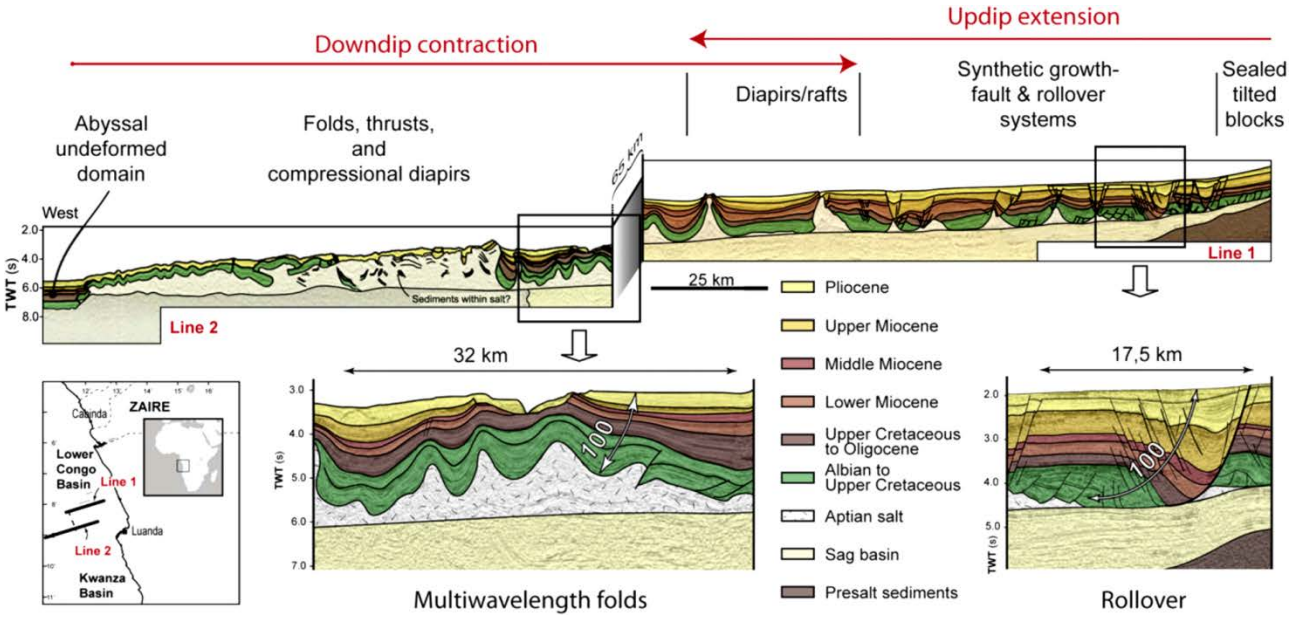

Figure 4: Composite regional-scale cross-section of the north Angolan margin showing the extensional and contractional deformation domains and the type of individual structures. See location of the two sub-lines 1 and 2 in the lower left insert. The two enlargements of the cross-section show the growth character of structures since 100 Ma, in extension to the right and contraction to the left. (Brun and Fort 2011)

Salt kinematic styles have characteristic salt related depocenter types. For example, in the extension domain, salt evacuation create salt rollers and listric growth faults with roll-over downlaps and growth packages in intervening depocenters (Weijermars et al. 1993b) (Fig. 5).

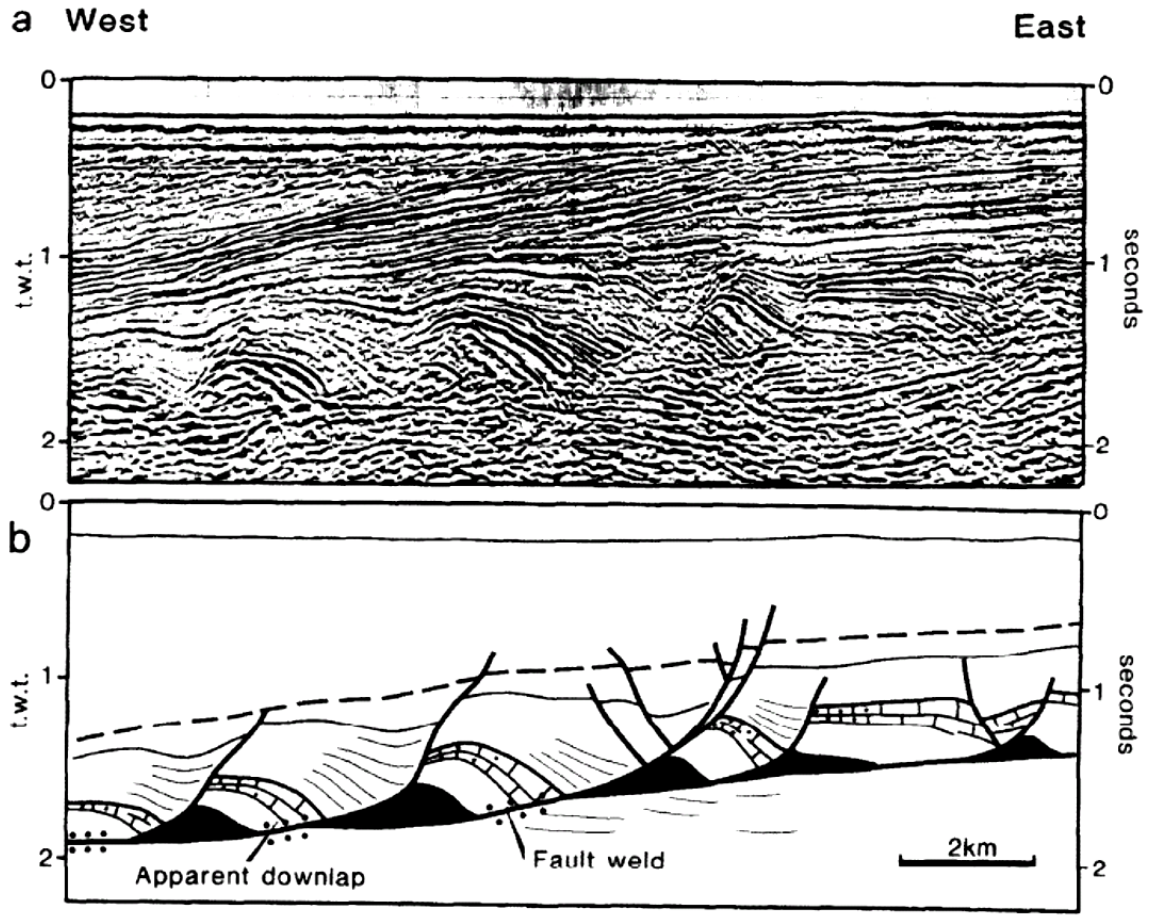

Figure 5: Migrated seismic reflection profile from the Kwanza basin, Angola (a), interpreted seismic section showing salt rollers and growth faults (b), and a scale model. Two-way travel time (t.w.t.) is in seconds (Weijermars et al. 1993b).

In the contraction domain, regional shortening and salt withdrawal create contractional salt folds, squeezed to welded diapirs etc. see examples in (Fig. 6, Fig. 7). Tilted to rotated minibasins typically form in the contraction domain (Fig. 6, Fig. 7) (Rowan and Vendeville 2006).

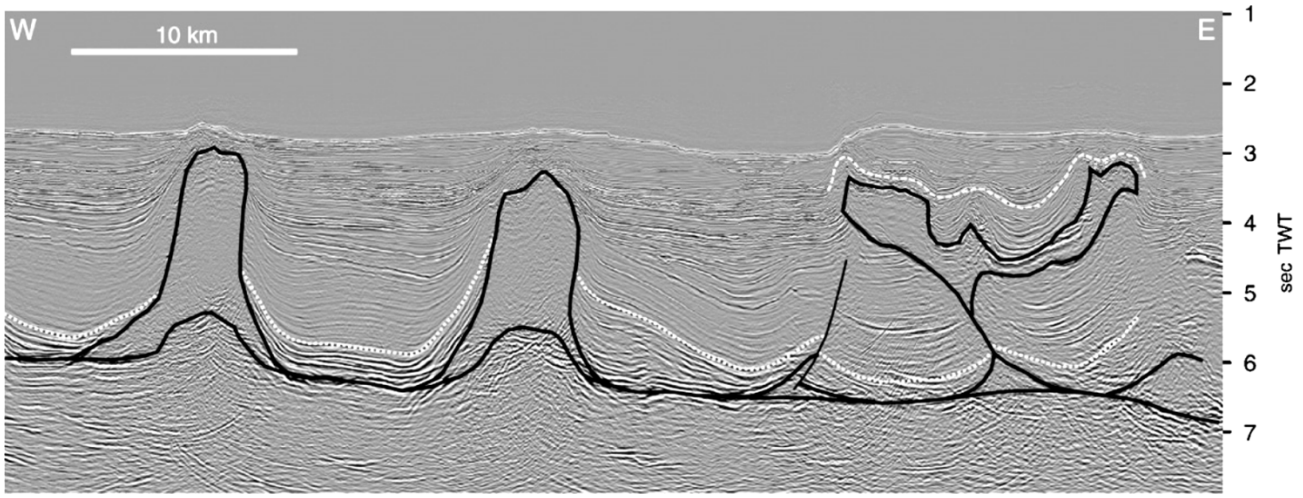

Figure 6: 3-D, time-migrated seismic profile from the deepwater Espirito Santo Basin of Brazil. The Aptian salt and its allochthonous equivalent are in black, the near-top Albian carbonates are in short white dashes, and an undated shallow horizon is in medium white dashes. Shortening at the basal detachment level has a regular wavelength and is accommodated by the squeezing of diapirs and by folding and thrusting. Shortening above the allochthonous salt is accommodated by smaller-wavelength folding because of the thinner section being deformed. (Rowan and Vendeville 2006)

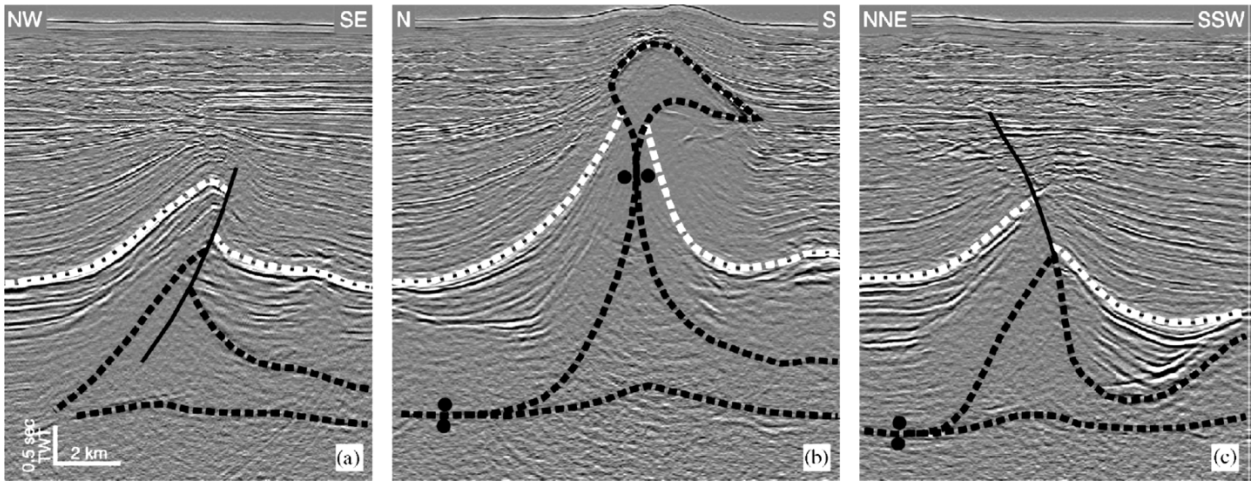

Figure 7: Three-dimensional, time-migrated seismic profiles showing variable geometries across the southern margin of a single minibasin, with salt in black dashed lines and the near-top Oligocene in white dashed lines. Vertical exaggeration is approximately 2.6:1. (a) thrusted salt-cored detachment fold; (b) squeezed diapir that may be welded shut, with extrusion of a small allochthonous tongue coincident with the timing of shortening; and (c) contractional high cut by a steep normal fault that may reflect late trans-tensional deformation during possible clockwise rotation of the minibasin. (Rowan and Vendeville 2006)

Halokinetic systems

In halokinetic systems, **differential topographic loading** and **density inversion** play a major role in the down-building of the thick depocenters into autochthonous or allochthonous salt i.e. minibasin (halokinetic) formation (Hudec et al. 2009b), model example of halokinetic minibasin formation is shown in (Fig. 8).

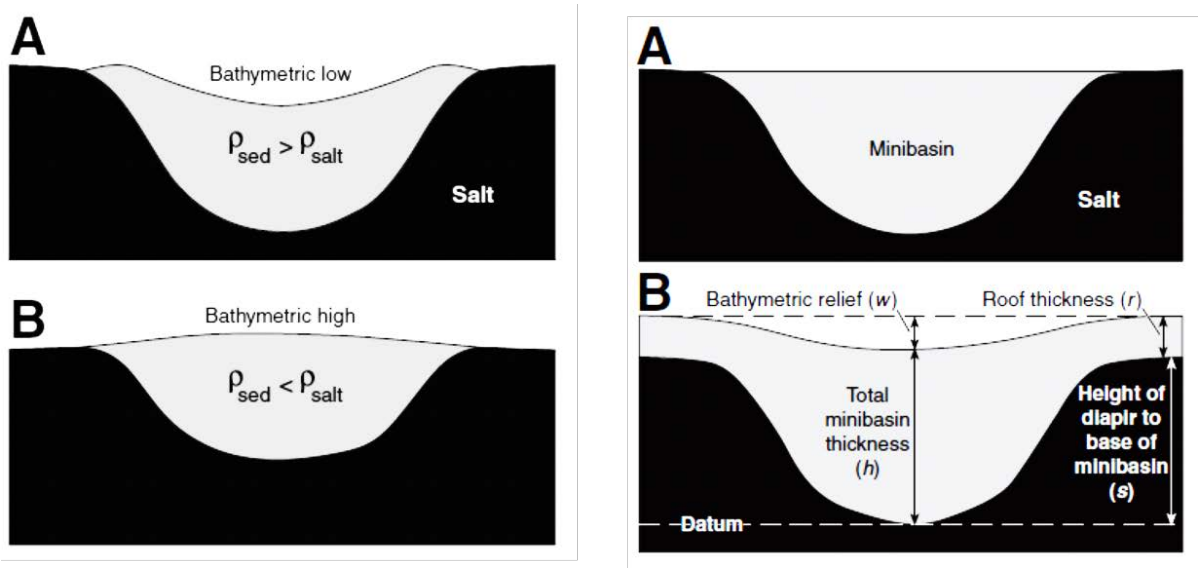

Figure 8: (Left) - Density-driven model of minibasin subsidence, where ρ is density. (A) Where sediments (grey) are denser than salt, static equilibrium produces a bathymetric low in the centre of the minibasin, which sinks under negative buoyancy. (B) Where sediments are less dense than salt, equilibrium produces a bathymetric high above the minibasin, which floats buoyantly. (Right) - Idealized minibasin cross sections. (A) Simplest case, in which exposed salt surrounds a minibasin that has no bathymetric relief. (B) More realistically, diapirs are buried beneath a roof, and the intervening minibasin has bathymetric relief (Hudec et al. 2009b).

In general, local halokinetic systems (summarised in workflow 4 at end of this section) are controlled by the relationship of **net diapir rise rate and net local sediment accumulation rate**. On diapir proximal scale, implications of net diapir rise rate and net local sediment accumulation rate can be observed as bathymetric failure or erosion of sediment material at the diapir crest (Andrie et al. 2012; Giles and Lawton 2002a; Giles et al. 2004; Giles and Rowan 2012; Kernen et al. 2012a; Rowan et al. 2012; Rowan et al. 2003b) and mechanical drag folding caused by syn-kinematic salt rise (Alsop et al. 2000; Callot et al. 2016; Nikolinakou et al. 2017; Rowan et al. 2016b; Schultz-Ela 2003). These analyses allow interpretations of salt-kinematic growth phases (reactive, active or passive growth phases) (Jackson et al. 1994a) (Fig. 9) or transitions from a pre-diapiric salt pillow phase, emergent phase to diapiric phase (Harding and Huuse 2015; Jackson et al. 1994a; Jackson et al. 1994b). Nature of failure and erosion surfaces proximal to diapirs and the degree of angular discordance at these surfaces are consequent of net diapir rise rate and net local sediment accumulation rate form halokinetic sequence boundaries and the basis

of the hook and wedge type member sequences or tabular and tapered end member composite halokinetic sequences (Giles and Rowan 2012) (Fig. 10), (Fig. 11).

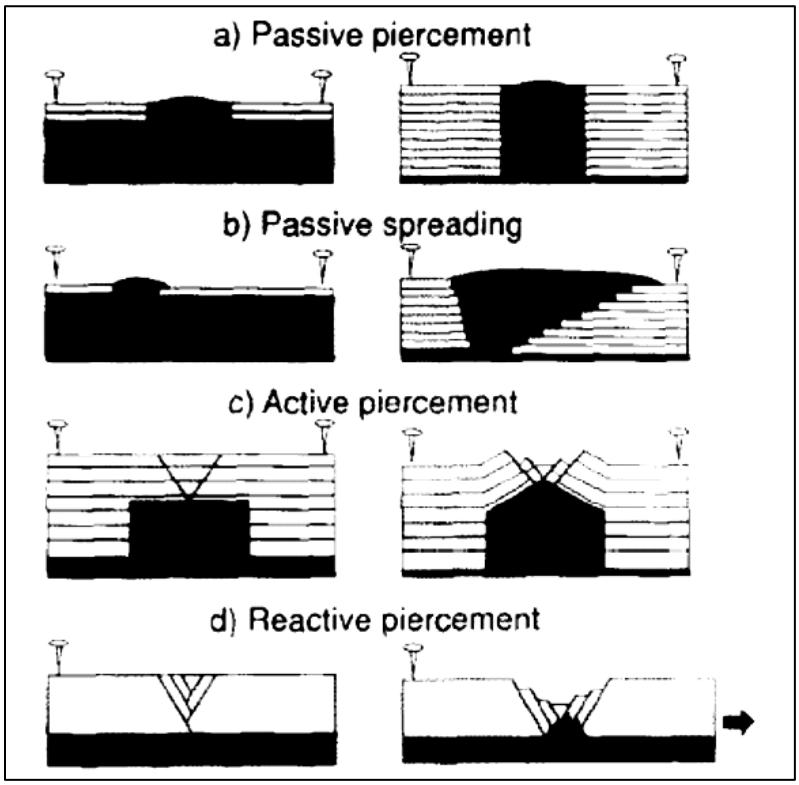

Figure 9: highly schematic illustrations of some mechanisms in salt tectonics. Syn-kinematic sedimentation is omitted for simplicity. (a) Diapir rises passively (down-builds) by remaining emergent while its base sinks. (h) Diapir spreads laterally while remaining emergent. (c) Diapir rises actively by forcefully intruding a relatively thin roof. (d) Diapir rises reactively below graben formed by regional extension (Jackson et al. 1994a).

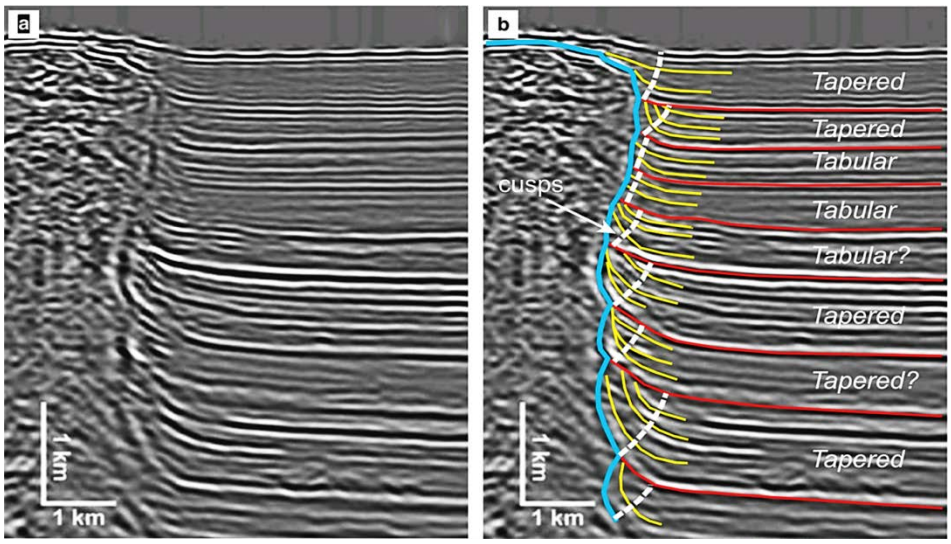

Figure 10: PSDM seismic profile a) un-interpreted and b) interpreted diapir and flanking strata from the northern Gulf of Mexico, the diapir edge is cuspate and stacked unconformities (red) define tapered or tabular composite halokinetic sequences. Dashed lines are axial traces of halokinetic folds and white arrow indicates a wedge-shaped body identified as mass-wasting deposit. V.E 1.5:1. (Giles and Rowan 2012)

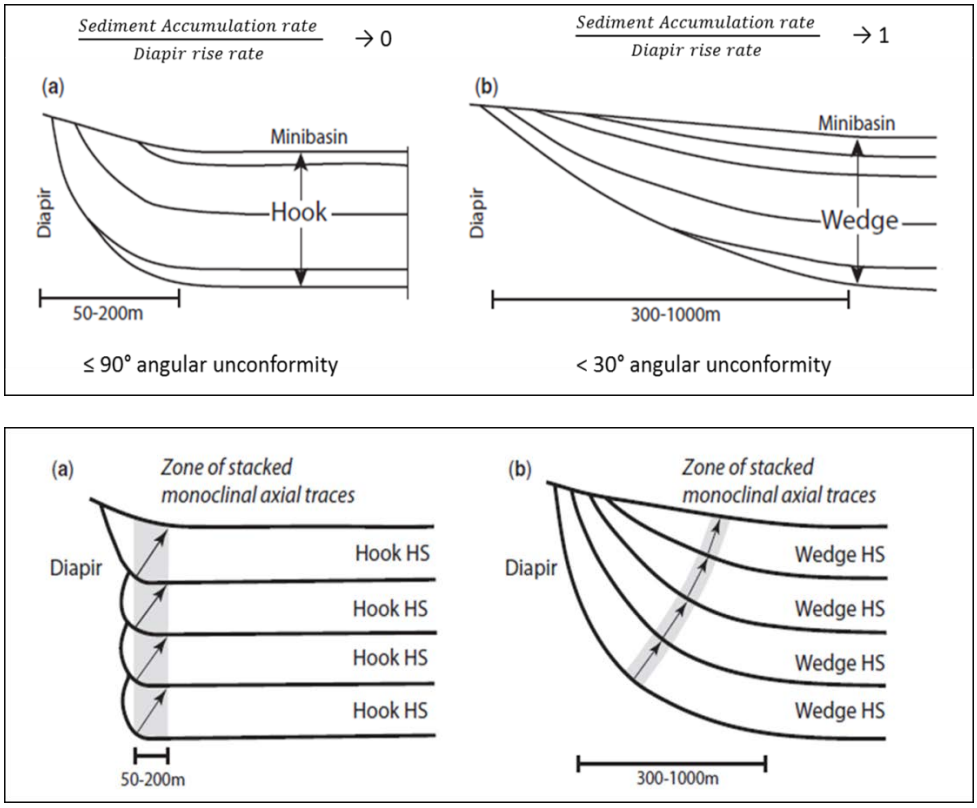

Figure 11: Hook and Wedge Halokinetic sequence model (Giles and Rowan 2012)

Syn-kinematic packages generally thin and upturn towards diapir flanks (Giles and Lawton 2002a). The widths of structural upturn known as drape geometries (Schultz-Ela 2003; Schultz-Ela et al. 1993) distinguish older sedimentary packages that form megaflaps (Callot et al. 2016; Nikolinakou et al. 2017) from younger syn-kinematic packages that form the halokinetic sequences (Giles and Lawton 2002a; Giles and Rowan 2012) (Fig. 12). Megaflaps are observed as steep stratal panels that extend far up the sides of diapirs or their equivalent welds. They exhibit strata that are structurally concordant with salt flank and concordant internal layering (Rowan et al. 2016b). The megaflaps are thus distinct from composite halokinetic sequences with smaller scale length upturns.

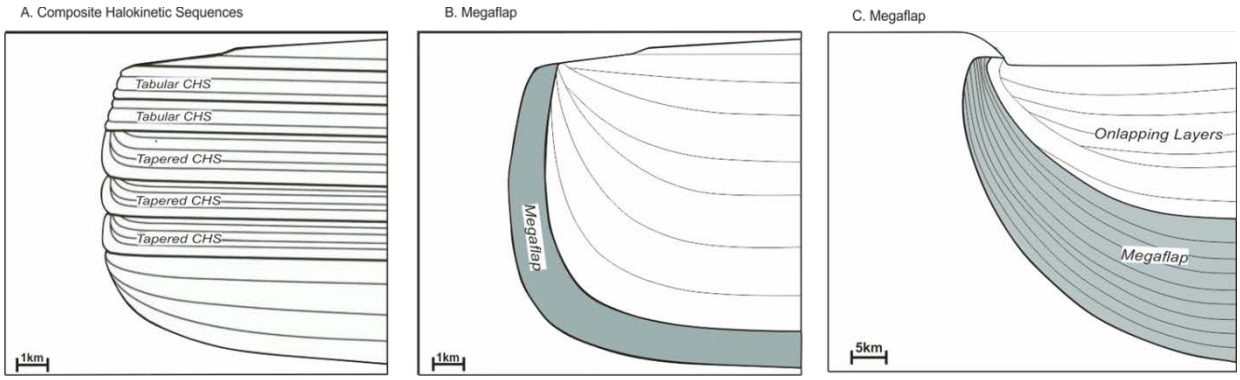

Figure 12: Published structural geometries of genetic halokinetic sequence packages critical for understanding diapir evolution. A. Stacked Composite Halokinetic Sequences defined by differences in shape and geometry of drape folds adjacent to passive diapirs (Rowan et al. 2016b). B. Megaflap (Pre-kinematic), defined by several kilometre fold widths and structural relief (Rowan et al. 2016a). C. Megaflap (syn-kinematic), defined by upturn of thick formerly roof sediments with onlap of younger downbuilding sediments (Nikolinakou et al. 2017)

Differential bathymetric profiles through time of salt structures that bound subsiding depocentres are recorded in the manner of accommodation or fill style within minibasins (Banham and Mountney 2013b; Guerra and Underhill 2012; Ribes et al. 2015b; Ribes et al. 2017). Dynamic models of minibasin subsidence and architectural sedimentation styles by (Hudec et al. 2009a; Jackson and Hudec 2009) all relate to bathymetric controls of rising salt structures. Diapiric bathymetries are able to divert sediment transport. This mechanism have been shown to control the architecture and internal organization of turbidite systems offshore Gulf of Lion e.g. from Dos Reis et al. (2005). Hence, initiation and formation of characteristic minibasin styles dominate particular kinematic provinces as discussed earlier.

Observational elements of minibasin accommodation are external geometries of stratigraphic packages, internal stratigraphic depositional patterns and overall minibasin architectures (Aschoff and Giles 2005). On minibasin scale, examples of external geometries of stratigraphic packages are trough, layer, wedge and bowl (Rowan and Weimer 1998) (Fig. 13). Recognisable internal stratigraphic depositional patterns e.g. parallel beds, convergent beds, divergent beds and up-

section changes from one depositional pattern to the other (Banham and Mountney 2013a; Guerra and Underhill 2012).

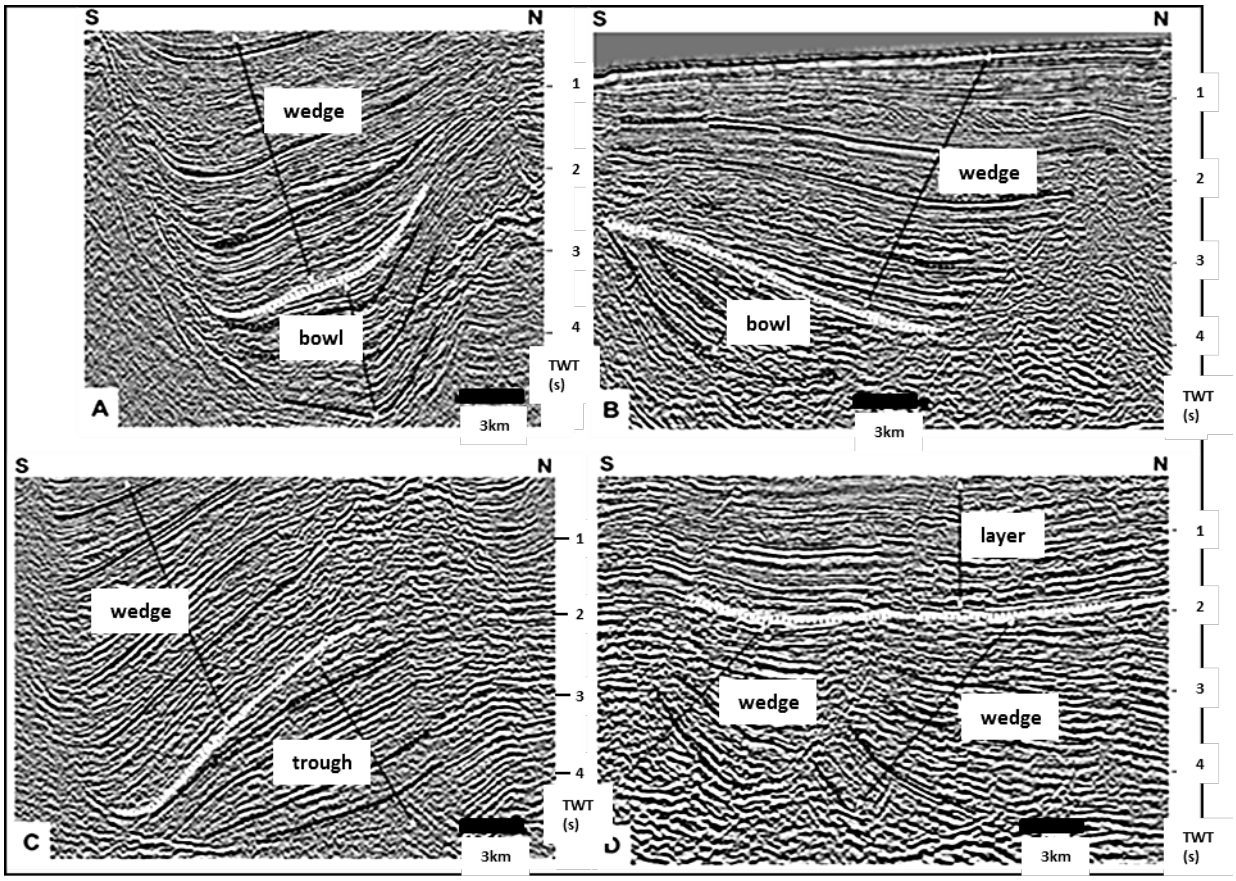

Figure 13: Tectono-stratigraphic packages within allochthonous minibasins in the Gulf of Mexico. Characterised based on external geometry of the packages. (McBride et al. 1998)

For interpretations of regional tectonic influences, interpretational element may consist of minibasin symmetry or rotation and stratigraphic depocentre shifts also known as migrating depocentres (Dooley et al. 2009; Hudec et al. 2009a) (Fig. 14). Concepts for minibasin scale salt tectonic interpretations applied in this project fall under stratigraphic architectures within minibasins (Banham and Mountney 2013a, b; Ribes et al. 2015b; Rowan and Weimer 1998) Minibasin fill patterns see (Hudec et al. 2009a) and depositional patterns within minibasins see (Andrie et al. 2012; Giles and Rowan 2012; Kernen et al. 2012b)

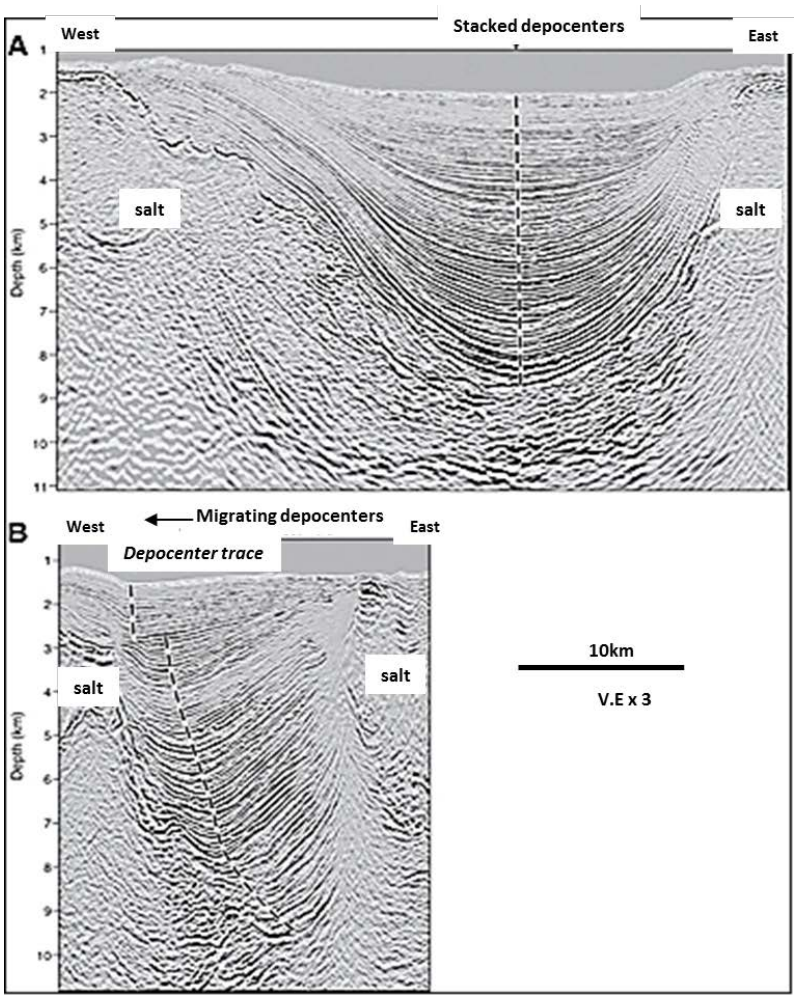

Figure 14: Seismic examples of minibasin fill patterns. Depocentre trace connects thickest parts of each stratigraphic package. A) Stacked depocentres above the thickest part of the minibasin are consistent with present day density-driven subsidence B) temporal rotation of depocentre suggesting that another mechanism controlled subsidence (Dooley et al. 2009)

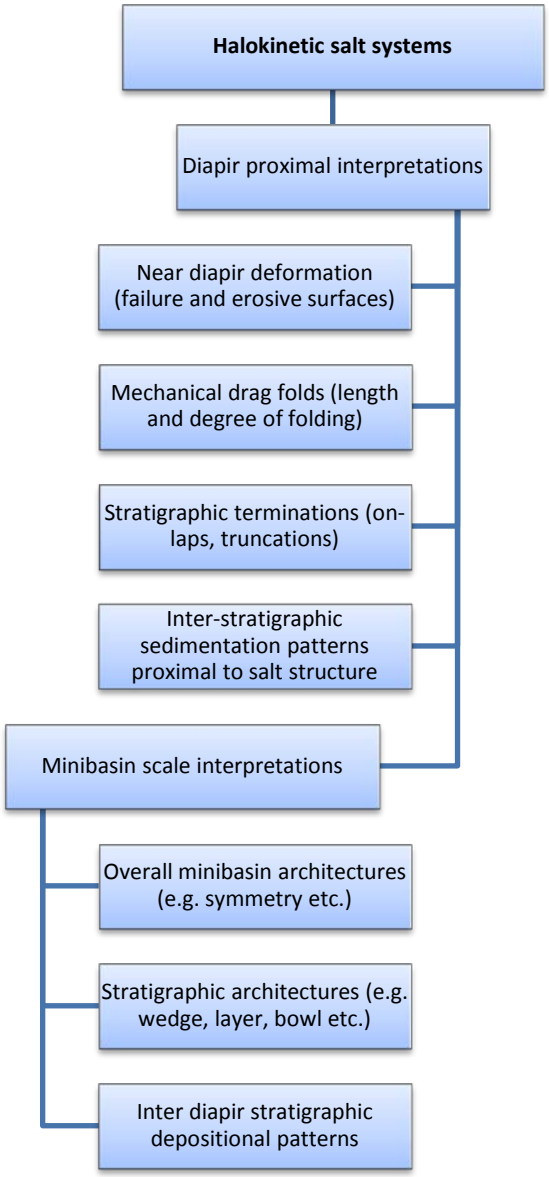

Workflow 4: Interpretational elements of halokinetic systems

C. Manuscript 1

Document type: Manuscript submitted for publication to the American Geophysical Union-Tectonics journal.

Authors: Mianaekere Victoria, Adam Jürgen

No of words: 12000

No of pages: 47

Convergent contractional salt tectonics in the Western Mediterranean Messinian salt basins: *Passive margin salt tectonics*

[1*]V. Mianaekere; [2] J. Adam
[1]*Earth Sciences department, Royal Holloway university of London*
[2]*Earth Sciences department, Royal Holloway university of London*
**Corresponding author: victoria.mianaekere.2014@live.rhul.ac.uk,*

Key Points

- Gravity driven, thin-skinned salt tectonics on passive margin with linked extensional – contractional salt system.
- Radial salt tectonic transport directions converge and influence evolution of contractional province.
- Evolution and landward migration of contractional province over time is evident from lateral variation in salt structural styles and salt-sediment relationships.

Abstract

This study investigates 2-Dimensional gravity-driven, thin-skinned salt kinematic processes in the Messinian salt basins of the Western Mediterranean with particular focus on the evolution of the contractional province in the distal deepwater Liguro-Provencal Basin. The present-day salt structural architecture results from regional gravity-driven thin-skinned basinward salt tectonic transport since early Pliocene times c.5 Ma which results in a characteristic kinematic segmentation of salt tectonic structures with a landward extensional, transitional, and basinward contractional domain. The landward migration of the contractional domain over time is documented by the late (upper Pliocene – Pleistocene) stage contractional deformation of the basinward part of the former transitional domain. Salt tectonic transport directions from the Gulf of Lion and Balearic promontory show a partial radial convergence in a common proximal to distal contractional province in the deepwater Provencal basin. The salt tectonic evolution of

the Provencal deepwater contractional domain showcases early stage, active salt tectonic processes such as in the Mesozoic salt basins which are now either deeply buried or strongly overprinted by the younger post-rift tectono-stratigraphic processes.

Keywords: gravity-driven salt tectonics, contractional salt tectonics, thin-skinned salt tectonics, Messinian salt basin

1. Introduction

Due to extensive exploration activities in the last decades, gravity driven thin-skinned salt tectonic processes on rifted continental margins have been studied in-depth, for example, in the mature Jurassic Atlantic salt basins [Gulf of Mexico, (Fort and Brun 2012; Peel et al. 1995; Schuster 1995; Seni 1992; Talbot 1993; Worrall and Snelson 1989; Wu et al. 1990), Scotian Margin, (Adam 2008; Cribb 2009; Ings and Shimeld 2006; MacDonald et al. 2008)] and Cretaceous Atlantic salt basins [Brazil (Adam et al. 2012a, b; Adam et al. 2012c; Demercian et al. 1993; Mohriak et al. 2008; Quirk et al. 2012) and West Africa, (Gottschalk et al. 2004; Hudec and Jackson 2002b; Liro and Coen 1995; Marton et al. 2000; Tari et al. 2003a)]. These salt basins are characterised by late syn-rift or early post-rift salt sediments originally deposited on extended continental crust. The much younger Cenozoic salt basins like the Red Sea (Mitchell et al. 2010) and the Mediterranean basins (dos Reis et al. 2005a) are characterised by a significantly different geodynamic and tectono-stratigraphic evolution and their gravity-driven salt tectonic processes are less well studied. In particular, in the Mediterranean Messinian salt basins we can analyse active salt tectonic processes in great detail that are comparable to early stage salt tectonic processes in the Mesozoic basins which are now either deeply buried or strongly overprinted by the younger post-rift tectono-stratigraphic processes.

The salt tectonic system in the Western Mediterranean has previously been analysed along the Gulf of Lion–Provencal margin segments (dos Reis et al. 2005a). This study analyses the regional gravity-driven thin-skinned salt tectonic and tectono-stratigraphy along the Gulf of Lion–Provencal and North Balearic-Provencal Basin segments. This study further documents regional salt tectonic structures, structural trends and kinematic domains on the NW rifted continental margin of the Western Mediterranean Basin including the North Balearic and Provencal oceanic basins. The regional kinematic analysis has been performed using structural and kinematic concepts of gravity-driven thin-skinned salt tectonic systems (Brun and Fort 2011b; Fort et al. 2004b; Rowan et al. 2004a; Vendeville 2005; Weijermars et al. 1993a) and salt tectonic regional contraction, (Dooley et al. 2009; Ge et al. 1997; Rowan et al. 2000; Vendeville and Nilsen 1995). Regional 2D seismic sections spanning from the continental margin to the deepwater oceanic basin have been interpreted to document the lateral variation in salt structural styles and distribution of the salt-kinematic domains. Based on the regional kinematic analysis of the gravity-driven thin-skinned extensional-contractional system, we analyse in the second part of this study in more detail, the salt tectonic evolution of the contractional deepwater diapiric domain.

2. Geological overview of study area

Tectonic setting

Plate-scale

Since the Palaeozoic, the NW continental margin of the Western Mediterranean Basin has evolved through diverse convergent and divergent plate tectonic phases (Dewey et al. 1989).

Major phases of plate convergence include a continental collision stage during the Palaeozoic Caledonian and Variscan orogeny as well as the Cretaceous to Paleogene Pyrenean orogeny (Gunnell et al. 2008b). The NW-directed subduction of Neo-Tethyan oceanic crust ended with the late Mesozoic collision of the NW European plate with the Apulian and Maghrebide continental platforms forming part of the African margin (Maillard et al. 2003; Mauffret et al. 2004; Gunnell et al. 2008; Driussi et al. 2015). Ongoing subduction of remnant oceanic crust in the Western Mediterranean Zone of Convergence caused hinge roll-back of the subducting slab with back-arc rifting along the NW continental plate margin, and the subsequent SE rotational roll-back of the Balearic, Corsica and Sardinia continental blocks (Gunnell et al. 2008b) (Fig. 1). Whereas back-arc extension and rotation of the Balearic block along the Spanish continental margin segment ceased in the Miocene (Carminati et al. 2004; Carminati et al. 2012; Storetvedt 1973), along the French continental margin segment subduction roll back and back-arc extension was continuing due to rotation of the Corsica-Sardinia block which led to the emplacement of oceanic crust in the Miocene (21-16 Ma) (Maillard et al. 2003).

Fig. 1: Tectonic map showing the West Mediterranean subduction system (Gunnell et al. 2008a), Basement Transfer Fracture Zones (Maillard et al. 2003) and subsequent formation of the North Balearic and Liguro-Provencal Basins caused by slab roll back of the Corsica (Co), Sardinia (Sa) and Calabria (Ca) blocks.

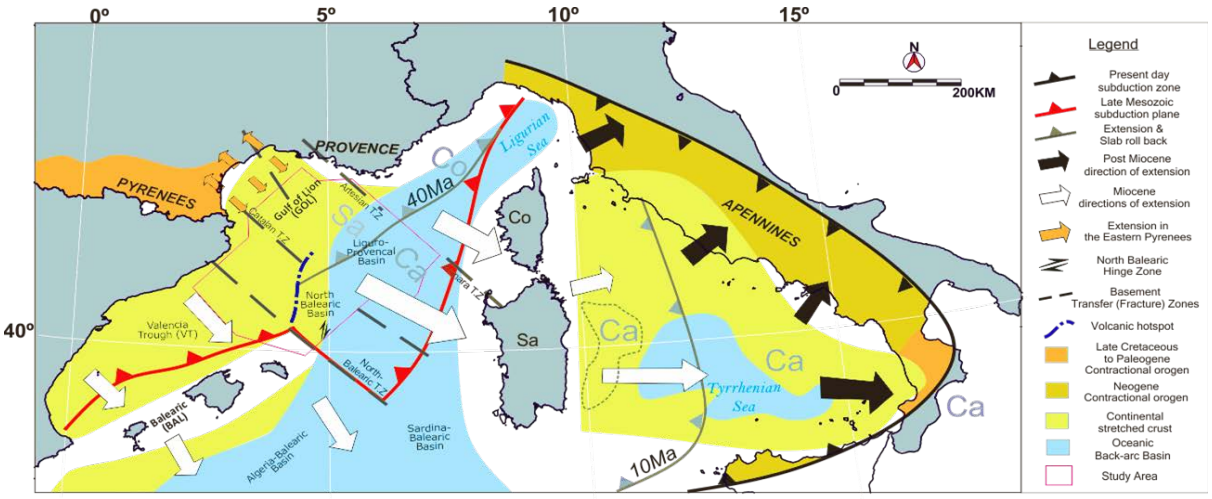

Regional structural variations

The complex structured basement beneath the modern NW continental margin is the expression of these Palaeozoic, Mesozoic and Cenozoic plate tectonic phases. Thus, the NW Mediterranean Cenozoic sedimentary basins, which developed during the NW-SE Miocene rifting and back-arc extension, are preferentially segmented along major basement suture zones, for example, the Catalan, Artesian and North-Balearic Transfer zones as shown in (Fig. 1). The early SE to late SSE rotational drift of the Balearic block led to stretched continental crust due to rifting and back-arc extension (Carminati et al. 2004; Carminati et al. 2012; Storetvedt 1973). The early SE to late E rotational drift of the Corsica-Sardinia block and contemporaneous back-arc extension led to the early formation of a highly stretched continental crust and the late

formation of oceanic crust. The architectures and basin fill history of the West-Mediterranean basins are strongly controlled by the nature of the underlying basement (Mauffret et al. 1995). The proximal Valencia Through and Gulf of Lion formed on highly stretched continental crust whereas the more distal North Balearic basin and Liguro-Provencal basin are overlying oceanic crust. Further prominent basement features include the North Balearic Fracture Zone (NBFZ) and an N-S trending line of intrusions of alkaline volcanoes along the Continent-Ocean transition (COT) south of the Valencia Trough (Fig. 1).

Basin domains and architecture in the study area

The study area focuses on the Cenozoic basins located NE of the North-Balearic Fracture Zone NBFZ including the proximal Gulf of Lion and the NW parts of the North-Balearic and Liguro-Provencal Basins (Fig. 1) and partly extends to the NE part of the Valencia Trough SW of the NBFZ. All these basins and underlying margin domains were controlled by thermal subsidence of oceanic crust since the late Miocene following the cessation of back arc extension (Biju-Duval et al. 1978). Re-organisation of basement structures and isostatic adjustments in response to thermal subsidence resulted in steep continental slopes and young oceanic basin with present-day water depths of ca. 2.8 km (Carminati et al. 2004). Subsequent uplift and basinward tilt of the continental shelves caused prograding sedimentary wedges, gravitational failure and gravity-driven deformation.

Tectono-stratigraphy

A schematic tectono-stratigraphic section of the West-Mediterranean basins stretching from the continental margin and highly extended continental (transition) margin to the deep oceanic basin is illustrated in (Fig. 2).

Fig. 2: Tectono-stratigraphic and litho-stratigraphic chart of the West Mediterranean basins.

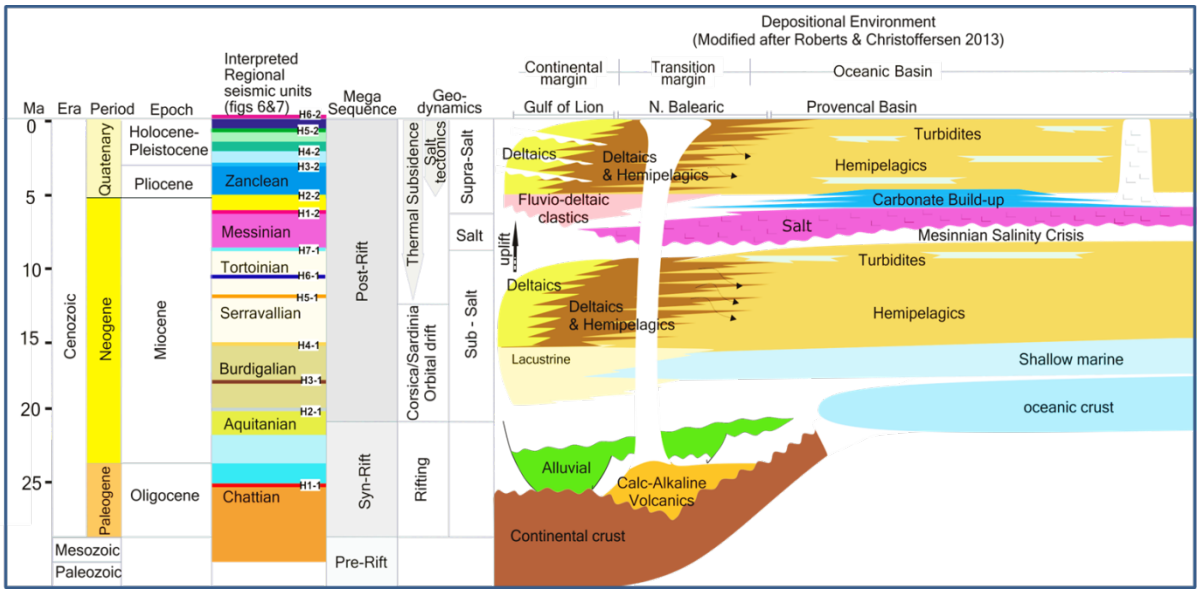

Basement

In the study area, the Gulf of Lion Basin represents the proximal rifted continental margin, and the North-Balearic Basin a highly extended transitional margin segment. The distal North-Balearic and Liguro-Provencal Basins are underlain by volcanic oceanic crust. The continental basement in the West Mediterranean continental margins is represented by Precambrian, Palaeozoic and Mesozoic rocks (Storetvedt 1973). The volcanic basement in the Valencia Trough is associated with the Paleogene rifting event (Carminati et al. 2004), (Fig. 2).

Synrift & postrift megasequences

The synrift and postrift megasequences (Fig. 2) consist in the proximal Gulf of Lion Basins dominantly of Oligocene to Holocene alluvial, lacustrine and fluvio-deltaic deposits and deltaic, hemipelagic and turbiditic sediments in the North Balearic and Provencal Basins (Guieu and Roussel 1990; Mauffret and Gorini 1996). The Early Oligocene to Aquitanian synrift megasequence consists of alluvial deposits that are confined to rifted grabens located beneath the modern continental margins (Leroux et al. 2015a). The Late Aquitanian to Holocene postrift megasequence shows a general uniformity in lithology with proximal deltaic and distal hemipelagic sediments throughout the West Mediterranean Basins (Roberts and Christoffersen 2013).

Messinian salinity crisis, salt deposition & Messinian unconformity

The Messinian Salinity Crisis in the West Mediterranean Basins spanned an estimated 1.5 Ma (Butler et al. 1999) (Fig. 2) and began during the pronounced late Miocene glacio-eustatic sea level regression (Ohneiser et al. 2015). Related desiccation and subaerial processes are marked in the basin fill succession by the regional Messinian unconformity; a prominent erosional surface traceable throughout the Western and Eastern Mediterranean basins (Bache et al. 2015; Driussi et al. 2015; Jolivet et al. 2006; Obone-Zue-Obame et al. 2011; Rouchy and Caruso 2006). In the West-Mediterranean back-arc basins the Messinian evaporites were deposited contemporaneously on extended continental crust and young oceanic crust. The megahalite sequence reached thicknesses up to 3 km and was deposited rapidly in pre-existing Miocene post-rift depressions during two cycles lasting less than 2 Ma (Butler et al. 1999). In the study area the early-stage evaporite deposition was confined to the deeper parts of the North Balearic

and Liguro-Provencal Basins. In the Gulf of Lion and Valencia Trough, the upper evaporite series extends further landward onto continental platforms and is onlapping on the Messinian Unconformity and pre-regression deposits while being conformable above marine transgressive deposits (Butler et al. 1999; Driussi et al. 2015; Gorini et al. 2015; Montadert et al. 1978; Roberts and Christoffersen 2013) In seismic data the Messinian evaporite succession shows an extensive distribution and a characteristic compositional layering into a lower, middle and upper evaporite series (Gorini et al. 2015; Montadert et al. 1978). The thick successions of the Lower Anhydrite and Middle Halite series are confined to deep basins overlying the oceanic crust. The thickness of the Middle Halite increases from 500 m in more landward positions up to 1.5 km in the deep basin. The Upper Mixed Evaporite succession consists of shallow marine basinal anhydrites deposited in a deep basin and marginal gypsum deposited in proximal basins and on the continental shelf (Cartwright et al. 2012). The upper evaporite series and carbonate build-ups are 500 m to 600 m thick and are overlying the halite in the deep basin (Gorini et al. 2015; Montadert et al. 1978). The depositional extent of this Miocene post-rift mega-halite (Warren 2010b) in the deep basins overlying oceanic crust is significantly different from the other major Mesozoic passive margin salt basins (Jackson 1995).

Post-Messinian succession

Stratigraphic studies of the geometries and patterns of the prograding postrift sequences (Fig. 2) estimate a total basin subsidence of 4 km since the Messinian. This includes ~1.5 km of subsidence in the Serravallian prior to the evaporate deposition and up to 2.5 km of post-Messinian subsidence in the Pliocene and Pleistocene (Biju-Duval et al. 1978). The post salt overburden in the NW Mediterranean basin has a cumulative thickness of 7 km to 9 km and

consists of fluvio-deltaic in the proximal margin and progradational deltaic sediments and in the distal deep basin. The latter consists of older carbonate build-ups overlain by younger hemi-pelagic and turbiditic successions. Extensive salt diapirism is situated in the deep basin overlying oceanic crust. (Montadert et al. 1978)

3. Data set & methods

Data sets

This study utilises a data set of 2D Kirchhoff pre-stack time-migrated regional seismic sections provided by TGS. The dataset consists of 16 NW-SE trending dip-lines with a maximum length of 250 km and 26 SW-NE trending strike-lines with a maximum length of 200 km (Fig. 3). The regional 2D seismic sections show a 10s record length and a 4 m/s sample interval. Lithological information and stratigraphic ages in the seismic sections were obtained from published stratigraphic information of the Gulf of Lion and Provencal Basin (Granado et al. 2016), the Gulf of Lion Drilling Project GOLD GLP2 well (Bache et al. 2015), and the Deep Sea Drilling Project DSDP 372 well (Kidd et al. 1978) (locations on Fig. 3).

Fig. 3: Bathymetric map of the West Mediterranean reproduced from the GEBCO, showing the locations of 2D regional lines used for regional salt tectonic analysis in this study. Red arrows show the directional trends of regional lines. Note the location of regional sections and diapir-minibasin sections in relation to main sediment input pathways and deep sea fan (Holser et al. 1988).

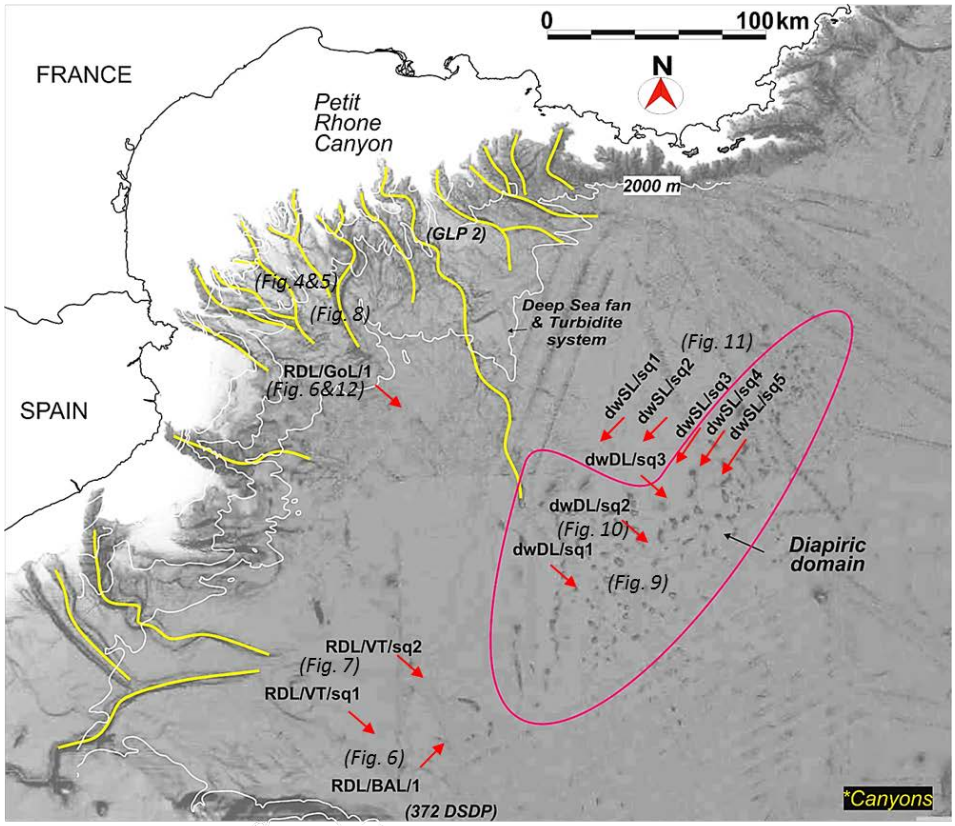

Explanation
R - regional
dw - deepwater
DL - dip line
SL - strike line
GoL - Gulf of Lion
BAL - Balearic
VT - Valencia Trough
sq. - sequence

Basin scale salt tectonic analysis

Regional-scale seismic interpretation and structural analysis include:

1) Mapping of key seismic marker horizons in dip & strike section
2) Sequence-stratigraphic analysis and establishment of the key seismic marker horizons and their stratigraphic correlation to well data
3) Interpretation of basin-wide sequence-stratigraphic markers and elements
4) Structural interpretation of salt structures and description of the lateral variation of salt tectonic styles
5) Identification of salt-kinematic elements and regional mapping of kinematic domains

Seismic marker horizons were interpreted from high-amplitude seismic reflection events and sequence-stratigraphic markers derived from seismic facies analysis; interpretations were tied to open source well data for stratigraphic control and age constraints. 13 seismic marker horizons consisting of 7 pre-salt and 6 post salt horizons were interpreted in this study (Fig. 4, Fig. 5, section 4).

Seismic marker horizons are interpreted via amplitude analysis of key seismic reflection events. The higher amplitude, homogenous frequency and continuous reflection events present the top of the acoustic basement, base salt, top salt, top post-salt carbonate reflectors and the sea bed. All these seismic horizons are characterized by a + ve polarity or positive impedance value except for the base salt which has a – ve polarity or negative impedance value. Seismic marker horizons are continuous, easily traceable reflectors and therefore extrapolated and correlated basin-wide. For mapping of regional sequence stratigraphic units, other delineating seismic horizons with heterogeneous frequency content and more discontinuous reflectivity indicate also key stratigraphic surfaces and have been interpreted from intersecting reflector terminations such as top-laps, on-laps, down-laps, off-laps and truncations and within stratigraphic units, reflector shapes such as dipping, divergent, convergent, oblique, sigmoid and parallel to sub-parallel are interpreted.

The regional salt tectonic trends were analysed on dip-lines of the Gulf of Lion, Balearic and Valencia Trough basin segments (see Fig. 6, Fig. 7, section 5). Dip-lines and strike-lines in the Provencal deepwater basin have been interpreted to determine the direction of basinward salt mobilisation. Kinematic styles in supra-salt sedimentary succession have been interpreted and separated in up-dip (proximal) extension and down-dip (distal) contractional domains.

4. Seismic stratigraphy

Seismic stratigraphic analysis was carried out for regional seismic interpretation of the Gulf of Lion to enable the correlation of seismic stratigraphic markers from the proximal shelf to the distal deep basin. The analysis also enables the integration of seismic-stratigraphic markers with stratigraphic markers from published data. The seismic stratigraphic interpretation for the pre-salt and post-salt sedimentary succession is shown in (Fig. 4, Fig. 5).

Fig. 4: Seismic stratigraphy of the pre-salt succession beneath the shelf-slope transition

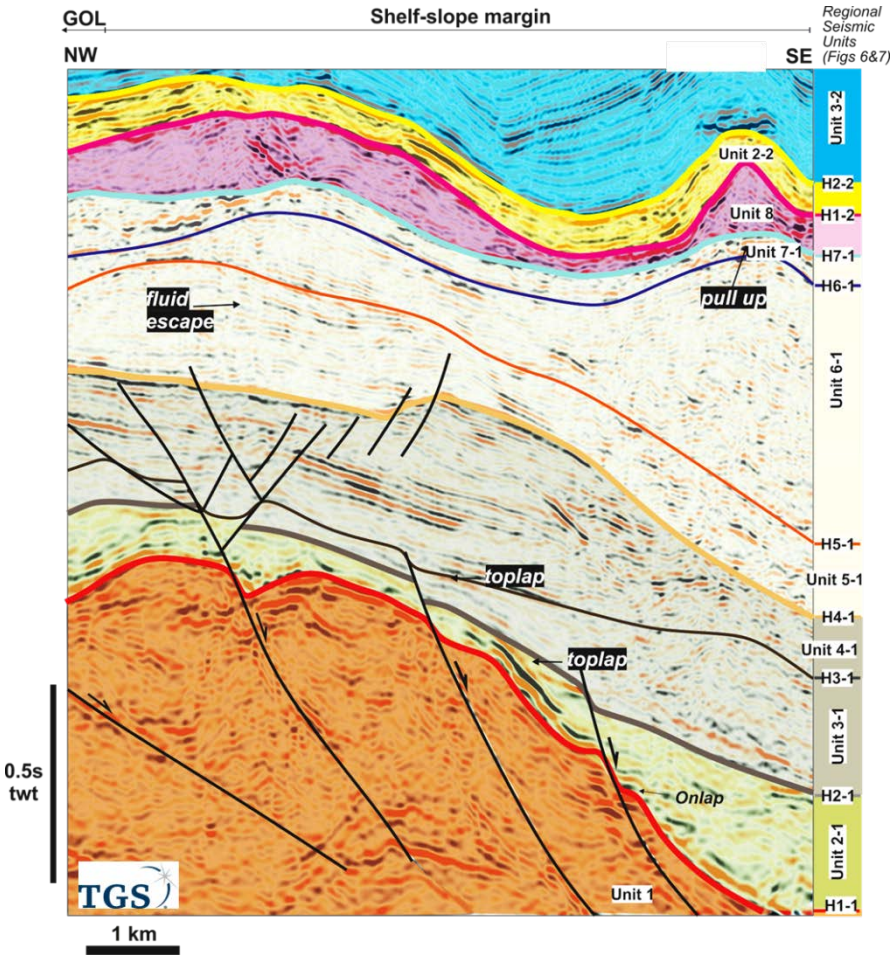

Fig. 5: Seismic stratigraphy of the supra-salt succession beneath the shelf-slope transition of the Gulf of Lion continental margin.

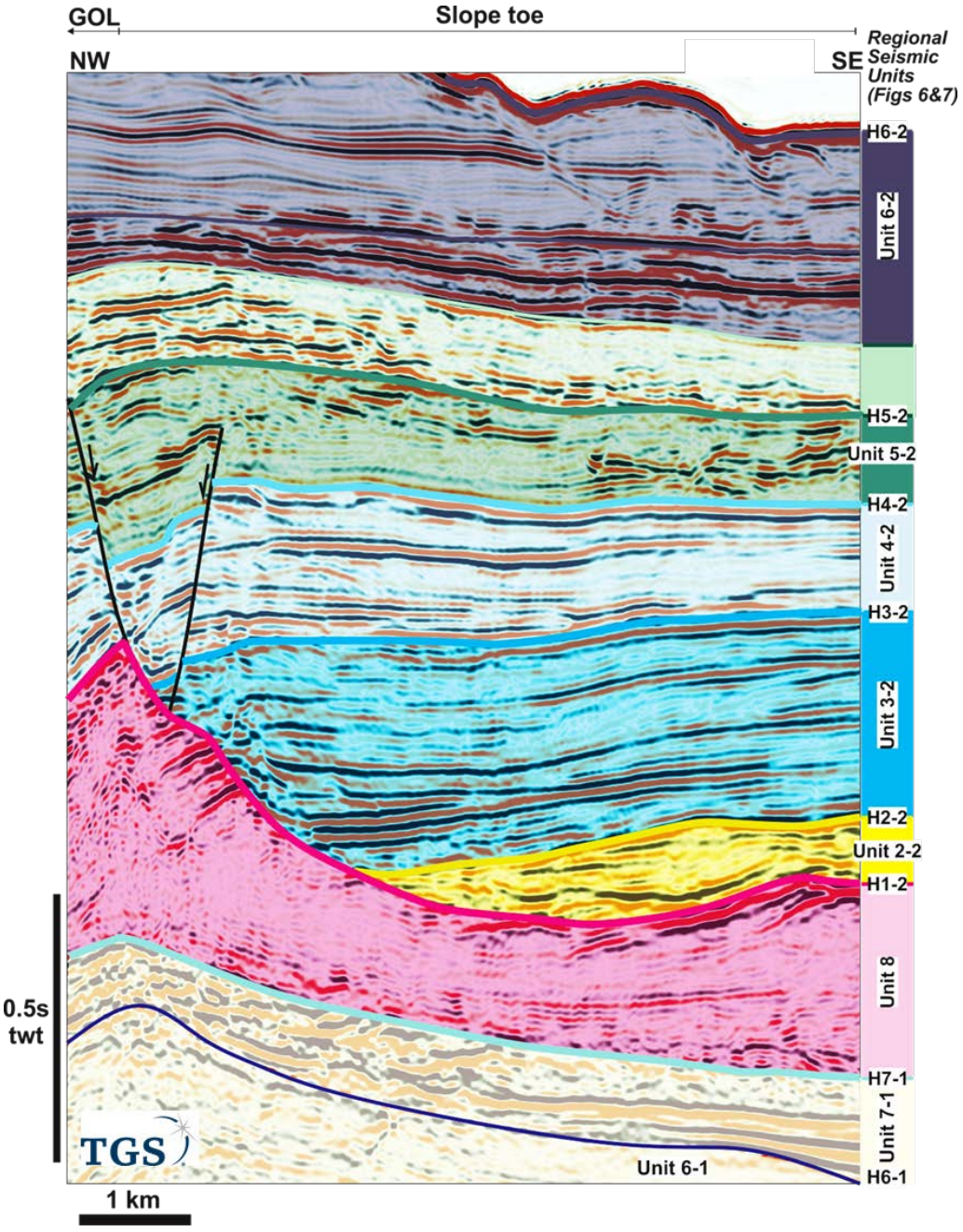

Seismic marker horizons

Strong-amplitude continuous seismic horizons mark major changes in lithology and depositional environments often associated with key stages of the regional stratigraphic evolution. Seven interpreted pre-salt seismic horizons are labelled H1-1 to H7-1 in (Fig. 4). The deepest horizon H1-1 is the acoustic basement top, a high amplitude reflector with wide side lobes exhibiting a high dip angle in basinward direction with offset by large throw basinward dipping basement faults. The acoustic basement shows the largest range for TWT values. The H2-1 to H4-1 horizons are subsequent basinward dipping lower amplitude reflectors with less pronounced side lobes displaced by the basement faults and other minor normal faults. The horizons H2-1 to H4-1 also show characteristic onlap and toplap reflector terminations. H5-1 to H7-1 horizons is typically sigmoidal, sub-parallel and show high amplitudes. H7-1 is the base salt horizon and can be described as parallel with reference to H6-1 in the proximal margin (Fig. 4) and is conformable to the underlying pre-salt reflectors in the deep basin.

Six interpreted post-salt seismic horizons are labelled H1-2 to H6-2 (Fig. 5). The deepest post-salt horizon H1-2 describes top-salt including the hangingwall contact of salt welds. Top-salt horizons are high amplitude reflectors and frequently show overlying down-lapping terminations and underlying truncations in the proximal margin. In general, post-salt seismic marker horizons are well constrained by strong amplitudes and clear frequency attributes, whereas pre-salt seismic marker horizons may be more affected by seismic wave attenuation and dispersion effects. Strong reflectors are the top-carbonate high amplitude reflector H2-2, the parallel to sub-parallel high amplitude reflectors H3-2 and H4-2 as well as H5-2 which is

characterized by its high amplitude attribute and apparent down-laps in the proximal margin. H6-2 is the seabed reflector described earlier.

Sequence stratigraphy

Sequence-stratigraphic interpretations aid in the understanding of temporal tectonic and sedimentary influences on the pre-salt and post-salt basin evolution and in identifying regional scale controls on the salt tectonic evolution. The sequence units are identified from seismic facies and are separated by seismic marker horizons discussed above. Identification of sequence-stratigraphic units has been done as a precursor to regional sequence-stratigraphic correlations. 12 sequence-stratigraphic units have been interpreted including seven pre-salt units which include the basement unit-1 and units 2-1 to 7-1 interpreted in the shelf – slope transition and five post-salt units including the Messinian evaporite unit-8 and unit 2-2 to unit 6-2 in the distal slope to basin plain.

Pre-salt sequence-stratigraphic units have been interpreted in the shelf-slope margin consisting of an Oligocene basement unit-1 and Miocene seismic-stratigraphic units 2-1 to 7-1 (Fig. 4). The basement unit shows a chaotic reflection character attributed to its association with fault blocks; the high-amplitude reflection is attributed to high acoustic impedance. Unit 2-1 is characterized by low-amplitude discontinuous reflections most likely due to slumping and sliding of sediments within graben segments. Unit 3-1 shows divergent reflectors, associated with a tilt in the depositional surface, low amplitude reflectors result from lithological composition probably of homogenous siltstones, marlstones or mudstones. Unit 4-1 shows a mix of high-amplitude shingles and low-amplitude divergent reflectors, Unit 5-1 and Unit 6-1 show prograding sigmoidal clinoforms. Divergent to prograding clinoforms are most likely an

outbuilding of deltaic systems (Patruno et al. 2015). Unit 7-1 shows high amplitude discontinuous reflectors. The Messinian evaporite unit-8 is largely transparent in the autochthonous salt layer and in low amplitude salt structures. In the distal basin, intra-salt stringers can be observed in tall salt structures with bathymetric expression and intra-salt deformation in multi-wavelength salt-cored folds.

Post-salt sequence-stratigraphic units have been interpreted in the distal slope to basin plain (Fig. 5). Pliocene seismic-stratigraphic units are unit 1-2, unit 2-2 and unit 3-2. Unit 1-2 is characterized by parallel highly reflective seismic facies composed of carbonates and is widely distributed in the deep basin. The units 2-2 and 3-2 exhibit parallel to sub-parallel seismic facies that include enveloping channels and lenses. In the deepwater basin unit 2-2 and unit 3-2 are characterized by a more continuous seismic character and are likely describing hemipelagic sediments. Here, seismic intervals with highly continuous seismic character and strong impedance contrast represent most likely condensed depositional sections. Pleistocene sequence-stratigraphic units, unit 4-2 and unit 5-2, exhibit chaotic, high amplitude seismic facies composed of turbiditic sediments and mass-transport deposits in the basin plain.

5. Regional salt tectonics

Regional salt tectonic styles

For the regional salt tectonic analysis the styles and variation of salt structures and related depocenters beneath the slope and deepwater basin were interpreted in two margin-scale seismic sections and further two regional seismic sections. One NW-SE margin-scale seismic section is oriented perpendicular to the Gulf of Lion - Liguro Provencal margin segment and

extends over 250 km from the mid-continental slope to the center of the deepwater basin (RDL/GoL/1, Fig. 6). The second SW-NE margin-scale seismic section is oriented parallel to the Gulf of Lion-Provencal margin segment, perpendicular to the Balearic-Provencal basin segment and North-Balearic Transform zone and extends over 200 km from the lower slope of the Balearic Islands into the deepwater basin (RDL/BAL/1, Fig. 6). In addition, two 100 km long NW - SE regional seismic sections have been chosen across the NW Valencia Trough and Provencal basin segment to illustrate the effect of the volcanic arc and the basement hinge zone on the basin architecture and salt tectonic structures of the deepwater basin (RDL/VT/sq1 and RDL/VT/sq2, Fig. 7).

Fig. 6: **(a)** Un-interpreted 2-Dimensional PSTM seismic dip lines along, (RDL/GoL/1) Gulf of Lion – Provencal Basin and (RDL/BAL/1) Balearic – Provencal Basin axis (Location shown in Fig. 3). Landmark colour bar is SEG Normal. **(b)** Interpreted seismic dip sections illustrating the regional salt tectonic styles and acoustic basement configuration along the Gulf of Lion-Provencal and Balearic-Provencal basin segments. Both trends differ in lateral extents of salt structural domains, amount of shortening in overburden and pre-salt sedimentary and structural configurations.

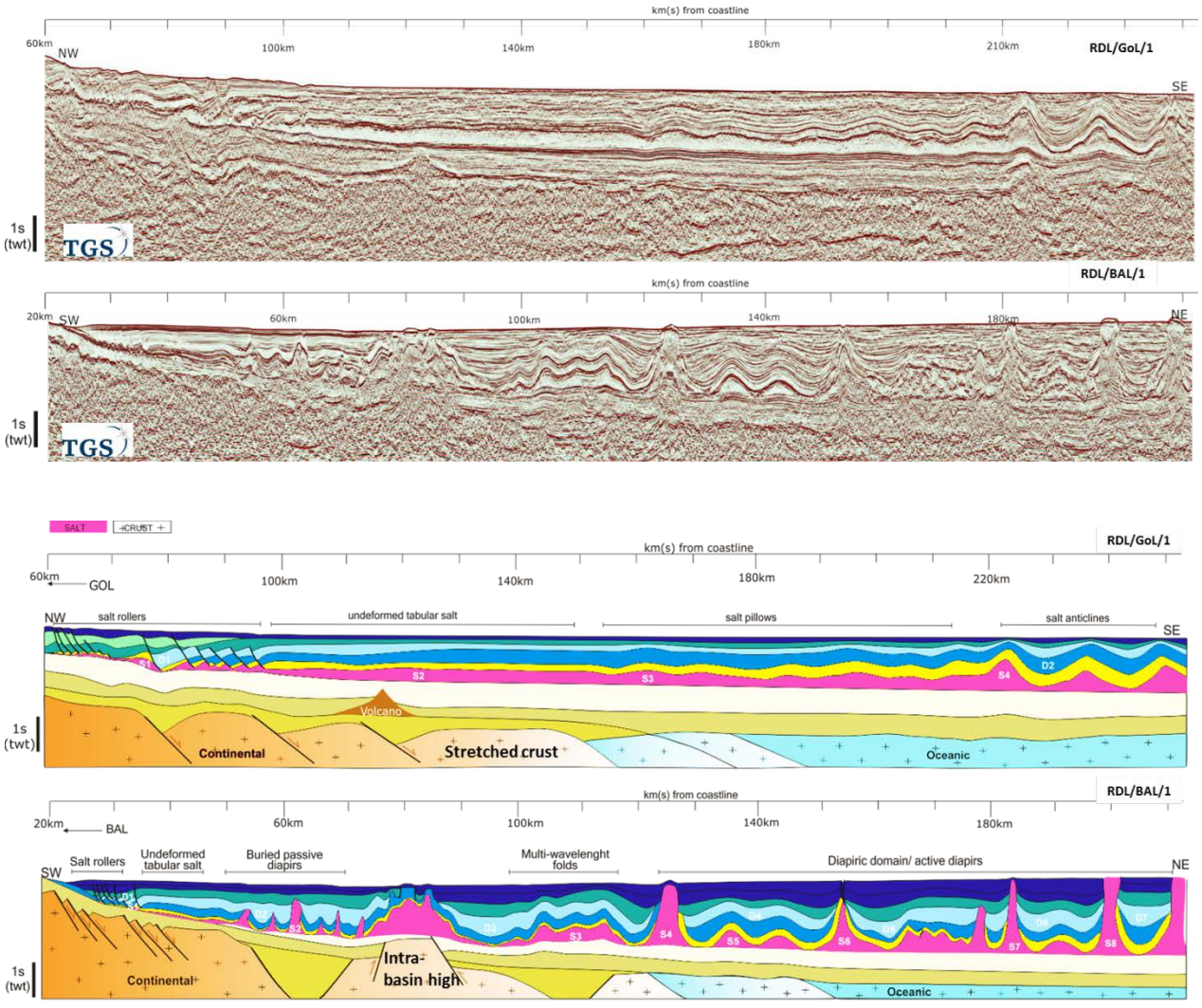

Fig. 7: **(a)** Un-interpreted 2D PSTM seismic dip lines south of the Valencia Trough (North Balearic Basin). Landmark colour bar is SEG Normal (Location shown in Fig. 3). **(b)** Interpreted seismic dip sections comparing regional salt tectonic styles and acoustic basement configuration south of the Valencia Trough and the volcanic arc. The sections RDL/VT/sq1 and RDL/VT/sq2 differ in lateral extent of salt and the western limit of deposited salt. The hinge zone and volcanic edifices form major basement structures in the Valencia Trough and North Balearic basin.

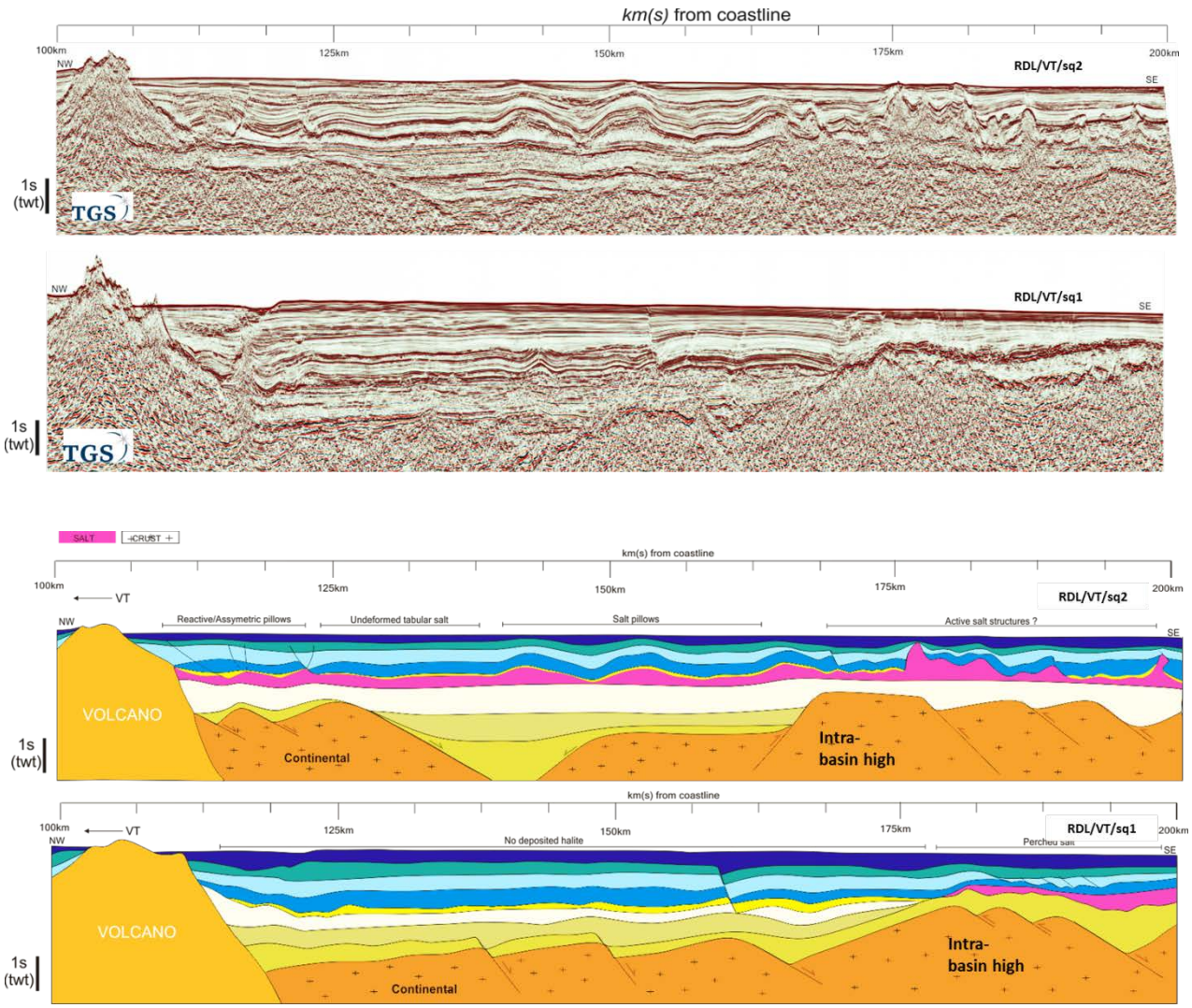

Characteristic regional salt-structural domains are delineated based on dominant structural styles and related depocenter geometries. Based on these structural observations the modern-day kinematic domains and the dominant regional tectonic transport directions have been derived. The salt tectonic evolution and temporal changes in kinematic styles were derived from additional kinematic analysis of characteristic multi-stage salt structures within all structural and kinematic domains. A more detailed kinematic analysis of characteristic salt structures in the landward extensional domain and in the proximal to distal contractional domains is discussed in (section 6).

Basement architecture and derived paleo salt basin geometry

The extent and geometries of salt structures derived regional salt-structural trends and kinematic domains in the West Mediterranean Basins may be controlled by the architectures of the rifted continental, transitional and young oceanic basement. Four major observational elements are of particular importance for the salt tectonic evolution:

1) Regional dip of the continental and oceanic basement
2) Distribution of Pre-Messinian basin fill (see Fig. 15, section 7) and its control on base-salt geometries and/or post Messinian salt tectonics
3) Landward margin of the Messinian salt basin
4) Original thicknesses and regional thickness variations of the Messinian megahalite.

Beneath the Gulf of Lion continental slope, the continental basement is buried up to depths of 10 km and is characterized by basinward dipping major rift normal faults separating 20 to 30 km wide rotated basement fault blocks (RDL/GoL/1, 60 – 140 km, Fig. 6). Beneath the Balearic continental shelf, the rift margin is characterized by a landward shallow basement hinge zone

and a prominent basement high beneath the lower slope separating two major rift grabens (RDL/BAL/1, 20 – 120 km, Fig. 6). The landward basement hinge zone is steeply dipping from shallow depths to depths of 5-6 km beneath the mid-slope (RDL/BAL/1, 20 – 50 km, Fig. 6). The hinge zone is structured by closely-spaced basinward-dipping normal faults with minor offsets and is limited basinward by a main rift border fault and adjacent 20 km wide and several km deep rift grabens. Beneath the lower slope a very prominent 30 – 40 km wide basement horst with major landward and seaward-dipping boundary faults is separating the landward rift graben from a deep basinward graben structure (RDL/BAL/1, 70 – 100 km, Fig. 6). The top of the central high of the horst structure is level with the basinward hinge zone. A seismically observable basinward extent of stretched continental crust in RDL/GoL/1 and RDL/BAL/1 is obvious from a basinward stepped transition and extent of the rift system.

Pre-Messinian syn-rift basins and post-rift succession

The distribution and thickness of Pre-Messinian syn-rift and post-rift sediments varies markedly in the Gulf of Lion-Provencal and Balearic-Provencal basin segments. In the landward Lion-Provencal segment, Chattian-Aquitanian syn-rift strata are blanketing the basement rift topography including the rift graben shoulders. In the Balearic-Provencal segment, thick Chattian-Aquitanian are restricted to the rift grabens and do not extend over the landward hinge zone or the mid-basin basement high.

The Pre-Messinian post-rift strata, which have been widely deposited during the early phase of post-rift thermal subsidence in both margin segments and the deepwater basin, is characterised my mostly horizontal reflectivity, only minor thickness variations and is not affected by basement faulting. In the Gulf of Lion-Provencal segment the early post-rift shallow marine

deposits of Langhian-Burdigalian age are deposited concordantly on top of the proximal syn-rift strata or onlap on volcanic complexes whereas they form a thick sediment blanket in the deepwater basin overlying young oceanic crust (see RDL/GoL/1, Fig. 6). The Serravallian-Tortonian deltaic- lacustrine turbiditic and hemi-pelagic strata of the later post-rift stage show a similar extend but cover the volcanic complex as well.

In the Balearic-Provencal basin segment, the thickness of the Pre-Messinian post-rift strata increases moderately in basinward direction and reaches a maximum average thickness of 3 km in the deepwater basin overlying oceanic crust (see RDL/GoL/1, Fig. 6). The early post-rift shallow marine deposits (Langhian-Burdigalian) are widely deposited covering the landward basement hinge zone, syn-rift sediments and oceanic basement. Only the central high of the intra-basin basement horst is not covered (see RDL/GoL/1 in Fig. 6, 70 km). In the deepwater basin these structurally undisturbed pre-salt sediments are characterized by horizontal strata with a homogenous thickness of ca. 2 km. The Serravallian-Tortonian deltaic- lacustrine turbiditic and hemipelagic strata are only deposited basinward of the landward hinge zone (see RDL/GoL/1 in Fig. 6, 50 km) and show a general thickness increase towards the basin center. The overall distribution of the Pre-Messinian basin fill and its control on post- Messinian salt tectonics, specifically the position of the highly deformed contraction domain over deep sub salt basin fill is shown in (Fig. 6) & (Fig. 15, section 7).

Salt basin extent

The major part of the Gulf of Lions, Liguro-Provencal and Balearic-Provencal basins formed part of the Messinian salt basin. Consequently, the Messinian megahalite forms a prominent and laterally extensive and variably thick seismic-stratigraphic unit in all regional seismic sections

(see Figs. 6 & 7). The NW and SW salt basin margin are both controlled by bathymetric elements of the continental slope, whereas the western salt basin margin is structurally controlled by volcanic complexes and intra-basin basement hinge zones related to the North Balearic transfer zone.

The north-western margin of the Messinian salt basin in the Gulf of Lion is not being observed in the NW-SE regional dip-section RDL/GoL/1 (Fig. 6). The landward part of the seismic section is characterized by extensional growth fault rollover anticlines and reactive salt diapirs typical for the landward extensional domain of thin-skinned gravity-driven salt systems. The NW margin of the salt basin is indicated by the limit of up-slope extension, which is approximately 25 km further landward in up-dip direction of RDL/GoL/1. In contrast, the SW margin of the Messinian salt basin in the Balearic-Provencal basin is clearly expressed in the regional seismic sections (see Figs. 6 & 7). In seismic line RDL/BAL/1, the SW salt basin margin is indicated by the up-slope limit of extensional salt rollers overlying the landward rifted basement and intra-basin high (Fig. 6).

The western margin of the Messinian salt basin in the Balearic-Provencal basin is structurally controlled and can be observed in the interpreted regional seismic sections RDL/VT/sq2 and RDL/VT/sq1 (see Fig. 7). In the NW part of seismic section RDL/VT/sq2, the salt basin is limited by a prominent volcanic complex and in SW part of seismic section RDL/VT/sq1, the salt basin margin is controlled by the structural high of a prominent intra-basin basement hinge zone with salt sediments pinching out on its SW flank and no salt sediments being deposited in the western basin beyond the basement intra basin high (Fig. 7).

Base of salt geometry

The base-salt geometries in the regional seismic sections of the Gulf of Lions – Provencal basin vary from basinward SW dipping segmented slopes of 25 km to 50 km widths with gentle dips of 0.5° to 1° in the landward salt basin underlying the lower continental slopes to a regional flat base-of-salt in the distal deepwater Liguro-Provencal Basin (RDL/GoL/1, Fig. 6).

In the Balearic-Provencal Basin, the base-of-salt is characterized by a steeper basinward NE dipping 20 km to 30 km wide slope segment in the salt basin overlying the landward hinge zone. More gentle dips of approximately 1° of the base-of-salt can be observed above the landward rift grabens (RDL/BAL/1, Fig. 6). South of the Valencia Trough, proximal to volcanic extrusion, the base salt shows mild undulations above rifted continental crust to flat base-salt geometries further basinward above syn-rift strata (RDL/VT/sq2, Fig. 7). RDL/VT/sq1 in Figure 7 shows a moderately structured base-salt overlying deformed syn-rift stratum.

With the exception of the structured base of salt overlying the intra-basin hinge zone in the W-Balearic Basin, the base of Messinian salt is concordant to the pre-Messinian post-rift basin fill and not affected by basement structures. Accordingly, thin-skinned gravity-driven deformation of the post-Messinian overburden is the dominant salt deformation mechanism observed in all seismic data causing a characteristic kinematic segmentation into landward extensional, transitional and basinward contractional salt-kinematic domain (see Fig. 14, section 7).

Original salt thickness

An approximate original thickness of the Messinian megahalite in the deepwater basin can be estimated from extensive undeformed tabular salt layers in the regional seismic lines RDL/GoL/1

(Fig. 6) and RDL/VT/sq2 (Fig. 7). Here, the average thickness of the salt sediments of 0.4 - 0.5 seconds TWT corresponds to a salt thickness of 900 – 1125 m (assuming seismic velocities of pure halite = 4500 m s–1 based on laboratory experiments (Jones and Davison 2014).

Due to extensive gravity-driven salt mobilization, original tabular salt layers are not preserved in the up-slope extensional salt domains along the margins of the Messinian salt basin in the Gulf of Lions (RDL/GoL/1, Fig. 6) and the W-Balearic basin (RDL/BAL/1, Fig. 6). Here the original thickness of the Messinian megahalite can be only estimated from the average thickness of low-amplitude salt structures ranging from 450 m to 625 m (0.2 – 0. 3 sec TWT) in RDL/GoL/1 to less than 450 m (< 0.2 sec TWT) in RDL/BAL/1. In the deep basin an of original salt thickness of approximately 2 to 3 km can be estimated from thickness of undeformed laterally extensive thickness autochthonous salt layer S2 on RDL/GoL/1. 1 to 2 km of original salt thickness on continental slope can be estimated from amplitude of salt structures specifically salt rollers on slopes (S1 on RDL/GoL/1 and S2 on RDL/BAL/1) (Fig. 6).

6. Salt kinematic domains

In this section, we briefly describe the structural styles and salt-structural domains which are characteristic for the three salt-kinematic domains observable in the regional seismic lines RDL/GoL/1, RDL/BAL/1, RDL/VT/sq1, RDL/VT/sq2 shown in previous section.

Extensional salt structures

The gravity-driven thin-skinned salt tectonics in the landward salt basin of the NW Gulf of Lion and SE Balearic Promontory is accommodated by a salt-detached extensional system beneath the continental slopes (see dos Reis, 2005). In the study area the characteristic extensional salt

structures consist of salt-detached listric normal faults and reactive triangular diapirs with variable spacing ranging from narrowly spaced normal faults with rotated fault blocks, to normal faults with intervening welded rollover anticlines, and more widely spaced listric normal faults separated by rafts and intervening syn-kinematic growth wedges (Fig. 8).

Fig. 8: Salt kinematic styles in the proximal slope **(.1)** of the Gulf of Lion margin and salt kinematic styles in the distal slope **(2)** of the Gulf of Lion, Line location is shown in Fig. 3. Segmentation of the extensional province is controlled by variable slope angles forming high to low angle slopes and terraced base-salt geometries that influence salt structural styles.

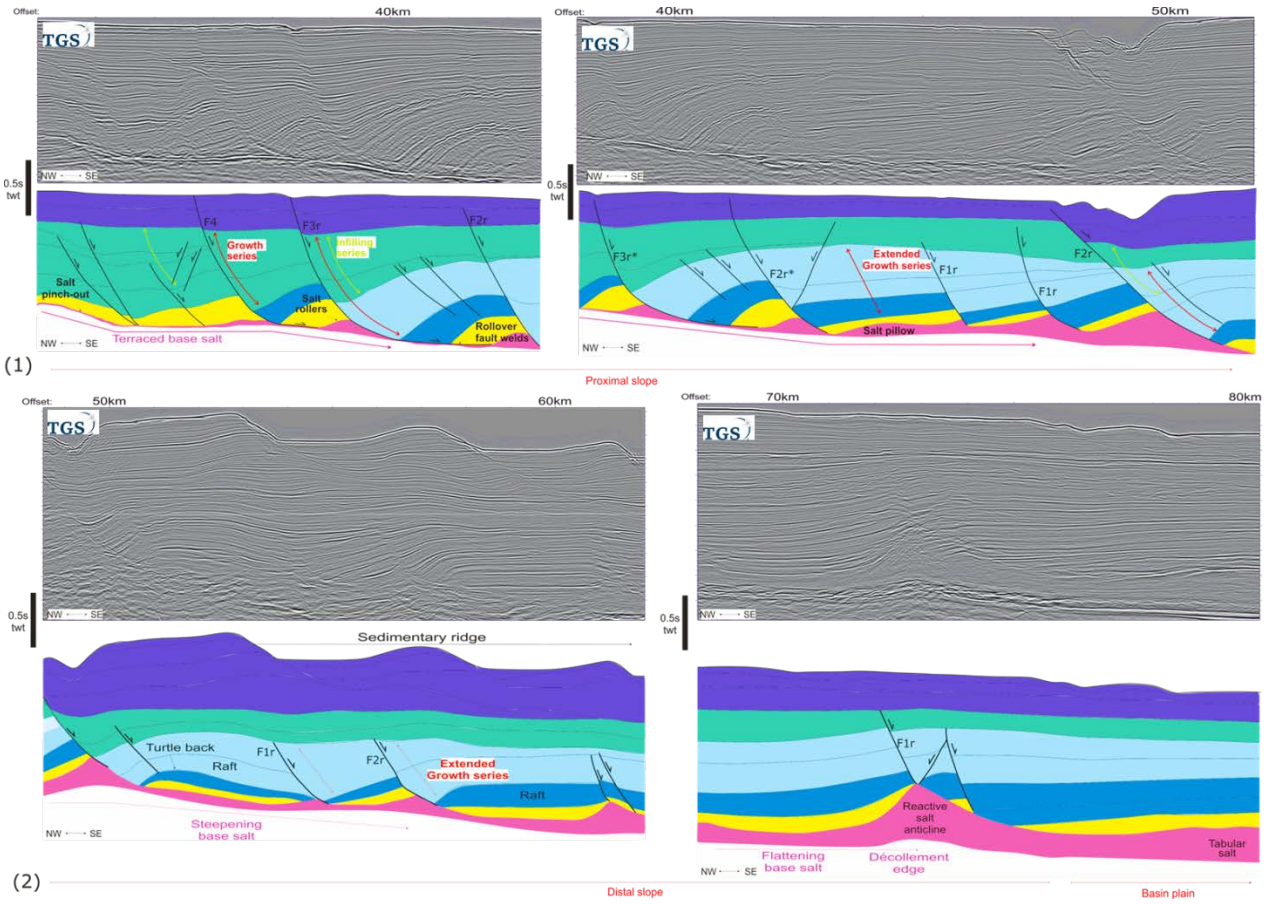

Typical basinward-dipping growth fault-rollover systems with reactive triangular diapirs can be seen in a 40 km wide zone in RDL/GoL/1 and a 20 km wide segment in RDL/BAL/1. In both regional seismic sections RDL/GoL/1 and RDL/BAL/1, reactive diapirs show a basinward increase in amplitudes from 200 m to 1 km.

Salt welds with less than 50 m of remnant salt have frequently developed beneath the subsiding rotated hanging-wall fault blocks. On the steep continental slope of the Balearic Islands, the extensional salt structures are characterized by a 10 km wide zone of narrowly spaced basinward-dipping growth faults, reactive diapirs and landward rotated hanging-wall fault blocks (RDL/BAL/1). The regional seismic line (RDL/VT/sq2) shows a 10 km wide zone of basinward-dipping growth faults, reactive diapirs and asymmetric salt pillows that formed on the SE flank of the volcanic complex in the transition between the Valencia Trough and North Balearic Basin.

(Fig. 8) shows a detailed interpretation of the structures and syn-kinematic depositional sequences in the proximal slope of the NW Gulf of Lion (landward part of the regional seismic section RDL/GoL/1, Fig. 6). This detailed interpretation illustrates that the geometries and kinematic evolution of fault and salt structures were influenced by the base-of-salt geometry (see following section, Fig. 13). Beneath the lower continental slope the base-of-salt is terraced with alternating shallower and steeper dipping segments with variable slopes 0.5^{o} in the proximal slope (Fig. 8) to 1^{o} in the distal slope (Fig. 8). Steeper base-of-salt segments in the proximal slope are overlain by asymmetric reactive diapirs, basinward-dipping listric growth faults and rollover anticlines with strongly rotated growth strata close to faults (F4, F3r & F3r* in Fig. 8). Beneath the hangingwall rollover anticlines the growth faults merge into the salt décollement which is represented by salt welds or an extremely thinned salt layer. In basinward

direction the steeper base-of-salt segments are separated by flatter terraces which are overlain by wider low-amplitude salt pillows and wider asymmetric half grabens with moderately rotated growth strata (F2r* & F1r in Fig. 8).

The extensional salt structures overlying the steeper dipping base-of-salt segments of the distal slope record significantly higher amounts of extension which is documented by rafts consisting of early post-Messinian sediment packages. The early pre- and synkinematic sequences in the footwall and hangingwall of high-displacement listric faults are no longer in contact across the faults but are separated by up to 2 km wide growth wedges of younger synkinematic strata.

Similar to the terraced base-of-salt segments in the proximal slope wider asymmetric half grabens with moderately rotated growth strata overlay the flatter base-of-slope segments in the transition of the distal slope to the distal basin plain. A wide reactive diapir overlying the transition of the distal slope into the basin plain marks the landward limit of the transitional salt kinematic zone (F1r in Fig. 8). Observed growth fault displacement, raft separation and wide younger half graben growth wedges document that gravity-driven extension and basinward translation of the post-Messinian sedimentary succession was enhanced above the steeper base-of-salt segments and sustained by high synkinematic sedimentation rates.

In the proximal and distal continental slope of the NW Gulf of Lions an overall extension of 35 % of the post-salt sequence and total horizontal basinward transport of 17.5 km of sediments at the base of the slope can be estimated from the sum of horizontal displacements of the listric growth faults and associated extensional salt structures (Fig. 8). SE of the Balearic Promontory even steeper base-of-salt segments with slope angles >3^{o} beneath the very narrow continental slope are characterised by narrowly spaced basinward-dipping listric faults and rotated fault

blocks with horizontal extension of more than 50 % and an estimated 5 km of total horizontal transport of salt kinematic structures at the base of the narrow slope segment.

Undeformed salt and halokinetic salt structures

In the Gulf of Lions - Provencal basin undeformed tabular salt stretches about 60 km from the base of slope into the basinal plain (RDL/GoL/1), in the Balearic-Provencal basin it extends 20 km from the basin slope (RDL/BAL/1) and in the Valencia Through – volcanic arc transition about 15 km (RDL/VT/sq2). The variable width of the tabular salt in the three basin segments is further discussed in later section. The thickness of the undeformed salt layer varies from less than 500 m to 2 km in the different basins.

Most of the observed salt structures in the study area are clearly related to gravity-driven extensional and contractional salt tectonic processes from the onset of post-Messinian salt deformation. Halokinetic salt structures are only locally developed in the landward part of the Balearic-Provencal basin in the lower continental slope. The halokinetic structures consist of buried passive diapirs with variable heights in a 20 km wide zone landward of the basement hinge zone (50-70 km/s RDL/BAL/1). Most passive diapirs are confined to Pliocene levels, one ca. 3 km tall passive diapir continued to grow till early Pleistocene times (S2 in RDL/BAL/1). Folding in the overlying strata indicates that all diapirs developed during an early passive stage, were subsequently buried and reactivated in a late contractional stage.

Contractional salt structures

Contractional salt structures are the most variable and widely distributed structures and can be observed in large parts of the deepwater basin including the distal Liguro-Provencal Basin (150 –

250 km in RDL/GoL/1) and most of the Balearic-Provencal Basin (70-210 km in RDL/BAL/1). The contractional salt structures show variable amounts of shortening and timing and range from low-amplitude salt pillows and poly-harmonic salt-cored folds via medium-high amplitude salt-cored folds to tall active and contractional diapirs (Fig. 9).

Fig. 9: Salt kinematic styles in the Liguro-Provencal deepwater basin. DIP direction of Gulf of Lion shows contractional salt structures show basinward amplification from a residual salt swell to an amplified salt swell and salt diapir **(3)**. STRIKE direction of Gulf of Lion shows salt structures show increased shortening from a reactive salt structure to a buried passive diapir and tall bathymetric squeezed diapir **(4)**. Note: possible intersection of section lines (3) & (4) means reactive salt anticline most likely falls between amplified salt swell and diapir on (3).

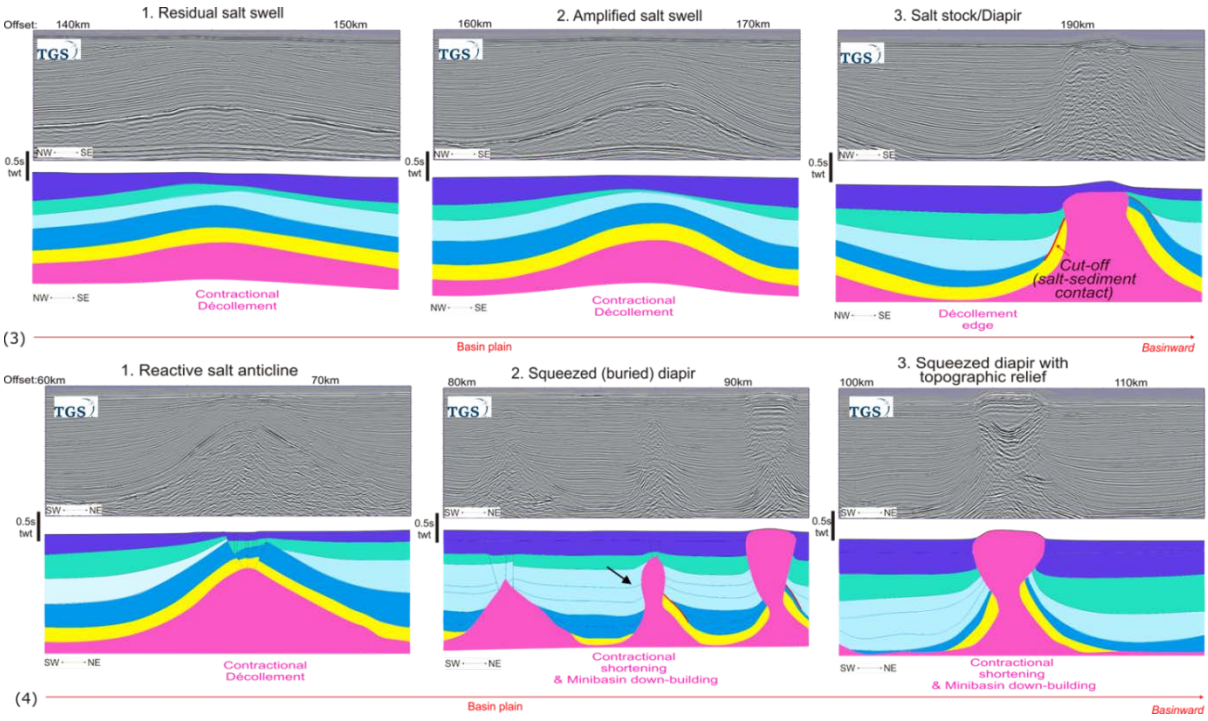

Low-amplitude salt pillows typically occur in wide zones located basinward of the tabular undeformed salt, for example in a 70 km wide segment in the Liguro-Provencal Basin (150 – 210 km in RDL/GoL/1) and a 30 km wide segment in the Balearic-Provencal Basin (140 – 170 km in RDL/VT/sq2). All salt pillows are characterized by pre-kinematic Messinian overburden and few even by Pliocene pre-kinematic strata with constant thickness indicating the late-stage formation of salt pillows since the Pliocene in areas previously occupied by tabular undeformed salt with concordant overburden sediments. The salt pillows show a basinward decrease in wavelength from 3.5 km to 3 km and a basinward increase in amplitude from ca. 500 m to 1 km. The salt pillows (Fig. 9) (3) are translated via basinward progradational sedimentary wedge terminating at a 3 km tall discordant diapir at the start of a diapiric domain. The progradational wedge is interpreted from syn-kinematic packages that thin above salt swells and grow significantly towards the salt diapir.

Similar to the salt pillows, salt-cored anticlines and poly-harmonic anticlines in the deepwater basin are characterized by concordant overburden but are further shortened with variable amplitudes and wavelengths. In the Liguro-Provencal Basin large harmonic salt anticlines with wavelengths of 10 km occur in a 30 km wide fold train (210 – 230 km, S4 in RDL/GoL/1). More complex poly-harmonic salt-cored fold structures have formed in the Balearic-Provencal basin with variable fold structures on the basin plain overlying the intra-basin high and distal continental crust (70 – 120 km, in RDL/BAL/1) displaying early km-scale short-wavelength folds of Messinian and Lower Pliocene sediments preserved at the base a large salt massif overlying the hinge zone and a 20 km wide Pleistocene-Holocene anticlinal structure (S3 in RDL/BAL/1). Harmonic salt-cored folds with 10 km wavelengths can be observed just basinward of the poly-

harmonic fold zone (120 – 150 km, S5 in RDL/BAL/1). In both basins salt-cored folds are characterized by pre-kinematic Messinian cover sediments and synkinematic Pliocene and younger sediments indicating the onset of contraction in the Early Pliocene. The poly-harmonic folds in the Balearic-Provencal basin are characterized by very thin Messinian sediments allowing early short-wavelength folding whereas the harmonic folds in the distal Balearic-Provencal and Liguro-Provencal Basin are covered by thicker Messinian post-salt sediments. Consequently, the wavelength of fold structures has been controlled by the thickness of the Messinian post-salt sediments deposited before the onset of Pliocene shortening. It is important to note that shortening of the salt-cored anticlines is ongoing in the Liguro-Provencal basin but seem to have ceased in the Balearic-Provencal basin. Further basinward beneath the distal deepwater basin plain of the Balearic-Provencal basin an extensive diapiric province can be observed stretching at least 40 km in NW-SE basinward direction and more than 100 km in SW-NE strike direction (120 – 220 km in RDL/BAL/1).

This diapiric domain (see RDL/BAL/1) is characterized by tall passive, active and contractional diapirs with variable widths ranging from 2 – 5 km and maximum heights of 3 km (S7, S8) which are separated by salt-cored anticlines (D4 & D6 or minibasins D7). Depocenter styles in the diapiric domain vary from 20 – 30 km wide W-shaped minibasins underlain by a remnant basal salt pillow (D4 & D5) and a narrower 10 km wide U-shaped minibasins with nearly vertical flanks (D6).

Representative examples of the range of contractional salt structures and their related depocenters are shown in (Fig. 9). The contractional salt structures show generally amplification and increase in shortening in basinward direction from low-amplitude salt pillows, moderate

and amplified salt-cored anticlines, to faulted salt-cored anticlines with active diapirs piercing the fold hinges to passive and contractional diapirs. Pre-kinematic strata is characterised by homogenous thicknesses and concordance with salt swells and the base of salt diapirs and is mostly discordant with flanks of salt diapir. Syn-contractional strata are characterized by thinning above salt swells and diapirs as well as growth sequences adjacent to salt diapirs. It is important to note that younger synkinematic layers are separated from the diapir flanks by upturned flaps. We consider that most diapirs in the deepwater basin plain developed from contractional salt pillows and salt-cored folds. Increased shortening has led to extensional faulting and erosion of fold hinges (Fig. 9) (4) allowing previously concordant salt to pierce the fold hinge as active diapir and to grow further as passive or contractional diapir. The kinematic evolution of the contraction province is described in section 4.4.

Buried triangular and columnar diapirs (Fig. 9) (4) are commonly characterised by extensional faulting in their roof sequences. Major contractional diapirs show a positive bathymetric expression near or at the seafloor with upward folded mega-flaps, bulbous diapir heads and characteristic hourglass geometries. Whereas the upward widening of diapirs can be seen in passive diapirs when the rate of diapir rise exceeds the local sedimentation rate, we consider all diapirs with bathymetric seafloor expression to grow as contractional diapirs today. All these diapirs are characterised by flanking depocenters that are already welded to the base-of-salt. Consequently, the diapirs are isolated from the source layer. Further diapir growth in case of passive diapirs would be driven by sediments accumulating in the diapir flanks. This switch of depocenters and typical growth sequences of younger strata (e.g. rim synclines, turtle structures) close to the diapir flanks cannot be observed. In contrast, all stratal geometries in

the diapir flanks are turned upwards into the diapir flank or show normal geometries demonstrating that continued diapir growth must be driven by regional gravity-driven shortening of the columnar diapir stems (Fig. 9).

7. Spatial arrangement of contractional structures and regional tectonic transport

The spatial arrangement and regional variation of contractional salt structures in the deepwater salt basin is reflecting the dominant regional tectonic transport directions and the impact of sediment loading caused by the Rhone deep sea fan (see Fig. 13). This has been analyzed and mapped in more detail in seismic sections trending in dip and strike directions of the NW Gulf of Lions – Provencal margin (Figs. 10 & 11). As already briefly discussed in previous section, a general trend of amplification and increase in shortening of salt structures from low-amplitude salt pillows, salt-cored anticlines to contractional diapirs can be clearly seen in the NW-SE regional seismic sections (Fig. 10). This trend describes the overall tectonic transport direction of salt structures and the post-Messinian sediment cover from the NW slope towards the deepwater basin plain due to the gravity-driven thin-skinned deformation processes.

Fig. 10: **(a)** Un-interpreted 2D seismic dip sections, Landmark colour bar is SEG Normal **(b)** Interpreted NW-SE 2D seismic dip lines (dwDL/sq1,dwDL/sq2,dwDL/sq3) of the Gulf of Lion showing variation of salt structural styles delineated in Zones 1 – 3 perpendicular to the shelf margin and derived kinematic domains.

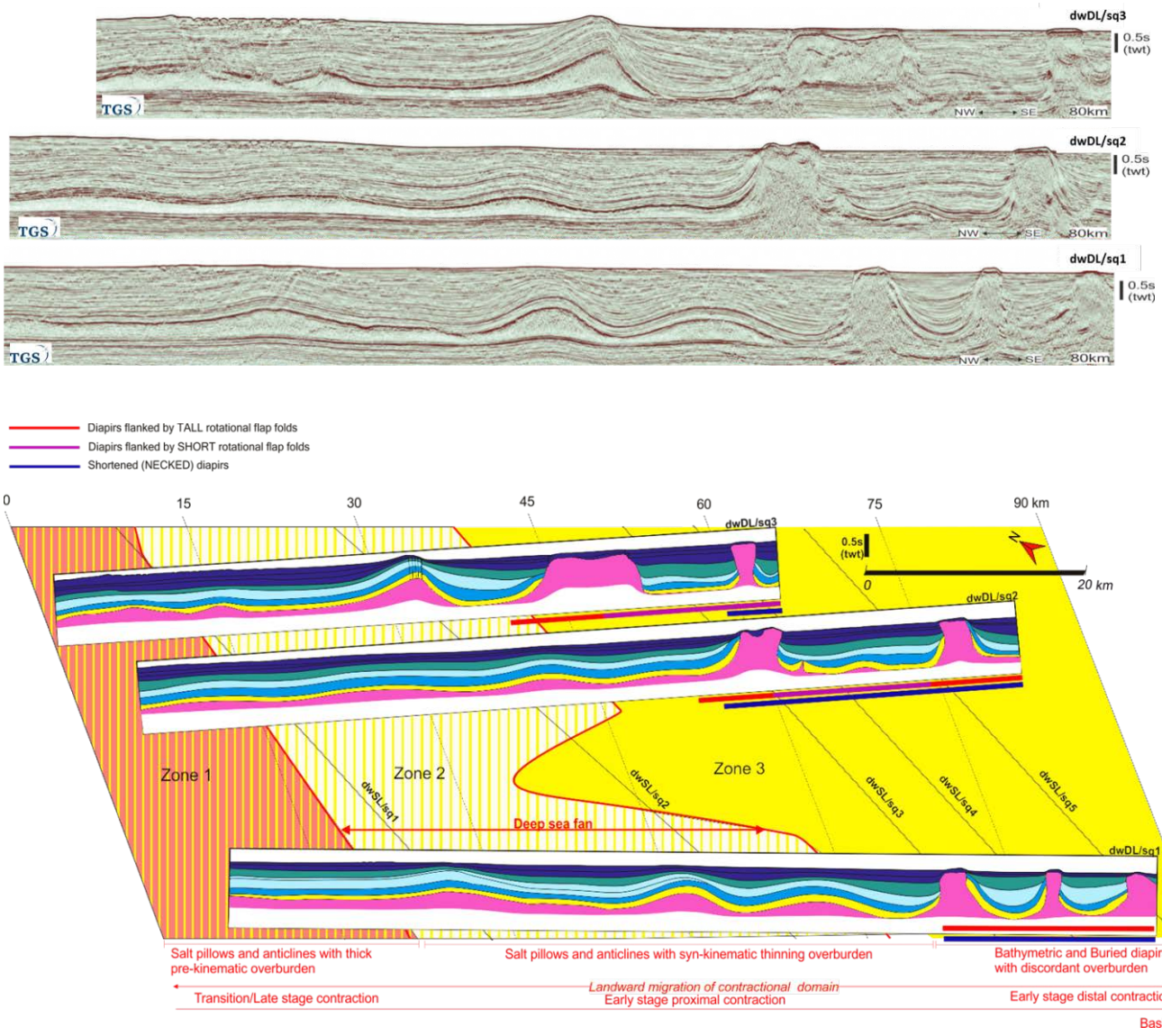

Fig. 11: **(a)** Un-interpreted 2D seismic strike sections, Landmark colour bar is SEG Normal **(b)** Interpreted SW-NE 2D seismic lines (dwSL/sq1,dwSL/sq2,dwSL/sq3,dwSL/sq4,dwSL/sq5) parallel to the Gulf of Lion shelf margin showing variation of salt structural styles and derived kinematic domains delineated in Zones 1 – 3.

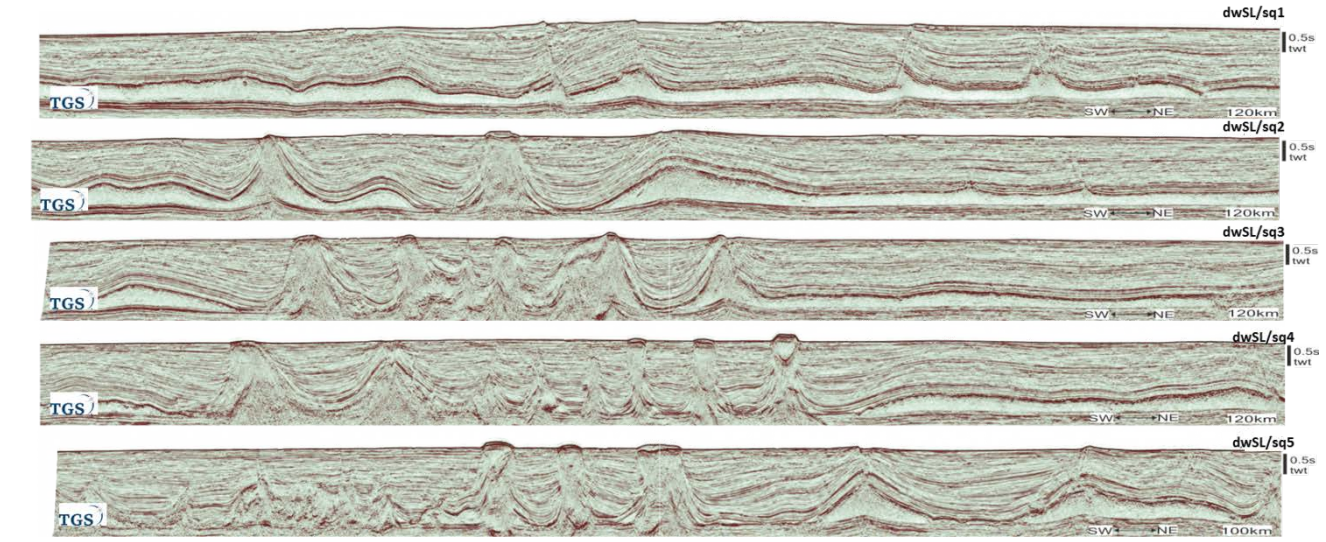

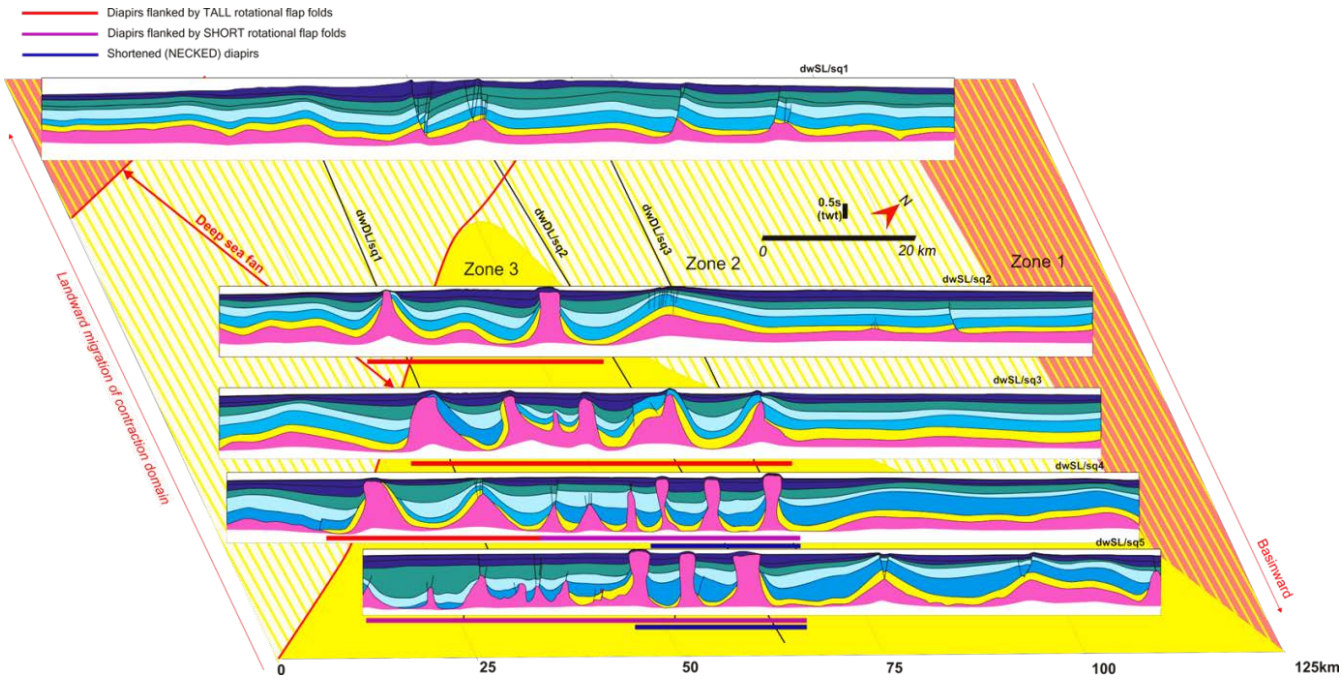

The structural zonation and the basinward salt tectonic transport direction in the Provencal–Liguro deepwater basin have been mapped in more detail in the seismic dip sections (Fig. 10). The NW-SE basinward-directed salt tectonic transport parallel to the dip seismic sections is documented by:

1) An increase in amplitude to wavelength ratios of salt swells and salt anticlines in the late-stage and early proximal contraction domains (Fig. 10).
2) Progradational syn-kinematic sedimentary wedges in the NW flanks of salt diapirs at the up-dip limit of the early-stage distal contractional domain (dwDL/Sq1 and dwDL/sq3 in Fig. 10).
3) Pronounced rotational upturn of flaps overlying the flanks of salt diapirs in the early-stage distal contraction (Fig. 10).
4) Ponding of younger syn-kinematic sediments, which are separated from the salt diapir and are onlapping on rotated basal layers overlying the diapir flanks in the early-stage contraction domain examples on diapirs (Fig. 11).
5) Contractional necked diapirs with hour-glass shapes in the early-stage distal contraction domain in (Figs. 10 & 11).

Based on these general observations, the variable contractional salt structural styles can be subdivided into three NE-SW trending structural zones, which can be identified and correlated between all dip seismic sections. From landward to basinward direction, these structural zones are:

1) Salt pillows and salt anticlines with thick Messinian - Early Pliocene pre-kinematic overburden

2) Salt pillows and salt anticlines with dominantly Pliocene -recent syn-kinematic overburden

3) Contractional diapirs, either buried or with bathymetric expression at the sea floor, with Pliocene - recent dominantly syn-kinematic overburden.

The post-Messinian synkinematic overburden in zones 2 & 3 demonstrate that both zones were controlled by contractional salt tectonics since Early Pliocene times, whereas the thick Messinian - Early Pliocene pre-kinematic sediments in zone 1 indicate only younger contractional deformation of tabular salt with Late Pliocene onset. This clearly demonstrates the up-dip migration of the landward boundary of the contractional domain in opposite direction of the overall regional basinward tectonic transport since Late Pliocene times (see Fig. 12). Indicators of tectonic transport along the deep sea fan pathway (see Fig. 13) are proximal reactive salt structure (dwDL/sq3 in Fig. 10), N-S propagation of salt swells (dwDL/sq2) to amplified swells and anticlines (dwDL/sq1) and an increase in lateral frequency of salt structures for each profile.

Fig. 12: Spatial and temporal evolution of salt kinematic domains in seismic line RDL/GoL/1 from the Early Pliocene to present times based on time constraints of syn-kinematic sediments and related structural zoning shown in Fig. 10.

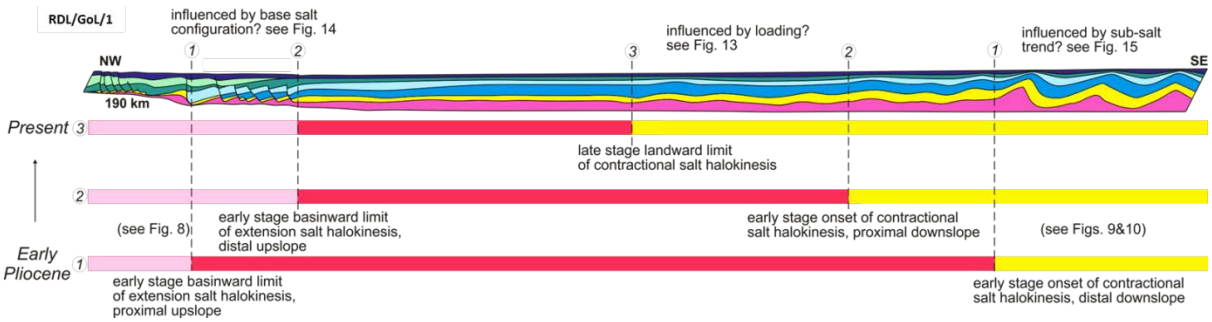

Similar structural trends and structural zones can be identified in the seismic strike-sections dwSL/sq1, dwSL/sq2, dwSL/sq3, dwSL/sq4 and dwSL/sq5 (Fig. 11) which are trending parallel to the Gulf of Lion margin. Here, the amplification and shortening of salt structures in the seismic sections increases from the landward strike-section dwSL/sq1 containing low-amplitude salt pillows, anticlines and reactive diapirs continuously towards the basinward seismic strike-section dwSL/sq5 with its narrowly spaced buried and emerging contractional diapirs.

The major observations in the individual seismic strike-sections (Fig. 11) include:

1) Basinward increase in frequency of contractional salt structures in structural zones 2 & 3.
2) Basinward decrease in width of minibasins.
3) Basinward change from symmetric to asymmetric axial trace of minibasins from SW to NE part of seismic section.
4) Basinward decrease of size and degree of rotation of mega flaps overlying the pedestals of diapirs.
5) Basinward decrease in width and increase in height of salt diapirs towards tall columnar diapirs.
6) Buried reactive diapirs and breached salt-cored anticlines with active salt diapirs border the tall contractional diapirs in strike direction in the SW and NE in the distal seismic sections (dwSL/sq2 to dwSL/sq5, Fig. 11).

The symmetry of structural zones in the individual sections demonstrates that the amount of shortening is increasing basinward from section to section and additionally towards the center of individual seismic sections indicating a slightly convergent tectonic transport in the central

deepwater basin plain (See section 8 for detailed discussion of the basin-wide kinematic segmentation and regional tectonic transport pattern). Increased contractional deformation of salt structures due to sediment loading of deep sea fan (Fig. 13) is apparent from the following salt structural changes:

1) A proximal reactive salt structure (dwDL/sq3).

2) N-S propagation of salt swells (dwDL/sq2) to amplified swells and anticlines (dwDL/sq1).

3) And an increase in frequency of salt structures for each profile dwDL/sq1, dwDL/sq2 and dwDL/sq3.

Fig. 13: Overlay of interpreted seismic lines and limits of kinematic domains on the interpolated structure-time map of the sea bed showing the spatial correlation of the deep sea Rhone fan and contractional salt structures in the deepwater Provencal Basin.

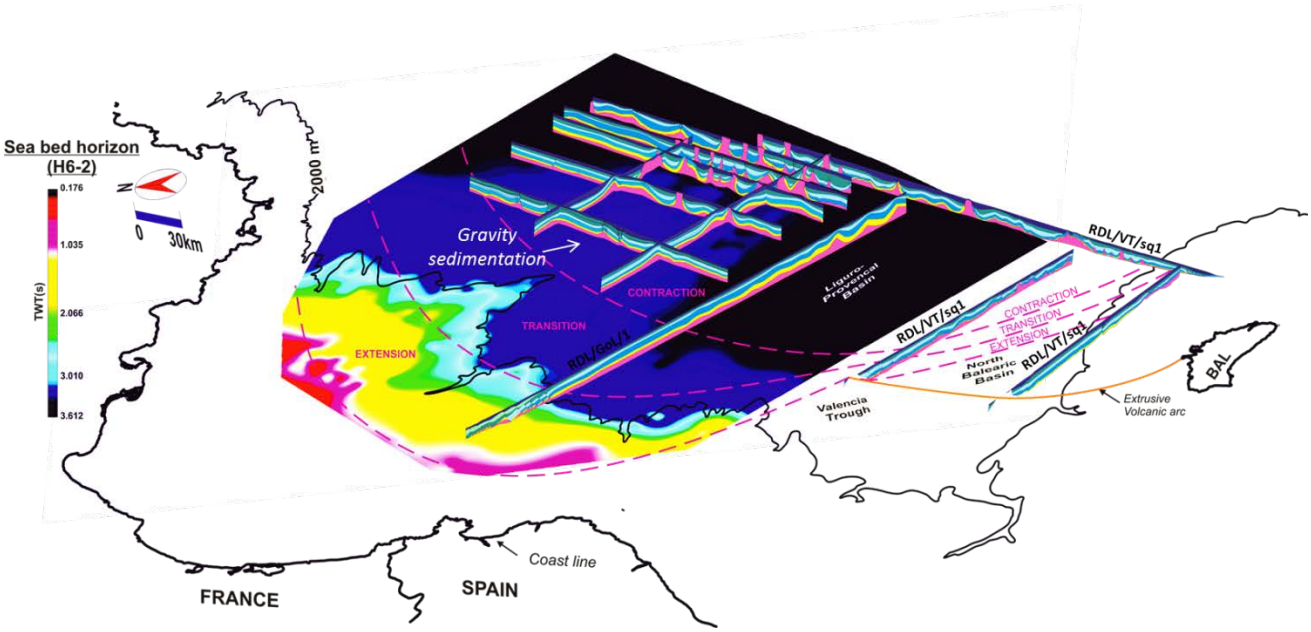

Fig. 14: Overlay of interpreted seismic lines and limits of kinematic domains on the interpolated base salt structure-time map.

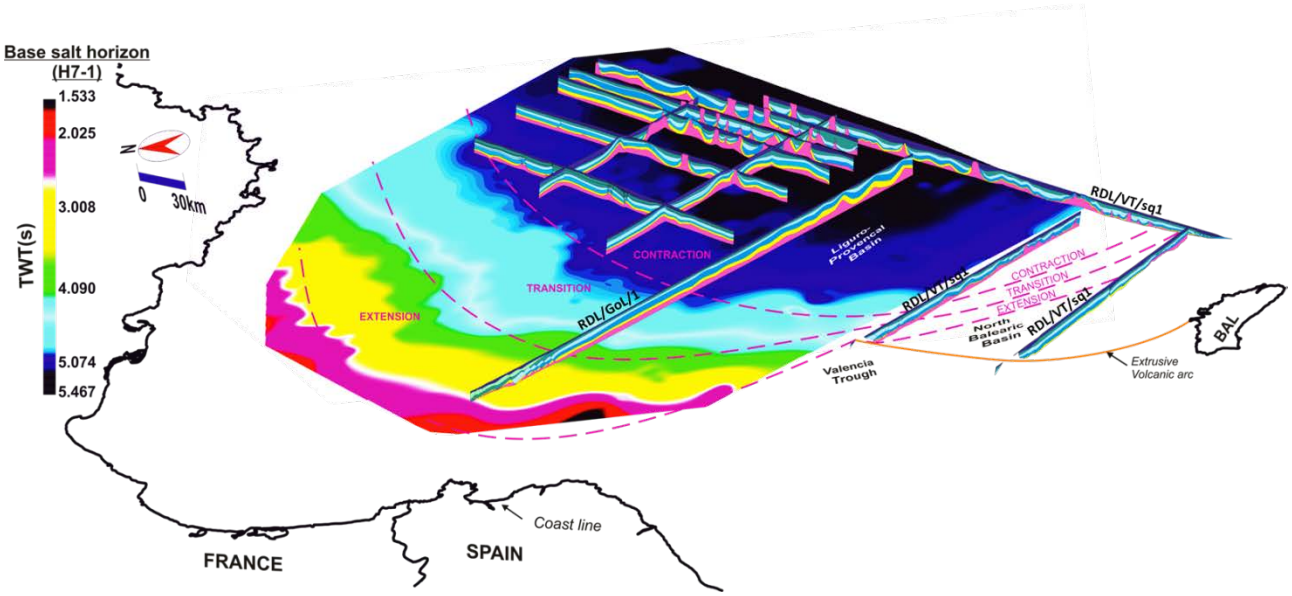

Fig. 15: Overlay of interpreted seismic lines on the interpolated structure-time map of the sub-salt horizon H1-1. Figure illustrates the possible relationship of the distribution of Pre-Messinian basin fill and its control on post Messinian salt tectonics.

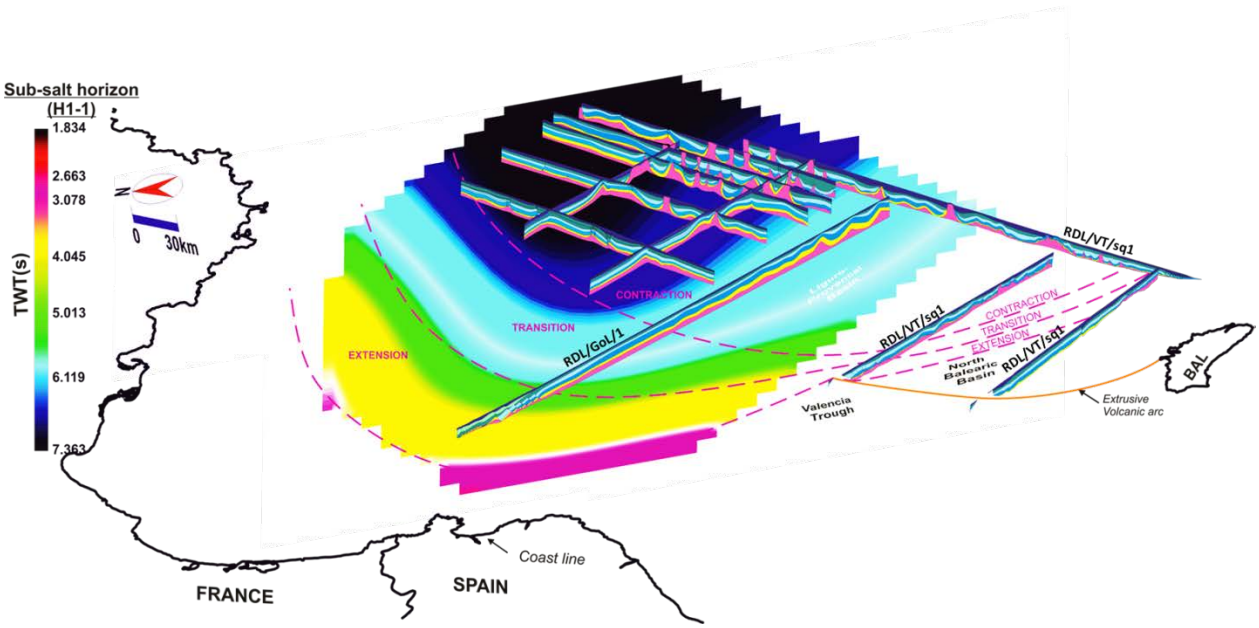

8. Discussion

Regional salt kinematic domains

The spatial-temporal pattern salt structures and derived structural zones describe a characteristic linked gravity-driven thin-skinned salt-detached system with a characteristic kinematic segmentation of landward extensional, transitional and basinward contractional salt kinematic domains stretching from the margin slope to the deepwater basin plain (Fig. 16). In the Gulf of Lion and the Valencia Trough the kinematic segments are oriented parallel to the NE-SW trending margin segment and the landward extensional, intermediate transitional and basinward contractional domains reflect the overall NW-SE directed tectonic transport into the basin centre. In contrast, in the SW along the NNW-SSE trending Balearic Promontory with its steep and narrow slope the orientation of the kinematic domains changes from NE-SW to NNW-

SSE indicating an overall W-E to WNW-ESE directed tectonic transport into the basin centre of the Liguro-Provencal basin.

Fig. 16: Regional distribution of kinematic domains in the North Balearic and Liguro-Provencal Messinian salt basin controlled by gravity-driven thin-skinned salt tectonic processes.

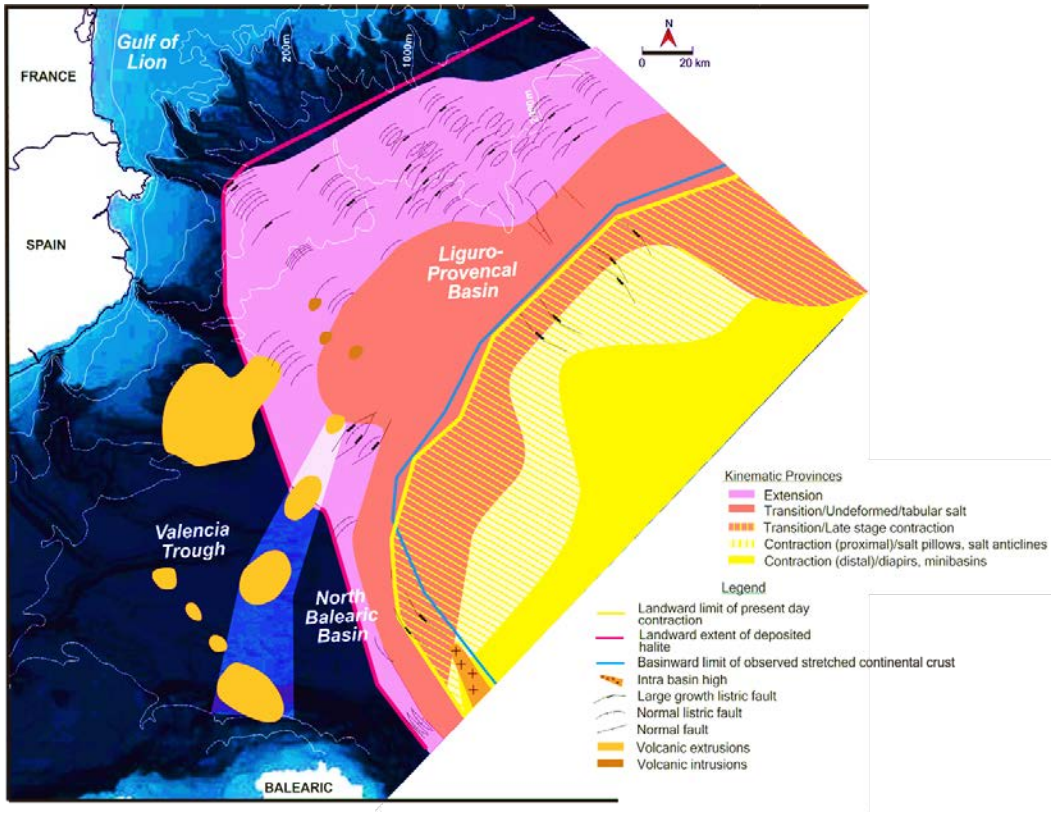

It is important to note that the NW-SE transport direction is dominant due to the much wider NW continental slope and margin as shown by the much wider extensional and transitional domains in this margin segment, whereas the extensional and transitional domains on the Balearic slope are less than 20 km wide. Nevertheless, tectonic transport towards the contractional domain beneath the deepwater basin plain can be described as partial convergent. Distinctive salt tectonic styles observed in the regional sections (RDL/GoL/1, RDL/BAL/1,

RDL/VT/sq1, RDL/VT/sq2) and derived regional kinematic segments summarized for the three main basin segments in (Fig. 16). As already described for other salt basins (Adam et al. 2012a, b; Adam and Krezsek 2012a), the extent of the kinematic provinces varies over time.

The salt tectonic trends in the three main basin segments are:

1) NE-SW strike trend parallel to the Gulf of Lion margin (RDL/GoL/1, Fig. 6) with well-developed several 10's km wide landward extensional domain beneath the continental slope with proportional undeformed transitional segment at the base of slope and a wide contractional segment in the central basin plain.
2) NNW-SSE strike trend parallel to the Balearic promontory (RDL/BAL/1, Fig. 6), a less than 10 km wide landward extensional segment beneath the steep slope is accompanied in basinward direction by a narrow transitional domain (< 20 km width) leading towards and a wide contractional segment in the central basin plain.
3) NNW-SSE strike trend parallel to the Valencia Trough (RDL/VT/sq2, Fig. 7), a narrow landward extensional domain on the basinward side of the volcanic arc leads in basinward direction to mildly deformed transitional domain in the distal basin plain. The absence of salt structures south of the volcanic arc (RDL/VT/sq1, Fig. 7) defines the western limit of Messinian salt deposition in the Valencia Trough.

The relationship between the landward extensional domain, the intermediate translational domain and the basinward contractional domain in each of the basin segments is typical for the strain distribution and kinematics of a thin-skinned gravity-driven linked salt kinematic system, (Adam et al. 2012a; Brun and Fort 2004; Fort et al. 2004b; Rowan et al. 2004b; Vendeville 2005). The widths of the kinematic provinces and their evolution over time are partly influenced by

changes in the basin geometry and the post-Messinian sediment input. For example, the changes in the geometry of the wide and gently dipping continental slope in the Gulf of Lion margin towards the narrow and more steeply dipping slopes in the Balearic margin are reflected in the variable widths of the kinematic domains.

NE-SW of the Gulf of Lion, indicates late-stage landward migration of the contractional domain or a gradual evolution of the behaviour from predominantly asynchronous dominated by halokinetic growth to synchronous with the increase of horizontal stress leading to lateral contraction strain growth (Ge et al. 2019). Along the NE-SW trending Gulf of Lion margin segment, landward contraction in Provencal Basin has been increased by sediment input into the basin plain during mid Pliocene to Pleistocene times (see Rowan 2014) from the Alps, Massif Central and the Pyrenees (Berné and Gorini 2005). These sediments were routed via multiple delivery canyons on the Gulf of Lion margin into deep sea fan systems into the deepwater basin plain (Fig. 3, Fig. 13).

The present-day distribution of the kinematic domains (see Fig. 16) with its early and late-stage contractional domains documents the up-dip migration of the landward limit of the contractional domain over time affecting the basinward part of the former transitional domain. For example, in the Gulf of Lion-Provencal basin the Early Pliocene transitional domain would have stretched further in the basin plain into the area characterized today by the 60km wide late-stage contractional domain consisting of low-amplitude salt pillows with thick Messinian-Early Pliocene pre-kinematic overburden. In contrast, the early contractional domain is characterized by long-term contractional salt tectonics since the onset of Late Messinian post-salt synkinematic sedimentation and is sub-divided by a 30 km wide landward zone with salt-

cored anticlines (RDL/GoL/1 in Fig. 6) and the basinward contractional diapiric province occupying the centre of the basinal plain.

Salt tectonic process model

A conceptual process model of gravity-driven thin-skinned salt tectonic processes in the Gulf of Lion – Provencal Messinian salt basins is illustrating the spatial variation and temporal evolution of the characteristic kinematic segments and their indicative salt tectonic structures (Fig. 17).

Fig. 17: Conceptual process model showing the evolution of salt kinematic domains and respective salt-structural styles in the Gulf of Lion – Provencal Messinian salt basin controlled by gravity-driven thin-skinned salt tectonics.

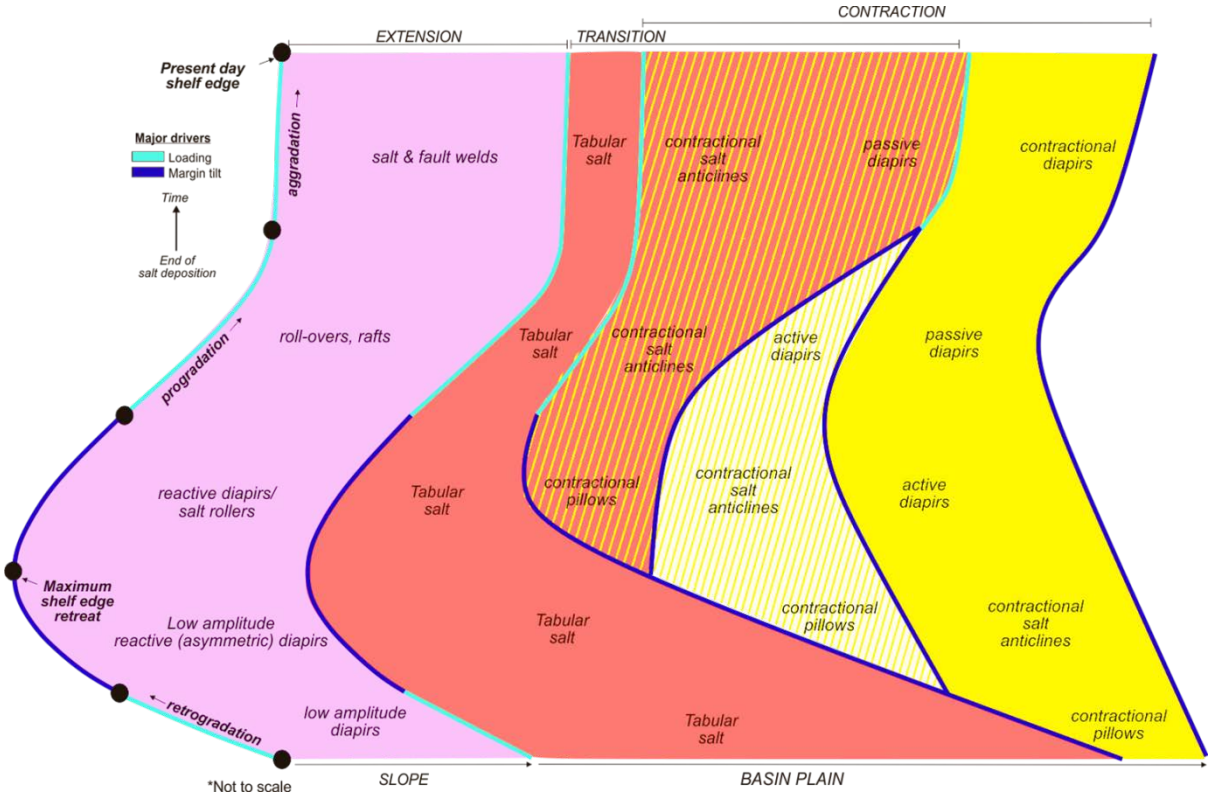

The temporal evolution of the salt kinematic domains is mainly controlled by factors such as overburden thickness, differential loading and margin tilt due to thermal subsidence. Subsequent to the salt deposition, early stage salt pillows form with negligible lateral tectonic forces in the distal basin plain see example in (Hughes and Davison 1993; Tari et al. 2003a). Regional extension in the landward salt basin initiated by margin tilt due to post-rift thermal subsidence leading to reactive diapirism and associated basinward-dipping listric growth fault-rollover systems while regional basin-wide sedimentation stabilises the para-autochthonous salt of the transitional domain in the lower slope to basin transition. The overall basinward translation of the post-salt overburden in the extensional and transitional domains is accommodated by salt pillows, salt-cored anticlines, active and contractional diapirs in the contractional domain occupying the deepwater basin plain. The formation of mature listric growth fault rollover systems and rafts indicate high strain rates due to localised sedimentary input and high sedimentation rates (Adam and Krezsek 2012a; Hudec and Jackson 2002a). For example, in our study, mature roll-over anticlines and rafts are formed during deep sea fan formation related to prograding shelf deltas. Post-salt sediment loading and margin tilt enabled regional contraction. Over time, thinning and welding of the salt detachment in the upslope extensional domain along with the increase in overburden thickness and lateral shortening in the basin plain, impeded short-wavelength folding enabling the upslope migration of the contractional domain and evolution of active diapirs and contractional salt anticlines into passive diapirs and contractional diapirs.

9. Conclusions

This study entails the assessment of the partially convergent salt tectonic system along Gulf of Lion– Provencal, Balearic–Provencal and Valencia Trough–Provencal basin segments. We document a gravity-driven thin-skinned salt-detached linked system with a characteristic kinematic segmentation of extensional, transitional and contractional salt kinematic domains. Salt-structural styles and the basin architecture are controlled by basin subsidence and margin uplift which contributed to the regional salt halokinetic response to subsequent sedimentary loading and regional gravitational processes. The present day kinematic segmentation is documented by a landward extensional, transitional, and basinward contractional domain with distinctive early and late stage phases. The late stage contractional domain describes the landward migration of the contractional domain over time affecting the basinward part of the former transitional domain.

10. Further work

Subsequent study investigates the halokinetic processes in the contractional diapiric domain of the Liguro-Provencal deepwater basin overlying young oceanic crust. Preserved seismic stratigraphic patterns within minibasin depocenters in the deepwater basin will enable the interpretations of kinematic phases and stages of salt growth and provide insights into the temporal local halokinetic processes and controls. The study of local halokinetic processes may support a better understanding between local and regional drivers of salt tectonic processes in the Messinian salt basins of the Western Mediterranean. Further study also builds on the current composite halokinetic sequence-stratigraphic concepts which were originally developed

for the analysis of local-scale salt-sediment interactions based on characteristic structural geometries formed close to passive salt diapirs.

11. ACKNOWLEDGEMENTS

We are especially grateful to TGS for providing the seismic data used in this study. At TGS, we are particularly thankful to Karyna Rodriguez and Neil Hodgkinson for detailed review of this work and for granting the permission to publish. We address our gratitude to IHS Markit for authorising the use of Kingdom: Seismic and geological interpretation software as part of the Royal Holloway academic licence agreement. Finally, our uttermost gratitude is to Petroleum Technical Development Fund (PTDF), Nigeria for the financial support throughout the PhD Programme.

12. References

Adam, J., Ge, Z. & Sanchez, M. 2012a. Post-rift salt tectonic evolution and key control factors of the Jequitinhonha deepwater fold belt, central Brazil passive margin: Insights from scaled physical experiments. Marine and Petroleum Geology, **37**, 70-100, doi: 10.1016/j.marpetgeo.2012.06.008.

Adam, J., Ge, Z. & Sanchez, M. 2012b. Salt-structural styles and kinematic evolution of the Jequitinhonha deepwater fold belt, central Brazil passive margin. Marine and Petroleum Geology, **37**, 101-120, doi: https://doi.org/10.1016/j.marpetgeo.2012.04.010.

Adam, J. & Krezsek, C. 2012. Basin-scale salt tectonic processes of the Laurentian Basin, Eastern Canada: insights from integrated regional 2D seismic interpretation and 4D physical experiments. Geological Society, London, Special Publications, **363**, 331-360.

Adam, J., Krezsek, C., MacDonald, C., Campbell, C., Cribb, J., Nedimovic, M., Grujic, D. 2008. Basin-scale salt tectonic processes at the North-Central Scotian Margin: Insights from integrated regional 2D seismic interpretation and 4D physical experiments. *AAPG Annual Convention*, San Antonio, Texas.

Adam, J., Zhiyuan, G. & Sanchez, M. 2012c. Post-rift Basin Evolution and Kinematics of the Salt-detached Deepwater Fold-Belt of the Jequitinhonha Basin, Central East Brazil Passive Margin. *AAPG Annual Conference & Exhibition*, Long Beach, California.

Bache, F., Gargani, J., Suc, J.-P., Gorini, C., Rabineau, M., Popescu, S.-M., Leroux, E., Couto, D.D., Jouannic, G., Rubino, J.-L., Olivet, J.-L., Clauzon, G., Dos Reis, A.T. & Aslanian, D. 2015. Messinian evaporite deposition during sea level rise in the Gulf of Lions (Western Mediterranean). Marine and Petroleum Geology, **66**, 262-277, doi: 10.1016/j.marpetgeo.2014.12.013.

Berné, S. & Gorini, C. 2005. The Gulf of Lions: An overview of recent studies within the French 'Margins' programme. Marine and Petroleum Geology, **22**, 691-693, doi: 10.1016/j.marpetgeo.2005.04.004.
Biju-Duval, B., Letouzey, J. & Montadert, L. 1978. Structure and evolution of the Mediterranean basins. Initial Reports of the Deep Sea Drilling Project, **42**, 951-984, doi: 10.2973/dsdp.proc.42-1.150.1978.
Brun, J. & Fort, X. 2004a. Compressional salt tectonics (Angolan margin). Tectonophysics, **382**, 129-150.
Brun, J.P. & Fort, X. 2011. Salt tectonics at passive margins: Geology versus models. Marine and Petroleum Geology, **28**, 1123-1145, doi: doi:10.1016/j.marpetgeo.2011.03.004.
Butler, R.W.H., McClelland, E. & Jones, R.E. 1999. Calibrating the duration and timing of the Messinian salinity crisis in the Mediterranean: linked tectonoclimatic signals in thrust-top basins of Sicily. Journal of the Geological Society, London, **156**, 827-835.
Carminati, E., Doglioni, C., Gelabert, B., Panza, G.F., Raykova, R.B. & Roca, E. 2004. Evolution of the Western Mediterranean. Principles of Phanerozoic Regional Geology, 1-29.
Carminati, E., Lustrino, M. & Doglioni, C. 2012. Geodynamic evolution of the central and western Mediterranean: Tectonics vs. igneous petrology constraints. Tectonophysics, **579**, 173-192, doi: 10.1016/j.tecto.2012.01.026.
Cartwright, J., Jackson, M., Dooley, T. & Higgins, S. 2012. Strain partitioning in gravity-driven shortening of a thick, multilayered evaporite sequence. Geological Society, London, Special Publications, **363**, 449-470, doi: 10.1144/sp363.21.
Cribb, J. 2009. *Analogue modelling of salt tectonic processes beneath the shelf and deepwater slope of the eastern Nova Scotian margin.* B.Sc. Thesis, B.Sc. Thesis, Dalhousie University.
Demercian, S., Szatmari, P. & Cobbold, P.C. 1993. Style and pattern of salt diapirs due to thin-skinned gravitational gliding, Campos and Santos basins, offshore Brazil. Tectonophysics, **228**, 393-433.
Dewey, J., Helman, M., D. Knott, S., Turco, E. & H. W. Hutton, D. 1989. Kinematics of the western Mediterranean. **45**, 265-283.
Dooley, T.P., Jackson, M. & Hudec, M.R. 2009. Inflation and deflation of deeply buried salt stocks during lateral shortening. Journal of Structural Geology, **31**, 582-600.
dos Reis, A.T., Gorini, C. & Mauffret, A. 2005. Implications of salt–sediment interactions on the architecture of the Gulf of Lions deep-water sedimentary systems—western Mediterranean Sea. Marine and Petroleum Geology, **22**, 713-746, doi: 10.1016/j.marpetgeo.2005.03.006.
Driussi, O., Maillard, A., Ochoa, D., Lofi, J., Chanier, F., Gaullier, V., Briais, A., Sage, F., Sierro, F. & Garcia, M. 2015. Messinian Salinity Crisis deposits widespread over the Balearic Promontory: Insights from new high-resolution seismic data. Marine and Petroleum Geology, **66**, 41-54, doi: 10.1016/j.marpetgeo.2014.09.008.
Fort, X. & Brun, J.P. 2012. Kinematics of regional salt flow in the northern Gulf of Mexico.
Fort, X., Brun, J.P. & Chauvel, F. 2004. Salt tectonics on the Angolan margin, synsedimentary deformation processes. AAPG Bulletin, **88**, 1523-1544.
Ge, H., Jackson, M. & Vendeville, B. 1997. Kinematics and dynamics of salt tectonics driven by progradation. AAPG Bulletin, **81**, 398-423.
Ge, Z., Rosenau, M., Warsitzka, M. & Gawthorpe, R.L. 2019. Overprinting translational domains in passive margin salt basins: insights from analogue modelling. Solid Earth, **10**, 1283-1300, doi: 10.5194/se-10-1283-2019.

Gorini, C., Montadert, L. & Rabineau, M. 2015. New imaging of the salinity crisis: Dual Messinian lowstand megasequences recorded in the deep basin of both the eastern and western Mediterranean. Marine and Petroleum Geology, **66**, 278-294, doi: 10.1016/j.marpetgeo.2015.01.009.
Gottschalk, R.R., Anderson, A.V., Walker, J.D. & Da Silva, J.C. 2004. Modes of contractional salt tectonics in Angola Block 33, Lower Congo Basin, West Africa. *Sediment Interactions and Hydrocarbon Prospectivity, Concepts, Applications and Case Studies for the 21st Century*, SEPM, Houston, TX., 705-734.
Granado, P., Urgeles, R., Sàbat, F., Albert-Villanueva, E., Roca, E., Muñoz, J.A., Mazzuca, N. & Gambini, R. 2016. Geodynamical framework and hydrocarbon plays of a salt giant: the NW Mediterranean Basin. Petroleum Geoscience, **22**, 309-321, doi: 10.1144/petgeo2015-084.
Guieu, G.r. & Roussel, J. 1990. Arguments for the pre-rift uplift and rift propagation in the Ligurian-Provencal Basin (northwestern Mediterranean) In the light of Pyrenean Provencal Orogeny. Tectonics, **9**, 1113-1142.
Gunnell, Y., Zeyen, H. & Calvet, M. 2008a. Geophysical evidence of a missing lithospheric root beneath the Eastern Pyrenees: Consequences for post-orogenic uplift and associated geomorphic signatures. Earth and Planetary Science Letters, **276**, 302-313, doi: 10.1016/j.epsl.2008.09.031.
Holser, W.T., Clement, G.P., Jansa, L.F. & Wade, J.A., 1988. . In (ed.): . 1988. Evaporite deposits of the North Atlantic rift. *In*: Manspeizer, W. (ed.) *Triassic and Jurassic Rifting, Continental Breakup and the Origin of the Atlantic Ocean and Passive Margins, Dev. Geotecton*, 525-556.
Hudec, M.R. & Jackson, M.P.A. 2002. Structural segmentation, inversion, and salt tectonics on a passive margin: Evolution of the Inner Kwanza Basin, Angola. Bulletin of the Geological Society of America, **114**, 1222-1244.
Hughes, M. & Davison, I. 1993. Geometry and growth kinematics of salt pillows in the southern North Sea. Tectonophysics, **228**, 239-254.
Ings, S.J. & Shimeld, J.W. 2006. A new conceptual model for the structural evolution of a regional salt detachment on the northeast Scotian margin, offshore eastern Canada. American Association of Petroleum Geologists Bulletin, **90**, 1407-1423.
Jackson, M.P.A. 1995. Retrospective Salt Tectonics. *In*: Jackson, M.P.A., Roberts, D.G. & Snelson, S. (eds.) *Salt tectonics: a global perspective: AAPG Memoir*. AAPG, 1-28.
Jolivet, L., Augier, R., Robin, C., Suc, J.-P. & Rouchy, J.M. 2006. Lithospheric-scale geodynamic context of the Messinian salinity crisis. Sedimentary Geology, **188**, 9-33.
Jones, I.F. & Davison, I. 2014. Seismic imaging in and around salt bodies. Interpretation, **2**, SL1-SL20, doi: 10.1190/int-2014-0033.1.
Kidd, R., Bernoulli, D., Garrison, R.E., Fabricius, F.H. & Mélières, F. 1978. 56. LITHOLOGIC FINDINGS OF DSDP LEG 42A, MEDITERRANEAN SEA.
Leroux, E., Aslanian, D., Rabineau, M., Moulin, M., Granjeon, D., Gorini, C. & Droz, L. 2015. Sedimentary markers in the Provençal Basin (western Mediterranean): A window into deep geodynamic processes. Terra Nova, **27**, 122-129, doi: 10.1111/ter.12139.
Liro, L.M. & Coen, R. 1995. Salt Deformation History and Postsalt Strucutral Trends, Offshore Southern Gabon, West Africa. *In*: Jackson, M.P.A., Roberts, D.G. & Snelson, S. (eds.) *Salt tectonics: a global perspective: AAPG Memoir*. AAPG, 323-331.

MacDonald, C., Campbell, C., Cribb, J., Adam, J., Nedimovic, M., Louden, K. & Krezsek, C. 2008. Salt Tectonics and Basin Evolution of the North-Central Scotian Margin. *Nova Scotia Energy Forum*, Antigonish, Nova Scotia, Canada.
Maillard, A., Gaullier, V., Vendeville, B.C. & Odonne, F. 2003a. Influence of differential compaction above basement steps on salt tectonics in the Ligurian-Provencal Basin, Northwest Mediterranean. Marine and Petroleum Geology, **20**, 13-27.
Marton, L., Tari, G. & Lehmann, C. 2000. Evolution of the Angolan passive margin, West Africa, with emphasis on post-salt structural styles. Atlantic rifts and continental margins, **115**, 129–149.
Mauffret, a. & Gorini, C. 1996. Structural style and geodynamic evolution of Camargue and Western Provencal basin, southeastern France. Tectonics, **15**, 356-375, doi: 10.1029/95TC02407.
Mauffret, A., Pascal, G., Maillard, A. & Gorini, C. 1995. Tectonics and deep structure of the north-western Mediterranean Basin. Marine and Petroleum Geology, **12**, 645-666, doi: 10.1016/0264-8172(95)98090-R.
Mitchell, N.C., Ligi, M., Ferrante, V., Bonatti, E. & Rutter, E. 2010. Submarine salt flows in the central Red Sea. Geological Society of America Bulletin, **122**, 701-713, doi: 10.1130/B26518.1.
Mohriak, W.U., Nemcok, M. & Enciso, G. 2008. South Atlantic divergent margin evolution: rift-border uplift and salt tectonics in the basins of SE Brazil. *In*: Pankhurst, R.J., Trouw, R.A.J., Brito Neves, B.B. & de Wit, M.J. (eds.) *West Gondwana: Pre-Cenozoic Correlations Across the South Atlantic Region*. Geological Society, London, Special Publications, 365-398.
Montadert, L., Letouzey, J. & Mauffret, A. 1978. MESSINIAN EVENT: SEISMIC EVIDENCE. Initial reports of the deep sea drilling project 42.
Obone-Zue-Obame, E.M.M., Gaullier, V., Sage, F.F., Maillard, A., Lofi, J., Vendeville, B.C., Thinon, I. & Rehault, J.-P.P. 2011. The sedimentary markers of the Messinian salinity crisis and their relation with salt tectonics on the Provençal margin (western Mediterranean):: results from the" MAURESC" cruise. Bulletin De La Societe Geologique De France, **182**, 181-196, doi: 10.2113/gssgfbull.182.2.181.
Ohneiser, C., Florindo, F., Stocchi, P., Roberts, A.P., DeConto, R.M. & Pollard, D. 2015. Antarctic glacio-eustatic contributions to late Miocene Mediterranean desiccation and reflooding. Nature Communications, **6**, 8765, doi: 10.1038/ncomms9765.
Patruno, S., Hampson, G.J. & Jackson, C.a.L. 2015. Quantitative characterisation of deltaic and subaqueous clinoforms. Earth-Science Reviews, **142**, 79-119, doi: 10.1016/j.earscirev.2015.01.004.
Peel, F.J., Travis, C.J. & Hossack, J. 1995. Genetic Structural Provinces and Salt Tectonics of the Cenozoic Offshore U.S. Gulf of Mexico: A Preliminary Analysis. *In*: Jackson, M.P.A., Roberts, D.G. & Snelson, S. (eds.) *Salt tectonics: a global perspective: AAPG Memoir*. AAPG, 153-175.
Quirk, D.G., Schødt, N., Lassen, B., Ings, S.J., Hsu, D., Hirsch, K.K. & Von Nicolai, C. 2012. Salt tectonics on passive margins: examples from Santos, Campos and Kwanza basins. Geological Society, London, Special Publications, **363**, 207-244, doi: 10.1144/sp363.10.
Roberts, G. & Christoffersen, T. 2013. The West Mediterranean Salt Basin – A Future Petroleum Producing Province ?*. **50791**.
Rouchy, J.M. & Caruso, A. 2006. The Messinian salinity crisis in the Mediterranean basin: A reassessment of the data and an integrated scenario. Sedimentary Geology, **188â€“189**, 35-67.

Rowan, M.G., Peel, F.J. & Vendeville, B.C. 2004a. Gravity-driven fold belts on passive margins. *In*: McClay, K.R. (ed.) *Thrust tectonics and hydrocarbon systems*. AAPG Memoir, 157-182.
Rowan, M.G., Trudgill, B.D. & Fiduk, J.C. 2000. Deepwater, salt-cored fold belts: lessons from the Mississippi Fan and Perdido fold belts, northern Gulf of Mexico. *In*: Mohriak, W. & Talwani, M. (eds.) *Atlantic rifts and continental margins*. American Geophysical Union, Washington, DC, United States, 173-191.
Schuster, D.C. 1995. Deformation of Allochthonous Salt and Evolution of Related Salt-Structural. *In*: Jackson, M.P.A., Roberts, D.G. & Snelson, S. (eds.) *Salt tectonics: a global perspective: AAPG Memoir*. AAPG, 177-198.
Seni, S.J. 1992. Evolution of salt structures during burial of salt sheets on the slope, northern Gulf of Mexico. Marine and Petroleum Geology, **9**, 452-468.
Storetvedt, K.M. 1973. Genesis of West Mediterranean basins. Earth and Planetary Science Letters., **21**, 22-28, doi: 10.1016/0012-821X(73)90221-5.
Talbot, C.J. 1993. Spreading of salt structures in the Gulf of Mexico. Tectonophysics, **228**, 151-166.
Tari, G., Molnar, J. & Ashton, P. 2003a. Examples of salt tectonics from West Africa: a comparative approach. Geological Society, London, Special Publications, **207**, 85-104, doi: 10.1144/gsl.sp.2003.207.01.05.
Vendeville, B. 2005. Salt tectonics driven by sediment progradation: Part I--Mechanics and kinematics. AAPG Bulletin, **89**, 1071-1079.
Vendeville, B.C. & Nilsen, K.T. 1995. Episodic growth of salt diapirs driven by horizontal shortening. *In*: Travis, C.J., Harrison, H., Hudec, M.R., Vendeville, B.C., Peel, F.J. & Perkins, B.F. (eds.) *Salt, Sediment and Hydrocarbons.* Gulf Coast Section Society of Exploration Paleontologists and Mineralogists Foundation 16th Annual Research Conference, 285-295.
Warren, J.K. 2010. Evaporites through time: Tectonic, climatic and eustatic controls in marine and nonmarine deposits. Earth-Science Reviews, **98**, 217-268.
Weijermars, R., Jackson, M. & Vendeville, B. 1993. Rheological and tectonic modeling of salt provinces.
Worrall, D.M. & Snelson, S. 1989. Evolution of the northern Gulf of Mexico, with emphasis on Cenozoic growth faulting and the role of salt. *In*: Bally, A. & Palmer, A. (eds.) *The Geology of North America-An Overview*. Geological Society of America, Boulder, Colorado, 97-138.
Wu, S., Bally, A.W. & Cramez, C. 1990. Allochthonous salt, structure and stratigraphy of the north-eastern Gulf of Mexico. Part II: Structure. Marine and Petroleum Geology, **7**, 334-340.

D. Manuscript 2

Document type: Manuscript submitted for publication to the Journal of Marine and Petroleum Geology.

Authors: Mianaekere Victoria, Adam Jürgen

No of words: 9000

No of pages: 41

'Halo-kinematic' sequence stratigraphic analysis adjacent to salt diapirs in the deepwater contractional province, Liguro-Provencal Basin, Western Mediterranean.

[1*]V. Mianaekere; [2] J. Adam

[1]Earth Sciences department, Royal Holloway university of London

[2]Earth Sciences department, Royal Holloway university of London

**Corresponding author: victoria.mianaekere.2014@live.rhul.ac.uk,*

Key points

- The kinematic evolution of salt structures in the combined halokinetic-contractional province is analysed from preserved seismic stratal patterns in successive genetic depocenters adjacent to salt diapirs.
- The classifications of the minibasin stratigraphic fill are re-defined in this study as pre-kinematic layer or layered sequence, pre-diapiric and halo-kinematic sequence packages.
- Unique stratal patterns; layered sequence (Ls), onlap wedge sequence (Ow), truncated hook sequence (Thk) and truncated onlap wedge sequence (T-Ow) directly infer kinematic growth phases of salt growth.

Abstract

This study investigates the coupled halokinetic and depositional processes of the contractional diapiric-minibasin province in the distal deepwater Liguro-Provencal basin. The Liguro-Provencal basin is situated above young oceanic crust developed during the NW-SE Miocene rifting and back-arc extension. Messinian evaporites succession was deposited contemporaneously on extended continental crust and young oceanic crust. Post-rift isostatic adjustments of the continental shelves influenced prograding sedimentary wedges, gravitational failure and gravity-driven deformation, hence extensive salt diapirism is situated a contractional domain in the deep basin overlying oceanic crust. The kinematic evolution of salt structures in the combined halokinetic-contractional province is analysed from preserved seismic stratal patterns in successive genetic depocenters adjacent to salt diapirs. Within minibasin successions, four dominant seismic stratal patterns have been classified as a layered, truncated-onlap wedge, onlap-wedge and truncated-hook. The truncated-onlap wedge sequences are early syn-kinematic depositional packages contemporaneous to salt growth and may converge towards the rising salt structure prior to diapirism. They are therefore categorised as the pre-diapiric sequence. The onlap wedge and truncated hook styles form later syn-kinematic packages in diapiric growth phase and are labelled as halo-kinematic sequences. The layered sequence, maybe pre-kinematic and show parallel beds all truncating on the diapir flank. This onlap wedge consists of on-lapping beds at the basal sequence boundary, stratal thinning or convergence towards the diapir flank and angular truncations on an erosional surface on the top depositional boundary proximal to the diapir flank. The truncated-hook sequence reflects an absence of beds on-lapping on the diapir roof within the sequence, beds truncate at diapir flank and on an erosional/slip surface on top depositional boundary proximal to diapir flank. Truncated-onlap

wedge sequence reflects on-lapping beds in the middle of the sequence and older and younger beds that truncate on the top depositional boundary.

Keywords: halokinetic-contractional salt tectonics, halo-kinematic sequences

1. Introduction

This study analyses the halokinetic processes in the contractional diapiric domain of the Liguro-Provencal deepwater basin overlying Miocene oceanic crust. The NW Mediterranean Cenozoic sedimentary basins the North Balearic and Provencal basins, developed during the NW-SE Miocene rifting and back-arc extension. Back-arc extension and rotation of the Balearic block along the Spanish continental margin segment ceased in the Miocene (Carminati et al. 2004; Carminati et al. 2012; Storetvedt 1973), along the French continental margin segment subduction roll back and back-arc extension was continuing due to rotation of the Corsica-Sardinia block which led to the emplacement of oceanic crust in the Miocene (21-16 Ma) (Maillard et al. 2003) (Fig. 1). In the West-Mediterranean back-arc basins the Messinian evaporites consisting of gypsum, halite and gypsum succession (Droz et al. 2006) were deposited contemporaneously on extended continental crust and young oceanic crust (Fig. 1). Post-rift isostatic adjustments of the continental shelves influenced prograding sedimentary wedges, gravitational failure and gravity-driven deformation, hence extensive salt diapirism is situated a contractional domain in the deep basin overlying oceanic crust (Mianaekere and Adam In review-a).

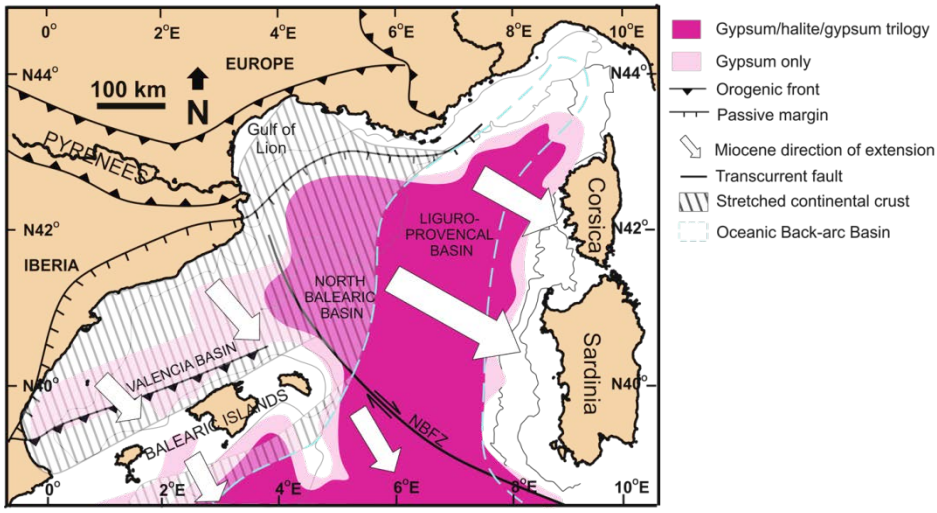

Fig. 1: Tectonic and salt distribution map of the West Mediterranean passive margin system modified from (Droz et al. 2006), Miocene rifting and consequent formation of the North Balearic and Liguro-Provencal Basins from slab roll back of the Corsica (Co), Sardinia (Sa) and Calabria (Ca) (Gunnell et al 2008), (Maillard et al 2003)

The contractional diapiric domain in the deepwater Messinian salt basin forms the distal kinematic domain of a gravity-driven thin-skinned salt-detached extensional-contractional system (Mianaekere and Adam In review-a). In this study we analyse in detail the syn-kinematic local halokinetic depositional systems in the deepwater minibasin province by the detailed mapping of salt structures and seismic-stratal analysis of minibasin depositional sequences in the deepwater diapiric province. This enabled the analysis of kinematic phases and stages of salt growth. Additionally, the analysis of stratal patterns in syn-kinematic depositional sequences provides insights into the temporal local halokinetic processes and controls. Our study builds on the current halokinetic sequence stratigraphic and megaflap concepts (Callot et al. 2016; Giles and Rowan 2012; Schultz-Ela 2003) which were originally developed for the analysis of local-scale salt-sediment interactions based on characteristic structural geometries formed close to passive salt diapirs (Fig. 2), (see section 1.1).

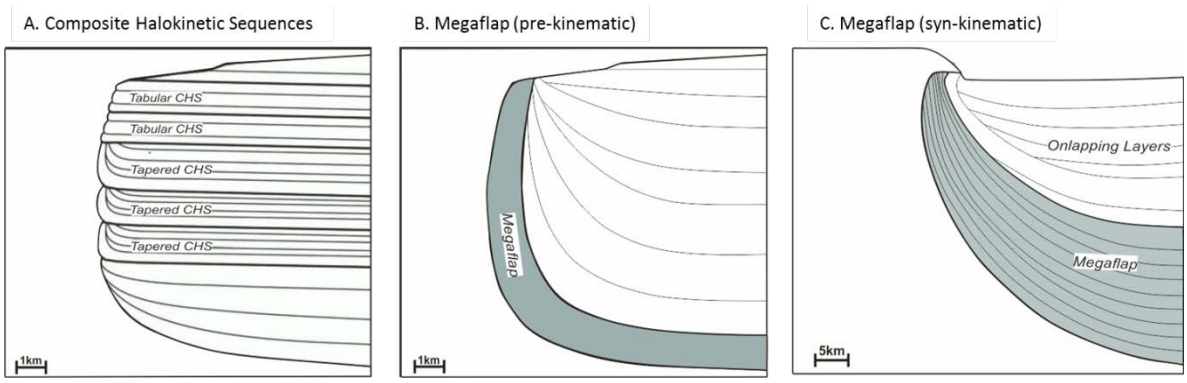

Fig. 2: Structural geometries of genetic halokinetic sequence packages critical for understanding diapir evolution. A. Stacked Composite Halokinetic Sequences defined by differences in shape and geometry of drape folds adjacent to passive diapirs (Giles & Rowan 2012, Rowan et al. 2016). B. Megaflap (Pre-kinematic), defined by several kilometre-wide fold and structural relief (Rowan et al. 2016). C. Megaflap (syn-kinematic), defined by upturn of thick formerly concordant roof sediments of salt structures with onlap of younger downbuilding sediments (Nikolinakou et al. 2017)

We aim to identify and classify characteristic internal stratal seismic patterns within genetically related salt-controlled depocenters that record all kinematic phases of salt diapir growth i.e. seismic patterns within active early syn-kinematic depocenters in comparison to C. in (Fig. 1) and seismic patterns within depocenters formed in passive salt growth phase in comparison to A. in (Fig. 1). Unique seismic stratigraphic patterns are classified as pre-kinematic, pre-diapiric and diapiric stages. Sedimentary wheeler diagrams are used to demonstrate local temporal diapir proximal processes that result in the genetic seismic-stratal patterns and depositional sequences adjacent to salt structures. We infer relative rates between local sedimentation and multi-stage diapir growth in the contractional domain. Correlation of regional depositional sequence interpretations and the minibasin depositional sequences supports a better correlation between local and regional drivers of salt tectonic processes in the Messinian salt basins of the Western Mediterranean. To further build on methods of interpretation of evolution of salt growth and intervening minibasins, subsequent study integrates structural

concepts of megaflaps and Composite Halokinetic Sequences with concepts of genetic seismic stratal patterns developed in this study on a minibasin scale.

Diapir proximal studies

Halokinetic Sequences (HKS) interpreted at flanks of salt diapirs suggest initiation of passive diapirism or continued passive diapirism controlled by sediment aggradation rates (Giles and Rowan 2012; Jackson and Hudec 2011). The top and basal boundaries of a HKS consist of unconformable erosional surfaces proximal to diapirs. The erosional surfaces known as halokinetic boundaries are influenced by relative rates of sedimentation and salt growth (Giles and Lawton 2002b; Giles and Rowan 2012; Jackson and Hudec 2011). The degree of angular unconformity formed at halokinetic boundaries are classified as 'hook' also known as 'tabular' Composite Halokinetic Sequences which represents a period of high salt rise rate relative to sedimentation or as 'wedge' also known as 'tapered' Composite Halokinetic Sequences which represents a period of high sedimentation rate relative to salt rise (Fig. 1) (Andrie et al. 2012; Giles and Lawton 2002b; Giles et al. 2004).

Significant rotational upturn of early syn-kinematic packages are currently assigned as basal megaflap (Nikolinakou et al. 2017; Rowan et al. 2016a). They may be observed as small scale flap folds to steep stratal fold panels concordant to diapir flank (Rowan et al. 2016). The basal megaflap has been said to originate from active kinematic growth phase of an amplified salt swell or anticline (Jackson and Hudec 2017). In order words, they form the pre-diapiric stratigraphic layers addressed in this study. The rotated flap has been observed at minibasin flanks, on-lapped by younger syn-kinematic layers. Hence the amount of upturn may be

proportional in timescales to the sedimentary layers cut-off from the salt structure by the upturned flap (Hearon IV et al. 2014; Rowan et al. 2016a).

The minibasin stratigraphic classifications employed in this study stem from much early studies of active/passive salt kinematic salt rise and pre/syn/post minibasin stratigraphic layers that constitute sedimentation geometries that make up the widely accepted classifications of conforming (salt controlled) stratal packages that infer the timing of salt growth, further discussed in methods (see section 2.2.2).

2. Dataset & Methods

Dataset

Regional 2D Kirchhoff pre-stack time migrated seismic data provided by TGS was used in this study. The diapir–minibasin seismic profiles analysed in section 4, details a 5s record length from sea bed to base salt. (Fig. 3) shows locations of the study strike and dip seismic profiles of bathymetric salt structures in the early contraction domain hosting dominantly shortened and tilted salt stocks. The interpreted salt structural domains and salt structural styles were analysed in precedent study (Mianaekere and Adam In review-a) and re-iterated in section 3 of this study.

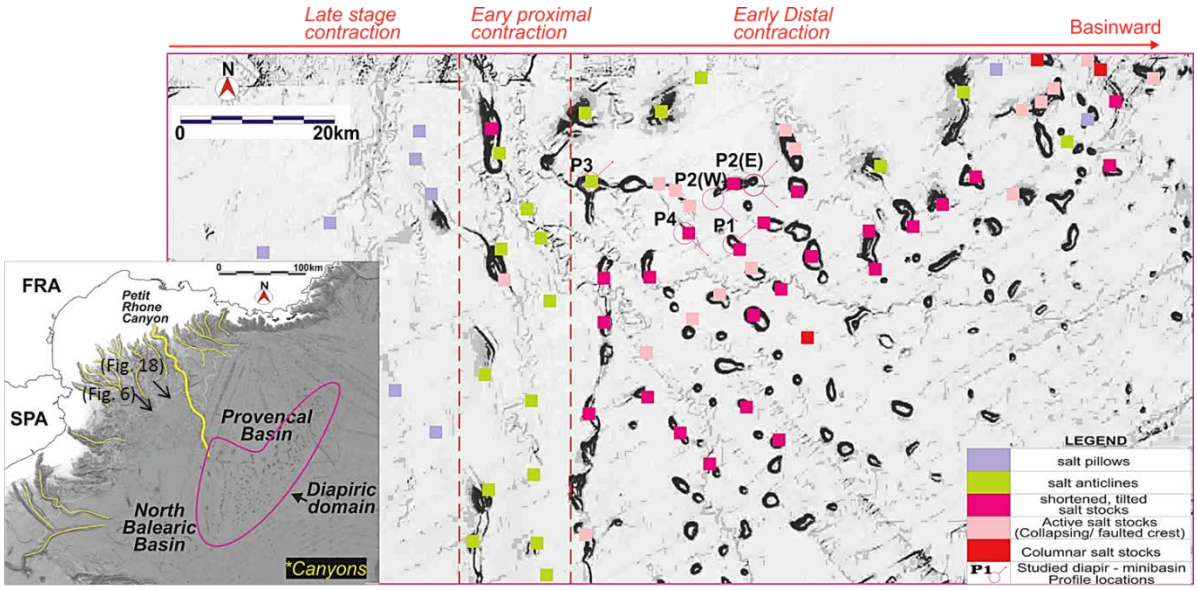

Fig. 3: Bathymetric map of the Western Mediterranean reproduced from the GEBCO showing sedimentary pathways and diapiric domain.

Method

Minibasin sequence-stratigraphic analysis & definition of terminology

The new minibasin sequence-stratigraphic classifications developed in this study builds on previously published classification schemes of active and passive kinematic phases of salt growth (Hudec et al. 2009a) (Fig. 4). The classifications of the minibasin stratigraphic fill into early stage active, late stage active and passive stage diapirism (Alsop et al. 2016) based on the kinematic phases of diapir evolution, are logically re-defined in this study as *pre-kinematic layer or layered sequence*, *pre-diapiric* and *halo-kinematic* sequence packages discussed below (Fig. 4), (Table 1).

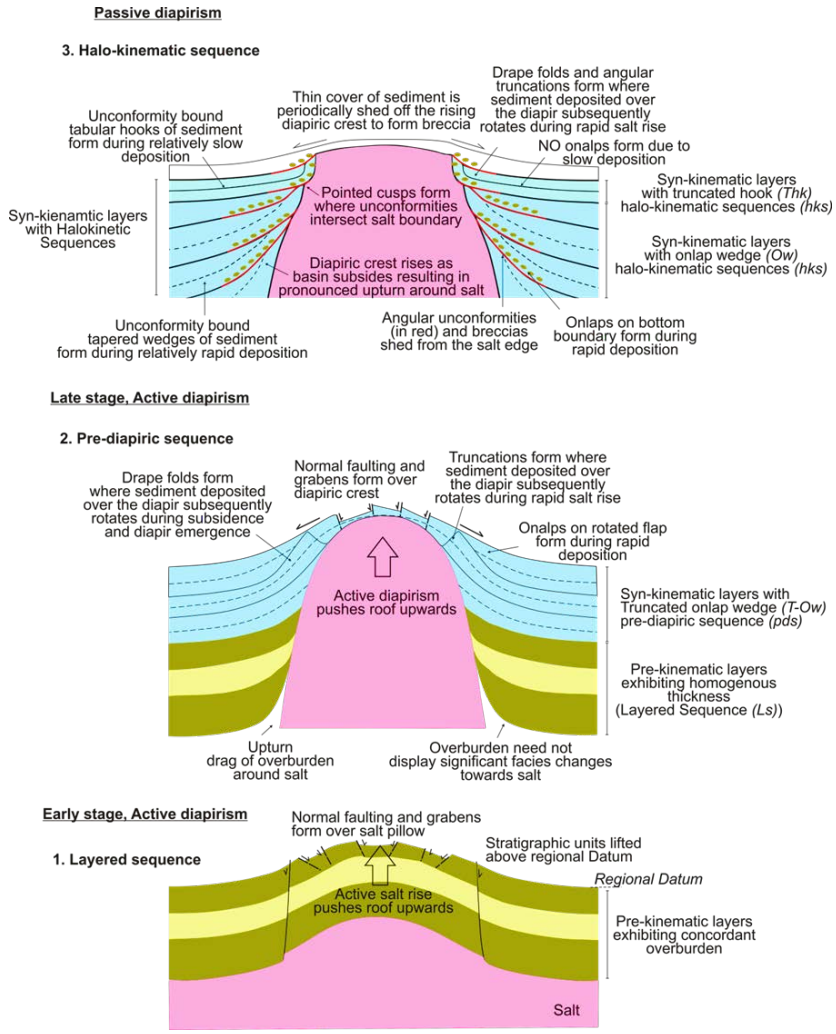

Fig. 4: Schematic cartoons showing anatomical features of active and passive diapirism (modified from Alsop et al. 2016). Note depositional patterns of pre-kinematic layers, pre-diapiric sequence and halo-kinematic sequence.

Salt kinematic growth phase	Stratigraphic Sequence (This study)	Abv.	Minibasin stratigraphic fill pattern (This study)	Abv.	Minibasin evolution phase	Minibasin stratigraphic fill pattern recognition
1. Early stage active phase	Layered sequence	*pkl, Ls*	Layered	*Ls*	Pre-kinematic	Parallel beds, lateral homogenous thickness
2. Late stage active phase	Pre-diapiric sequence	*pds*	Truncated onlap wedge	*T-Ow*	Early syn-kinematic	Drape folded strata on-lapped by early syn-kinematic ponded sediments
3. Passive phase	Halo-kinematic sequence	*hks*	1. Onlap wedge 2. Truncated hook	1. *Ow* 2. *Thk*	Late syn-kinematic	1. Ponded sediments onlap on lower stratigraphic boundary, convergent strata, angular truncation on upper stratigraphic boundary. 2. No ponded sediments in stratigraphic layer, angular truncations on upper stratigraphic boundary

Table 1: Clarification of terminology

The early stage active salt kinematic growth phase initiates from active piercement of the pre-kinematic concordant overburden. Hence minibasin stratigraphic fills exhibiting parallel seismic patterns with lateral homogeneous thickness are designated the pre-kinematic layer *pkl*, layered sequence *Ls*. The late stage active phase initiates from active piercement of early syn-kinematic stratigraphic overburden. Early syn-kinematic strata exhibit drape folding concordant to diapir flank that are consequent to diapir emergence and subsequently on-lapped by ponded sediments that are consequent to an increase in minibasin subsidence. The early syn-kinematic strata are therefore defined as the pre-diapiric sequence *pds*.

Syn-kinematic layers in this study are classified and labelled based on the presence or absence of onlapping beds and their location within any of the unconformity bound seismic-stratigraphic sequence adjacent to salt diapirs, the early syn-kinematic strata with lower boundary beds up-turned and truncated proximal to diapir edge and on-lapping beds within the sequence strata are labelled as Truncated on-lap wedge *T-Ow,* pre-diapiric sequence.

Later syn-kinematic layers that form in diapiric phase i.e. in discordant relationship with diapir flank are defined as halo-kinematic sequences *hks*. Halo-kinematic Sequences (*hks* in Fig. 4*)* located in the flanks of salt diapirs indicate initiation of passive diapirism or continued passive diapirism controlled by sediment aggradation and down-building of the minibasin sediments (Giles and Lawton 2002b; Giles and Rowan 2012; Jackson and Hudec 2011). A halo-kinematic sequence *hks* may truncate directly on diapir flank or maybe cut-off from diapir by older rotated flap folds. A halo-kinematic sequence *hks* boundary is delineated at top stratigraphic surface from angular truncations and at bottom surface from onlaps proximal to diapirs. The halo-kinematic sequence with onlaps on lower halo-kinematic boundary is labelled as onlap wedge *Ow* (hks). Halo-kinematic sequence with an absence of onlaps within the strata is labelled as truncated hook *Thk* (hks).

In summary, pre kinematic layers deposited on a mostly stationary and stable salt layer exhibit parallel layering with no apparent thickness changes related to salt growth (Jackson and Hudec 2017), hence the pre kinematic layer(s) in this study is described and labeled as layered sequences (Fig. 4). On the other hand, syn-kinematic layers exhibit sub-parallel to angular layers accumulated during salt-withdrawal and adjacent salt growth. In the minibasin depositional succession, the truncated onlap wedge sequence forms the earliest syn-kinematic layer directly overlying the pre-kinematic layered sequence. While either of the end-members, onlap-wedge and truncated-hook sequence form the younger successive layer(s) and are classified as halo-kinematic sequences.

Detailed seismic–stratigraphic analyses have been carried out on diapirs and their adjacent minibasins in the deepwater diapir province on strike and dip seismic sections (Fig. 3).

Interpretation of uncertainties close to salt diapirs due to seismic imaging limitations as a result of steeply dipping flanks, salt forms and complex geology (Jones and Davison 2014; Ratcliff et al. 1992; Rojo et al. 2016) were considered in detailed seismic interpretations.

Sedimentary Wheeler diagrams

Minibasin halo-kinematic sequences have been delineated from the character of the sequence-bounding unconformities and their internal sedimentation patterns and have been classified using the halo-kinematic classifications scheme discussed in Chapter 2.2.1. The local depositional processes controlling the formation of the minibasin halo-kinematic sequences are visualised by sedimentary Wheeler diagrams. The Wheeler diagram is a 2D representation of the interpreted geo-seismic section with relative geological time as the vertical axis and space in meters as the horizontal axis (Wheeler 1958). Each geological stratum in the cross section is plotted at a relative geological time and extrapolated horizontally according to its measured line length on the interpreted geo-seismic section. Stratal thicknesses on the wheeler diagrams are diagrammatic representations obtained from the two-way-time geo-sections. With relative geological time as the vertical axis, the stratal thicknesses and inclinations of surfaces demonstrate relative timescales or rates of deposition to rates of associated salt rise (Mianaekere and Adam In review-a).

3. Regional salt tectonic overview

Tectono-stratigraphy, Sequence stratigraphy

Tectono-stratigraphy in the Western Mediterranean include the early Oligocene to Aquitanian synrift megasequence deposited in asymmetric rift grabens located beneath the modern

continental margins (Bache et al. 2015; Leroux et al. 2015b) (Fig. 5) and the late Aquitanian to Holocene postrift megasequence (Roberts and Christoffersen 2013) consisting of thick laterally continuous strata beneath and above the regional Messinian unconformity related to the Messinian Salinity Crisis; a prominent erosional surface traceable throughout the Western and Eastern Mediterranean basins (Bache et al. 2015; Driussi et al. 2015; Gorini et al. 2015).

The postrift megasequence has been subdivided in six sequence stratigraphic units Sq-1 to Sq-6 (further discussed in section 5), constrained by high amplitude, laterally continuous seismic marker horizons with clear frequency attributes. Geodynamics of the pre Messinian stratigraphy marks the onset of tectonic quiescence and the early onset of thermal subsidence. Geodynamics of post Messinian stratigraphy includes continued thermal subsidence of the distal deepwater basin relative to the continental shelf margin and regional salt tectonics. Therefore basin-wide sequence-stratigraphic correlation is carried out especially for post-salt sub-sequence units in other to support the analysis of the impact of regional sedimentary events and basin isostatic adjustments on the post-Messinian salt tectonics.

Sequence stratigraphic boundaries include Unconformities recognized by angular terminations or canyon incisions in the shelf and traced as correlative conformities *cc* in the slope and basin plain, Maximum Regressive Surfaces *MRS* are traced from the shelf margin interpreted below a back-stepping shelf edge trajectory and Maximum Flooding Surfaces *MFS* interpreted below a positive (aggrading or prograding) shelf edge trajectory.

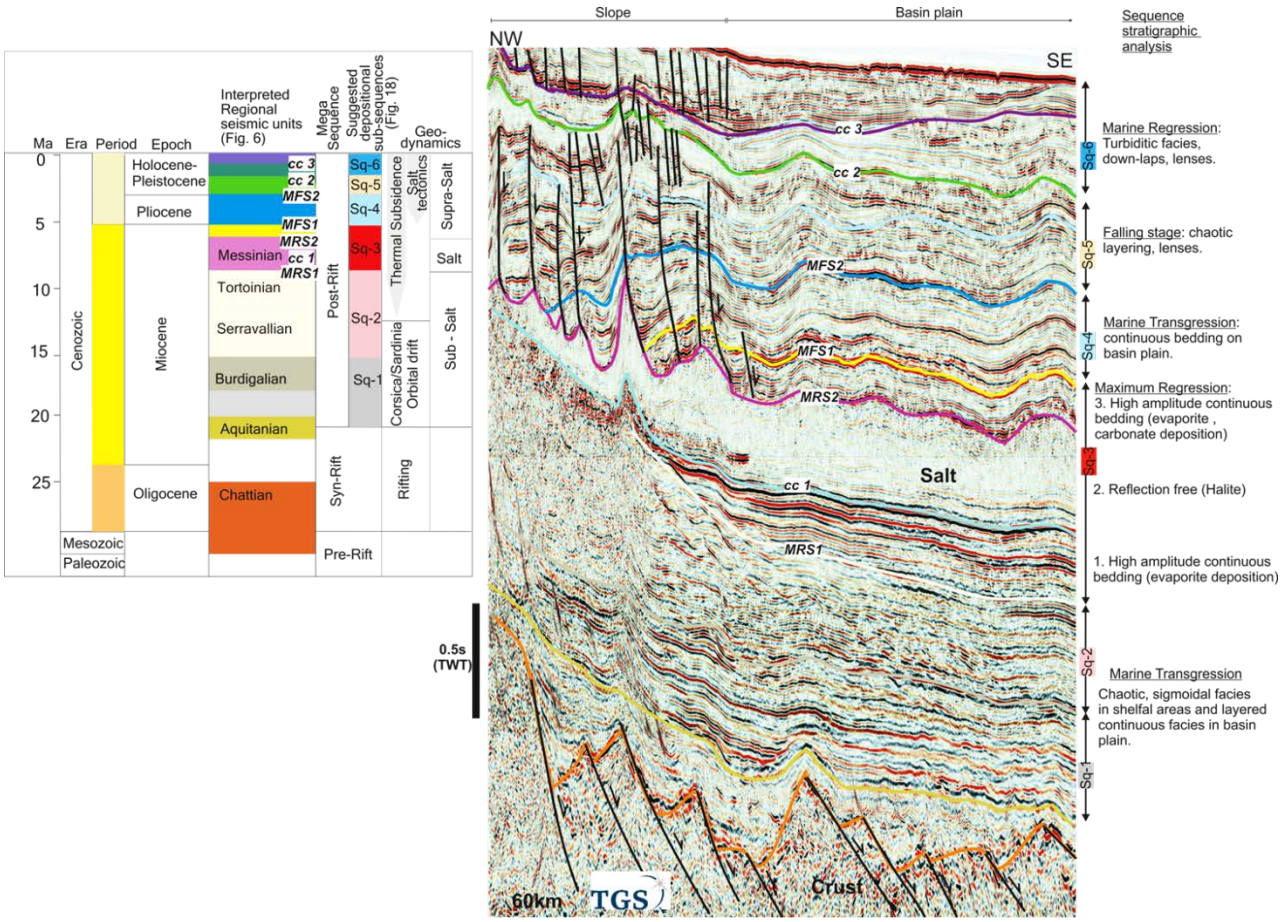

Fig. 5: Sequence stratigraphic interpretation of the Gulf of Lion

Early post-rift mid-Miocene sequence stratigraphic units Sq-1, Sq-2 consist at large of chaotic to sigmoidal facies in shelfal areas and layered continuous, uniform facies in the basin plain indicating a period of marine transgression. Sq-3 marks a period of the Messinian marine regression and consists of lower and upper evaporitic layers and reflection free mega halite in the middle (Bourillot et al. 2010; Butler et al. 1999; Rouchy and Caruso 2006). The lower evaporitic layer shows on-lapping terminations on the bottom sequence boundary *MRS1*, is conformable in the basin plain and unconformable in paleo slope with base of halite *cc1* and Messinian unconformity. The top of halite seismic horizon is interpreted as a Maximum

Regressive Surface *MRS2*. Top of halite horizons are high amplitude reflectors and frequently show overlying progradational down-lapping terminations and underlying truncations on salt welds in the paleo shelf. Overlying the halite are strong reflectors evaporite and carbonate high amplitude, continuous band of reflectors related to waning of the Marine regression and delineated at the top by a Maximum Flooding Surface *MFS1*. Overlying Pliocene depositional sequence unit Sq-4 is controlled by major sea level transgression and is widely deposited on the paleo basin plain. Sq-4 exhibits parallel to sub-parallel high amplitude reflectors and large growth strata down-lapping on salt and salt welds on continental slope. The marine transgression sequence unit Sq-4 most likely contain hemipelagics given relative thicknesses, timescales and depositional environment. Sq-4 terminates at a Maximum Flooding Surface MFS2 and marks a transition to a sequence unit Sq-5 consisting of chaotic, discontinuous facies and lenses related to a Falling Stage Stand. Sq-6 consists largely of chaotic, turbiditic facies owing to a marine regressive phase. Seismic marker horizons cc2, cc3 are correlative conformities within Sq-6 traced from incised sub-aerial stratigraphic boundaries in the shelf (see regional section, Fig. 6) and are characterized by its high amplitude attribute with apparent down-laps in the slope margin. (Granado et al. 2016; Roberts and Christoffersen 2013)

Regional salt tectonics

The regional salt tectonic style of the Western Mediterranean passive margin was analysed in precedent study (Mianaekere and Adam In review-a). Salt tectonics evolved from a gravitational salt system with an up-dip extensional domain and a down-dip combined contractional-halokinetic minibasin domain (Fig. 6)

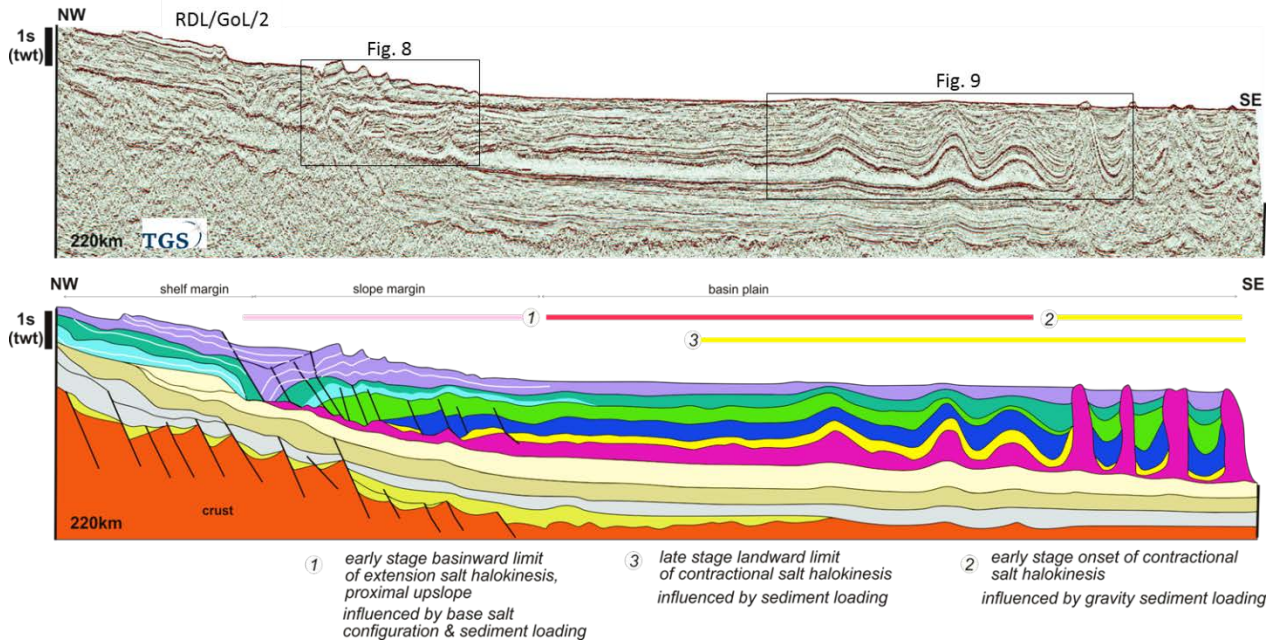

Fig. 6: Un-interpreted 2-Dimensional PSTM seismic dip line along Gulf of Lion-Provencal Basin (Location shown in Fig. 3), Landmark colour bar is SEG Normal. Interpreted section (bottom) shows regional salt tectonic styles, lateral extents of salt kinematic segmentations and pre-salt sedimentary and structural configurations.

Thin-skinned gravity deformation in the West Mediterranean is driven by margin tilt and sediment loading in shelf and slope and high gravity sedimentation in basin plain. Basinward translation of salt and overburden sediment overtime resulted in a characteristic kinematic segmentation with landward extensional limit of salt halokinesis, intermediate transitional domain and a landward migration over time of the contractional province. Present day salt structural segmentations show a contractional province with progradational salt displacement and emplacement in overburden as pillows, anticlines, and stocks. The contractional domain is located in the deepwater transect between the North Balearic and Liguro-Provencal Basins (Fig. 7). The overall regional salt structural styles NW of the Gulf of Lion, NW of the Valencia Trough and EW of the Balearic Promontory have been described in detail by (Mianaekere and Adam In

review-a) (see seismic lines in Fig. 7). Regional controls to the salt tectonic evolution and salt structural domains in the West Mediterranean is summarised below.

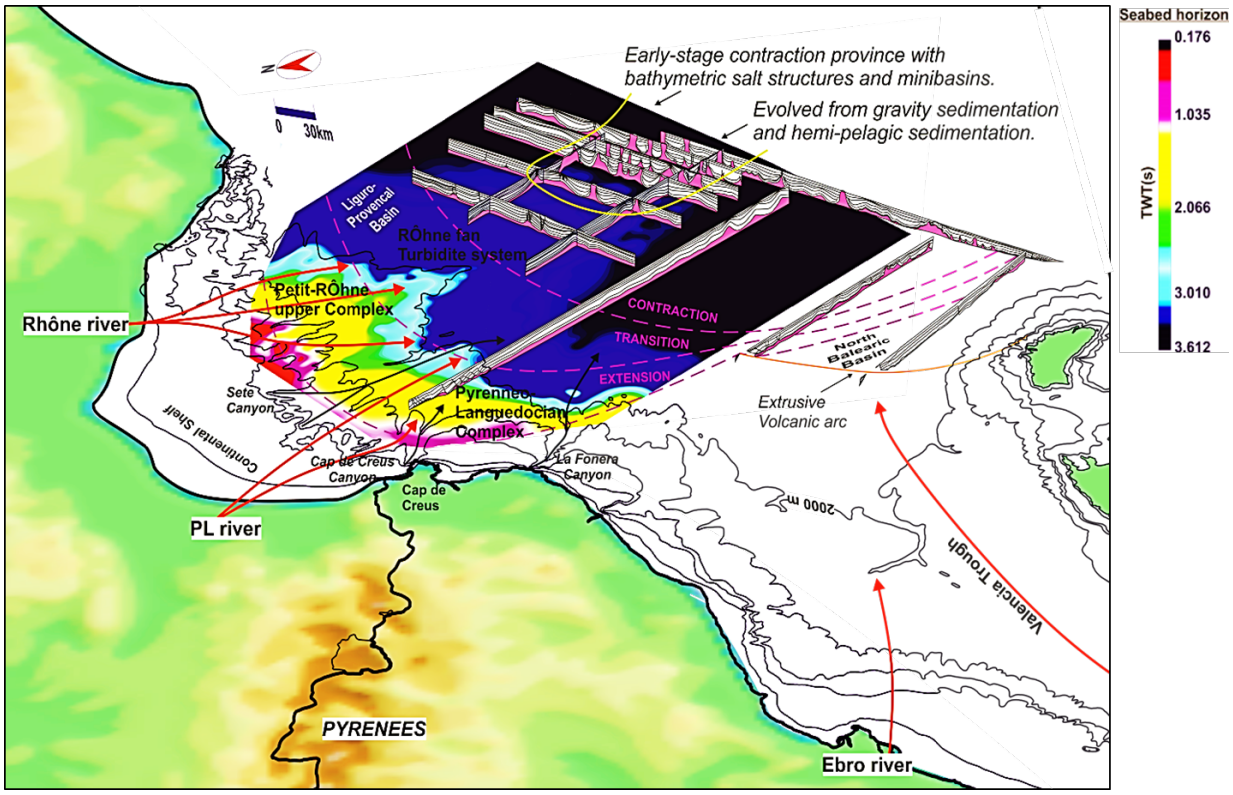

Fig. 7: Regional salt kinematic segmentation in the West Mediterranean. (Mianaekere and Adam In review-a)

1. NE-SW salt tectonics parallel to the Gulf of Lion margin is sustained by gentle margin tilt ca. 1^{o} and high sediment loading, mainly the Pyreneo-Languedocian complex (Whipple 2004) and Petit-Rhone upper complex constrained to the proximal continental margin resulting in a well-developed several 10's km wide up-dip extensional domain beneath the continental slope and a basinward progradational sedimentation from the Rhone fan and turbidite system resulting in

an undeformed transitional segment at the base of slope and a down-dip contractional segment in the central deepwater basin plain.

2. NNW-SSE salt tectonics parallel to the Balearic promontory is sustained by a steep margin slope and high rates of continued sedimentation resulting in a less than 10 km wide landward extensional segment beneath the steep slope is accompanied in basinward direction by a narrow transitional domain (< 20 km width) leading towards and a wide contractional domain in the central basin plain.

3. NNW-SSE salt tectonics parallel to the Valencia Trough, a narrow landward extensional domain on the basinward side of the volcanic arc leads in basinward direction to mildly deformed transitional domain in the distal basin plain.

The salt tectonic trends NE-SW of the Gulf of Lion, NNW-SSE of the Valencia Trough and NNW-SSE of the Balearic Promontory converges in a common contractional province in the deepwater Liguro-Provencal Basin (Fig. 7).

4. Halo-kinematic sequence-stratigraphic analysis

Depocenters and internal geometries associated with extensional salt structures

Apparent stratal patterns in depocenters associated with the extensional salt structures prominent in the landward extensional domains were created by salt evacuation and down-dip translation and extension of the overburden sequences (Fig. 8). The extensional structural styles are controlled by varying slope angles and base-of-salt geometries in the proximal shelf-slope margin and distal slope and relate to characteristic stratal pattern in syn-kinematic depocenters.

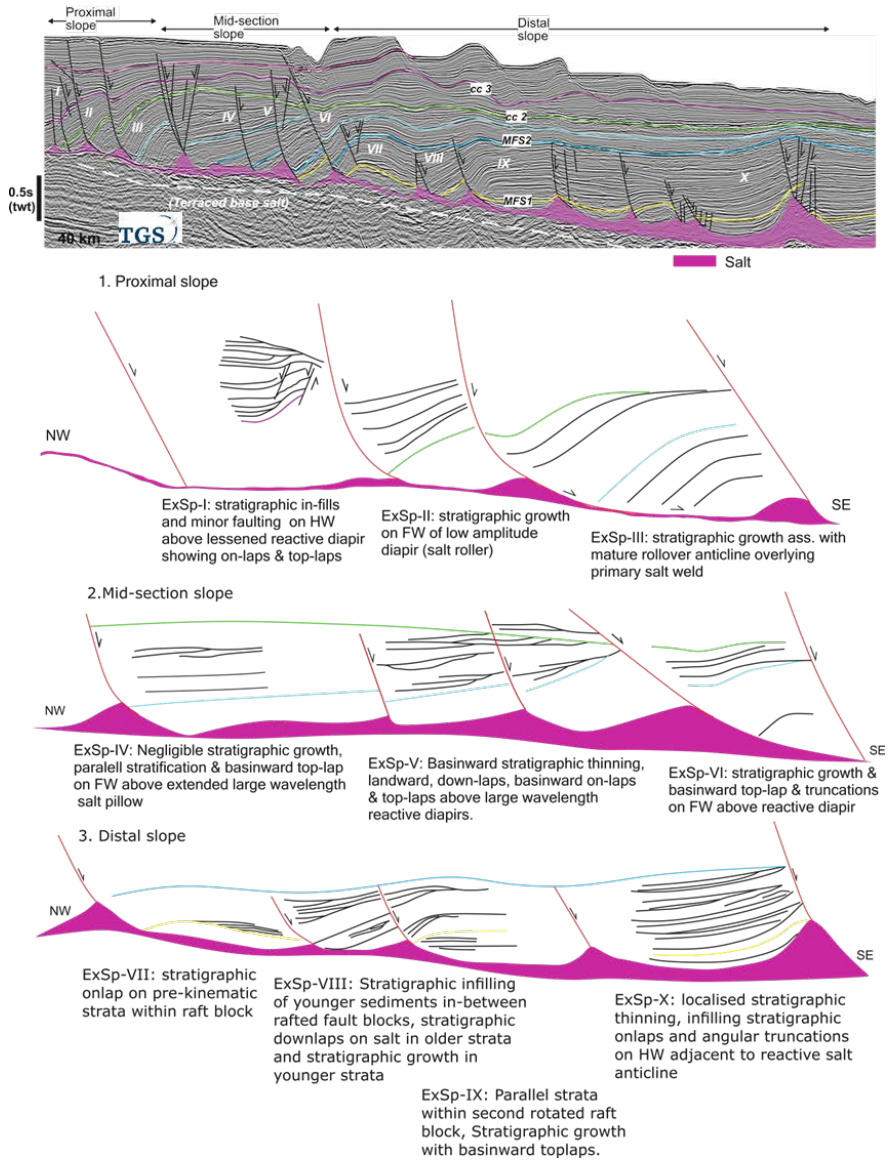

Fig. 8: Stratal geometries in landward extensional kinematic domain in the Gulf of Lion slope margin. Salt structural and depocentre styles are interpreted in dip NW-SE directions, sub-divided into proximal slope, mid-section slope and distal slope having varying slope angles. Note: (ExSp – Extensional sedimentation patterns).

The proximal slope displays listric growth fault rollovers with underlying low-amplitude asymmetric reactive diapirs (salt rollers). In the segments with a flat base of salt, the depocenters in the hanging-wall of extensional faults show basinward onlap and toplap infills

(ExSp-I) above lessened reactive diapir, whereas the depocenter on more steeply basinward sloping base-of-salt segments are characterized by stratal growth patterns with significant growth towards the listric faults (ExSp-II). Also in the proximal slope, associated with high-extension listric faults steeply dipping growth strata (ExSp-III) can be seen near the base of mature rollover anticlines overlying primary salt welds.

Flat-base salt segments in the mid-slope are characterized by normal faults with variable geometries that detach on a thicker primary salt layer. Related depocenters are characterized by basal parallel strata and subsequent basinward toplap geometries with negligible stratigraphic growth (ExSp-IV). Further basinward, reactive diapirs overlying inclined base-of-salt segments are related to depocenters with basinward stratigraphic thinning, landward downlap, basinward onlap and toplap (ExSp-V) terminating on asymmetric reactive diapirs. Rollover anticlines related to shallow dipping normal faults above medium-amplitude reactive diapirs above inclined base-of-salt segments show extensive stratigraphic growth, basinward toplap and truncations (ExSp-VI).

In the distal slope, high amount of extension is documented by rotated rafted fault blocks. Here, synkinematic strata show onlap geometries on basal pre-kinematic strata within the raft block (ExSp-VII), parallel strata within pre-kinematic strata and stratigraphic growth with basinward top-laps in a second raft block (ExSp-IX) can be observed. Stratigraphic infilling of younger sediments in between raft blocks show stratigraphic downlaps on older strata and stratigraphic growth in younger strata (ExSp-VIII). The toe of slope is marked by a salt-cored anticline (or high-relief reactive diapir) in the transition to the zone of the undeformed horizontal salt layer in the basin plain. Synclinal depocenter in the hanging wall show stratigraphic onlap, toplap and

localized thinning towards fault (ExSp-X). Overall, in the extensional regime, fill styles in synkinematic depocenters most certainly dominated by salt withdrawal and basinward transport on the salt detachment rather than being controlled by local depositional processes.

Internal geometries in contractional depocenters

Salt structures localised in the contractional domain vary in structural zones, i.e. in the early contraction further basinward in the distal basin plain and in the late contraction (refer to section 3) each with characteristic depocenter styles. In the late contraction province, sparsely distributed salt pillows with varying amplitudes are shown in 'dip' NW-SE seismic section (Fig. 9). Localised in the early contraction province is salt anticlines, buried passive or active diapirs i.e. collapsing or faulted crests salt stocks and dominantly shortened i.e. necked, thinned or tilted salt stocks shown in strike SW-NE seismic section (Fig. 10). The synkinematic depocenters in the contractional structural domains show characteristic stratal patterns associated with the varied salt structural styles which document variable local-scale salt flow with salt withdrawal beneath synkinematic depocenters adjacent to vertical salt flow in active and contractional diapirs.

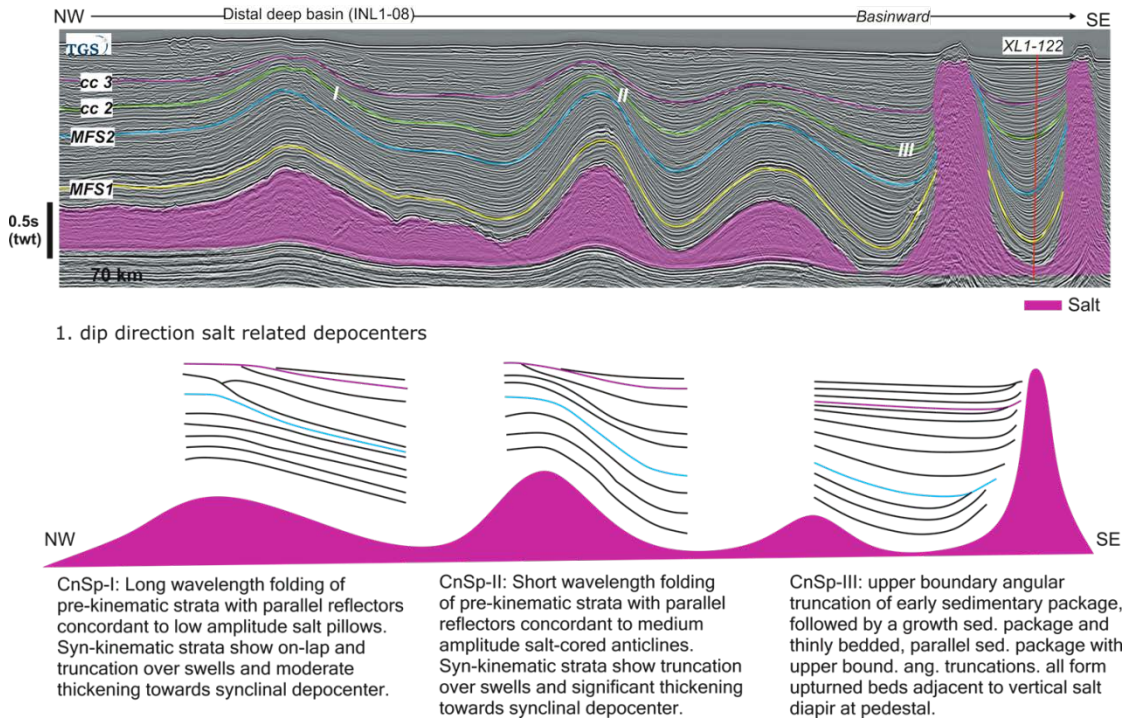

Fig. 9: Contractional sedimentation patterns in the late contraction domain on basin plain, Provencal Basin. Salt structural and depocentre styles in dip NW-SE directions. (CnSp - contractional sedimentation pattern)

In NW-SE direction (Fig. 9), the landward late-stage contractional structural zone is characterised by salt pillows with thick Messinian to Early Pliocene pre-kinematic strata and Late Pliocene to recent synkinematic strata. These depocenters developed typical stratal pattern related to the dominant wavelength and amplitude of contractional salt structures. Low-amplitude salt pillows caused large-wavelength folding of concordant pre-kinematic strata with parallel reflectors whereas synkinematic strata show onlap and truncation over swells and moderate thickening towards synclinal depocenter (CnSp-I). Medium-amplitude salt-cored anticlines are accompanied by short-wavelength folding of concordant pre-kinematic strata and synkinematic strata characterised by truncation over swells and significant thickening towards synclinal depocenter (CnSp-II). It is notable that in asymmetrical depocenters the dominant

stratigraphic growth can be observed on the basinward side of pillows and anticlines. The basinward transition from the early-stage to late-stage contractional structural zone is marked by a tall ca. 3km salt diapir. The landward NW side of the diapir depocenter shows progradational synkinematic growth wedges, basal depocenter sequences show narrowly spaced parallel reflectors with top boundary angular truncations near the diapir flank (CnSp-III).

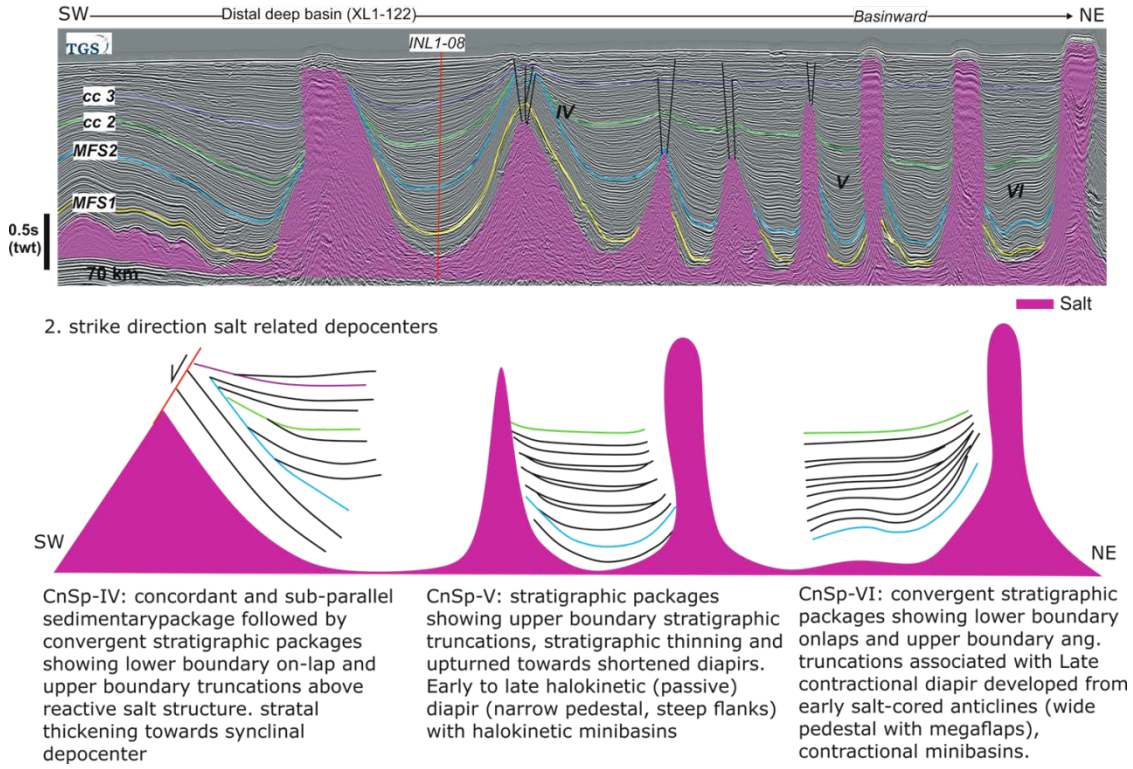

Fig. 10: Contractional sedimentation patterns in the early contraction domain in the distal basin plain, Provencal Basin. Salt structural and depocentre styles in strike SW-NE directions. (CnSp- contractional sedimentation pattern)

In SW-NE direction (Fig. 10), synkinematic depocenters related to early-stage salt-cored anticlines show basal depositional sequences with convergent stratal patterns above salt anticlines whereas younger synkinematic strata show upper surface truncations above the anticlines and stratal thickening towards the synclinal depocenters (CnSp-IV). Halokinetic U-

shaped minibasins formed between early to late halokinetic (passive) diapirs (narrow pedestal, steep flanks) and show stratal pattern with upper boundary truncations, thinning and upturn near the flank (CnSP-V). Contractional minibasins formed between late contractional diapirs that developed from early salt-cored anticlines (wide pedestal with megaflaps) and are characterised by convergent stratal pattern with lower boundary onlaps and upper boundary truncations, basal strata concordant to pedestals forming upturned flap fold (CnSP-VI).

Diapiric/ contractional domain

In the deepwater Provencal Basin, salt displacement and emplacement vertically as stocks in the overburden in present day consists of 2km to 3km tall bathymetric diapirs [see Leroux et al (2015), Maillard et al (2003), Mianaekere and Adam (In review)]. Hence the diapiric domain is easily traced from bathymetric relief map (Fig. 11, C). The generated isochron (Fig. 11, B) and bathymetric maps show density, shapes and regional trends of bathymetric salt structures.

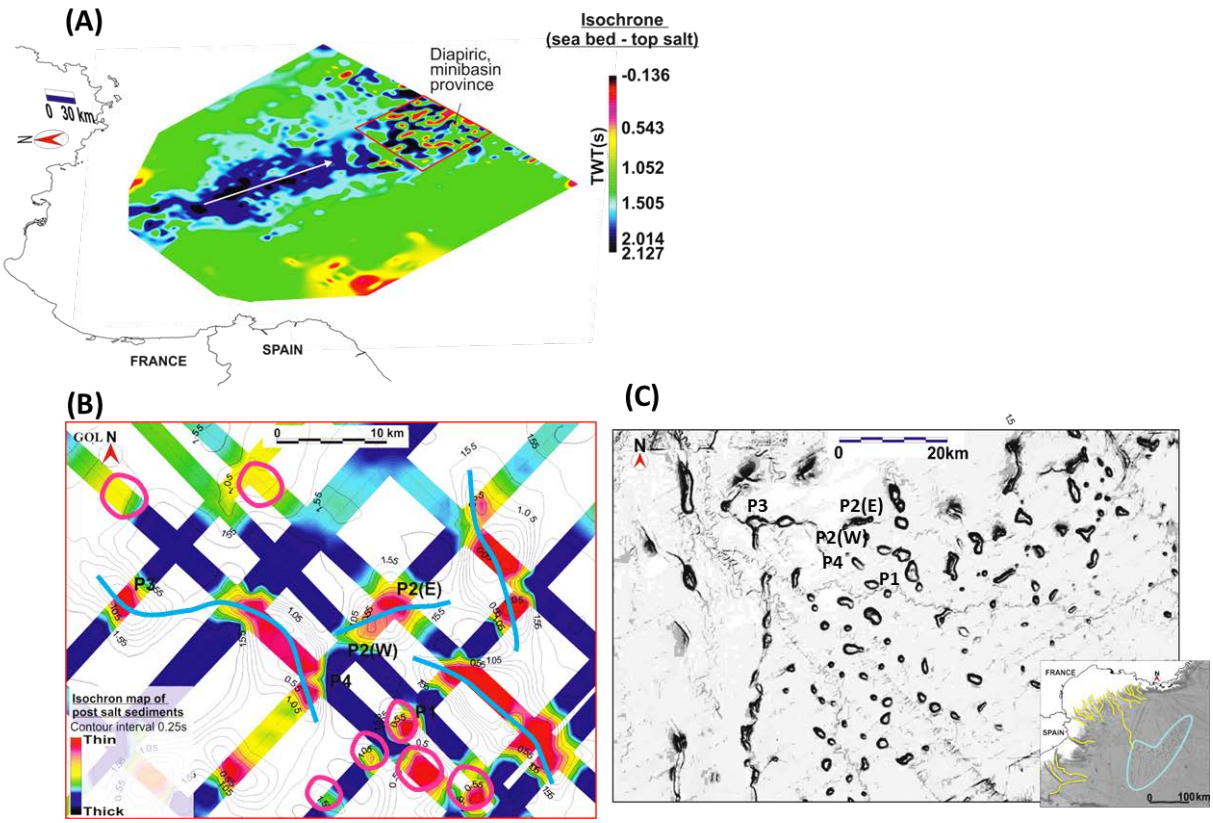

Fig. 11: (A) Interpolated Isochron map of post-salt sediments derived from 2D seismic survey. (B) The derived grid reflects an inverse distance of 1km from data control points and the contour overlay is computed with a flex grid interpolation algorithm, white polygonal areas are low confidence areas. Suggested salt stocks (pink circles) and salt walls (blue lines) backed by bathymetric map in C. (C) Bathymetric map showing bathymetric salt diapirs and walls in the deep basin.

An interpolated isochron map of post-salt sediments (Fig. 11, A) derived from 2D whole seismic survey shows concentration of thickest post salt sediments and minibasin fill in the distal deepwater, contraction province. The grid of the diapiric domain (Fig. 11, B) reflects an inverse distance of 1km from data control points hence white polygonal areas are low confidence areas. The contour overlay is computed with a flex grid interpolation algorithm. Extracted trends from

flex grid contour overlay corroborated with bathymetric map (Fig. 11, C) show interpreted salt stocks, trends and connectivity of salt peaks/salt walls in the contractional province.

Sedimentation patterns in contractional-halokinetic minibasins; comparison to halokinetic sequence stratigraphy

The seismic stratigraphic sequences of minibasins in the diapiric domain of the deepwater basin can be subdivided into pre-kinematic, pre-diapiric (early/older syn-kinematic) and halo-kinematic (younger syn-kinematic) sequences, with respect to internal seismic-stratigraphic patterns (refer to section 2.2.1). The detailed analysis of the stratal patterns within successive minibasin depositional sequences has been conducted for three local strike seismic sections P1 (Fig. 12), P2(E) (Fig. 13) and P3 (Fig. 14) stretching from diapir to minibasin centers. Note, strike seismic sections parallel to the NW-SE gravity sediment loading from the Gulf of Lion (refer to section sections 3.2, 4.3) are used given minibasin fills may better represent a regional sediment sink.

1. Profile P1 (Fig.12) is located in the most distal position in the contractional diapir domain and shows a 2 km long diapir - minibasin center seismic profile with a contractional (necked) diapir with hourglass geometry and bathymetric expression.
2. Profile P2 (E) (Fig. 13) shows a 3 km long diapir - minibasin center profile with a flat-topped diapir with wide pedestal and moderately inclined flanks.
3. Profile P3 (Fig. 14) is located in the most proximal position in the contractional diapir domain and shows a 3 km long diapir - minibasin center seismic profile with a diapir with wide pedestal and a narrow top and moderately inclined flanks.

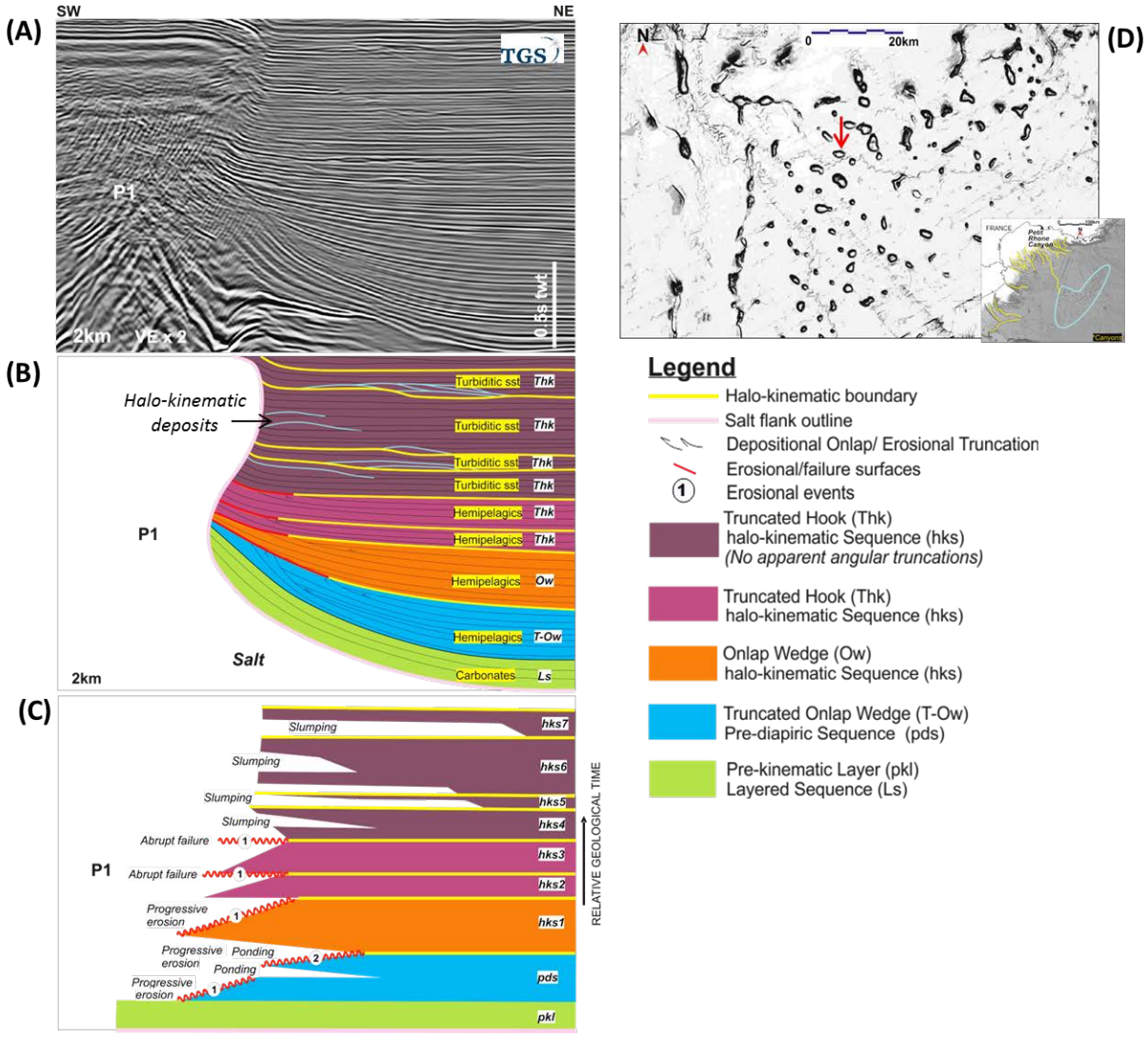

Fig. 12: Diapir-minibasin profile P1. (A) Un-interpreted seismic section (B) Interpreted stratal geometries and minibasin sequences (C) Sedimentary wheeler diagram (D) Bathymetric map and location of diapir P1.

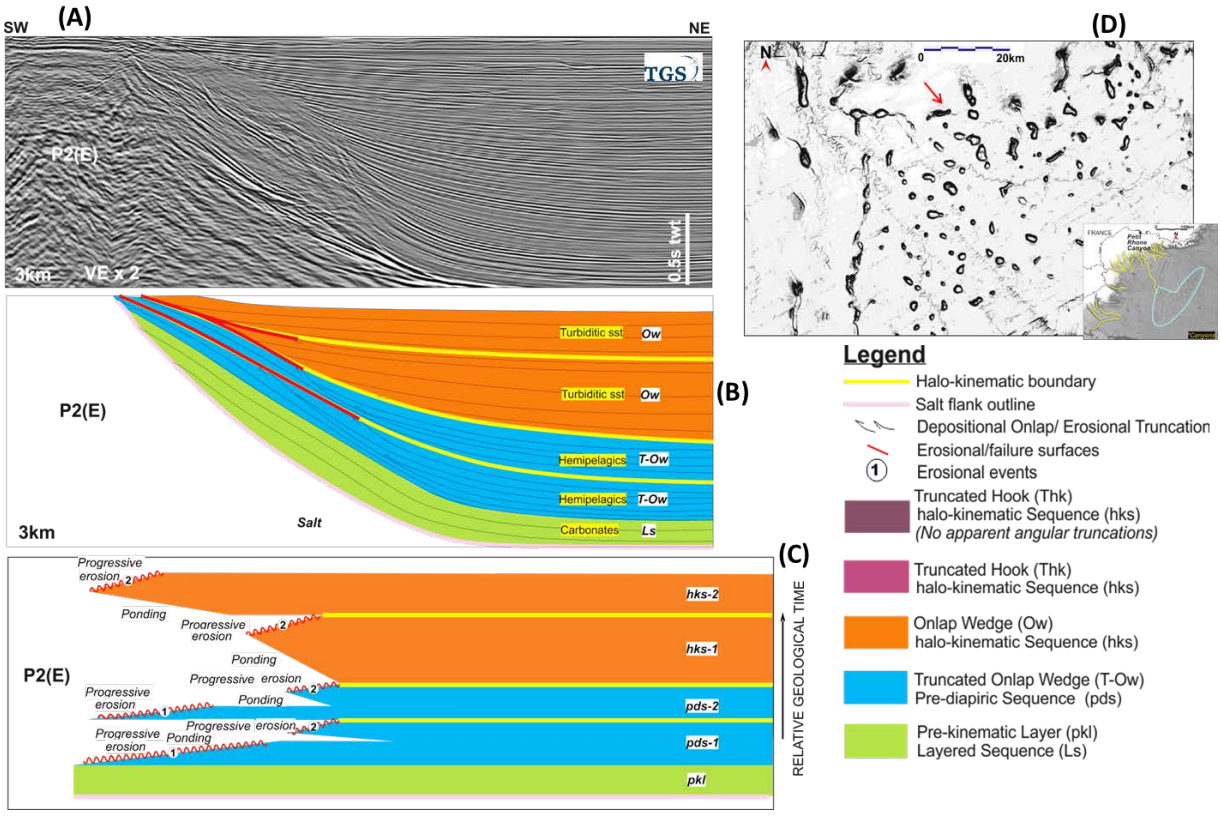

Fig. 13: Diapir-minibasin profile P2(E). (A) Un-interpreted seismic section (B) Interpreted stratal geometries and minibasin sequences (C) Sedimentary wheeler diagram (D) Bathymetric map and location of diapir P2(E).

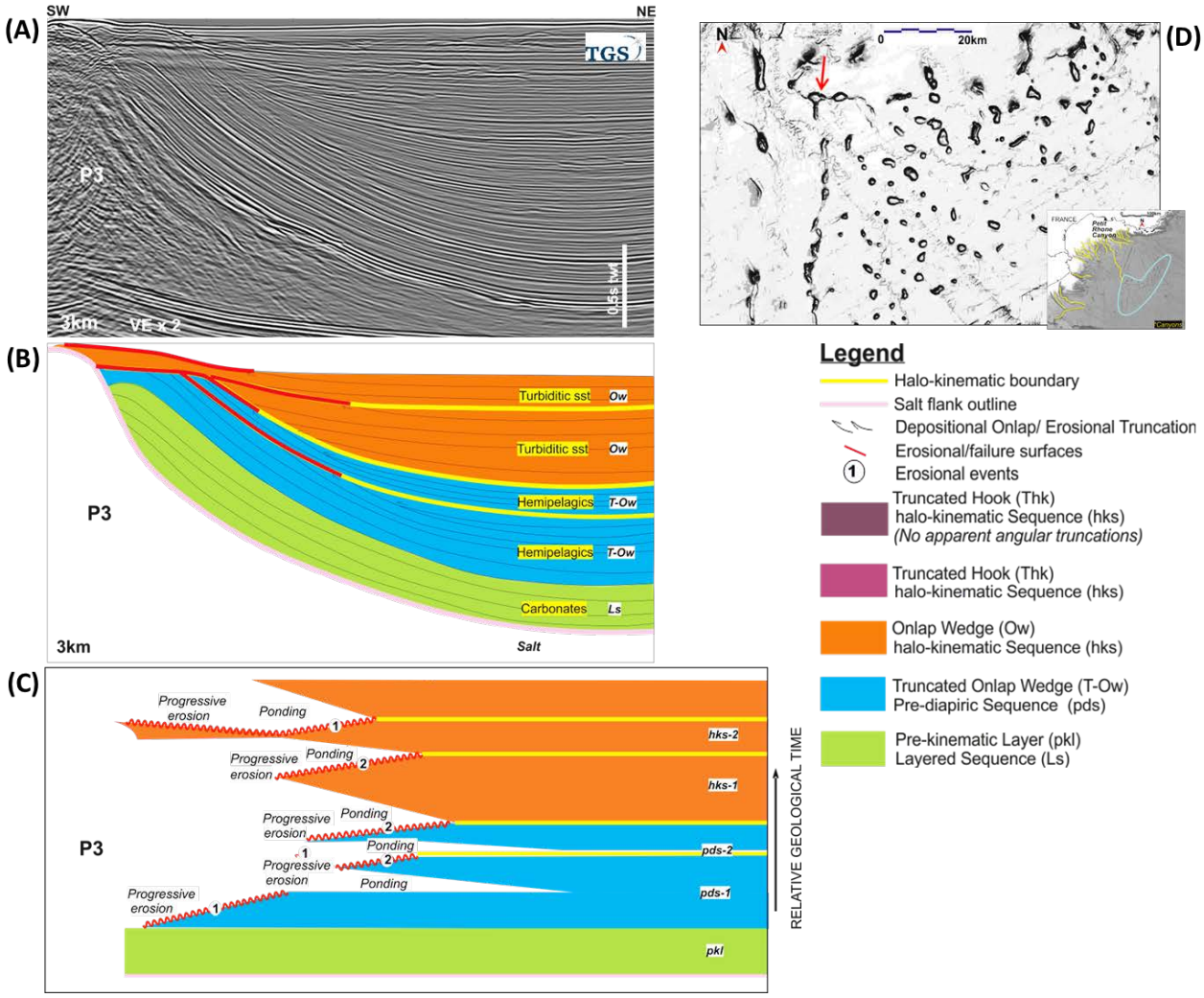

Fig. 14: Diapir-minibasin profile P3. (A) Un-interpreted seismic section (B) Interpreted stratal geometries and minibasin sequences (C) Sedimentary wheeler diagram (D) Bathymetric map and location of diapir P3.

The minibasin in profile P1 (Fig. 12) is completely welded, whereas the minibasins in P2(E) (Fig. 13) and P3 (Fig. 14) are only partly welded. Four types of halo-kinematic sequences can be identified in all three seismic profiles P1, P2(E) and P3.

1. *Layered sequences (Ls)* are characteristic for the pre-kinematic depositional units and have all beds truncating at the diapir flank with no onlaps or top boundary angular truncations.

2. *Truncated-onlap wedge sequences (T-Ow)* are typical in syn-kinematic, pre-diapiric sequences and show onlapping beds in the middle of the sequence, while overlying and underlying beds within the stratal unit are truncated by an erosional surface proximal to the diapir flank. This halokinetic sequence style exhibits two (*could be more in other analogues*) progressive erosional event surfaces separated by a period of sediment ponding in minibasin centers.
3. *Onlap wedge sequences (Ow)* are present in synkinematic, syn-diapiric sequences and show onlapping bottom boundaries. Younger beds show stratigraphic thinning towards the diapir flank and truncations of the top surface by an erosional surface proximal to the diapir flank. A period of ponding and subsequent progressive erosion of depositional sequences complete the halokinetic sequence.
4. *Truncated hook sequence (Thk)* form part of the synkinematic, syn-diapiric sequences and are characterized by an absence of onlap geometries in the sequence. Older units show truncated top surfaces at diapir flanks and younger beds are truncated by an erosional or slump surface proximal to diapir flank.

Overall in this study, the truncated onlap wedge and onlap wedge sequences consist of thick stratal units. The progressive erosive surfaces of the truncated onlap wedge and onlap wedge depicted in the wheeler diagrams suggest longer depositional periods and relative high ratios of sedimentation to salt rise. Truncated hook sequence with thinner stratal units and flat erosive surfaces suggest shorter depositional periods during stages of high diapir growth rates.

Profile P1 shows a minibasin succession where all halo-kinematic sequences show discordant contacts and truncations towards the diapir flanks. The minibasin succession consists of a layered pre-kinematic sequence, a truncated onlap wedge pre-diapiric sequence, a unconformity-bound onlap wedge halo-kinematic sequence and two unconformity-bound truncated hook halo-kinematic sequences. Erosional surfaces at halo-kinematic sequence boundaries can be identified in ca. 200 - 300m wide zones near the diapir flank [see also Giles and Rowan (2012)]. Younger halo-kinematic sequences with no apparent angular truncations are interpreted from accumulations of lobe-like deposits suggested to be slump deposits or debris flows triggered during diapir rise. Timing of weld formation is interpreted from the onset of syn-kinematic sequences with no apparent angular unconformities. Profile P2(E) shows a minibasin succession of a layered pre-kinematic layer, two truncated-onlap wedge pre-diapiric sequences and two unconformity bound onlap wedge halo-kinematic sequences. Erosional surfaces on halo-kinematic sequence boundaries extend ca. 1km away from diapir flanks (see also Giles and Rowan, 2012). Pre-kinematic and pre-diapiric sequences are rotated on diapir pedestals. The rotated pre-diapiric sequences separate the younger syn-kinematic sequences from the diapir flanks. Profile P3 shows a minibasin succession of a layered pre-kinematic sequence, two truncated-onlap wedge pre-diapiric sequences and two unconformity-bound onlap wedge halo-kinematic sequences. Like P2(E), erosional surfaces of the halo-kinematic sequence boundaries extend ca. 1km away from diapir flanks. The pre-kinematic sequence and pre-diapiric sequences are rotated and dragged (Schultz-Ela 2003) to the diapir edge. Pre-diapiric sequences separate younger discordant syn-kinematic sequences from the diapir flanks.

Comparison of seismic stratigraphic patterns in alternate facing diapir flanks

An arbitrary seismic section (Fig. 15) compares stratal geometries and sequence stacking in alternate facing flanks for diapir profile P2(E) in strike-dip directions with respect to the Gulf of Lion margin. Observed contrast in the dip profile is a stacking of onlap wedge and truncated hook sequences and in strike profile onlap wedge kinematic sequences only.

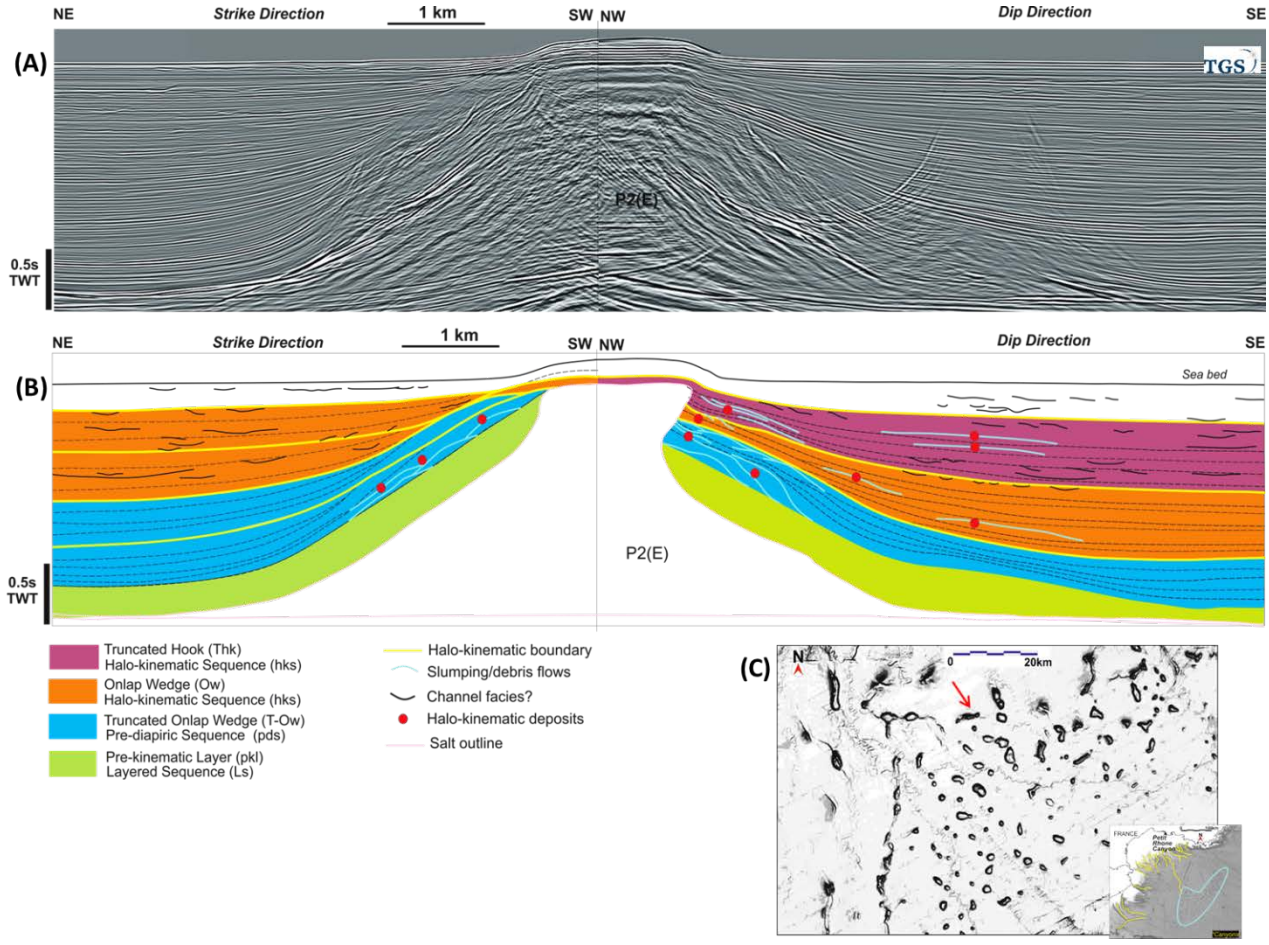

Fig. 15: Diapir-minibasin profile P2(E) in strike SW-NE and dip NW-SE directions (. (A) Un-interpreted seismic section (B) Interpreted stratigraphic sedimentation patterns and minibasin sequences (C) Bathymetric map and location of diapir P3.

Also in the dip direction, slump deposits/debris flows and lobe-like deposits interpreted as amalgamated sand sheets or minibasin floor fans by (Rowan and Weimer 1998) are used as proxies for interpretation of minibasin sequence boundaries in dip profile section. The lobe-like bodies above the boundaries most likely are redistributed sediments eroded from diapir edge. Prominent in the strike profile and in contrast to the dip profile is an abundance of channelized facies observed in onlap wedge sequences with an absence of kinematic redistributed lobes.

Overall, the dip section profile with truncated hook sequences shows dominant sedimentary successions with re-distributed kinematic deposits in comparison to the strike section profile with onlap wedge sequences. Salt controlled minibasins from the Sivas Basin, Turkey (Ribes et al. 2015a), hosts channelized sand bodies in minibasin sequences with stratal geometries comparable to onlap wedge sequences in this study and in contrast, sequences with stratal geometries comparable to truncated hook sequences show no evidence of lateral facies change and apparent conformity in minibasin centre. Furthermore, since regional and local processes interact differently on alternate facing flanks of an evolving diapir, preserved stratal patterns and structural styles are usually different around diapirs or salt walls. The alternate facing flanks may in tandem recreate the structural evolution of the salt diapir and best analysed on a 3D dataset.

5. Discussion

Seismic analogue of minibasin sequences

The diapir-minibasin profile P2(W) (Fig. 16) oriented NW-SE in dip direction to the Gulf of Lion margin shows a buried salt anticline with an analogue of preserved early stage formation of pre-

diapiric sequences within depocentre on basinward side of the profile section. Note that diapir profiles P2(W) and P2(E) analysed in section 4.3 are different points along the same salt wall.

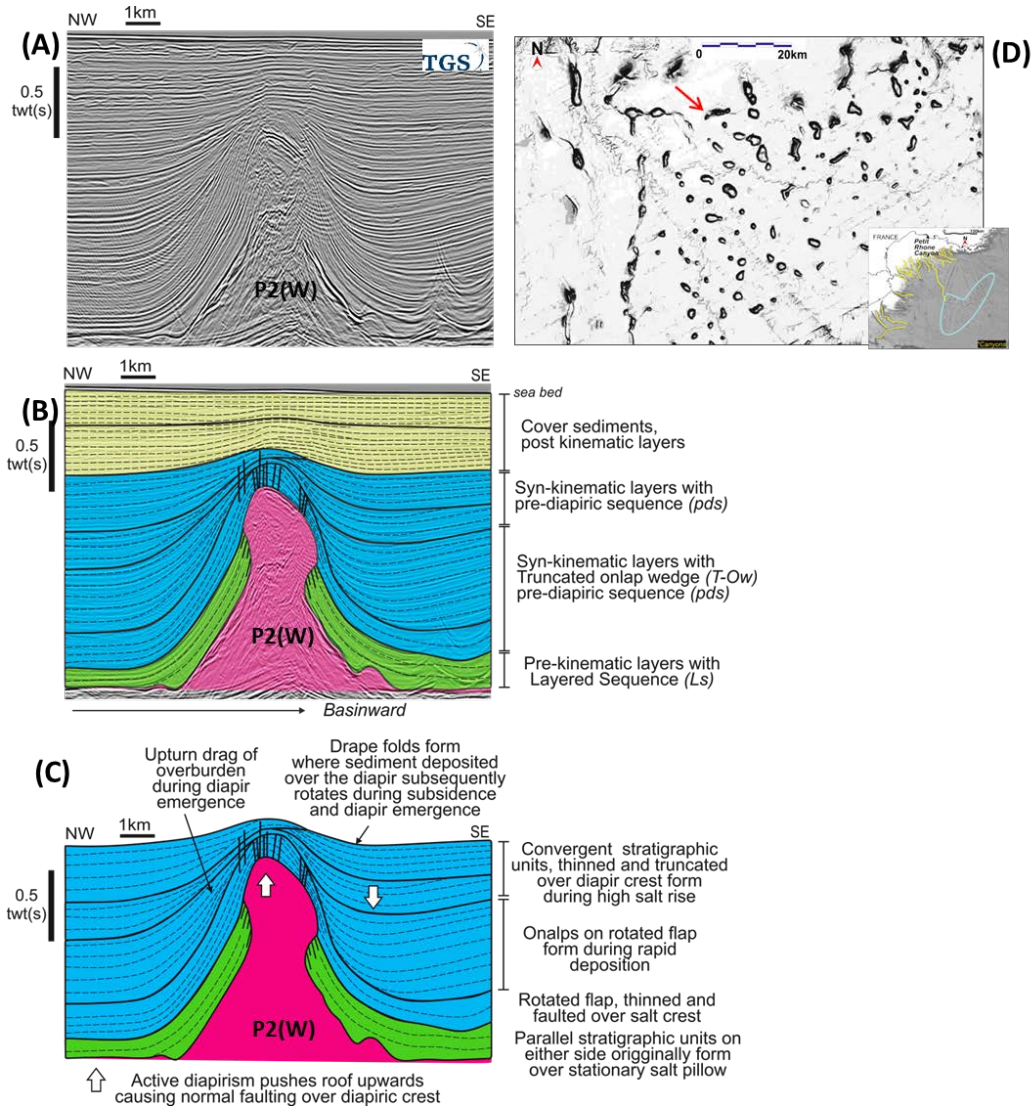

Fig. 16: P2(W) diapir-depocentre profile showing a diapir buried in early kinematic growth phase.

1. Salt anticline P2(W) exhibits drag strata in depocenter on landward side and subsidence strata in depocenter on basinward side.

2. On either side of P2(W), basal discordant stratigraphic unit with parallel sedimentation pattern form the pre-kinematic layer originally from concordant overburden above stationary salt pillow.
3. Basal stratigraphic pre-diapiric sequence formed from initial active salt rise, drag folded and faulted over salt anticline show thinning on basinward side of salt crest and subsequent onlaps from syn-kinematic deposition.
4. Syn-diapiric units formed during continued active salt rise show convergent sedimentation patterns towards salt anticline, apparent thinning and faulting over salt crest.
5. Thick post-kinematic roof sediments bury salt anticline.

The diapir-minibasin profile P4 (Fig. 17) oriented NW-SE in dip direction to the Gulf of Lion margin shows a passive diapir with adjacent minibasin sequences, pre-kinematic layer, pre-diapiric sequence and halo-kinematic sequences on basinward side.

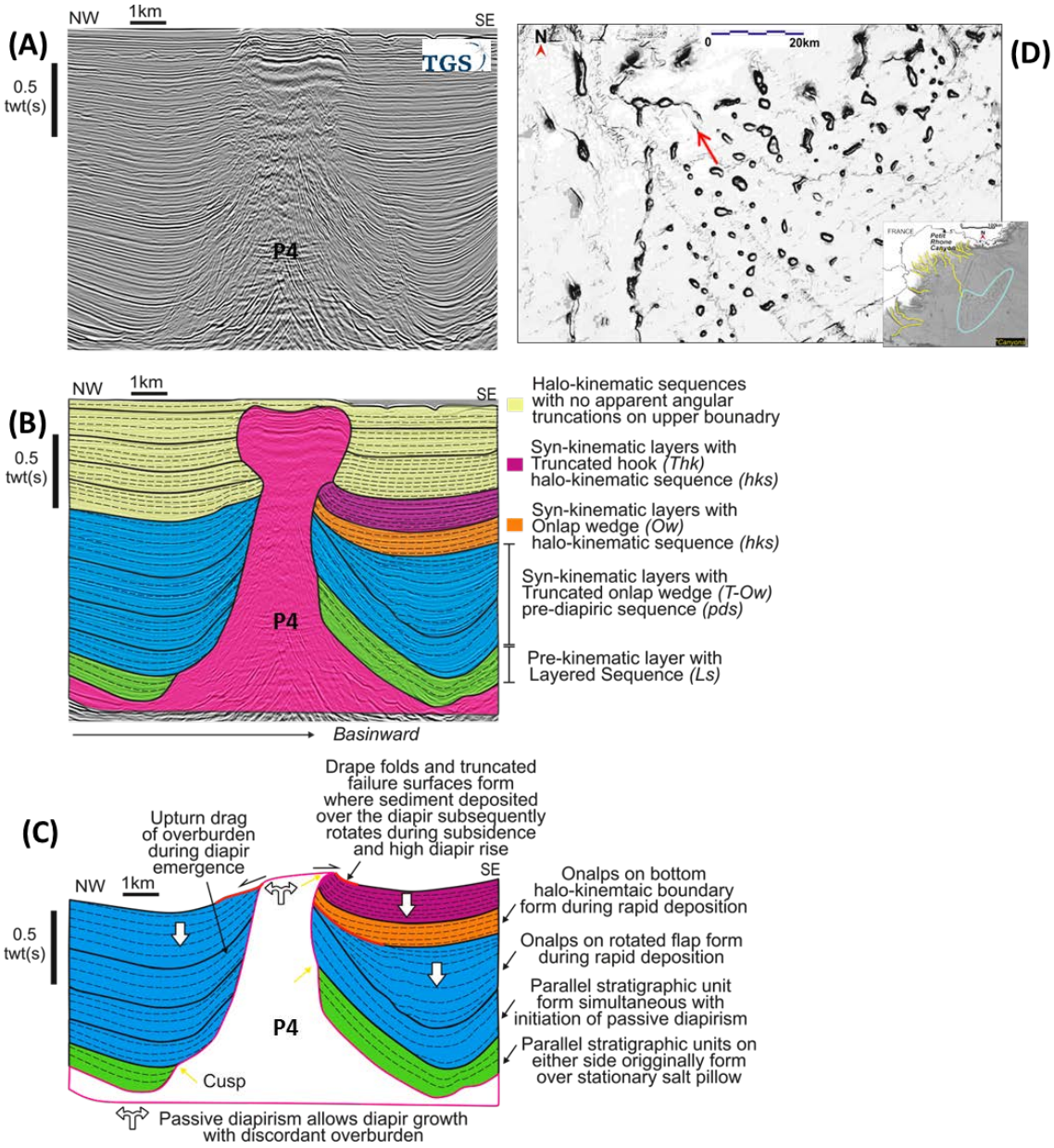

Fig. 17: P4 diapir-depocentre profile showing a passive diapir (B) & (C) Interpretation of salt kinematic growth phases.

1. Salt diapir P4 exhibits drag strata with diapir proximal thinning on landward side and subsidence strata in depocenter on basinward side.

2. On either side of P4, basal discordant stratigraphic unit with parallel sedimentation pattern form the pre-kinematic layer originally form concordant overburden above stationary salt pillow.
3. Truncated onlap wedge, pre-diapiric sequence on basinward side of P4; basal discordant stratigraphic unit formed from initial active salt rise, drag folded on emerging salt diapir with subsequent onlaps from syn-kinematic deposition.
4. Onlap wedge, halo-kinematic sequence on basinward side of P4; discordant stratigraphic unit formed from syn-kinematic passive salt rise shows onlaps on bottom halo-kinematic boundary and convergent towards salt diapir resulting from rapid sedimentation rates.
5. Truncated hook, halo-kinematic sequence on basinward side of P4; discordant stratigraphic unit formed from syn-kinematic passive salt rise shows no onlaps within halo-kinematic sequence, all beds are folded proximal to the diapir and truncated at cusp (Giles and Rowan 2012). The *Thk* sequence results from high salt rise rates.
6. Halo-kinematic sequences with no apparent angular truncation form in a late stage passive diapirism, i.e. waning minibasin down-building.

Correlation of regional sequence-stratigraphic and minibasin halo-kinematic sequences

Correlation of the regional sequence-stratigraphic units of the Gulf of Lion-Provencal basin with local minibasin halo-kinematic sequence-stratigraphic units identified in this study is shown in (Fig. 18).

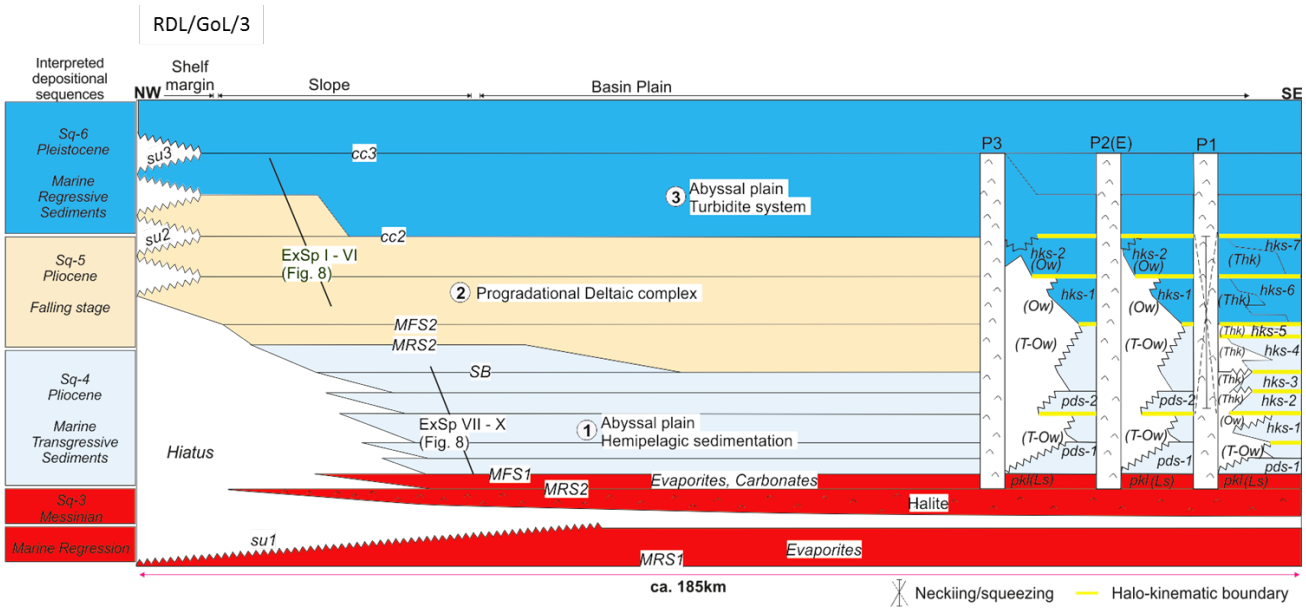

Fig. 18: Correlation of the regional sequence-stratigraphic units of the Gulf of Lion-Provencal basin with local minibasin halo-kinematic sequence-stratigraphic units (Mianaekere and Adam In review-a). (Location shown in Fig. 3)

A chronostratigraphic correlation of pre-kinematic and syn-kinematic depositional units from the up-slope margin to the deepwater basin and across minibasins may raise uncertainties because salt structures and minibasins in different kinematic segments develop at different times and rates (Trudgill 2011). In contrast to the mature Atlantic salt basins, uncertainties can be reduced in this study due to the relatively young age of the salt tectonic processes in the Messinian salt basin. Regional correlations of key seismic horizons are constrained by interpretations of associated kinematic deformation and internal geometries in depocenters adjacent to salt structures in up-dip Gulf of Lion margin and the down-dip Provencal Basin. For example, timing of halokinesis in the updip NE of the Gulf of Lion are inferred from normal listric faults that penetrate younger stratigraphic packages in the proximal slope and constrained to older syn-kinematic packages in the distal slope see (Wu et al. 1990). Also, older (Pliocene)

stratigraphic units are observed down-lapping on salt structures; salt welds are associated with kinematic growth faults in the proximal slope and younger (Pleistocene) units are parallel.

Sq-3 represents the lower evaporite layer, Messinian Hiatus, unconformity and Messinian halite layer and upper evaporite layer. The base-halite horizon is a regional correlative conformity related to the sub-aerial unconformity *su1* characterized by prominent angular truncations on the paleo shelf and paleo slope. The Early Pliocene marine transgressive unit Sq-4 describes a period of low (hemipelagic) sedimentation rates and early stage contraction in the deep basin. The marine transgressive unit include depocenters (ExSp-VII, ExSp-VIII, ExSp-IX and ExSp-X) related to extensional salt structures created on the up-dip distal slope and in basinward direction correlates with the pre-kinematic and syn-kinematic (pre-diapiric) sequences in the proximal diapiric domain, and with later halo-kinematic sequences in the distal diapiric domain. The Pliocene falling stage unit Sq-5 and Pleistocene marine regressive unit Sq-6 represents a period of increasing sedimentation rates related to the progradational deltaic complex in margin slope and turbidite sedimentation in the basin plain, contributing to higher rates of regional contraction. Sq-5 and Sq-6 depositional units include synkinematic depocenters (ExSp-I, ExSp-II, ExSp-III, ExSp-IV, ExSp-V and ExSp-VI) in the up-dip extensional domain formed on a terraced base-of-salt segment in the proximal and mid-section slope. Sq-5 and Sq-6 correlates down-dip with onlap wedge syn-kinematic halo-kinematic sequences in proximal diapiric domain and syn-kinematic halo-kinematic sequences characterised by slump deposits in the distal diapiric domain. Overall, the minibasin sequence boundaries that delineate truncated onlap wedges, onlap wedges and truncated hooks are equivalent in timescales to parasequence boundaries (Andrie et al. 2012; Giles and Rowan 2012; Rowan et al. 2012).

Halo-kinematic sequence stratigraphy vs. halokinetic sequence stratigraphy

In literature, halokinetic depocenters and minibasins have been categorized as depocenters which are created by the reciprocal interactions of sediment loading and salt withdrawal (Hudec and Jackson 2002b; Jackson and Hudec 2009). Genetically related pre-diapiric and halo-kinematic depocenters that hosts truncated onlap wedge, onlap wedge and truncated hook depositional patterns in this study also result from reciprocal interactions of sediment loading and salt withdrawal.

Halo-kinematic sequences defined by stratal depositional patterns in this study are regarded in comparison to sequence classifications defined by stratal structural geometries and salt-sediment geometric relationships by researchers such as (Alsop et al. 2000; Giles and Rowan 2012; Nikolinakou et al. 2017; Rowan et al. 2016a; Rowan et al. 2003a; Schultz-Ela 2003) (Fig. 19).

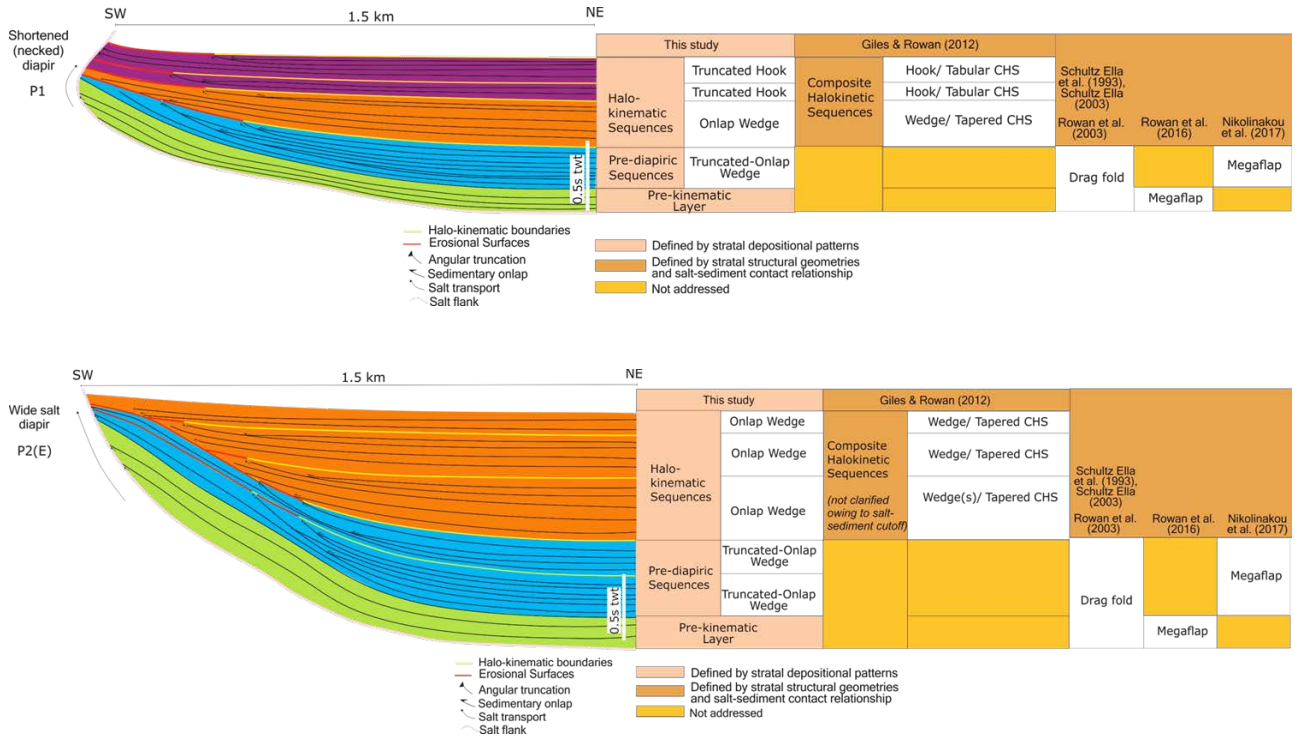

Fig. 19: Comparison table showing classifications of minibasin depositional packages from published studies compared to results from this study. The table compares classifications defined by stratal depositional patterns and stratal structural geometries.

On diapir proximal scale, the onlap wedge sequence defined in this study can be compared to tapered composite halokinetic sequences (Giles and Rowan 2012) with folded convergent boundaries and broad zones of upper boundary erosion in the near-diapir zone. The truncated hook sequence may be likened to tabular composite halokinetic sequences (Giles and Rowan 2012) with folded angular boundaries and narrow zones of upper boundary deformation near the diapir flanks. The tapered, tabular structural styles and onlap wedge, truncated hook sedimentation geometries result from the advancement of passive salt diapirs as described in the current model of Giles and Rowan (2012).

Formation of truncated onlap wedge sequence in this study follows the drag dogma from (Alsop et al. 2000; Callot et al. 2016; Dooley et al. 2009; Hudec and Jackson 2007; Schultz-Ela 2003) which suggests that during diapiric inflation and radial salt growth through susceptible overburden roof, drag folding may initiate from near surface deformation; initial expressions of strata onlapping a downbuilding diapir and an originally continuous roof are upturned to flap folds at diapir flanks (Nikolinakou et al. 2017; Rowan et al. 2016a). In tectonically stable settings, structural configurations of flap folds are used to identify basal megaflaps (Hearon et al. 2015; Nikolinakou et al. 2017; Rowan et al. 2016a; Saura et al. 2016) and halokinetic sequences (Giles and Lawton 2002b; Hearon IV et al. 2014; Kernen et al. 2012b; Rowan et al. 2016a; Rowan et al. 2003a; Yohann et al. 2016). Basal megaflaps and truncated onlap wedge sedimentation patterns suggests the initiation and nature of structural evolution of a salt swell to diapir, kinematic translations from reactive or active to passive phases, (Schultz-Ela 2003), relative rates and time scales of sedimentation and salt growth (Giles and Lawton 2002b; Giles and Rowan 2012; Rowan et al. 2016a).

6. Conclusion

The stratal patterns; layered sequence (Ls), onlap wedge sequence (Ow), truncated hook sequence (Thk) and truncated onlap wedge sequence (T-Ow) discussed in this study directly result from local interactions of salt inflation rates, sedimentation rates, salt withdrawal from beneath minibasins. Characteristic internal stratigraphic patterns within genetically related salt-controlled depocenters that inform on all kinematic phases of salt diapir growth i.e. active or passive and growth stages i.e. pre-kinematic, pre-diapiric and diapiric stages of salt-sediment interactions. The classifications; pre-kinematic layered sequence, pre-diapiric truncated onlap

wedge sequence and halo-kinematic onlap wedge and halo-kinematic truncated hook sequences directly infer kinematic growth phases of salt growth. Minibasin stratigraphic interpretation on alternate facing flanks for diapir profile P2(E) in strike-dip (in-line - x-line) arbitrary line section, showed dominant kinematic successions and kinematic deposits in the dip section profile (NW-SE) in comparison to the strike section profile (SW-NE). This observation may suggest the minibasin stratal patterns discussed in this study are influenced by regional sedimentation and contraction.

7. Future work

Current concepts of halokinetic sequence stratigraphy by Giles and Rowan (2012) apply to near diapir scale i.e. within 3km from diapir flank hence; further work would extend concepts of halokinetic sequence stratigraphy and concepts of halo-kinematic sequence stratigraphy developed in this study on a minibasin scale to highlight influences of regional scale contractional salt tectonics. Future work would incorporate published concepts on drag folding and models of basal megaflaps for the pre-kinematic, early syn-kinematic layers. This study showcases that onlapping beds may appear at the bottom or enveloped within rotated beds in a stratigraphic sequence, in other words, they infer relative timings of structural folding and sedimentation within a sequence; structural wheeler diagram will demonstrate the folding and sedimentation cycle of events.

8. ACKNOWLEDGEMENTS

We are especially grateful to TGS for providing the seismic data used in this study. At TGS, we are particularly thankful to Karyna Rodriguez and Neil Hodgkinson for detailed review of this work and for granting the permission to publish. We address our gratitude to IHS Markit for

authorising the use of Kingdom: Seismic and geological interpretation software as part of the Royal Holloway academic licence agreement. We extend our thanks to Ian Watkinson at and Peter Burgess (former) at Royal Holloway, Earth Sciences department for invaluable discussions on sequence stratigraphic interpretations that inspired the near diapir scale wheeler diagrams in this study. Special thanks to Mark Rowan for stimulating discussions on Halokinetic Sequence Stratigraphy aspects of this work.

9. References

Alsop, G.I., Brown, J.P., Davison, I. & Gibling, M.R. 2000. The geometry of drag zones adjacent to salt diapirs. Journal of the Geological Society of London, **157**, 1019-1029.

Alsop, G.I., Weinberger, R., Levi, T. & Marco, S. 2016. Cycles of passive versus active diapirism recorded along an exposed salt wall. Journal of Structural Geology, **84**, 47-67, doi: 10.1016/j.jsg.2016.01.008.

Andrie, J.R., Giles, K.a., Lawton, T.F. & Rowan, M.G. 2012. Halokinetic-sequence stratigraphy, fluvial sedimentology and structural geometry of the Eocene Carroza Formation along La Popa salt weld, La Popa Basin, Mexico. Geological Society, London, Special Publications, **363**, 59-79, doi: 10.1144/SP363.4.

Bache, F., Gargani, J., Suc, J.-P., Gorini, C., Rabineau, M., Popescu, S.-M., Leroux, E., Couto, D.D., Jouannic, G., Rubino, J.-L., Olivet, J.-L., Clauzon, G., Dos Reis, A.T. & Aslanian, D. 2015. Messinian evaporite deposition during sea level rise in the Gulf of Lions (Western Mediterranean). Marine and Petroleum Geology, **66**, 262-277, doi: 10.1016/j.marpetgeo.2014.12.013.

Bourillot, R., Vennin, E., Rouchy, J.M., Blanc-Valleron, M.M., Caruso, A. & Durlet, C. 2010. The end of the Messinian Salinity Crisis in the western Mediterranean: Insights from the carbonate platforms of south-eastern Spain. Sedimentary Geology, **229**, 224-253, doi: 10.1016/j.sedgeo.2010.06.010.

Butler, R.W.H., McClelland, E. & Jones, R.E. 1999. Calibrating the duration and timing of the Messinian salinity crisis in the Mediterranean: linked tectonoclimatic signals in thrust-top basins of Sicily. Journal of the Geological Society, London, **156**, 827-835.

Callot, J.-p., Salel, J.-f., Letouzey, J., Daniel, J.-m. & Ringenbach, J.-c. 2016. Three-dimensional evolution of salt-controlled minibasins : Interactions , folding , and mega fl ap development. **9**, 1419-1442, doi: 10.1306/0
3101614087.

Carminati, E., Doglioni, C., Gelabert, B., Panza, G.F., Raykova, R.B. & Roca, E. 2004. Evolution of the Western Mediterranean. Principles of Phanerozoic Regional Geology, 1-29.

Carminati, E., Lustrino, M. & Doglioni, C. 2012. Geodynamic evolution of the central and western Mediterranean: Tectonics vs. igneous petrology constraints. Tectonophysics, **579**, 173-192, doi: 10.1016/j.tecto.2012.01.026.

Dooley, T.P., Jackson, M.P.A. & Hudec, M.R. 2009. Inflation and deflation of deeply buried salt stocks during lateral shortening. Journal of Structural Geology, **31**, 582-600, doi: 10.1016/j.jsg.2009.03.013.
Driussi, O., Maillard, A., Ochoa, D., Lofi, J., Chanier, F., Gaullier, V., Briais, A., Sage, F., Sierro, F. & Garcia, M. 2015. Messinian Salinity Crisis deposits widespread over the Balearic Promontory: Insights from new high-resolution seismic data. Marine and Petroleum Geology, **66**, 41-54, doi: 10.1016/j.marpetgeo.2014.09.008.
Droz, L., dos Reis, a.T., Rabineau, M., Berné, S. & Bellaiche, G. 2006. Quaternary turbidite systems on the northern margins of the Balearic Basin (Western Mediterranean): A synthesis. Geo-Marine Letters, **26**, 347-359, doi: 10.1007/s00367-006-0044-0.
Giles, K.A. & Lawton, T.F. 2002. Halokinetic Sequence Stratigraphy Adjacent to the El Papalote Diapir, Northeastern Mexico. American Associacion of Petroleum Geologists Bulletin, **86**, 823-840, doi: 10.1306/61eedbac-173e-11d7-8645000102c1865d.
Giles, K.A., Lawton, T.F. & Rowan, M.G. 2004. Summary of Halokinetic Sequence Chacteristics from Outcrop Studies of La Popa Salt Basin, Northeastern Mexico. *24th Bob F. Perkins Research Conference*, Houston, Texas, 625-634.
Giles, K.A. & Rowan, M.G. 2012. Concepts in halokinetic-sequence deformation and stratigraphy. Geological Society, London, Special Publications, **363**, 7-31, doi: 10.1144/sp363.2.
Gorini, C., Montadert, L. & Rabineau, M. 2015. New imaging of the salinity crisis: Dual Messinian lowstand megasequences recorded in the deep basin of both the eastern and western Mediterranean. Marine and Petroleum Geology, **66**, 278-294, doi: 10.1016/j.marpetgeo.2015.01.009.
Granado, P., Urgeles, R., Sàbat, F., Albert-Villanueva, E., Roca, E., Muñoz, J.A., Mazzuca, N. & Gambini, R. 2016. Geodynamical framework and hydrocarbon plays of a salt giant: the NW Mediterranean Basin. Petroleum Geoscience, **22**, 309-321, doi: 10.1144/petgeo2015-084.
Hearon IV, T.E., Rowan, M., A., G.K. & H., a.H.W. 2014. Halokinetic deformation adjacent to the deepwater Auger diapir, Garden Banks 470, northern Gulf of Mexico: Testing the applicability of an outcrop-based model using subsurface data. Special section: Salt tectonics and interpretation, **2**, SM57-SM76.
Hearon, T.E., Rowan, M.G., Giles, K.A., Kernen, R.A., Gannaway, C.E., Lawton, T.F. & Fiduk, J.C. 2015. Allochthonous salt initiation and advance in the northern Flinders and eastern Willouran ranges, South Australia: Using outcrops to test subsurface-based models from the northern Gulf of Mexico. AAPG Bulletin, **99**, 293-331.
Hudec, M.R. & Jackson, M.P.A. 2002. Structural segmentation, inversion, and salt tectonics on a passive margin: Evolution of the Inner Kwanza Basin, Angola. Geological Society of America Bulletin, **114**, 1222-1244, doi: 10.1130/0016-7606(2002)114<1222:ssiast>2.0.co;2.
Hudec, M.R. & Jackson, M.P.A. 2007. Terra infirma: Understanding salt tectonics. Earth-Science Reviews, **82**, 1-28.
Hudec, M.R., Jackson, M.P.A. & Schultz-Ela, D.D. 2009. The paradox of minibasin subsidence into salt: Clues to the evolution of crustal basins. Bulletin of the Geological Society of America, doi: 10.1130/B26275.1.
Jackson, M.P.a. & Hudec, M.R. 2009. Interplay of Basement Tectonics, Salt Tectonics, and Sedimentation in the Kwanza Basin, Angola. *In*: Town, A.C. (ed.) *Search and Discovery Article*.
Jackson, M.P.A. & Hudec, M.R. 2011. Salt Tectonics: Priciples and Practice

Jackson, M.P.A. & Hudec, M.R. 2017. Salt Tectonics: Principles and Practice. Cambridge University Press.
Jones, I.F. & Davison, I. 2014. Seismic imaging in and around salt bodies. Interpretation, **2**, SL1-SL20, doi: 10.1190/int-2014-0033.1.
Kernen, R.A., Giles, K.A., Rowan, M.G., Lawton, T.F. & Hearon, T.E. 2012. Depositional and halokinetic-sequence stratigraphy of the Neoproterozoic Wonoka Formation adjacent to Patawarta allochthonous salt sheet, Central Flinders Ranges, South Australia. *In*: Archer, S.G., Alsop, G.I., Hartley, A.J., Grant, N.T. & Hodgkinson, R. (eds.) *Salt Tectonics, Sediments and Prospectivity*. Geological Society, 81-105.
Leroux, E., Aslanian, D., Rabineau, M., Moulin, M., Granjeon, D., Gorini, C. & Droz, L. 2015a. Sedimentary markers in the Provençal Basin (western Mediterranean): a window into deep geodynamic processes. Terra Nova, **27**, 122-129, doi: 10.1111/ter.12139.
Maillard, A., Gaullier, V., Vendeville, B.C. & Odonne, F. 2003a. Influence of differential compaction above basement steps on salt tectonics in the Ligurian-Provencal Basin, Northwest Mediterranean. Marine and Petroleum Geology, **20**, 13-27.
Mianaekere, V. & Adam, J. in review. Convergent contractional salt tectonics in the Western Mediterranean Messinian salt basins: Passive margin salt tectonics. *In*: London, R.H.U.o. (ed.).
Nikolinakou, M.A., Heidari, M., Hudec, M.R. & Flemings, P.B. 2017. Initiation and growth of salt diapirs in tectonically stable settings: Upbuilding and megaflaps. AAPG Bulletin, **101**, 887-905, doi: 10.1306/09021615245.
Ratcliff, D.W., Gray, S.H. & Whitmore, N.D. 1992. Seismic imaging of salt structures in the Gulf of Mexico. The Leading Edge, doi: 10.1190/1.1436876.
Ribes, C., Kergaravat, C., Bonnel, C., Crumeyrolle, P., Callot, J.-P., Poisson, A., Temiz, H. & Ringenbach, J.-C. 2015. Fluvial sedimentation in a salt-controlled mini-basin: stratal patterns and facies assemblages, Sivas Basin, Turkey. Sedimentology, **62**, 1513-1545, doi: 10.1111/sed.12195.
Roberts, G. & Christoffersen, T. 2013. The West Mediterranean Salt Basin – A Future Petroleum Producing Province ?*. **50791**.
Rojo, L.A., Escalona, A. & Schulte, L. 2016. The use of seismic attributes to enhance imaging of salt structures in the Barents Sea. First Break, doi: 0.3997/1365-2397.2016014.
Rouchy, J.M. & Caruso, A. 2006. The Messinian salinity crisis in the Mediterranean basin: A reassessment of the data and an integrated scenario. Sedimentary Geology, **188**, 35-67.
Rowan, M.G., Giles, K.a., Hearon IV, T.E. & Fiduk, J.C. 2016. Megaflaps adjacent to salt diapirs. AAPG Bulletin, **100**, 1723-1747, doi: 10.1306/05241616009.
Rowan, M.G., Lawton, T.F. & Giles, K.A. 2012. Anatomy of an exposed vertical salt weld and flanking strata, La Popa Basin, Mexico. Geological Society, London, Special Publications, **363**, 33-57, doi: 10.1144/sp363.3.
Rowan, M.G., Lawton, T.F., Giles, K.A. & Ratliff, R.A. 2003. Near-salt deformation in La Popa basin, Mexico, and the northern Gulf of Mexico: A general model for passive diapirism. AAPG Bulletin, **87**, 733-756.
Rowan, M.G. & Weimer, P. 1998. Salt-Sediment Interaction, Northern Green Canyon and Ewing Bank (Offshore Louisiana), Northern Gulf of Mexico.
Saura, E., Ardèvol i Oró, L., Teixell, A. & Vergés, J. 2016. Rising and falling diapirs, shifting depocenters, and flap overturning in the Cretaceous Sopeira and Sant Gervàs subbasins (Ribagorça Basin, southern Pyrenees). Tectonics, **35**, 638-662, doi: 10.1002/2015tc004001.

Schultz-Ela, D.D. 2003. Origin of drag folds bordering salt diapirs. AAPG Bulletin, **87**, 757-780, doi: 10.1306/12200201093.
Storetvedt, K.M. 1973. Genesis of West Mediterranean basins. Earth and Planetary Science Letters., **21**, 22-28, doi: 10.1016/0012-821X(73)90221-5.
Trudgill, B.D. 2011. Evolution of salt structures in the northern Paradox Basin: Controls on evaporite deposition, salt wall growth and supra-salt stratigraphic architecture. Basin Research, **23**, 208-238, doi: 10.1111/j.1365-2117.2010.00478.x.
Wheeler, H.E. 1958. Time-stratigraphy. AAPG Bulletin, **42**, 1047-1063.
Whipple, K.X.M., B.J. 2004. Controls on the strength of coupling among climate, erosion, and deformation in two-sided, frictional orogenic wedges at steady state. Journal of Geophysical Research, **109**, doi:10.1029/2003JF000019.
Wu, S., Bally, A.W. & Cramez, C. 1990. Allochthonous salt, structure and stratigraphy of the north-eastern Gulf of Mexico. Part II: Structure. Marine and Petroleum Geology, **7**, 334-340.
Yohann, P., Christophe, B., Etienne, J., Matthieu, G. & Michel, L. 2016. Halokinetic sequences in carbonate systems: An example from the Middle Albian Bakio Breccias Formation (Basque Country, Spain). Sedimentary Geology, **334**, doi: 10.1016/j.sedgeo.2016.01.013.

E. Manuscript 3

Document type: Manuscript submitted for publication to the Journal of Marine and Petroleum Geology.

Authors: Mianaekere Victoria, Adam Jürgen

No of words: 7500

No of pages: 45

'Halo-kinematic' sequence-stratigraphic analysis of minibasins in the deepwater contractional province of the Liguro-Provencal Basin, Western Mediterranean

V. Mianaekere*; J. Adam
Earth Sciences department, Royal Holloway university of London

**Corresponding author: victoria.mianaekere.2014@live.rhul.ac.uk,*

Abstract

This study investigates the co-evolution of gravity-driven thin-skinned salt tectonic processes and minibasin-scale halokinetic-depositional sequences for the kinematic analysis of salt diapirs in the diapiric province of the contractional domain of the deepwater Liguro-Provencal basin. We apply minibasin-scale halo-kinematic sequence-stratigraphic concepts to investigate local controls of diapir growth, creation of accommodation space in related salt-withdrawal minibasins and the spatial-temporal changes in depositional patterns respectively within minibasins. Sequentially restored 2D Minibasin depositional sequences and derived sedimentary wheeler diagrams and structural Wheeler diagrams show the syn-kinematic cycle of events consisting of *ponding, flap folding and erosion* within halo-kinematic sequences. Halo-kinematic sequences show periods of onlapping of ponded sediments and erosional truncations near diapir flanks that delineate halo-kinematic sequence boundaries, while structural folding of minibasin flanks punctuate the ponding and erosional events. Structural wheeler diagrams demonstrate the transition from large length scale folding above diapir pedestals to small length scale folding proximal to steep diapir flanks. Large length scale folds are associated with early pre-kinematic layers; they rotate from minibasin anchor point. Small length scale folds are associated with younger depositional sequences; they rotate from local depocentre focus points. New methods and concepts developed in this study may be integrated into an approach

for hydrocarbon prospectivity analysis, e.g. reservoir mapping within minibasin sequences and dynamics of trap formation around multi-stage salt structures

Keywords: Halo-kinematic sequence stratigraphy, Minibasins, depositional patterns, salt tectonics, Messinian salt.

1. Introduction

This study investigates the co-evolution of passive margin gravity-driven thin-skinned salt tectonic processes and minibasin-scale salt tectonics in the diapiric province of the contractional domain of the deepwater Liguro-Provencal basin [see (Mianaekere and Adam (in review)]. The regional salt tectonic style of the west Mediterranean passive margin was analysed in precedent study. Salt tectonics evolved from a gravitational salt system with an up-dip extensional domain and a down-dip combined contractional-halokinetic minibasin domain (Mianaekere and Adam In review-a). Distribution of primary minibasins in the deepwater contractional domain of a linked thin-skinned gravity-driven salt basin are demonstrated in Figure 1, (a) and (b) showing different magnitudes of regional contraction. Figure 1 (a) Shows minibasins (A) formed in the contractional domain associated with passive down-building and regional squeezing or shortening. Minibasins (A) bound by vertical salt stocks may range in geometry from symmetrical to asymmetrical to rotated minibasins. Figure 1 (b) shows minibasins (B) formed in transitional zone, associated with passive downbuilding and minibasins (C) formed in the contractional domain associated with folding and thrusting (Brun and Fort 2011a). Minibasins (A) formed under low deformation rates and moderate total shortening.

Figure 1: Salt tectonic styles on passive margins (Modified from Brun and Fort 2011). Note distribution of primary minibasins labelled A, B and C.

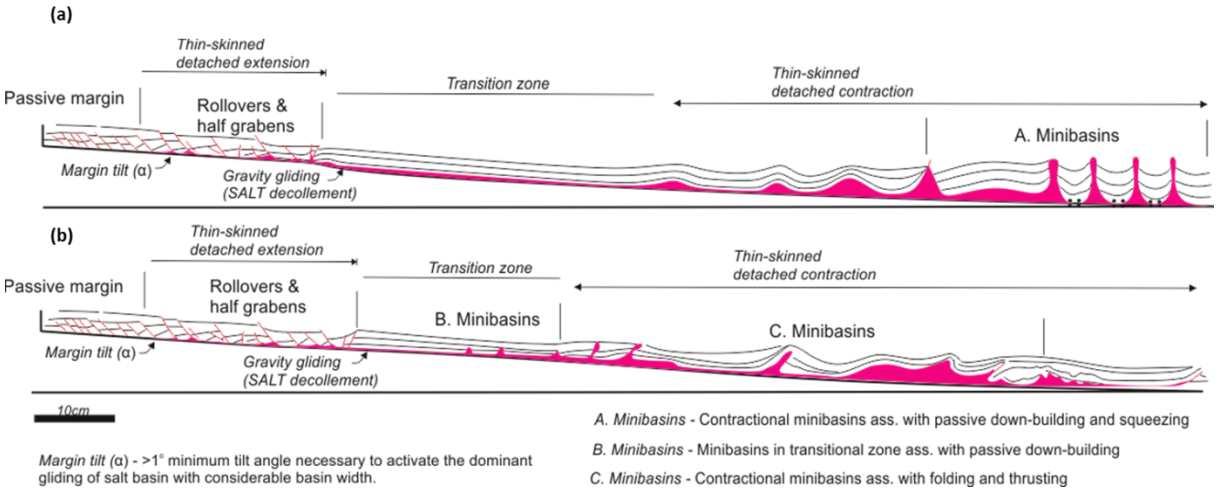

Study area

The NW Mediterranean North Balearic and Liguro-Provencal Cenozoic sedimentary basins (Fig. 2) developed during the NW-SE directed rifting and back-arc extension in Miocene times (Gunnell et al. 2008b). The SE to late SSE rotational drift of the Corsica-Sardinia block and contemporaneous back-arc extension led to the early formation of a highly stretched continental crust and the late formation of the Miocene (21-16 Ma) oceanic crust beneath the Liguro-Provencal basin (Carminati et al. 2004; Maillard et al. 2003; Storetvedt 1973). The Messinian evaporite succession were deposited contemporaneously on extended continental crust and young oceanic crust during the pronounced late Miocene glacio-eustatic sea level regression (Butler et al. 1999; Droz et al. 2006). Post-Messinian isostatic adjustments of the continental shelves relative to the basin plain influenced prograding sedimentary wedges, gravitational failure and gravity-driven thin-skinned deformation, hence extensive salt diapirism

is situated in the down-dip contractional domain in the deepwater basin overlying oceanic crust (Mianaekere and Adam In review-a).

Figure 2: Tectonic and salt distribution map of the West Mediterranean passive margin system, Miocene rifting and subsequent formation of the North Balearic and Liguro-Provencal Basins from slab roll back of the Corsica (Co), Sardinia (Sa) and Calabria (Ca) (Gunnell et al. 2008b), (Maillard et al. 2003), (Droz et al. 2006).

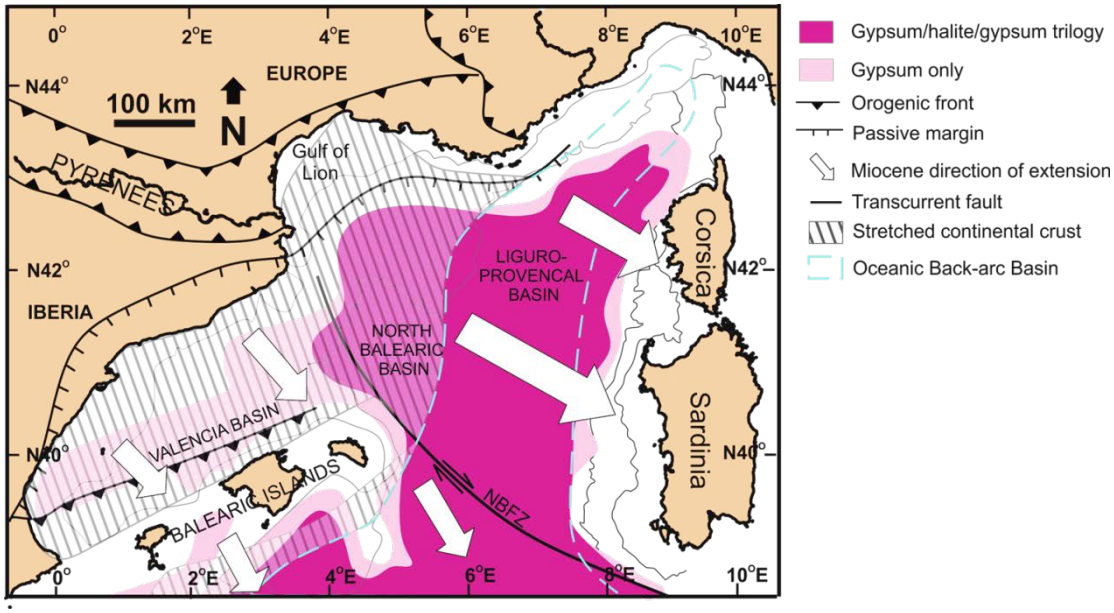

Study aims

We apply minibasin scale halo-kinematic sequence-stratigraphic concepts from Mianaekere and Adam (in review) for the detailed analysis of syn-kinematic depositional sequences to further investigate local controls of diapir growth and creation of accommodation space in related salt-withdrawal minibasins. This study combines the concepts of seismic stratigraphy based on the identification of unique seismic stratigraphic geometries within minibasin sequences (Aschoff and Giles 2005; Hudec et al. 2009a; Madof et al. 2009; Mannie et al. 2014; Saura et al. 2016)

with the concepts of basal megaflaps (Maria A. Nikolinakou and Flemings 2017; Rowan et al. 2016a) and halokinetic sequences (Giles and Lawton 2002b; Kernen et al. 2012b; Rowan et al. 2003a) which employ recognition of structural geometries of depositional packages associated with diapir growth. Identification of unique internal stratal patterns within minibasin sequences and structural geometries of related depositional packages typical of each syn-kinematic growth phase or stage (Jackson and Hudec 2011) of salt structures may enable a better understanding of local halokinetic processes and intermittent response to regional contraction (Duffy et al. 2017).

Our understanding of regional contractional salt tectonics and the evolution of a diapiric and minibasin domain has so far been driven by detailed seismic studies e.g. (Adam et al. 2012b; Brun and Fort 2011a; Brun and Fort 2004; Gottschalk et al. 2004; Tari et al. 2003b, a; Vendeville et al. 1990) and scaled analogue experiments e.g. (Adam et al. 2005; Adam et al. 2006; Adam and Salt Dynamics Group 2008; Gemmer et al. 2004; Ings et al. 2004; Schreurs et al. 2003). On the other hand, local-scale salt halokinesis and resulting conforming stratal architectures and stratal depositional patterns within genetic stratigraphic packages are interpreted proximal to diapirs mostly on outcrops or seismic data e.g. (Andrie et al. 2012; Giles et al. 2004; Giles and Rowan 2012). Small scale analogue modelling [see Koyi et al (1995)] of these commonly observed diapir proximal geometric and internal depositional patterns may be impossible to replicate with scaled physical modelling. Therefore, the aims of this study are to

1. Identify small-scale minibasin depositional and structural geometries evident of minibasin response to regional contraction

2. Identify minibasin depositional units evident of local halokinetic events, i.e. local influences of diapir growth, salt-withdrawal style and depositional style on temporal structural configurations and depositional patterns respectively within minibasins.

3. Analyse and demonstrate intermittent local halokinetic events on minibasin scale using sedimentary wheeler and structural wheeler diagrams.

4. Identify characteristic salt kinematic sequences for different styles of diapir growth and minibasin down-building using schematic structural restorations.

2. Comparative studies

Halo-kinematic sequence stratigraphy, Halokinetic sequence stratigraphy and megaflap

In this section, we highlight and compare established concepts of structural geometries and depositional sequences within salt-related minibasins. A comparative distinction between minibasin halo-kinematic sequence stratigraphic classifications defined by stratal depositional patterns (Mianaekere and Adam In review-b) with published classifications defined by stratal structural geometries is shown in (Fig. 3).

Figure 3: Comparison table showing classifications of minibasin depositional packages established in precedent study (Mianaekere and Adam In review-b) defined by stratal depositional patterns to published classification defined by stratal structural geometries.

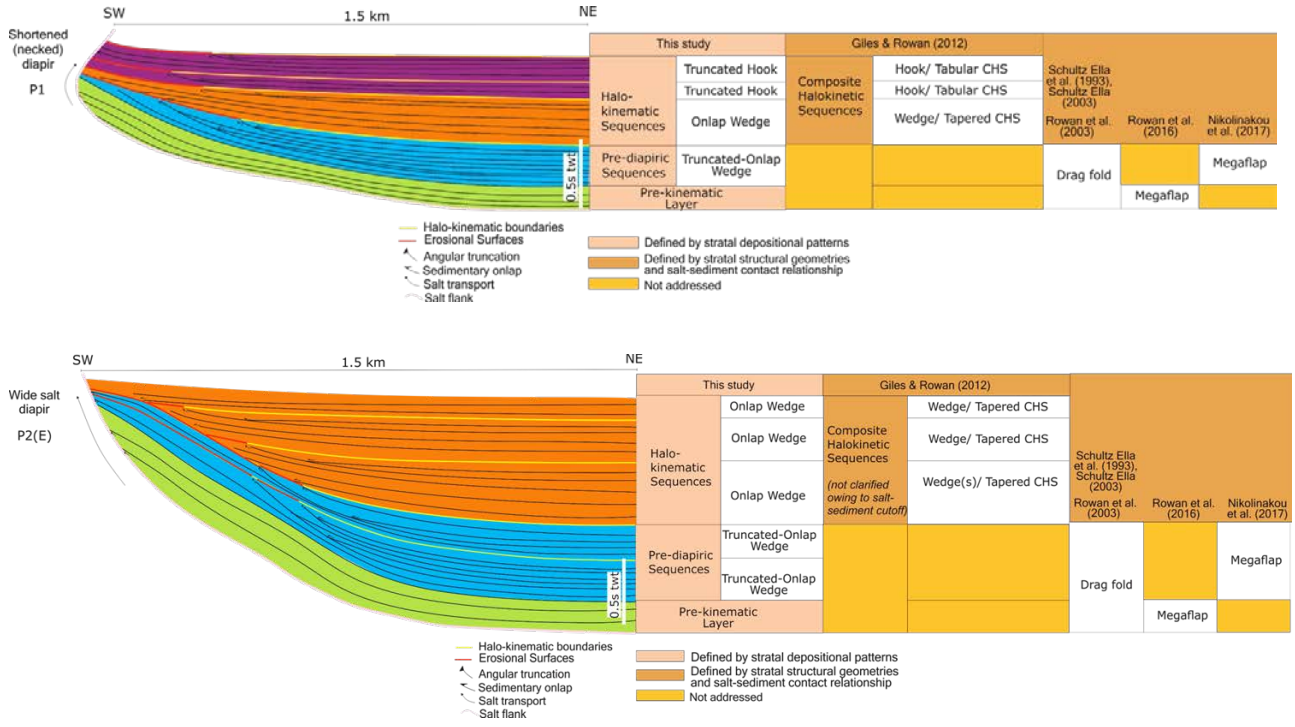

Halo-kinematic sequence stratigraphy was established in precedent study on diapir proximal scale and is developed in this study on minibasin scale. A comparative analysis of formation of halo-kinematic sequences on minibasin scale is demonstrated with diagrammatic cross-sections of the Emirhan mini-basin documenting subsidence through time and formation of a basal megaflap followed by Hook and Wedge halokinetic sequences (Fig. 4).

Figure 4: Diagrammatic cross-sections of the Emirhan mini-basin illustrating subsidence through time showing formation of a basal megaflap followed by Hook and Wedge halokinetic sequences. This classification can be compared to the formation of truncated onlap wedge pre-diapiric sequences and onlap wedge, truncated hook style halo-kinematic sequences (Modified from Ribes et al. 2015). See Table 1 for clarification of terminology and abbreviations.

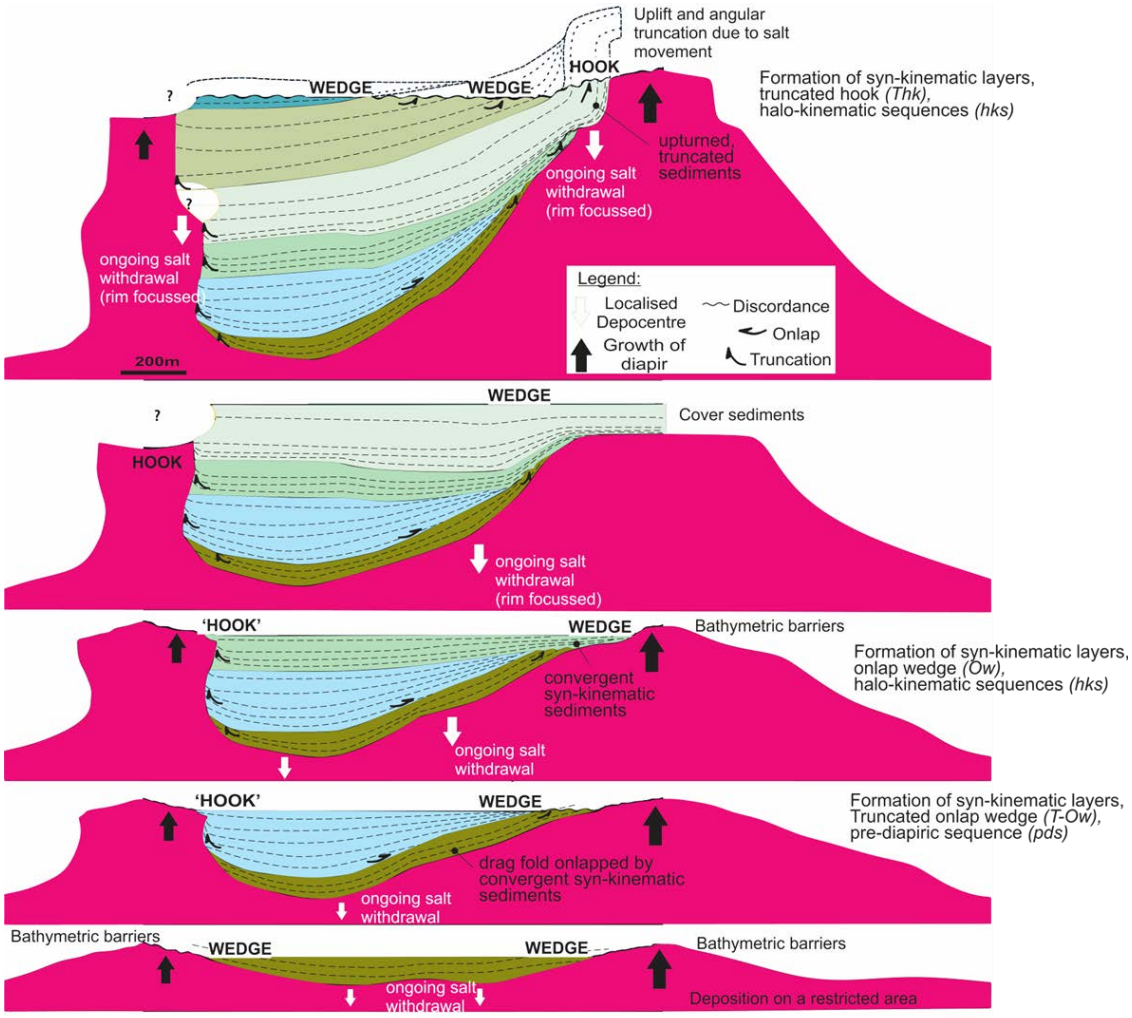

Figure 4 demonstrates how the variable ratio between net diapir rise rate and net local sediment accumulation rate has led to the bathymetric failure or erosion of material at the diapir crest (Andrie et al. 2012; Giles et al. 2004; Giles and Rowan 2012; Kernen et al. 2012b;

Rowan et al. 2012; Rowan et al. 2003a). The mechanical drag folding of strata in the diapir flank was caused by syn-kinematic salt rise (Alsop et al. 2000; Callot et al. 2016; Nikolinakou et al. 2017; Rowan et al. 2016a; Schultz-Ela 2003).

Significant rotational upturn or drag folding (see Fig. 4) of early syn-kinematic packages are currently described as basal megaflaps (Nikolinakou et al. 2017). Basal megaflaps are significant length scale fold panels concordant to diapir flank (Rowan et al. 2016). The basal megaflap has been said to originate from amplification of a salt swell or salt-cored anticline (Jackson and Hudec 2017). In this study, significant structural folds concordant to diapir flank that cut-off subsequent syn-kinematic packages from diapir flank are used to distinguish basal megaflaps (Hearon IV et al. 2014; Nikolinakou et al. 2017; Rowan et al. 2016a; Saura et al. 2016) or pre-diapiric syn-kinematic sequences from halokinetic sequences (Andrie et al. 2012; Giles and Lawton 2002a; Giles et al. 2004; Giles and Rowan 2012; Kernen et al. 2012a) and halo-kinematic sequences (Mianaekere and Adam In review-b) with smaller length scale folds proximal to diapir flank.

Table 1: Clarification of terminology

Salt kinematic growth phase	Stratigraphic Sequence (This study)	Abv.	Minibasin stratigraphic fill pattern (This study)	Abv.	Minibasin evolution phase	Minibasin stratigraphic fill pattern recognition
1. Early stage active phase	Layered sequence	*pkl, Ls*	Layered	*Ls*	Pre-kinematic	Parallel beds, lateral homogenous thickness
2. Late stage active phase	Pre-diapiric sequence	*pds*	Truncated onlap wedge	*T-Ow*	Early syn-kinematic	Drape folded strata on-lapped by early syn-kinematic ponded sediments
3. Passive phase	Halo-kinematic sequence	*hks*	1. Onlap wedge 2. Truncated hook	1. *Ow* 2. *Thk*	Late syn-kinematic	1. Ponded sediments onlap on lower stratigraphic boundary, convergent strata, angular truncation on upper stratigraphic boundary. 2. No ponded sediments in stratigraphic layer, angular truncations on upper stratigraphic boundary

3. Methodology

Dataset

Regional 2D Kirchhoff pre-stack time migrated seismic data provided by TGS were used in this study. A set of regional seismic lines (Fig. 5) with maximum length of 120 km trending in strike and dip direction of the NW Provencal margin were used for the regional kinematic analysis. The seismic sections used for minibasin analysis show a 5s record length from sea bed to base salt. Strike and dip minibasin profiles selected from the regional lines are analysed in detail in (section 5).

Figure 5: Bathymetric map of the Western Mediterranean reproduced from the GEBCO (*www.gebco.net/dgridded_bathymetry_data/)* showing sediment transport pathways and the location of the diapiric domain. Within the diapiric domain the location of strike line (SL) in sequence (sq) (dwSL/sq2 to dwSL/sq5) and dip lines (DP) (dwDL/sq1 to dwDL/sq3) the deepwater (dw) Provencal basin and diapir-minibasin profiles are shown.

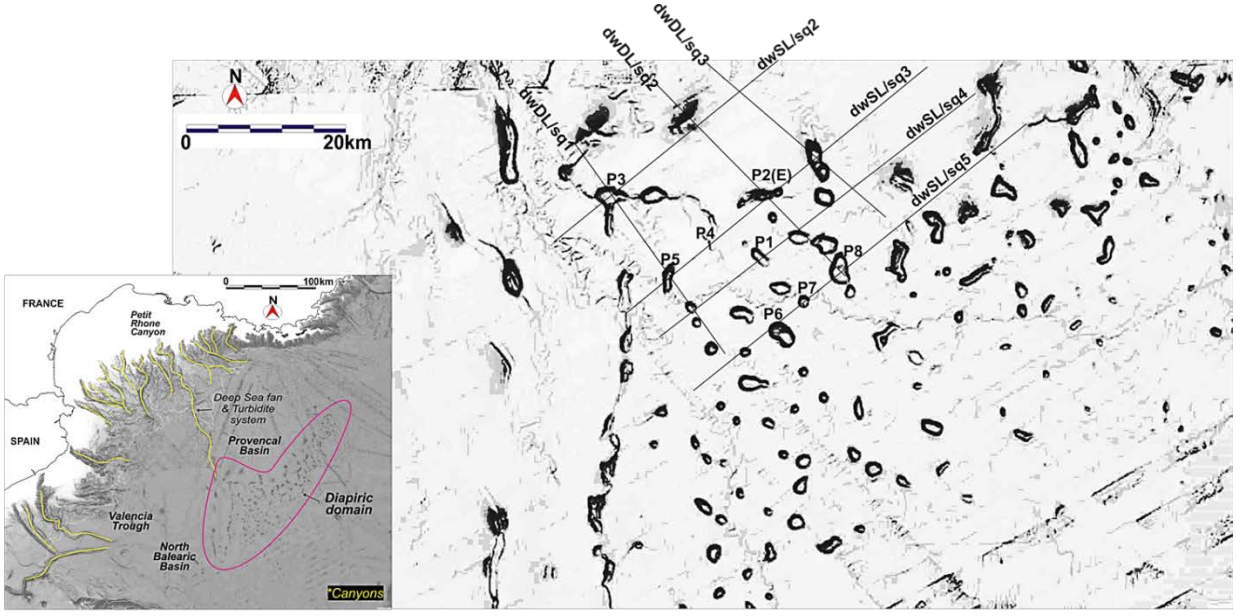

Minibasin sequence stratigraphy

The detailed regional depositional sequence stratigraphic interpretation and tectono-stratigraphic interpretation of the Western Mediterranean have been discussed in precedent study (Mianaekere and Adam in review-c). In this study, a high-resolution seismic-stratigraphic analysis delineated by four post-salt horizons (pslt-1 to pslt-4 in Fig. 6) have been correlated across minibasins in the deepwater Liguro-Provencal basin in (section 5, Fig. 10, 11 & 12) to derive a detailed local minibasin scale halo-kinematic sequence-stratigraphy for the Provencal deepwater contractional diapiric province.

This local minibasin scale halo-kinematic sequence-stratigraphy of the distal basin then can be correlated with the regional stratigraphic framework of the Liguro-Provencal basin which was derived from seismic facies analysis of the proximal Gulf of Lion margin (Mianaekere and Adam In review-a).

Figure 6: Minibasin seismic stratigraphy in the deepwater Provencal basin (right) and stratigraphic chart with regional sequence-stratigraphic units of the Liguro-Provencal Basin (left).

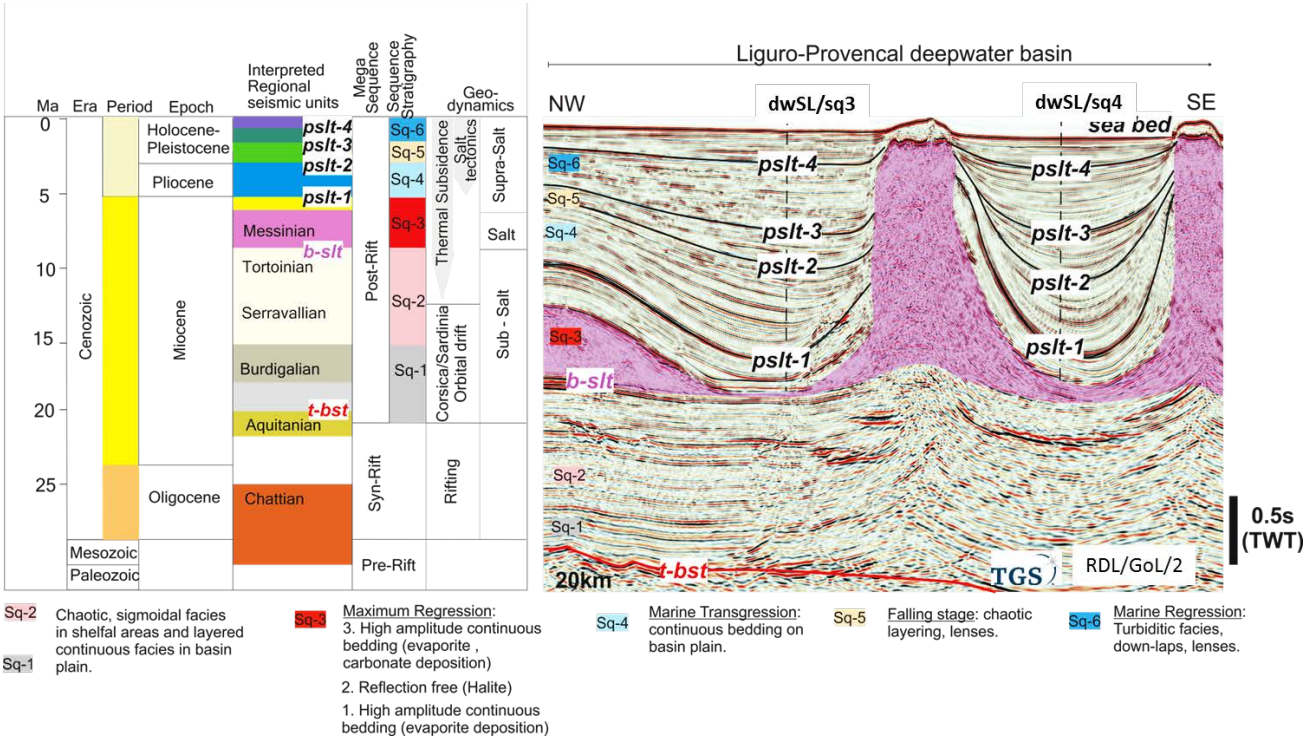

Sedimentary Wheeler diagrams

Syn-kinematic minibasin sequence packages are delineated from the depositional patterns. The local halo-kinematic processes, e.g. the interaction of diapir growth and minibasin down-building can be visualised by sedimentary wheeler diagrams. The Wheeler diagram is a 2D representation of the interpreted geo-seismic section with relative geological time as the vertical axis and section position in meters as the horizontal axis (Wheeler 1958). Each geological stratum in the cross section is plotted at a relative geological time line and extrapolated horizontally according to its measured line length in the interpreted geo-seismic section. Stratal thicknesses on the wheeler diagrams are diagrammatic representations obtained

from the time-migrated geo-sections. With relative geological time as the vertical axis, the derived stratal thicknesses and inclinations of surfaces demonstrate relative timescales or rates of deposition to rates of associated salt rise.

Schematic structural restoration of diapir-minibasin profiles (Fig. 13), (Fig. 14)

For the analysis of the depositional and structural cycles and overall evolution of the minibasins,

Interpreted diapir-minibasin sections are sequentially restored by flattening of key seismic-stratigraphic horizons. It is important to note that this seismic horizon flattening produces only a schematic restoration and does not consider decompaction of the sediments or isostatic adjustment of the base-of-salt usually being performed for the construction of a structurally balanced section restoration (Hudec 2003; Rowan and Ratliff 2012), The flattening exercise preserves bed lengths in adjacent minibasins. Cross-section restoration typically assumes plane-strain deformation and area conservation, constraints that are usually invalid for the salt layer itself because of its characteristic three-dimensional flow and possible dissolution, and (2) for supra-salt layers because of the variable movement directions of separate minibasins or vertical-axis rotation during translation above salt (Rowan and Ratliff 2012). Pre-emptively, orientation of the cross section are chosen parallel to the tectonic transport direction of the overburden strata in downslope direction due to the gravitational processes (Rowan and Ratliff 2012). In summary, the kinematic restorations may not account for thinning of sedimentary layers caused by shear strain due to active diapir piercement (Hudec and Jackson 2007), out-of-section deformation, and diapiric shapes resulting from lateral deformation and mechanical drag folds (Nikolinakou et al. 2017).

Structurally restored Wheeler diagrams (Fig. 15)

The sequentially restored cross-sections have been complemented by a series of restored structural Wheeler diagrams. The structural deformation derived from each restoration stage is overlain in the structural Wheeler diagram with separate colour overlays according to the line length of the given geological strata affected by structural deformation. The colour overlay delimits the extent of structural deformation for each geological stratum onto the wheeler diagram.

4. Contractional salt kinematics

The present-day contractional domain in the Provencal deepwater basin is governed by thin-skinned salt-detached gravity-driven deformation and is separated from the landward extensional domain by an intermediate transitional domain underlying the continental slope. Contractional overprinting of former halokinetic salt structures like salt pillows and salt-cored anticlines that proof the landward migration of the contractional domain since the Late Pliocene can be observed in dip seismic profiles (Fig. 7). Also, the contractional domain represents the major sediment sink in the deepwater Provencal Basin. Hence, the subsidence history in salt-withdrawal minibasins is recorded in the variation of stratigraphic thicknesses in early (dark grey) and late (light grey) syn-kinematic depositional sequences.

Figure 7: Un-interpreted and interpreted NW-SE trending seismic DIP sections perpendicular to the Gulf of Lion shelf margin.

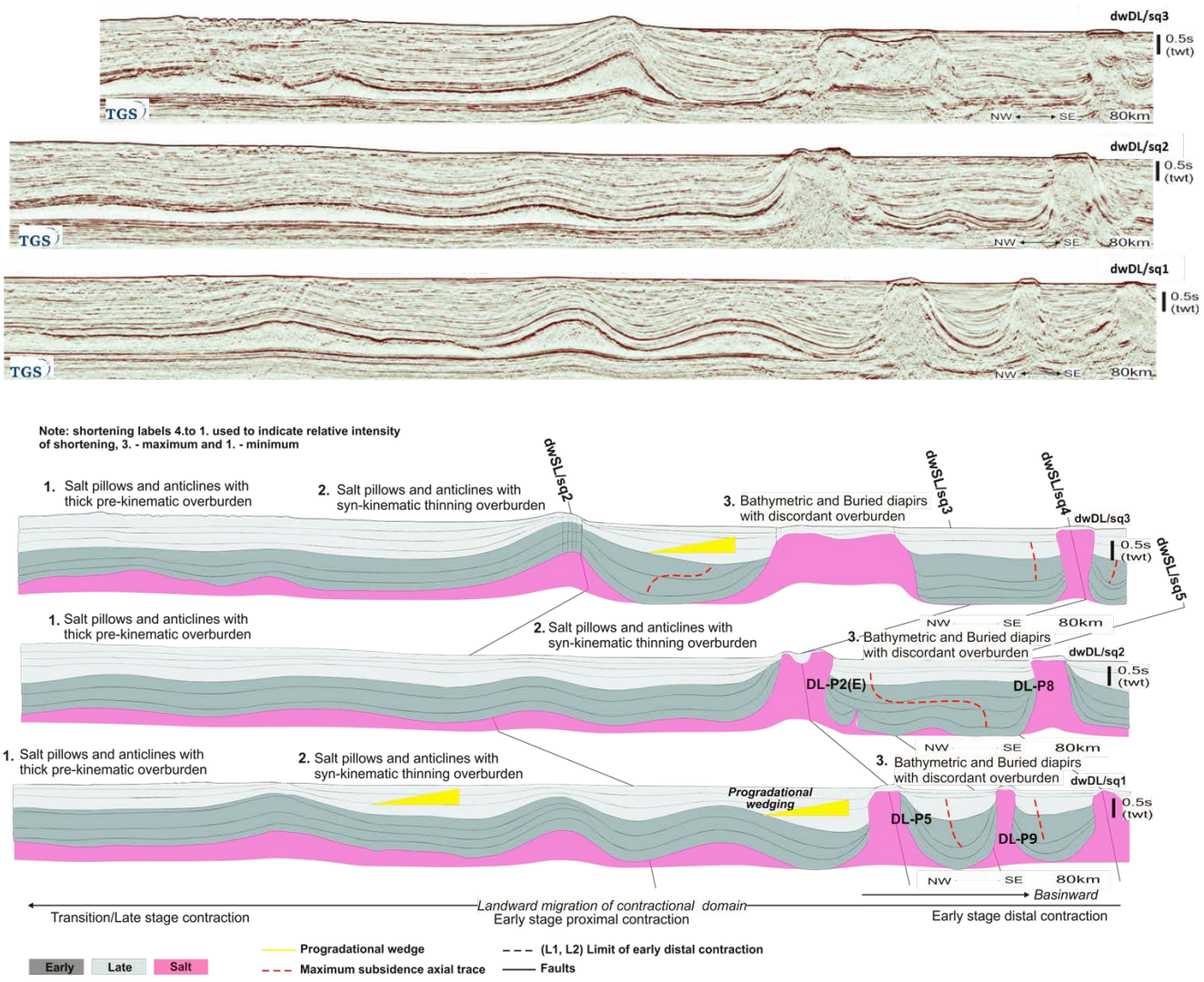

The NW-SE trending dip lines dwDL/sq1, dwDL/sq2 and dwDL/sq3 (Fig. 7) show a progressive segmentation in basinward direction in contractional sub-domains consisting of an early transitional/late stage contractional, early stage proximal contractional and early stage distal contractional sub-domain. The intensity of shortening of salt structures in each sub-domain is indicated by labels 1 (minimum) to 3 (maximum) in Figure 7. In the landward early

transitional/late stage contractional zone, minor shortening (1 in Fig. 7) is represented by low-medium amplitude salt pillows and salt-cored anticlines with thick pre-kinematic overburden. In the early stage proximal contractional domain, moderate shortening (2 in Fig. 7) is represented by salt pillows and salt-cored anticlines with syn-kinematic thinning in overburden. In the early stage distal contractional domain, maximum shortening (3 in Fig. 7) is represented by bathymetric diapirs with discordant overburden. Basinward salt detached contraction and shortening of the early sage distal contraction is further analysed from SW-NE trending 2-Dimensional seismic strike sections dwSL/sq2, dwSL/sq3, dwSL/sq4 and dwSL/sq5 in the deepwater contractional province (Fig. 8).

The boundary of the early distal contraction (L1 in Fig. 8) is indicated in the SW part of the seismic profiles dwSL/sq2, dwSL/sq3, dwSL/sq4 and dwSL/sq5. The boundary is indicated by compressional salt pillows terminating at bathymetric diapirs and active salt diapirs. In the NE part of the strike seismic section the boundary of the early distal contractional domain (L2 in Fig. 8) is marked by contractional diapirs and active contractional salt anticlines.

Figure 8: Un-interpreted and interpreted SW-NE trending 2-Dimensional seismic STRIKE lines parallel to the Gulf of Lion shelf margin. Observe variation of salt structural styles, minibasin geometries and variations in timing and intensity of syn-kinematic subsidence in minibasins across the sections.

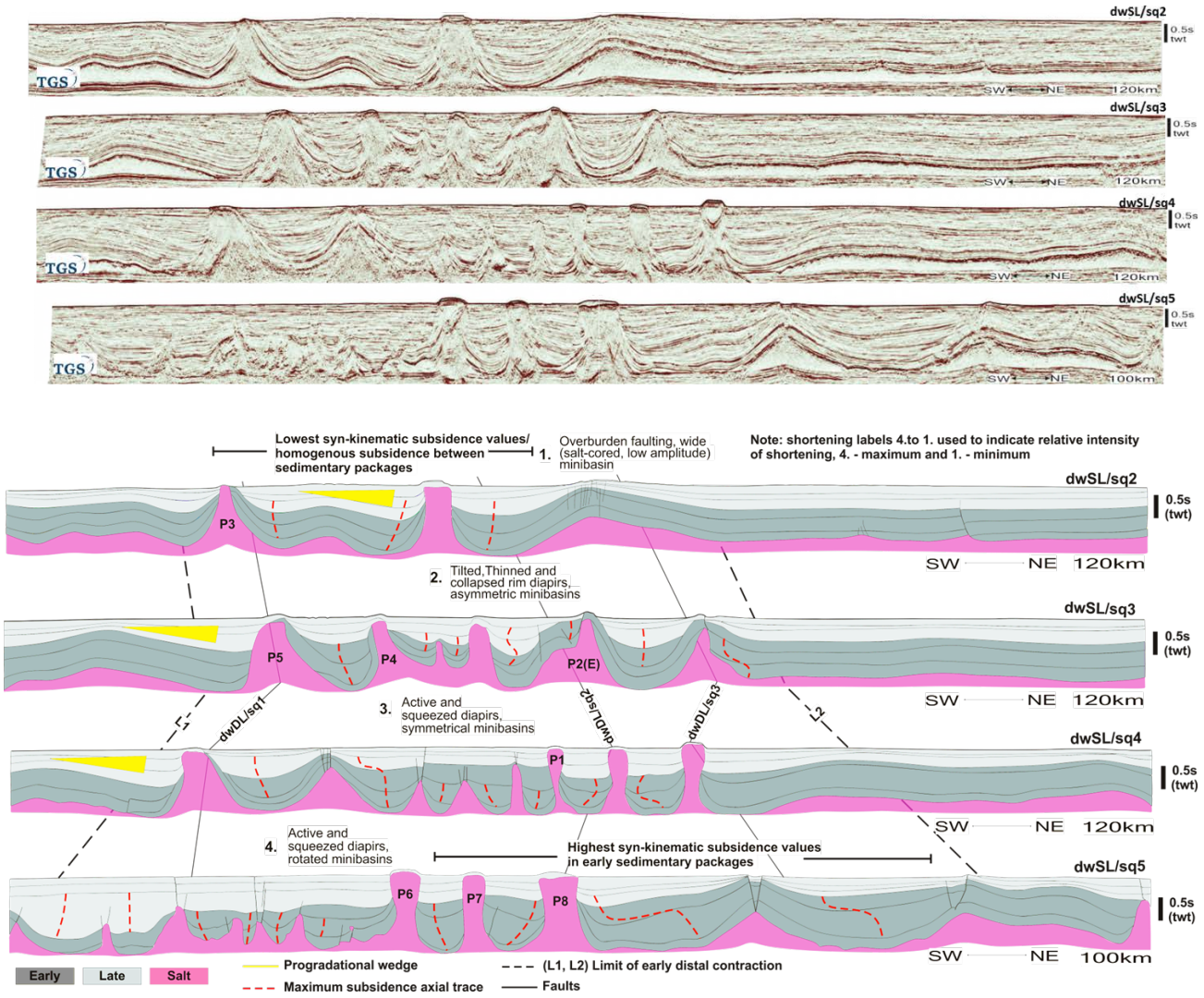

The SW limit of early distal contraction L1 coincides with the basinward termination of the progradational sedimentary wedge against the furthest landward contractional diapir. The NE limit of early distal contraction L2 also indicates the maximum basinward extent of contractional diapirs and contractional minibasins. Landward migration of the contraction domain is also

recorded the subsidence history in salt-withdrawal minibasins across the strike seismic profiles (Fig. 8) showing the variation of stratigraphic thicknesses in early and late syn-kinematic depositional sequences. Maximum syn-kinematic 'subsidence values' are recorded in early sedimentary packages within minibasins furthest in the contractional province on seismic profile dwSL/sq5 (Fig. 8) while minimum syn-kinematic 'subsidence values' are recorded in early sedimentary packages within minibasins most proximal in the contractional province on dwSL/sq2 (Fig. 8).

Spatial variation of contraction styles and shortening in the early stage distal contraction domain are evident by the variation of salt structural geometries, minibasin geometries and timing of syn-kinematic subsidence in minibasins interpreted across the strike seismic profiles dwSL/sq2, dwSL/sq3, dwSL/sq4 and dwSL/sq5 in figure 8.

Relative intensity of shortening across the strike seismic profiles vary from 4-maximum on dwSL/sq5 to 1-minimum on dwSL/sq2 (Fig. 8). DwSL/sq5 being the furthest from margin, exhibits salt structures and minibasins with greater intensity of shortening. Maximum shortening (4) on dwSL/sq5 shows active diapirs to the SW and significantly squeezed (necked) diapirs to the NE bound rotated minibasins between P6, P7 and P8 diapirs (discussed in section 5, Fig. 11). Shortening (3) on dwSL/sq4 shows active diapirs bound symmetrical minibasins and significantly squeezed (necked) diapirs bound asymmetric minibasins. Shortening (2) on dwSL/sq3 shows tilted, thinned and collapsed rim diapirs with flared base bound asymmetric minibasins. Minimum shortening observed on dwSL/sq2 shows faulting of concordant overburden above salt pillow and wide salt cored minibasins with widths of ca. 20km adjacent to P3 diapir in comparison to ca. 10km minibasin widths on dwSL/sq3, between P5 and P4 and

north east of P2 (E), ca. 5km minibasin widths on dwSL/sq4 NE of P1 and ca. 4km to 5km on dwSL/sq5 between P6 and P7 and P8. Another crucial observation from strike seismic profiles (Fig. 8) is variation in length of flexural upturn (megaflap) of basal sedimentary layers against salt diapirs (further discussed in sections 6 and 7). The more proximal, landward strike profiles host large length upturns observed adjacent to P3, P5, P4 and P2 (E) diapirs and basinward, furthest strike profile host shorter length scale upturn adjacent to P1, P6, P7 and P8 diapirs.

5. Minibasin Sequence Stratigraphic analysis

Minibasin-scale halo-kinematic sequence stratigraphic analyses have been performed on strike and dip seismic sections including strike seismic sections of minibasins between diapirs P4/P5 (dwSL/sq3, Fig. 9), diapirs P6/P7 and P7/P8 (dwSL/sq5, Fig. 10) and dip seismic lines across the minibasin between diapirs P5 and P9 (dwDL/sq1, Fig. 11)). The resulting sedimentary wheeler diagrams of the minibasins are sum up at the end of this section. All discussed minibasins are positioned in the distal early contractional domain of in the Liguro-Provencal deepwater basin.

Figure 9: Un-interpreted (top) and interpreted seismic sections (middle) and sedimentary wheeler diagram (bottom) of the P4 and P5 strike diapir-minibasin profile.

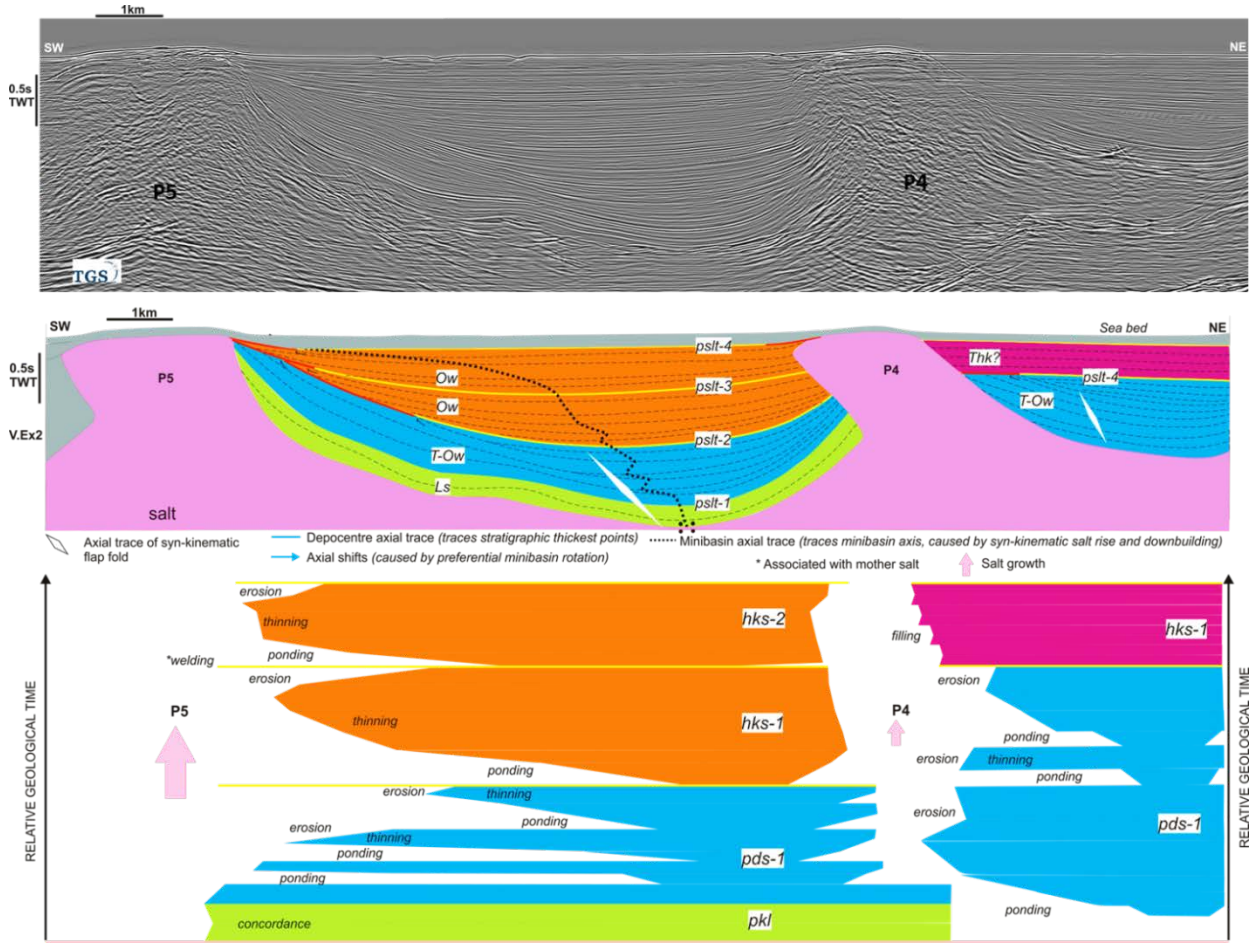

The diapirs P4 & P5 (Fig. 9) are tilted in SW direction of regional tectonic transport, hence a minibasin symmetry skewed preferential to the SW tilt. Angular halo-kinematic boundaries on the NE flank of diapir P5 and a depocenter axial trace skewed to the P5 diapir suggest a significant variation in growth rates between the bounding diapirs P5/P4 through time. Seismic stratal patterns within the minibasin depositional sequences consist of one layered sequence (Ls), one truncated onlap wedge sequence (T-Ow) and two onlap wedge sequences (Ow). Hence, in the sedimentary Wheeler diagram of the minibasin between P4/P5, distinct kinematic

sequences consist of one pre-kinematic layer (pkl), one syn-kinematic pre-diapiric sequence (pds) and two halo-kinematic sequences (hks).

Figure 10: Un-interpreted (top) and interpreted seismic interpretation (middle) and sedimentary wheeler diagram (bottom) of the P6, P7 and P8 strike diapir-minibasin profile.

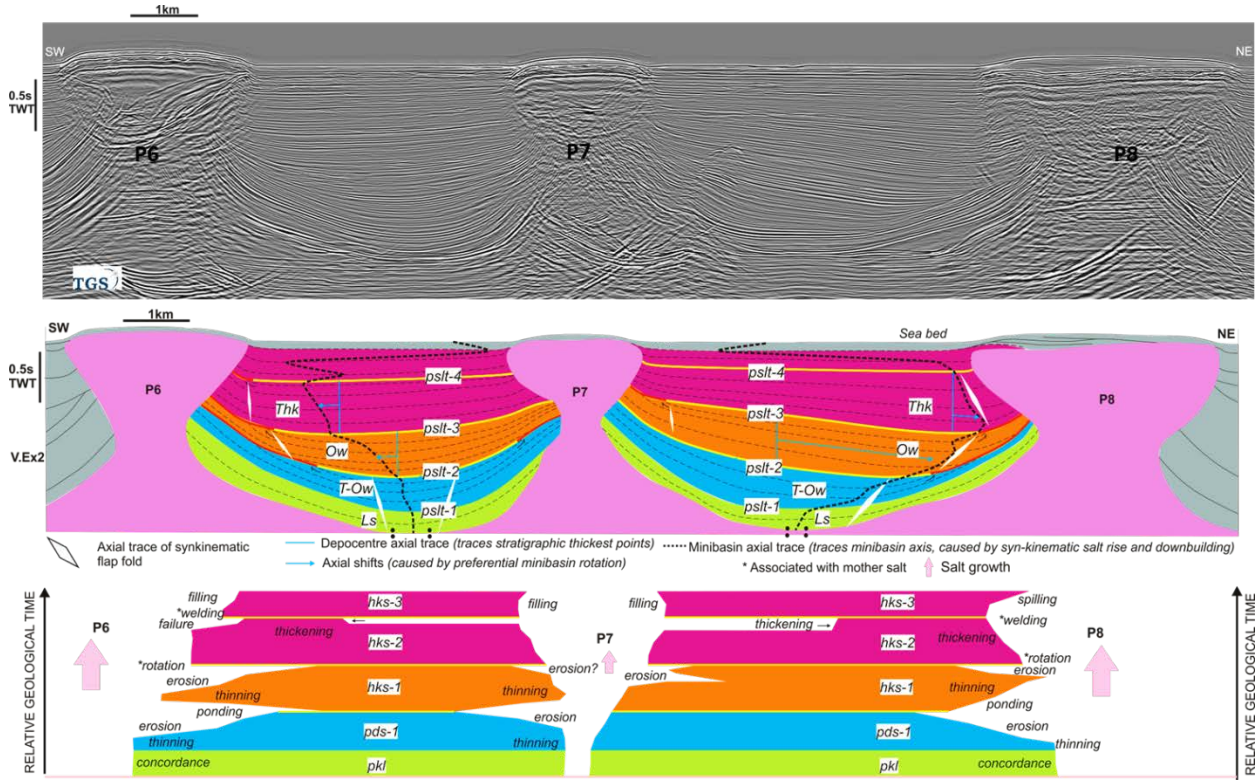

The diapirs P6, P7 & P8 (Fig. 10) are vertical and mostly symmetrical salt stocks with a characteristic hourglass geometry with a neck and bulbous head indicating late-stage and ingoing contraction. The minibasin profile between diapirs P6/P7 shows angular halo-kinematic boundaries on both flanks of the minibasins in the pre-diapiric sequence, suggesting no significant variation in growth rates of bounding diapirs at the time. Subsequent halo-kinematic sequences show angular halo-kinematic boundaries on the minibasin flank to the more rapidly growing diapir P6 as indicated by a depocenter axial trace advancing towards diapir P6 in

younger minibasin depositional sequences. In the P7/P8 minibasin profile, P8 diapir is the faster growing diapir through time and is evident from erosional halo-kinematic terminations in each stratigraphic sequence and a minibasin axial trace skewed towards diapir P8. Diapir P7 has no apparent erosional terminations on either side of the truncated hook sequences (Thk) which may suggest the absence of bathymetric relief due to ceasing salt flow into the diapir. Seismic stratal patterns within sequence packages in minibasin between diapirs P6 & P7 (Fig. 10), P7 & P8 (Fig. 10) consist of one layered sequence (Ls), one truncated onlap wedge sequence (T-Ow), one onlap wedge sequences (Ow) and two truncated hook (Thk) sequences. Hence, sedimentary wheeler diagrams of minibasins between diapirs P6/P7 and diapirs P7/P8 show one pre-kinematic layer (pkl), one syn-kinematic pre-diapiric sequence (pds) and three halo-kinematic sequences (hks).

Figure 11: Un-interpreted (top) and interpreted seismic interpretation (middle) and sedimentary wheeler diagram (bottom) of the DL-P5 and DL-P9 dip direction diapir-minibasin profiles.

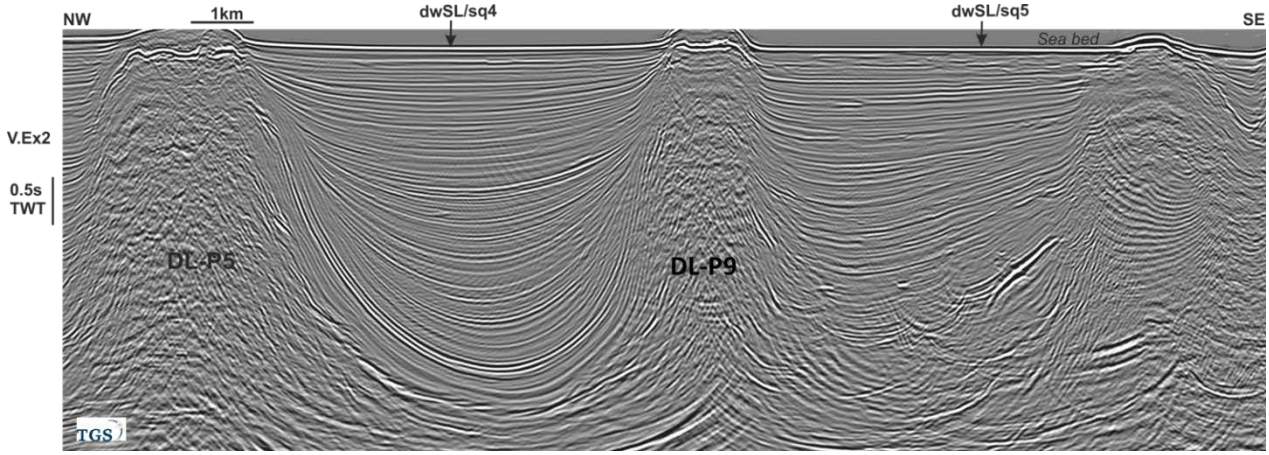

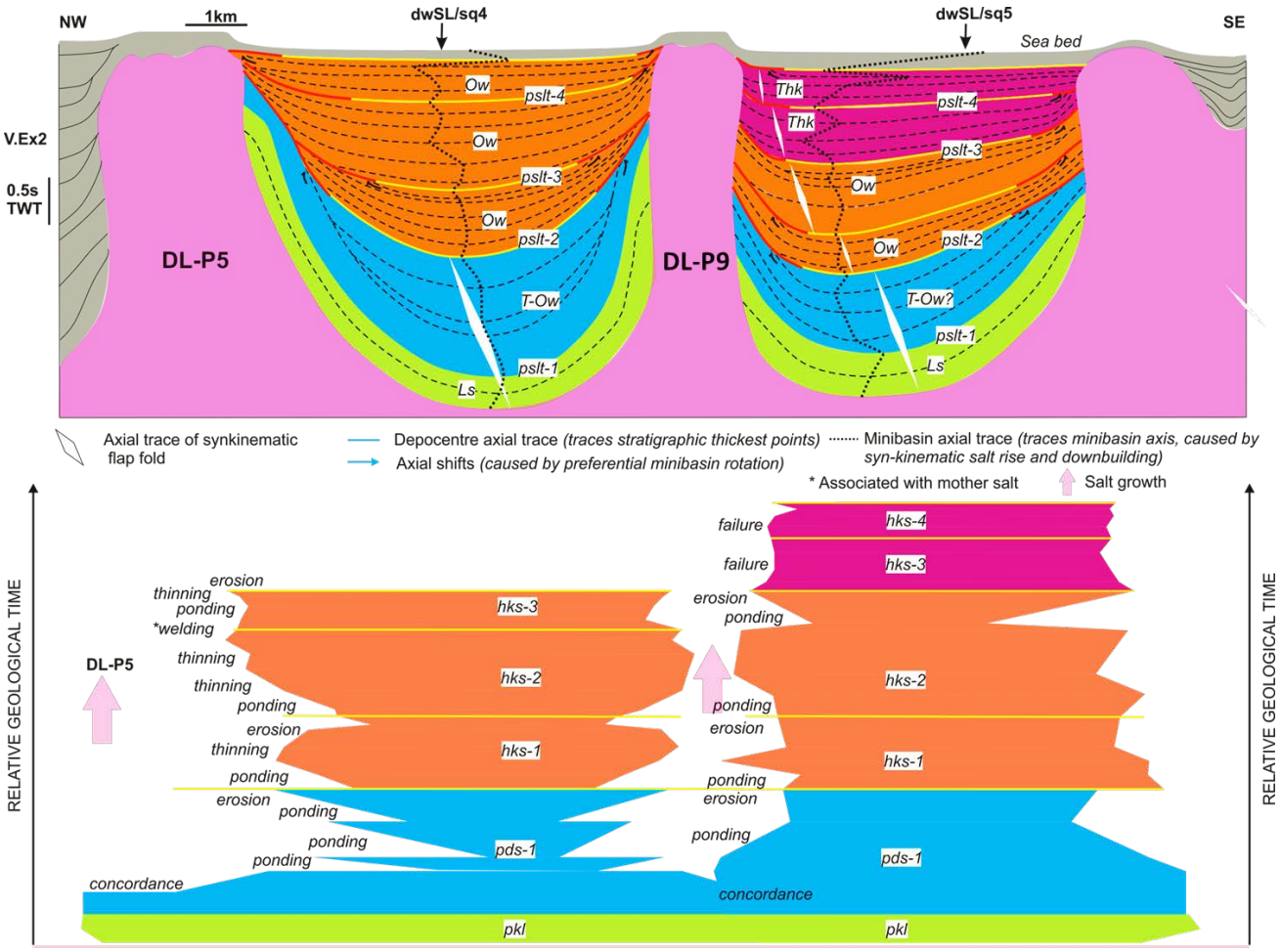

Diapir P5 (Fig. 11) features in dip section a c. 2 km wide stem and wide base. Diapir P9 (Fig. 11) to the SE features a c. 1km wide narrow stem and a relatively narrow base. The minibasin flank adjacent to diapir P5 shows angular erosional terminations on each syn-kinematic depositional sequence i.e. the pre-diapiric and subsequent halo-kinematic sequences and a symmetric minibasin axial trace suggesting similar growth rates between bounding diapirs P5 and P9 through time. The minibasin adjacent to the diapir P9 to the SE also shows angular erosional terminations on each syn-kinematic stratigraphic sequence. However, a minibasin axial trace skewed toward the diapir P9 still suggest varying growth rates of bounding diapirs and P9 being the faster growing diapir.

The sedimentary wheeler diagram show intermittent local halokinetic events in depositional successions within the minibasin stratigraphic sequences. Ponding occur during periods of high sedimentation prior to minibasin weld. Erosion/erosive processes results from topographic relief of inflating salt [see also Andrie et al (2012), Giles and Rowan (2012), Kernen et al (2012)] or in other words, bathymetric base level isostasy of folded strata above regional datum. The progressive erosive surfaces of the truncated onlap wedge and onlap wedge sequences suggest longer depositional periods and relative high ratios of sedimentation to salt rise. The truncated hook sequence with thinner stratal units and flat erosive surfaces suggest shorter depositional periods during stages of high diapir growth rates.

6. Schematic structural restorations

Schematic structural restoration is carried out for analysis of temporal structural configurations and depositional patterns respectively within minibasins. Restored temporal profiles for seismic cross section P1 (Fig. 12), P2(E) (Fig. 13) are labelled (*T.1* to *T.5)* further demonstrates formation of layered *pre-kinematic* sequence*,* truncated onlap wedge *pre-diapiric* sequence, onlap wedge halo-kinematic sequence and truncated hook halo-kinematic sequence developed in this study on a minibasin scale.

Figure 12: Kinematic restoration of the P1 diapir-minibasin profile. Five stratigraphic packages are restored from flattening individual stratigraphic boundaries.

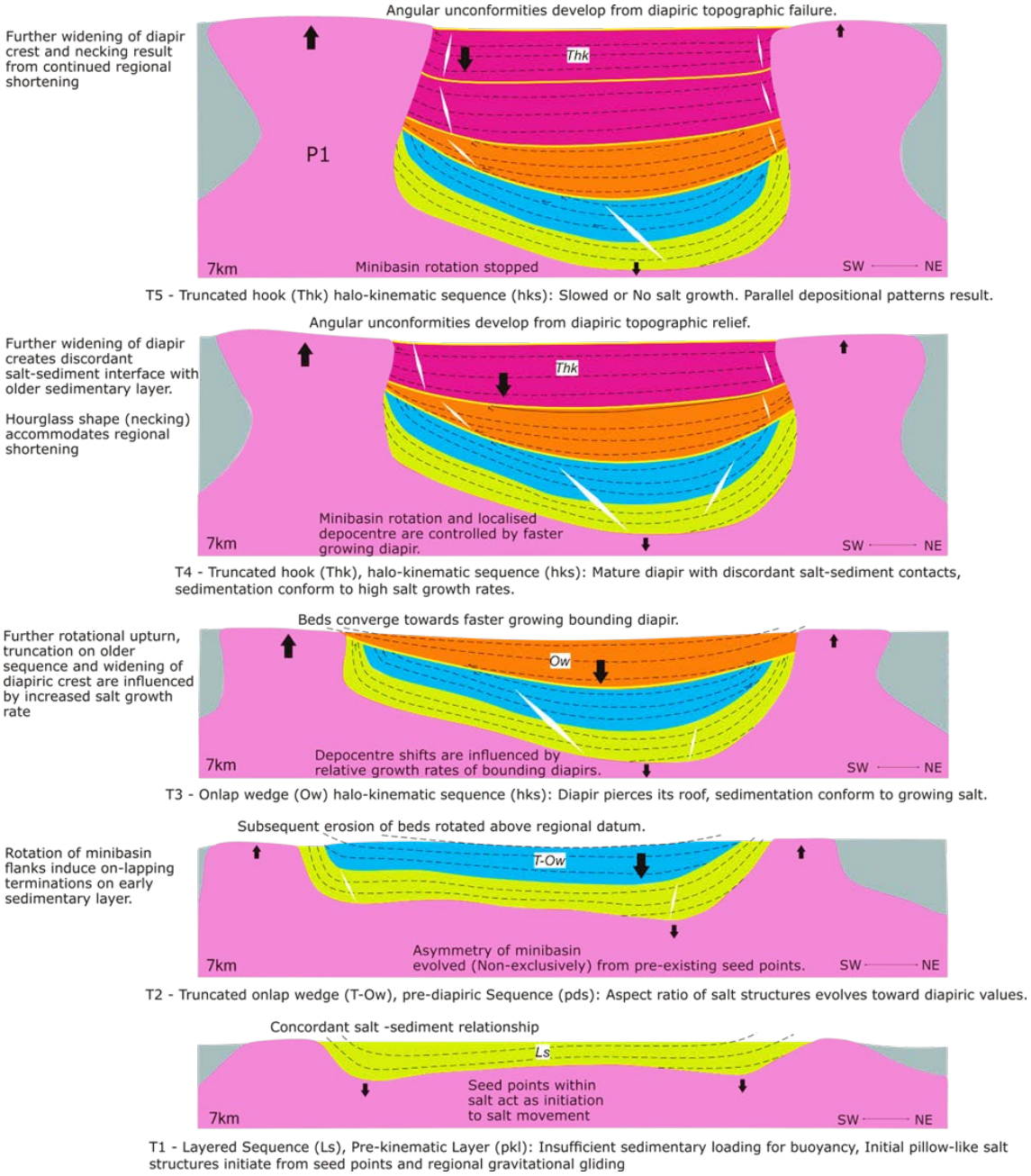

P1 diapir-minibasin profile:

T.1 shows a pre-kinematic depocentre profile. No discordant salt-sediment contacts. Salt pillows and seed points as the initial pre-kinematic configuration are assumed, implying minimal differential loading prior to initiation of regional halokinesis. Concordant sedimentary cover is over stationary salt pillows. The pre-kinematic layers include small thickness variation around seed points located at the foot of early salt structures flanks. The seed points may remain in subsidence until the onset of kinesis. Further explanations for seed points can be seen in (Peel 2014).

T.2 shows a pre-diapiric depocentre profile. Early syn-kinematic package converges towards the rising salt structure prior to diapirism. No apparent discordant salt-sediment contacts. Sequential erosional surfaces that later form the truncated onlap wedge sedimentary pattern develops from erosion of syn-kinematic beds plastically rotated above regional datum. The salt structure would most likely be in an active kinematic phase, penetrating a thin sedimentary roof.

T.3, *T.4*, shows syn-kinematic minibasin profiles. These syn-kinematic packages evolve in diapiric growth phase and are therefore labelled as halo-kinematic sequences in this study. Kinematic sequence boundaries are on-lapped by younger sediments or truncated by older underlying sediments. Kinematic sequences occur in diapiric growth phase and are bound at top and base by unconformable kinematic sequence boundaries.

T.3 shows a halo-kinematic sequence wit convergence of syn-kinematic beds and onlaps at bottom stratigraphic boundary. A continuous salt growth at or close to regional datum can be inferred. Significant shift in localised depocentre can be observed

T.4 shows a halo-kinematic sequence with sub-parallel sedimentary layers all truncating on diapir flank. An increased salt expansion and growth may have created a relief above the diapir. Significant shifts in localised depocentre are focused towards faster growing diapir.

T.5 shows a kinematic sequence and Present day minibasin profile. *T.1* a layered sequence, *T.2* a truncated onlap wedge sequence, *T.3* an onlap wedge sequence, *T.4* a truncated hook sequence and *T.5* most likely a truncated hook sequence. A residual halo-kinematic sequence may retain as stratigraphic thinning above the salt structure.

The minibasins depocentres T.2 to T.5 migrate towards the salt structures flanks in the later stages of kinesis.

Figure 13: Kinematic restoration of the P2(E) diapir-minibasin profile. Five stratigraphic packages are restored from flattening individual stratigraphic boundaries.

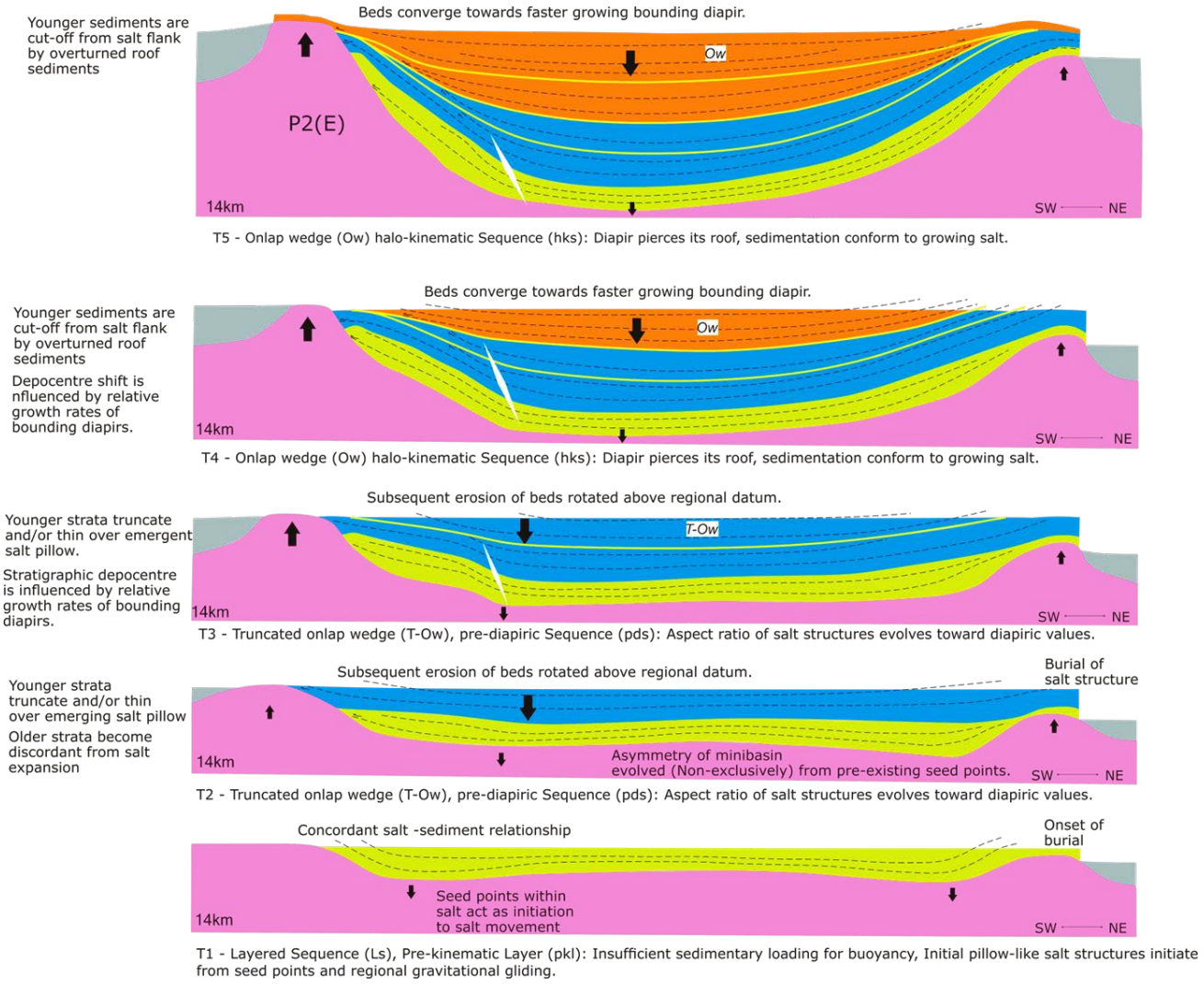

P2 (E) diapir-minibasin profile:

T.1 shows a pre-kinematic depocentre profile. No discordant salt-sediment contacts. Concordant sedimentary cover is over stationary salt pillows. The pre-kinematic layers include small thickness variation around seed points located at the foot of early salt structures flanks. Onset

of burial of adjoining salt structure is observed with implications for future growth rate and possibility for piercement.

T.2 shows a pre-diapiric depocentre profile. An early syn-kinematic package with early stage discordance and crestal thinning above an emerging salt structure is interpreted. Discordance of early pre-kinematic strata is formed from early expansion of salt pillow. Sequential erosional surfaces that later form the truncated onlap wedge sedimentary pattern develops from erosion of syn-kinematic beds plastically rotated above regional datum.

T.3 shows a pre-diapiric depocentre profile. A second syn-kinematic package converges towards an emerging salt structure. Discordance of older strata is formed from rapidly expanding salt pillow.

T.4 shows a syn-kinematic minibasin profile *kinematic sequence*. A syn-kinematic package converges towards an emergent salt structure. Stratigraphic package is cut-off from salt flank by overturned minibasin flank sediments.

T.5 shows a syn-kinematic sequence and Present day minibasin profile. *T.1* a layered sequence, *T.2* & *T.3* a truncated onlap wedge sequence, *T.4* & *T.5* onlap wedge sequences and *T.5,* an onlap wedge sequence with residual syn-kinematic thinning above the P2 diapir.

7. Discussion

Structural evolution of flap folding

Structural Wheeler diagram of P1 diapir-minibasin profile (Fig. 14) produced from schematic structural restorations of the P1 diapir-minibasin profile (Fig. 12, section 6), shows the evolution of drag folding [see Schultz-Ela (2003)] within a downbuilding minibasin. Syn-kinematic packages

generally thin and upturn towards diapir flanks. The widths of structural upturn also known as drape geometries (Schultz-Ela 2003; Schultz-Ela et al. 1993) distinguish older sedimentary packages that form megaflaps [see (Callot et al. 2016; Nikolinakou et al. 2017)] from younger syn-kinematic packages that form the halokinetic sequences [see Giles and Rowan (2012)] or halo-kinematic sequences in this study [see Mianaekere and Adam (In review-b).

Figure 14: Structural wheeler diagram of P1 diapir-minibasin profile. Shows 1) evolution of drag folding within a downbuilding minibasin 2) drag folding styles for minibasin sequence successions

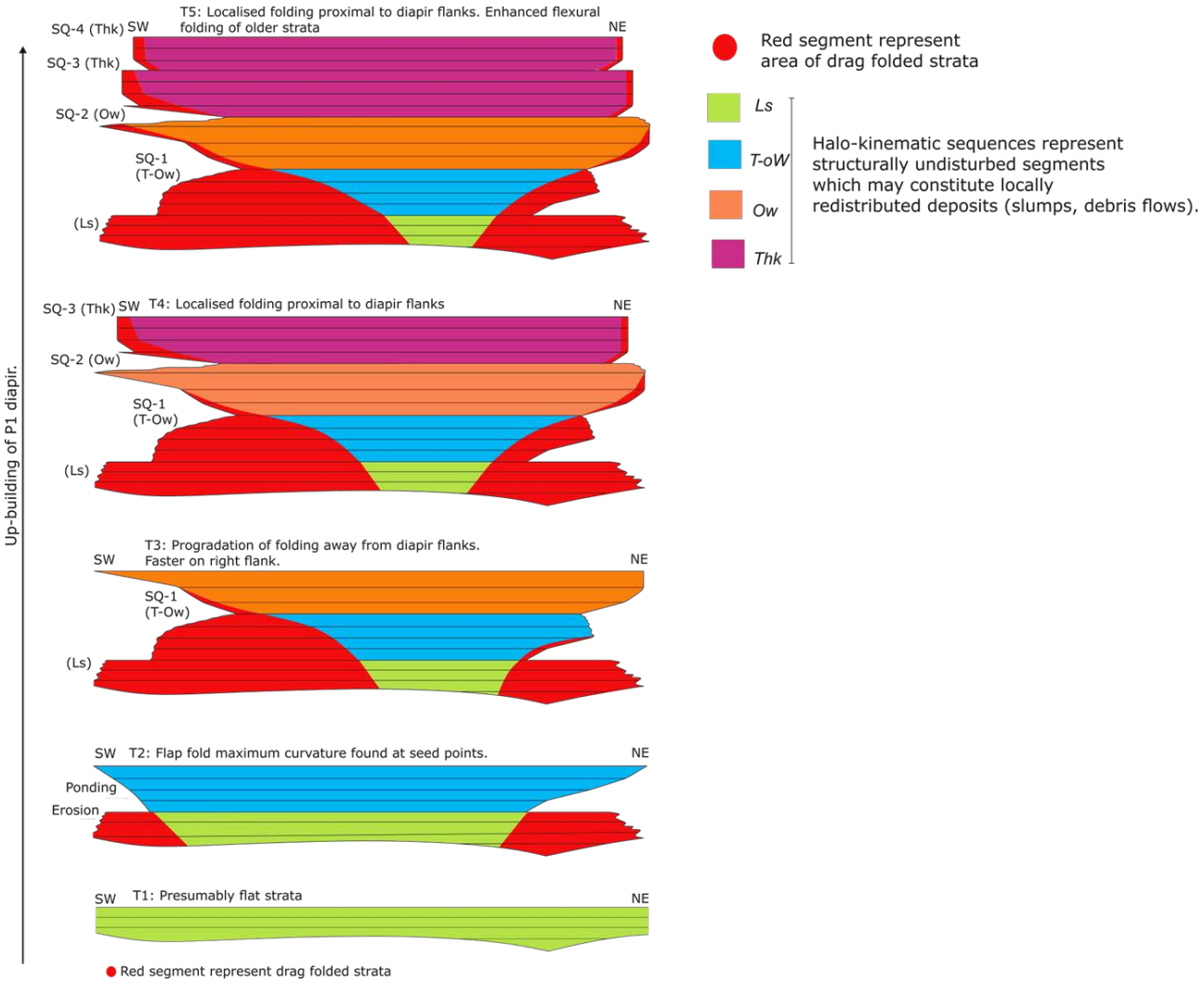

The wheeler diagram demonstrates 1) the transition from large length scale folding to small length scale folding proximal to diapir flank 2) transition from basal megaflaps to local halo-kinematic sequences. Distinguishing structural geometries of megaflaps and halo-kinematic sequences similarly analysed in recent studies are rotational upturn of stratigraphic layers, length scales of rotational upturn so that smaller scale upturn in syn-kinematic packages are categorised as halo-kinematic sequences in this study.

The rotation of depositional layer(s) starts with the onset of salt kinesis and downbuilding, hence the term flexural drag (Alsop et al. 2000). Preferential drag to one minibasin flank starts with differential salt growth rates of bounding diapir. Drag zones (Schultz-Ela 2003) indicated in the temporal profiles maybe categorised as 1) Large length scale folds associated with early depositional layers, these rotate from minibasin anchor points and 2) Small length scale folds associated with younger depositional layers, these rotate from local depocentre axis. The small scale length folds are associated with halo-kinematic sequences form in passive (diapiric) growth phase. The large scale length folds are associated with pre-diapiric sequences form in active (pre-diapiric) growth phase. Diapir flaring i.e. active high salt rise in the pre-diapiric growth phase and later minibasin welding enable large scale upturn/ flexural fold of the pre-diapiric sequence. Temporal profiles *T.3* to *T.5* shows preferential drag with faster growing diapir P1. *T.5*, present day configuration show minibasin weld and weld length constrain unfolded stratal segments and welded points in the mother salt that cannot be folded. Drag stops at minibasin weld time or at flanks of stationary salt.

Noteworthy, all flexural folds, small or large length scales form during active salt rise and downbuilding, with local aggradation rate playing a major role in its formation. The local

aggradation rate as a controlling factor is viewed cautiously since a high aggradation rate above a salt diapir results in a slower salt rise rate while a high aggradation rate above source layer increases salt supply to diapirs and hence a higher salt rise rate (Jackson and Hudec 2017). This differential loading on local scale may be in turn controlled by geometry of surrounding salt structures. Length scales of flexural upturn and thicknesses of basal minibasin depositional layers, relative timing of onset of syn-kinematic minibasin subsidence and shortening in diapir stem shown in (Fig. 15) are minibasin scale depositional patterns and structural geometries evident of minibasin response to regional contraction (refer to section 4).

Figure 15: Basinward distribution of basal flap folding and correlation of minibasin sequences to regional depositional sequence units.

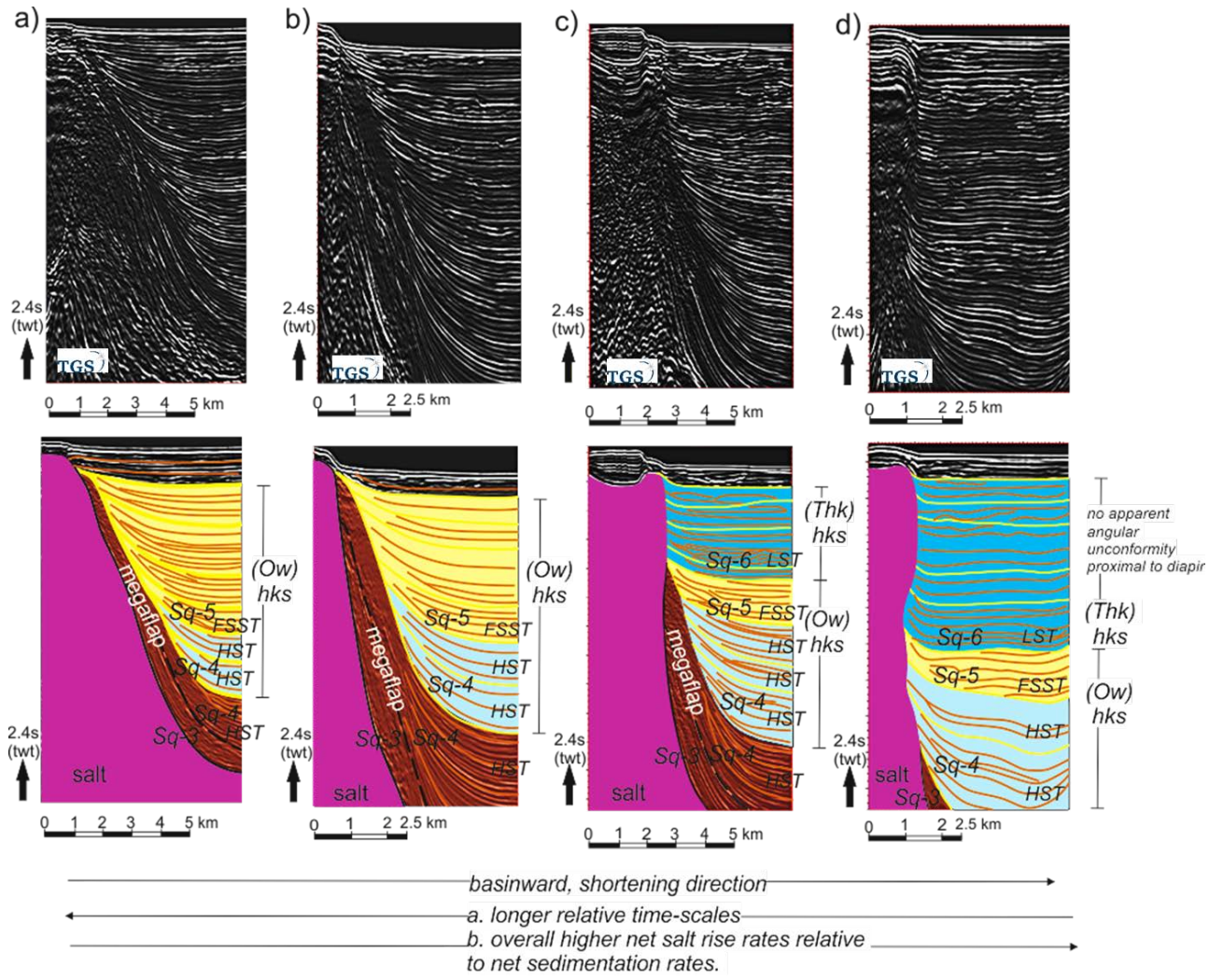

Relatively shorter megaflaps are interpreted adjacent to shortened diapirs in the distal early stage contraction province. Shorter megaflaps show thinner stratal thicknesses and are associated with early onset of high syn-kinematic subsidence. Shorter megaflaps therefore form under relatively shorter time scales i.e. higher regional contraction rates (Fig. 15) [see (Rowan et al (2016)]. The interpreted depositional sequence units (sq-3 to sq-6) shown in figure are extrapolated from proximal margin depositional sequence units (refer to section 3) to establish

influence of regional sedimentation on distal basin contractional salt tectonics. However minibasin sequences in this study form in deepwater environments.

Depositional and structural events in contractional, down-building minibasins

Stratal depositional patterns allowed for interpretations of intermittent syn-kinematic events demonstrated in wheeler diagrams and kinematic restorations of minibasin profiles. Ponding events result in onlaps, while surface erosion events result in angular truncations.

The cycle of events is depositional and structural components *ponding, flap folding and erosion* classified under the unique stratal patterns the truncated onlap wedge, onlap wedge and truncated hook sequences which are equivalent in timescales to parasequence sets likewise Composite Halokinetic Sequences by Giles & Rowan (2012).

Kinematic restorations (section 6) show period of onlap creation/ponding and erosional truncations relative to salt rise that make up sedimentary sequence events while structural folding of minibasin flanks punctuate these events. Flap folding events result from flexural drag during surgent salt rise (Schultz-Ela 2003; Waltham 1997). Therefore, the cycle of events may then be classified under the unique stratal patterns in halo-kinematic sequences in this study as follows i.e.

1. Ponding – folding – ponding – erosion: These make up syn-kinematic events within the truncated onlap wedge sequence.
2. Ponding – folding – erosion: These form syn-kinematic events within the onlap wedge sequence and

3. Folding – erosion: These make up syn-kinematic events within the truncated hook sequence.

Syn-kinematic events within minibasin sequence packages involving periods of ponding, flap folding and erosion result from significant changes in relative rates of local salt rise and local sedimentation. Influences of relative rates of salt rise and sedimentation have in previous studies been affiliated with geometrical configurations adjacent to salt structures [see Giles and Lawton (2002) and Kernen et al (2012)].

Significant changes in relative rates of salt rise and sedimentation are inferred from depocentre shifts and minibasin rotation observed in interpreted diapir-minibasin seismic profiles and restored seismic profiles in this study. Stratal depocentre shifts (migrating depocentres) (Hudec et al. 2009a) appear as overall minibasin rotation and are influenced by the preferential flexural drag caused by local differential growth rates of bounding diapirs (Hudec and Jackson 2007; Hudec et al. 2009a; Jackson and Hudec 2017) or as a direct response to regional contraction and shortening (Duffy et al. 2017).

Flanks of faster growing diapir become the focus of accommodation dictating stratigraphic depocentre axis. P5 diapir-minibasin profile (section 5) showing a highly skewed trajectory of overall minibasin axis towards the P5 diapir is the best case example in this study and in line with concepts of rim or peripheral synclines (Brandes et al. 2012). i.e. A shift from salt-floored downbuilding (Hudec et al. 2009a; Vendeville 2002) to peripheral sinks is a critical cue to changes in controlling factors during minibasin evolution. Such changes in controlling factors may be 1) depletion and welding of autochthonous layer (Ferrer et al. 2014; Heidari et al. 2016; Jackson et al. 2010), indicated here in sedimentary wheeler diagrams, 2) increased salt rise rate

resulting from increased contraction rates may affect salt shapes creating peripheral accommodation (Brun and Fort 2004; Letouzey et al. 1995; Massimi et al. 2007), in such a case, syn-kinematic packages show thickening as opposed to thinning [see (Giles et al. 2004; Giles and Rowan 2012)] towards faster growing diapir.

8. Conclusion

Minibasin sequence divisions are defined by internal stratal depositional patterns and external structural geometries. This is necessary to establish more robust definitions and classifications of minibasin sequences. This study provides an approach to improved kinematic analysis of diapir and minibasin evolution and interaction with depositional systems at local scale. Minibasin sequences consist of pre-kinematic layer, pre-diapiric and halo-kinematic sequence packages. Structural drags of the minibasin sequences initiates and evolve from the onset of vertical salt kinesis and therefore interplay in the sequence cycles of the pre-diapiric and kinematic sequences. The cycle of events is sedimentary and structural components *ponding, flap folding and erosion*

9. ACKNOWLEDGEMENTS

We are especially grateful to TGS for providing the seismic data used in this study. At TGS, we are particularly thankful to Neil Hodgkinson for detailed review of this work and for granting the permission to publish. We address our gratitude to IHS Markit for authorising the use of Kingdom: Seismic and geological interpretation software as part of the Royal Holloway academic licence agreement. We extend our thanks to Ian Watkinson at and Peter Burgess (former) at Royal Holloway, Earth Sciences department for invaluable discussions on sequence stratigraphic interpretations that inspired the near diapir scale wheeler diagrams in this study. Special thanks

to Mark Rowan for stimulating discussions on Halokinetic Sequence Stratigraphy aspects of this work.

10. References

Adam, J., Ge, Z. & Sanchez, M. 2012. Salt-structural styles and kinematic evolution of the Jequitinhonha deepwater fold belt, central Brazil passive margin. Marine and Petroleum Geology, **37**, 101-120, doi: https://doi.org/10.1016/j.marpetgeo.2012.04.010.

Adam, J., Grujic, D. & Ings, S. 2005. 4-D Physical Modeling of Tectonics and Basin Migration during Salt Mobilization at Passive Margins. *2006 AAPG Annual Convention*, Calgary.

Adam, J., Krezsek, C. & Grujic, D. 2006. Thin-skinned extension, salt dynamics and deformation in dynamic depositional systems at passive margins. *8th SEGJ International Symposium Conference Proceedings,*, Kyoto, Japan, 6.

Adam, J. & Salt Dynamics Group. 2008. 4D Physical Simulation of Basin-Scale Salt Tectonic Processes and Coupled Depositional Systems from the Rift Basin to Modern Continental Margin. Touch Briefings - Exploration & Production Oil&Gas Review, **6**, 94-97.

Alsop, G.I., Brown, J.P., Davison, I. & Gibling, M.R. 2000. The geometry of drag zones adjacent to salt diapirs. Journal of the Geological Society of London, **157**, 1019-1029.

Andrie, J.R., Giles, K.a., Lawton, T.F. & Rowan, M.G. 2012. Halokinetic-sequence stratigraphy, fluvial sedimentology and structural geometry of the Eocene Carroza Formation along La Popa salt weld, La Popa Basin, Mexico. Geological Society, London, Special Publications, **363**, 59-79, doi: 10.1144/SP363.4.

Aschoff, J.L. & Giles, K.A. 2005. Salt diapir-influenced, shallow-marine sediment dispersal patterns: Insights from outcrop analogs. AAPG Bulletin, **89**, 447-469.

Brandes, C., Pollok, L., Schmidt, C., Wilde, V. & Winsemann, J. 2012. Basin modelling of a lignite-bearing salt rim syncline: insights into rim syncline evolution and salt diapirism in NW Germany. Basin Research, **24**, 699-716, doi: 10.1111/j.1365-2117.2012.00544.x.

Brun, J.-P. & Fort, X. 2011. Salt tectonics at passive margins: Geology versus models. Marine and Petroleum Geology, **28**, 1123-1145, doi: 10.1016/j.marpetgeo.2011.03.004.

Brun, J. & Fort, X. 2004. Compressional salt tectonics (Angolan margin). Tectonophysics, **382**, 129-150.

Butler, R.W.H., McClelland, E. & Jones, R.E. 1999. Calibrating the duration and timing of the Messinian salinity crisis in the Mediterranean: linked tectonoclimatic signals in thrust-top basins of Sicily. Journal of the Geological Society, London, **156**, 827-835.

Callot, J.-p., Salel, J.-f., Letouzey, J., Daniel, J.-m. & Ringenbach, J.-c. 2016. Three-dimensional evolution of salt-controlled minibasins : Interactions , folding , and mega fl ap development. **9**, 1419-1442, doi: 10.1306/03101614087.

Carminati, E., Doglioni, C., Gelabert, B., Panza, G.F., Raykova, R.B. & Roca, E. 2004. Evolution of the Western Mediterranean. Principles of Phanerozoic Regional Geology, 1-29.

Droz, L., dos Reis, a.T., Rabineau, M., Berné, S. & Bellaiche, G. 2006. Quaternary turbidite systems on the northern margins of the Balearic Basin (Western Mediterranean): A synthesis. Geo-Marine Letters, **26**, 347-359, doi: 10.1007/s00367-006-0044-0.

Duffy, O.B., Fernandez, N., Hudec, M.R., Jackson, M.P.A., Burg, G., Dooley, T.P. & Jackson, C.A.L. 2017. Lateral mobility of minibasins during shortening: Insights from the SE Precaspian Basin, Kazakhstan. Journal of Structural Geology, **97**, doi: 10.1016/j.jsg.2017.02.002.

Ferrer, O., Roca, E. & Vendeville, B.C. 2014. The role of salt layers in the hangingwall deformation of kinked-planar extensional faults: Insights from 3D analogue models and comparison with the Parentis Basin. Tectonophysics, **636**, 338-350, doi: http://dx.doi.org/10.1016/j.tecto.2014.09.013.

Gemmer, L., Ings, S., Medvedev, S. & Beaumont, C. 2004. Salt tectonics driven by differential sediment loading Stability analysis and finite-element experiments.

Giles, K.A. & Lawton, T.F. 2002a. Halokinetic Sequence Stratigraphy Adjacent to the El Papalote Diapir, Northeastern Mexico. American Associacion of Petroleum Geologists Bulletin, **86**, 823-840, doi: 10.1306/61eedbac-173e-11d7-8645000102c1865d.

Giles, K.A., Lawton, T.F. & Rowan, M.G. 2004. Summary of Halokinetic Sequence Chacteristics from Outcrop Studies of La Popa Salt Basin, Northeastern Mexico. *24th Bob F. Perkins Research Conference*, Houston, Texas, 625-634.

Giles, K.A. & Rowan, M.G. 2012. Concepts in halokinetic-sequence deformation and stratigraphy. Geological Society, London, Special Publications, **363**, 7-31, doi: 10.1144/sp363.2.

Gottschalk, R.R., Anderson, A.V., Walker, J.D. & Da Silva, J.C. 2004. Modes of contractional salt tectonics in Angola Block 33, Lower Congo Basin, West Africa. *Sediment Interactions and Hydrocarbon Prospectivity, Concepts, Applications and Case Studies for the 21st Century*, SEPM, Houston, TX., 705-734.

Hearon IV, T.E., Rowan, M., A., G.K. & H., a.H.W. 2014. Halokinetic deformation adjacent to the deepwater Auger diapir, Garden Banks 470, northern Gulf of Mexico: Testing the applicability of an outcrop-based model using subsurface data. Special section: Salt tectonics and interpretation, **2**, SM57-SM76.

Heidari, M., Nikolinakou, M.A., Hudec, M.R. & Flemings, P.B. 2016. Geomechanical analysis of a welding salt layer and its effects on adjacent sediments. Tectonophysics, **683**, 172-181, doi: 10.1016/j.tecto.2016.06.027.

Holser, W.T., Clement, G.P., Jansa, L.F. & Wade, J.A., 1988. . In (ed.): . 1988. Evaporite deposits of the North Atlantic rift. *In*: Manspeizer, W. (ed.) *Triassic and Jurassic Rifting, Continental Breakup and the Origin of the Atlantic Ocean and Passive Margins, Dev. Geotecton*, 525-556.

Hudec, M.R. & Jackson, M.P.A. 2007. Terra infirma: Understanding salt tectonics. Earth-Science Reviews, **82**, 1-28.

Hudec, M.R., Jackson, M.P.A. & Schultz-Ela, D.D. 2009. The paradox of minibasin subsidence into salt: Clues to the evolution of crustal basins. Bulletin of the Geological Society of America, doi: 10.1130/B26275.1.

Ings, S., Beaumont, C. & Gemmer, L. 2004. Numerical Modeling of Salt Tectonics on Passive Continental Margins: Preliminary Assessment of the Effects of Sediment Loading, Buoyancy, Margin Tilt, and Isostasy. *24th Annual GCSSEPM Foundation Bob F. Perkins Research Conference Proceedings*, 38-68.

Jackson, M., Cloos, M., Hudec, M., Steel, R., Sen, M. & Peel, F. 2010. An Analysis of Salt Welding.

Jackson, M.P.A. & Hudec, M.R. 2011. Salt Tectonics: Priciples and Practice

Jackson, M.P.A. & Hudec, M.R. 2017. Salt Tectonics: Principles and Practice. Cambridge University Press.

Kernen, R.A., Giles, K.A., Rowan, M.G., Lawton, T.F. & Hearon, T.E. 2012a. Depositional and halokinetic-sequence stratigraphy of the Neoproterozoic Wonoka Formation adjacent to Patawarta allochthonous salt sheet, Central Flinders Ranges, South Australia. *In*: Archer, S.G., Alsop, G.I., Hartley, A.J., Grant, N.T. & Hodgkinson, R. (eds.) *Salt Tectonics, Sediments and Prospectivity*. Geological Society, 81-105.

Letouzey, J., Colletta, B., Vially, R. & Chermette, J.C. 1995. Evolution of Salt-Related Structures in Compressional Settings. *In*: Jackson, M.P.A., Roberts, D.G. & Snelson, S. (eds.) *Salt tectonics: a global perspective: AAPG Memoir*. AAPG, 41-60.

Madof, A.S., Christie-Blick, N. & Anders, M.H. 2009. Stratigraphic controls on a salt-withdrawal intraslope minibasin, north-central Green Canyon, Gulf of Mexico: Implications for misinterpreting sea level change. AAPG Bulletin, **93**, 535-561, doi: 10.1306/12220808082.

Maillard, A., Gaullier, V., Vendeville, B.C. & Odonne, F. 2003. Influence of differential compaction above basement steps on salt tectonics in the Ligurian-Provencal Basin, Northwest Mediterranean. Marine and Petroleum Geology, **20**, 13-27.

Mannie, A.S., Jackson, C.A.L. & Hampson, G.J. 2014. Shallow-marine reservoir development in extensional diaper-collapse minibasins: An integrated subsurface case study from the Upper Jurassic of the Cod terrace, Norwegian North Sea. AAPG Bulletin, **98**, 2019-2055, doi: 10.1306/03201413161.

Massimi, P., Quarteroni, A., Saleri, F. & Scrofani, G. 2007. Modeling of salt tectonics. Computer Methods in Applied Mechanics and Engineering, **197**, 281-293.

Mianaekere, V. & Adam, J. in review-a. Convergent contractional salt tectonics in the Western Mediterranean Messinian salt basins: Passive margin salt tectonics. *In*: London, R.H.U.o. (ed.).

Nikolinakou, M.A., Heidari, M., Hudec, M.R. & Flemings, P.B. 2017. Initiation and growth of salt diapirs in tectonically stable settings: Upbuilding and megaflaps. AAPG Bulletin, **101**, 887-905, doi: 10.1306/09021615245.

Peel, F.J. 2014. How do salt withdrawal minibasins form? Insights from forward modelling, and implications for hydrocarbon migration. Tectonophysics, **630**, 222-235, doi: 10.1016/j.tecto.2014.05.027.

Rowan, M.G., Giles, K.a., Hearon IV, T.E. & Fiduk, J.C. 2016. Megaflaps adjacent to salt diapirs. AAPG Bulletin, **100**, 1723-1747, doi: 10.1306/05241616009.

Rowan, M.G., Lawton, T.F. & Giles, K.A. 2012. Anatomy of an exposed vertical salt weld and flanking strata, La Popa Basin, Mexico. Geological Society, London, Special Publications, **363**, 33-57, doi: 10.1144/sp363.3.

Rowan, M.G., Lawton, T.F., Giles, K.A. & Ratliff, R.A. 2003. Near-salt deformation in La Popa basin, Mexico, and the northern Gulf of Mexico: A general model for passive diapirism. AAPG Bulletin, **87**, 733-756.

Rowan, M.G. & Ratliff, R.A. 2012. Cross-section restoration of salt-related deformation: Best practices and potential pitfalls. Journal of Structural Geology, doi: 10.1016/j.jsg.2011.12.012.

Saura, E., Ardèvol i Oró, L., Teixell, A. & Vergés, J. 2016. Rising and falling diapirs, shifting depocenters, and flap overturning in the Cretaceous Sopeira and Sant Gervàs subbasins (Ribagorça Basin, southern Pyrenees). Tectonics, **35**, 638-662, doi: 10.1002/2015tc004001.

Schreurs, G., Haenni, R., Panien, M. & Vock, P. 2003. Analysis of analogue models by helical X-ray computed tomography. Geological Society Special Publications, **215**, 213-223.

Schultz-Ela, D.D. 2003. Origin of drag folds bordering salt diapirs. AAPG Bulletin, **87**, 757-780, doi: 10.1306/12200201093.

Schultz-Ela, D.D., Jackson, M. & Vendeville, B. 1993. Mechanics of active salt diapirism.

Storetvedt, K.M. 1973. Genesis of West Mediterranean basins. Earth and Planetary Science Letters., **21**, 22-28, doi: 10.1016/0012-821X(73)90221-5.

Tari, G., Molnar, J. & Ashton, P. 2003a. Examples of salt tectonics from West Africa: a comparative approach. *In*: Arthur, T.J., MacGregor, D.S. & Cameron, N. (eds.) *Petroleum Geology of Africa: New Themes and Developing Technologies*. Geological Society of London, Special Publications, 85-104.

Vendeville, B. 2002. A new Interpretation of Trusheim's Classic Model of Salt-Diapir Growth. Gulf Coast Association of Geological Societies Transactions, **52**.

Vendeville, B.C., Jackson, M.P.A. & Anonymous. 1990. Physical modeling of the growth of extensional and contractional salt tongues on continental slopes. AAPG Bulletin, **74**, 784.

Waltham, D. 1997. Why does salt start to move? *Tectonophysics*, 117-128.

Wheeler, H.E. 1958. Time-stratigraphy. AAPG Bulletin, **42**, 1047-1063.

F. Discussion

Rationale for case study area

The high-quality regional seismic imaging of simple salt structures and depocentres allow in-depth analysis of the salt tectonic history and kinematic evolution of a Cenozoic post-rift salt basin from the shelf extensional domain to the contractional deepwater diapir province fully positioned on oceanic crust. Pros of regional basin-scale salt tectonics and local to minibasin-scale halokinetic-depositional kinematic analysis in the west Mediterranean salt basins are as follows;

1. Geologic age of the salt basin; Cenozoic age of the Liguro-Provencal salt basin in the western Mediterranean is key influencing factor for understanding salt tectonic style and kinematics. Longer time spans mean complex, poly-phase deformation histories (Unternehr and de Clarens 2004) with consequences in uncertainties in determining rates of geological processes (Jackson and Hudec 2011) and overprinting of tectonic features overtime.
2. Salt basin type; post rift salt as in the west Mediterranean. (Kukla et al. 2010; Rowan 2014b; Warren 2010a) influences the resulting salt systems. Gravity salt systems, on post rift salt basins, such as in the west Mediterranean, Gulf of Mexico, Brazil and Canada result in distinct linked structural and kinematic domains of updip extension, transition and downdip contraction (Brun and Fort 2011b; Brun and Fort 2010) that can be readily assessed even on 2D seismic data along with the regional salt tectonic influence on minibasin evolution in particular kinematic provinces.
3. Detached thin-skinned salt tectonics; the implication for studying regional controls on minibasin evolution is that with the former, rates of regional basin tectonics is considered and with the later rates of regional contraction and shortening is considered. In older more mature salt basins, stratigraphic architectures, depositional patterns including flank geometries of minibasins and stratigraphic depocenter shifts within minibasins maybe consequent of rates of regional basin tectonic triggers.

Overview of Manuscripts

Manuscript 1 contains detailed study of gravity driven thin-skinned salt tectonic processes including progradational loading by deltaic and pelagic sedimentation in the deepwater basins overlying the oceanic crust, where detached contractional diapirs and minibasins form. Distinct salt structural domains, extensional, transitional and contractional domains typical of passive margin salt tectonic trends are segmented throughout the survey area. In parallel to literature [see dos Reis et al. (2005) and Leroux et al. (2015)], salt structural zonations and present day kinematic provinces is identified. However, wide coverage 2D PSTM data uncovered convergent regional salt tectonic trends along Gulf of Lion – Provencal and the North Balearic – Provencal basin segments (refer to manuscript 1).

Manuscript 1 further uncovers gravity driven regional salt kinematic transport in the west Mediterranean, contributing to conceptual models and concepts from (Adam et al. 2012a, b; Adam and Krezsek 2012a; Brun and Fort 2011b). In contrast to most published interpretations of gravity driven salt systems with characteristic up-dip extension, transition and basinward early and late stage

contraction domains in that order, this project showcases landward creep of the deepwater contractional province over time, reducing lateral basinward lengths of the undeformed transition domain. Comparison example from Congo (Fig. 1) and scaled physical experiments (Adam et al. 2012a) (Fig. 2) which show a basinward evolution of the contraction domain, other such examples can especially be found in studies from the Gulf of Mexico.

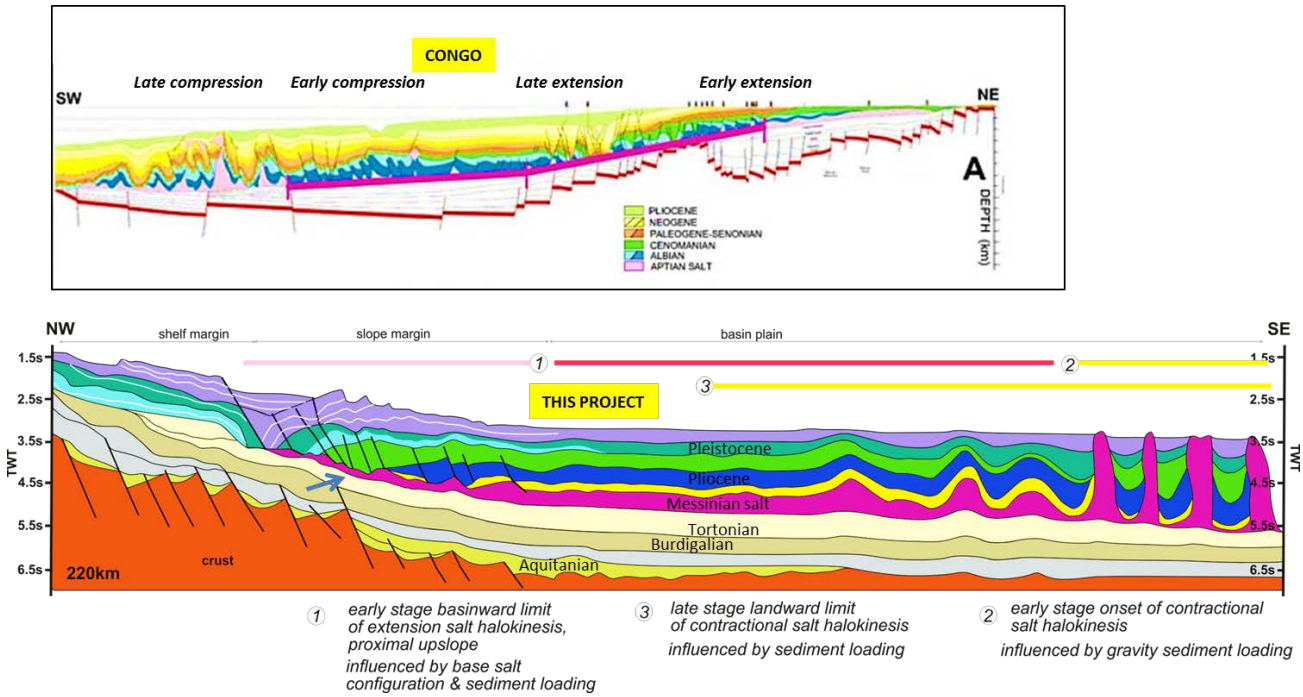

Fig, 1: Zonation of the gravity driven tectonics and the geological cross sections from Congo (top) and the west Mediterranean (bottom). Note the similar flat/ramp geometries at the base of salt (Congo- thick purple line, this project- blue arrow) that act as breaks in the continuity of the salt detachment

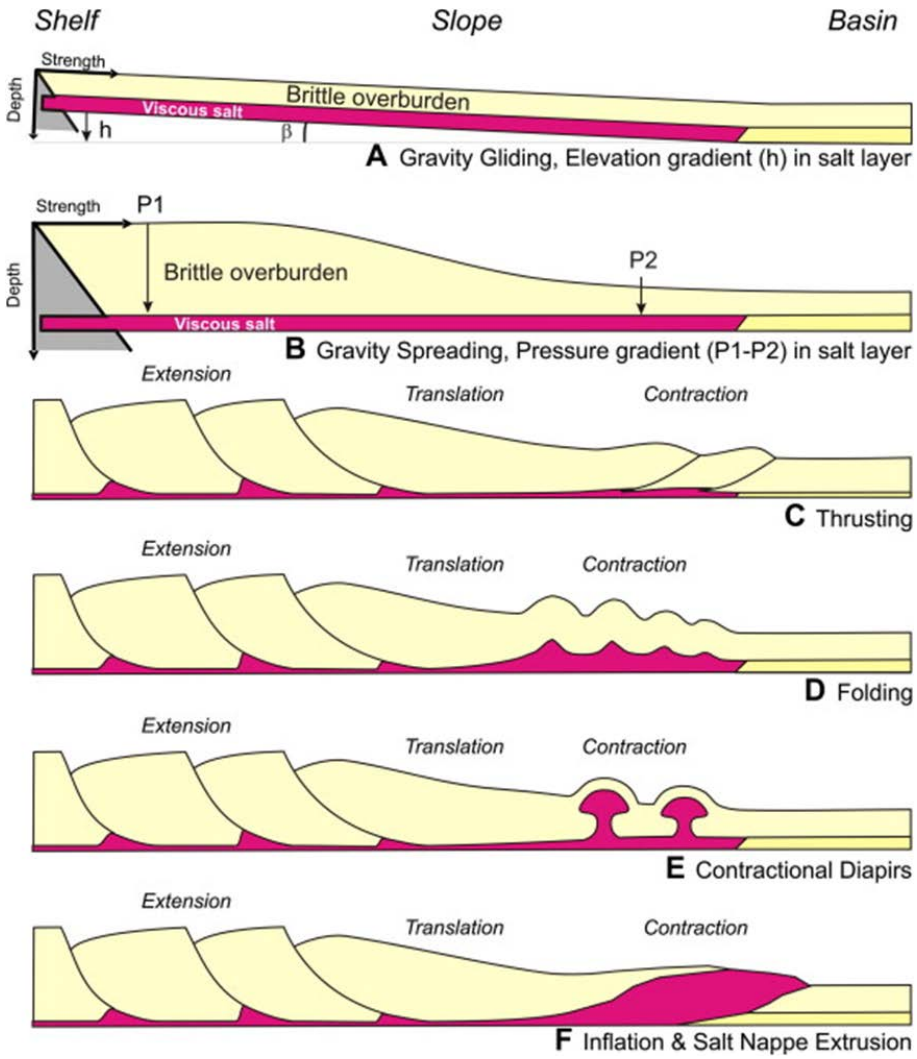

Fig, 2: Thin-skinned gravity-driven deformation in a passive margin sedimentary succession on salt substratum. A. Gravity-gliding above basinward-dipping detachment; B. Gravity spreading due to differential sediment loading; C–F: Different styles of contractional deformation in the distal salt basin: C. Thrust-dominated shortening; D. Fold-dominated shortening; E. Horizontal Contraction of pre-existing diapirs; and F. Inflation and extrusion of an allochthonous salt nappe. (Adam et al. 2012a)

Overprinting transitional domains in a gravity salt system congruent to results from this project have been established with analogue models by (Ge et al. 2019). They proposed mechanisms of overprinting translational domains and models illustrating strain transfer with undeformed translational domain, and areas of minibasins and diapirs (Fig. 3).

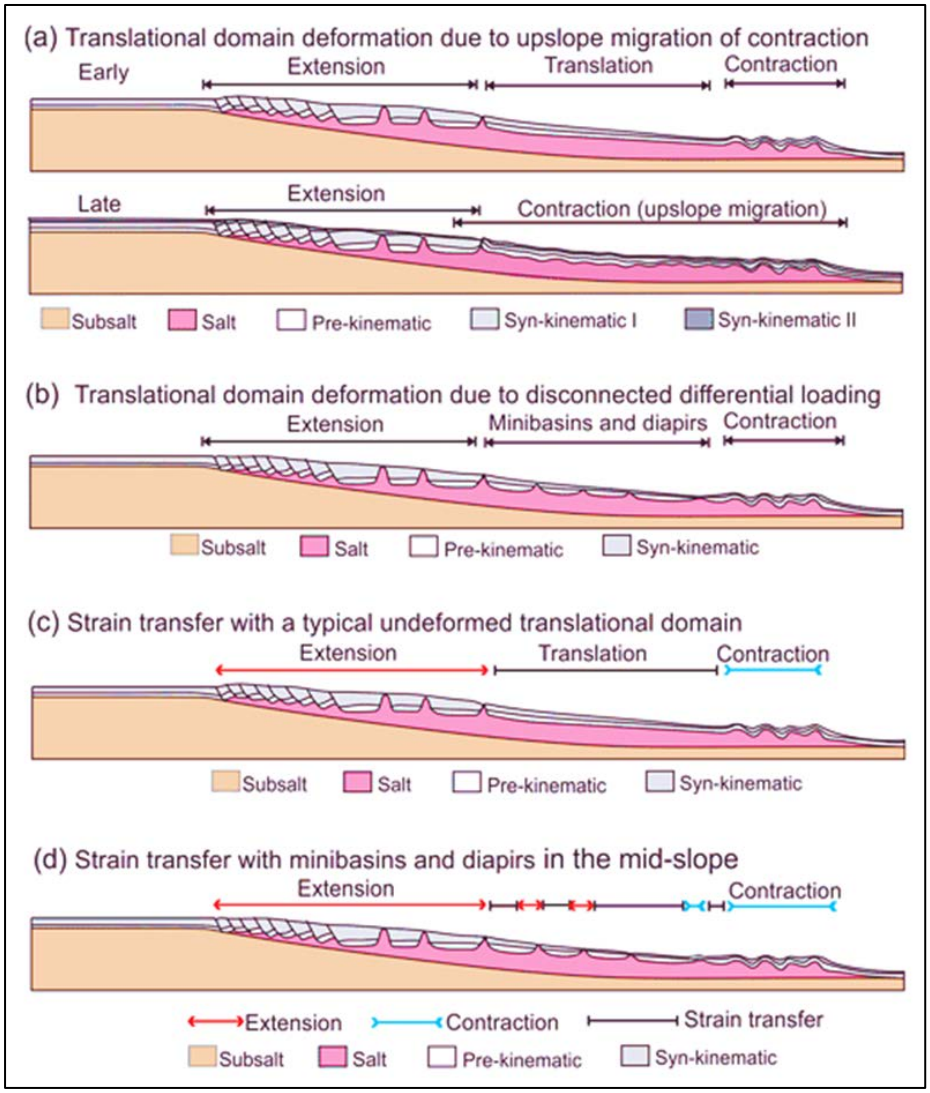

Fig, 3: Proposed mechanisms of overprinting translational domains and models illustrating strain transfer with undeformed translational domain, and areas of minibasins and diapirs. (a) Low sedimentation rate and thin supra-salt cover allows upslope migration of contraction resulting in overprinting the translational domain. (b) Sedimentary differential loading leads to the development of minibasins and diapirs in the mid-slope preventing the establishment of a stable, undeformed translational domain. (c) The undeformed translational domain in the mid-slope allows strain transfer (ST) without significant internal deformation. (d) The minibasins and diapirs in the mid-slope allow strain transfer (ST) through a combination of passive movement of minibasin and minor widening (extension) or shortening (contraction) of diapirs. (Ge et al. 2019)

Established concept from this project on the evolution of regional contraction in the West Mediterranean deepwater basin is that, the early contraction domain in the distal deep basin in early stage regional halokinesis initially contained salt pillows and anticlines that later evolved to present day bathymetric columnar diapirs and shortened diapirs and a late stage contractional domain

influenced from high continued sedimentation on basin plain contains low amplitude salt pillows which evolved from a tabular transition domain void of salt structures. (Fig. 4)

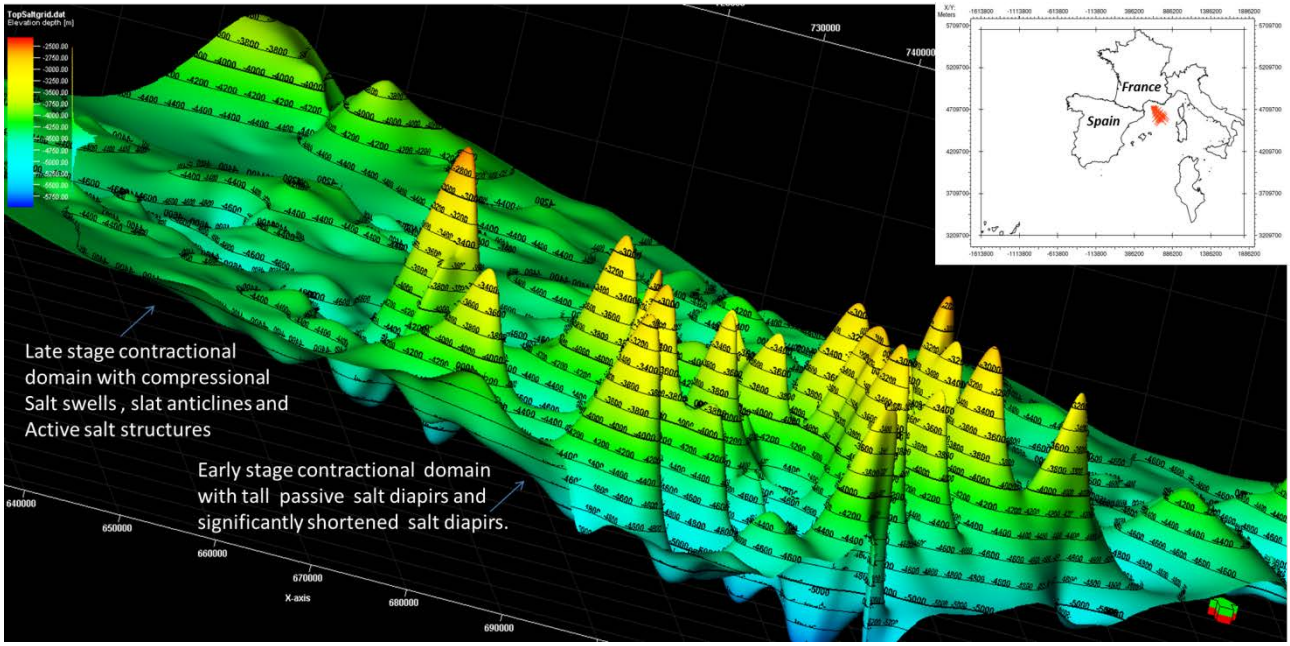

Fig, 4: Grid of top salt horizon along the Gulf of Lion – Provencal basin segment showing basin plain early and late stage contractional salt domains.

The salt kinematic history throughout the basin is controlled by basin-specific factors like sub-salt morphology, salt thickness, salt thickness variation, sedimentation rates and margin tilt. Basinward contraction and shortening of overburden is maintained by further tilting of the continental margins due to thermal subsidence and by differential loading caused by basinward progradation of clastic sediments. Contemporaneous salt withdrawal and diapir growth typically accompany basinward translation of the overburden and lead to thinning of the primary salt layer and partly welding hence slowing lateral movement of the overburden with time. Basinward contraction was more likely episodic SE of the Gulf of Lion with periods when halokinetic down-building in the distal basin was dominant salt tectonic process and periods when regional contraction and shortening were relatively high (Fig. 5). On the other hand basinward contraction was more continuous NE of the Balearic promontory which shows a diversity of salt structural styles including multiwavelength folds with vertical amplification in overburden (Fig. 5).

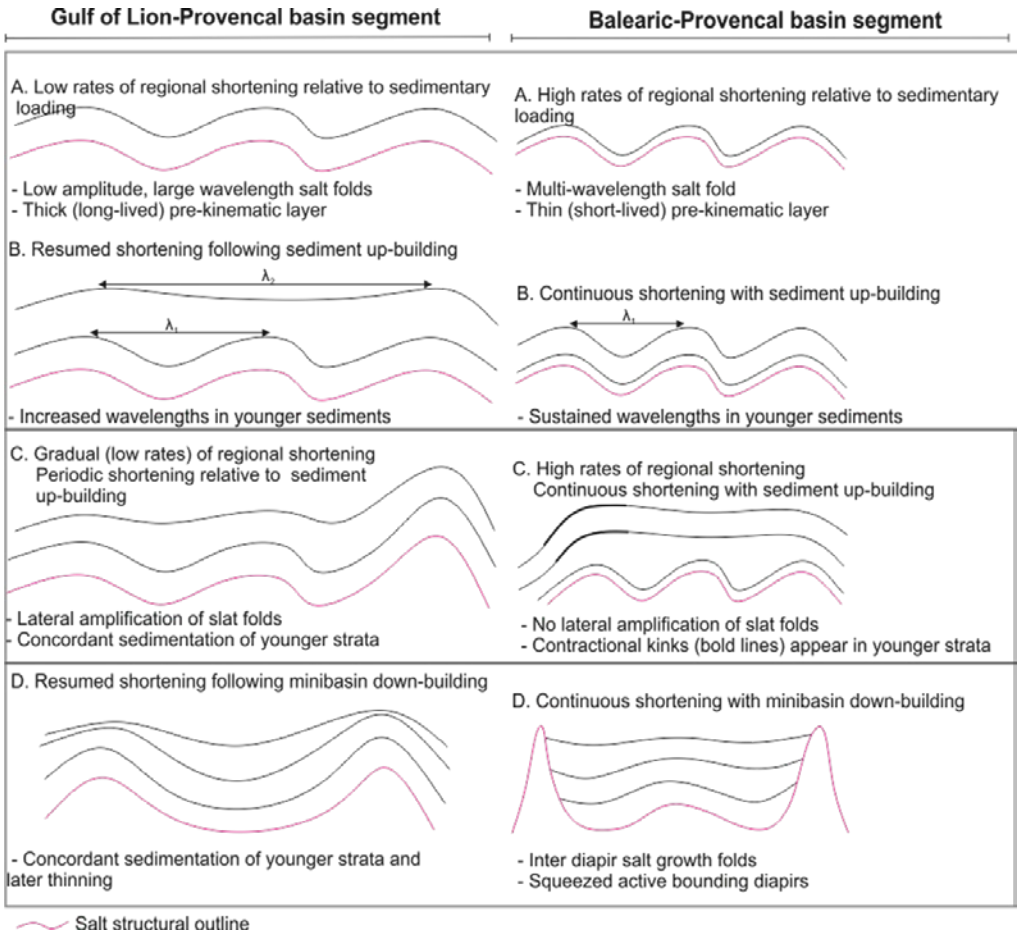

Fig, 5: Comparison of nature of contraction and analysis of periodic vs continuous contraction and shortening along the Gulf of Lion – Provencal and Balearic – Provencal basin segments.

In Manuscript 2 & 3, local scale salt tectonics analysis is focused in the down-dip contractional province with tall diapirs and mature down-building minibasins. (Fig. 6)

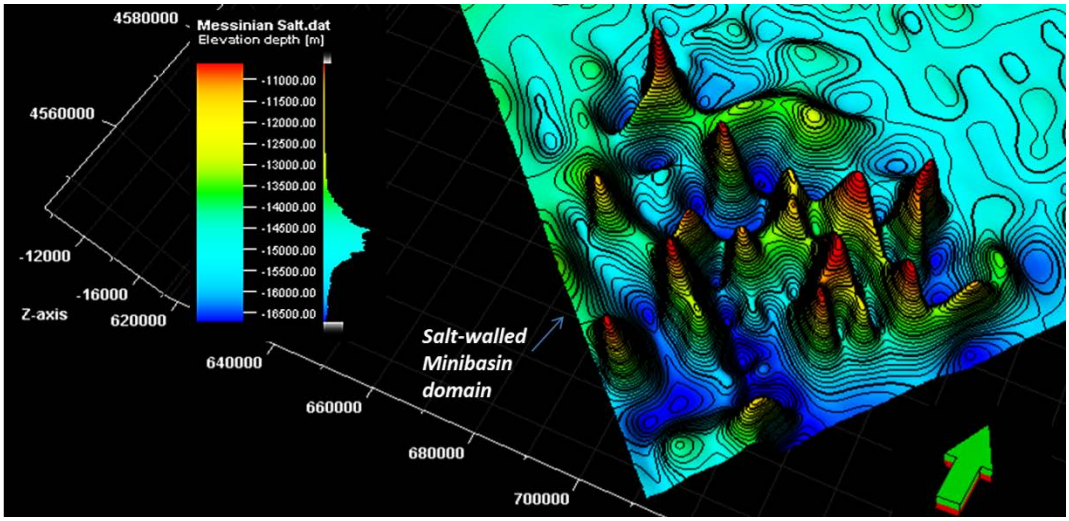

Fig, 6: Grid of top salt horizon, showing diapir and minibasin domain in the deepwater Provencal basin.

Detailed seismic interpretation of unique depositional patterns within stratigraphic sequences adjacent to salt diapirs allow inferences to kinematic growth histories of salt diapirs as a direct result from the reciprocal interactions of net salt rise rates and sedimentation rates, contributing to widely accepted concepts of halokinetic sequence stratigraphy from Giles and Rowan 2012. The tabular and tapered end member composite halokinetic sequences (Heidbach et al. 2007) were originally developed on an exposed salt weld, La Popa offshore Gulf of Mexico. The composite halokinetic sequences are unique structural configurations that form in passive salt rise phase. A recent addition to this was the basal megaflap (Callot et al. 2016; Nikolinakou et al. 2017), where pre-kinematic and early syn-kinematic stratigraphic structural configurations and related intervening sedimentation patterns aid direct recognition and interpretation of early active phase of salt rise via significant structural flap folds of early basal strata and subsequent stratigraphic onlaping. In comparison in this project, we show alternative structural and sedimentaion pattern for interpretation of early syn-kinematic active phase/pre-diapirc stage of salt growth constituting of cyclic stacking of structural folded and onlapped beds, shown as megaflap in (Fig. 7).

Later syn-kinemtaic packages with unqiue smaller scale structural flap identified in this project are comparable to halokinetic sequences by Giles & Rowan 2012 occuring in diapiric, passive phase of salt growth and are termed halo-kinematic sequences (hks) in this project. Halo-kinematic sequences like halokinetic sequences are genetically related, unconformity bound stratigraphic packages but defined mainly via unique sedimention patterns on diapir – minibasin centre scale thus labelled truncated hook (Thk) and onlap wedge (Ow) end member type halo-kinematic sequences as opposed to hook (tabular CHS) and wedge (tapered CHS) halokinetic sequences. Pre-diapiric sequence not addressed in the Giles & Rowan 2012 hook and wedge model are identified from a truncated-onlap wedge style sequence in basal strata, they also form the megaflap in this project (Fig. 7).

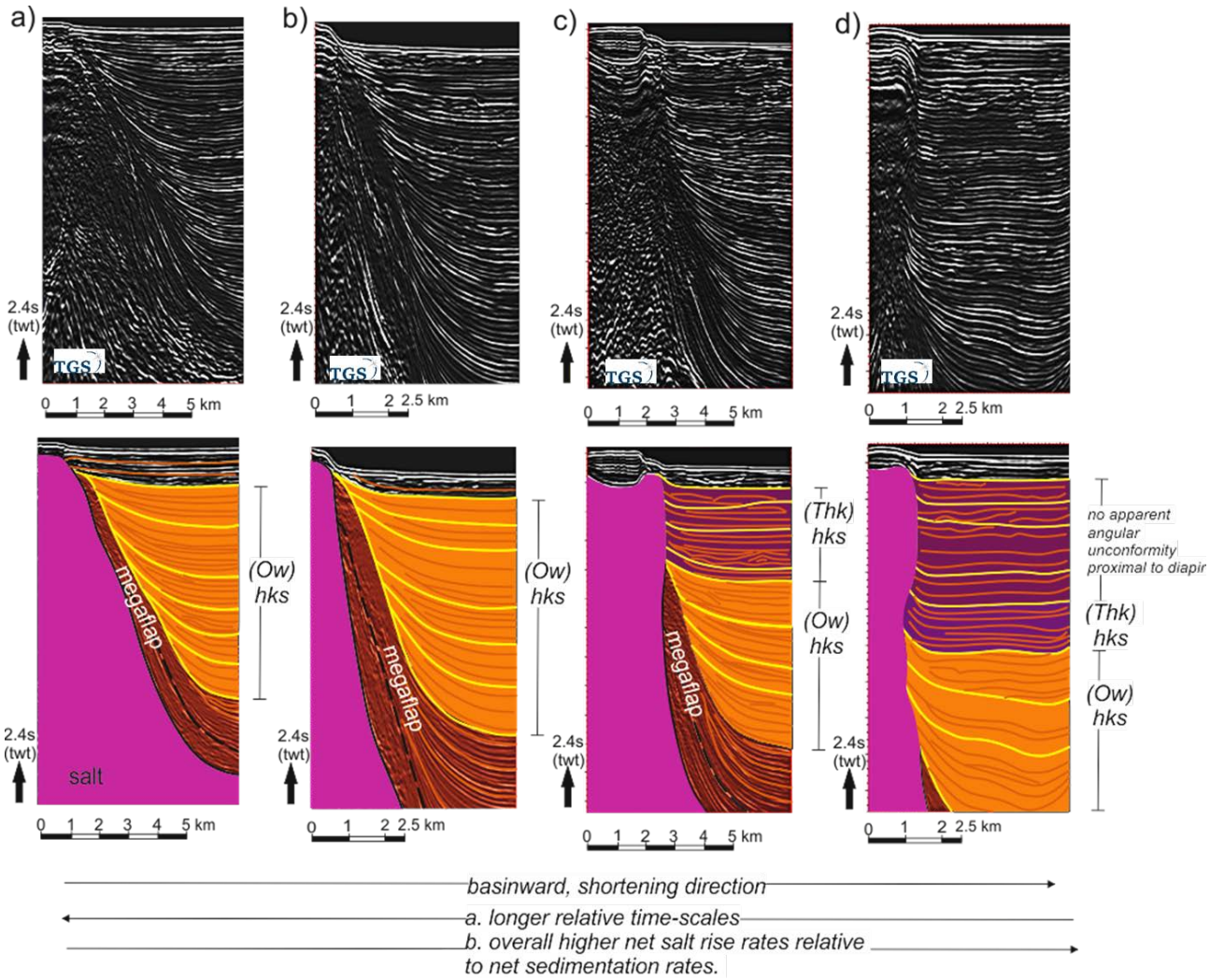

Fig, 7: Diapir proximal minibasin sequence interpretation

In Manuscript 3, we see that minibasin evolution and controls in the west Mediterranean are consequent of relative rates of salt rise, sedimentation and regional contraction. In the west Mediterranean, minibasin sequence stratigraphic analysis involved identification of unique stratigraphic depositional geometries addressed above and structural architecture of salt-walled minibasins. The minibasin domain in the deepwater Provencal Basin showcases variability in subsidence mechanism via overall minibasin architectures such as flank geometries and degree of tilt or rotation. Minibasin geometries in Provencal Basin are influenced by relative rates and timing of regional contraction and sediment loading. The interplay of regional contraction and local minibasin down-building in the Provencal Basin are apparent from structural configurations of minibasin flanks, degree of minibasin rotation and minibasin axial trace /stratigraphic depocentre trace (Fig. 8).

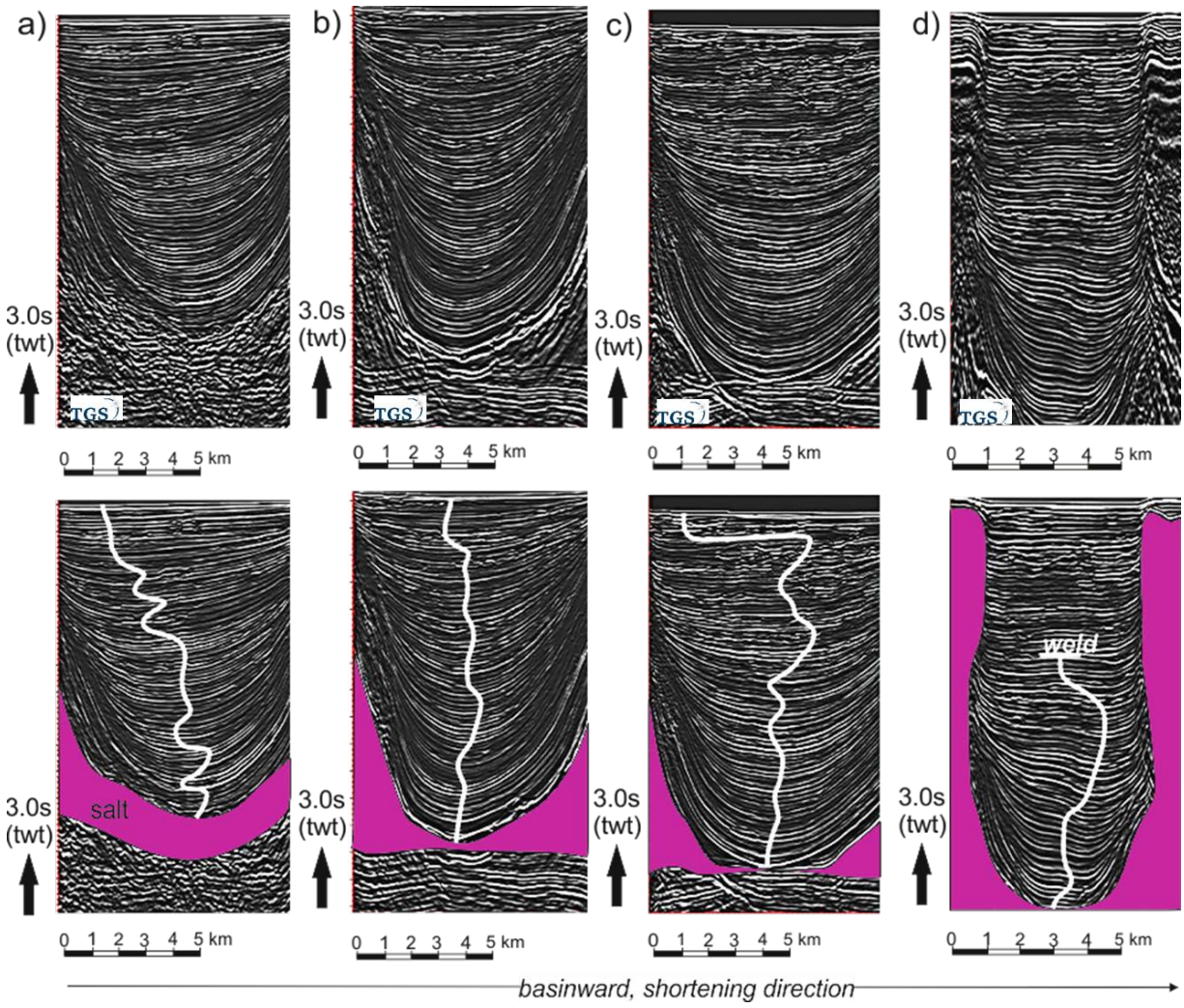

Fig, 8: Minibasin styles in basinward, shortening direction. (Thick white line) is minibasin axial trace or stratigraphic depocentre trace

Manuscript 3, therefore details application of derived concepts of formation of halo-kinematic sequences on minibasin in a contractional province. However, only U-shaped minibasins (Fig. 9) are addressed in this project. Development of W-shaped minibasin (Fig. 9) where remnant inter-diapir salt cored anticlines ripple through minibasin stratigraphic packages is still unclear in parallel with regional contraction and formation of minibasin sequence styles developed in this project. Formation of U & W-shaped minibasin was first introduced in (Peel 2014).

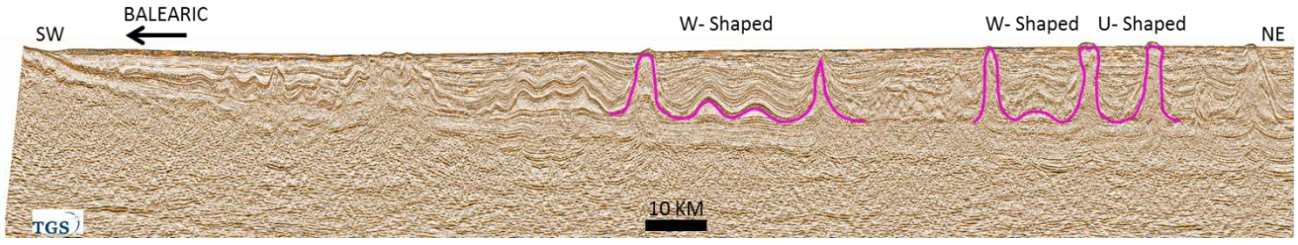

Fig, 9: Regional seismic line, along (dip direction) the Balearic – Provencal basin segment. Note w-shaped and U-shaped minibasin types.

Another aspect of results from this project in need of clarification is the interpretation of halo-kinematic sequence formed in diapiric phases of salt growth (Fig.10). Where approximately 2 to 3 km of tall salt stocks are flanked by large scale rotated flaps with minibasin stratigraphic packages that do not terminate on salt but rather on rotated flap, can a diapiric phase then been conclusively interpreted?

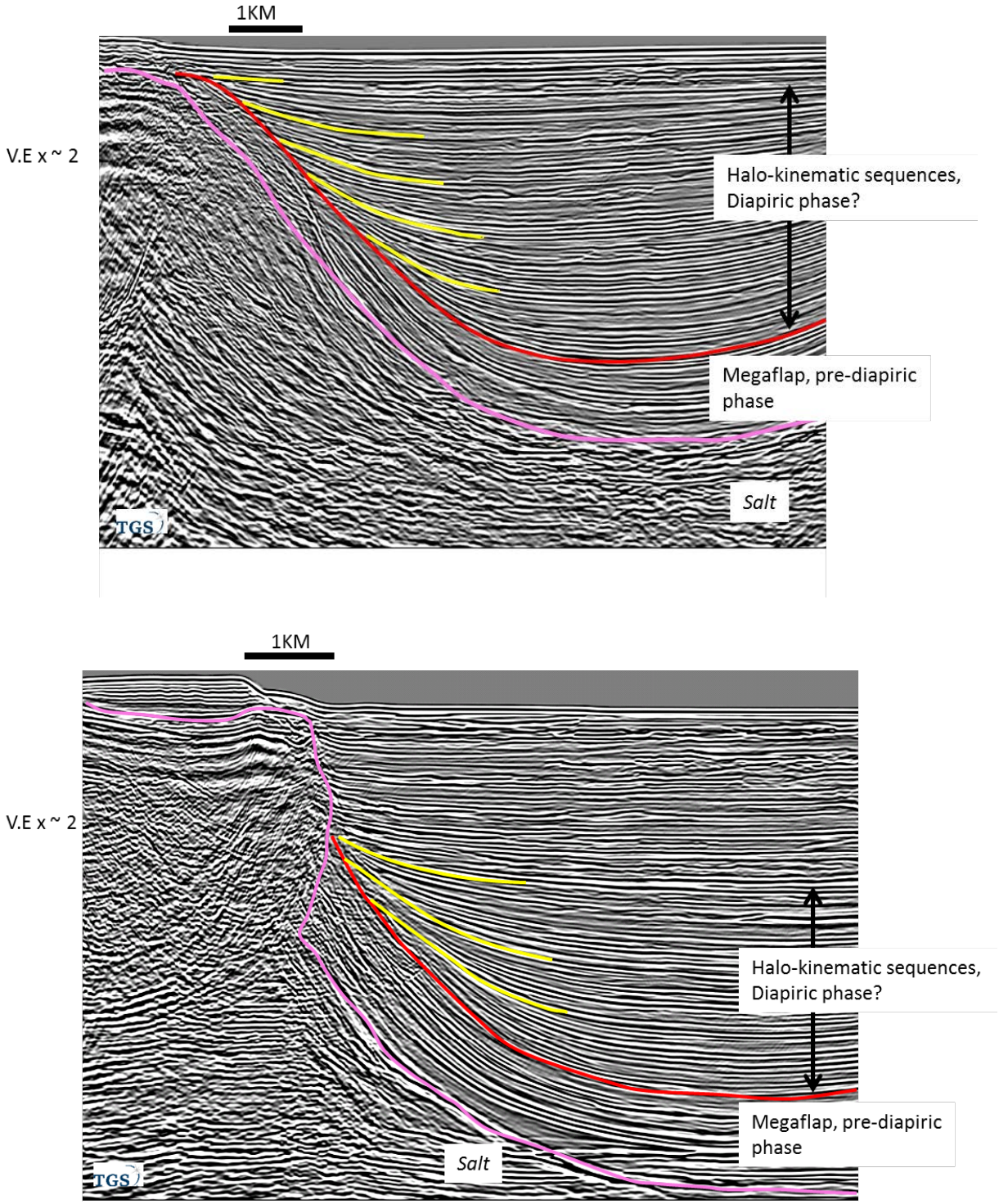

Fig, 10: Interpretation of halo-kinematic sequences and diapiric phases of salt growth.

Overview of applied methodologies: 2D vs 3D

The 2D seismic survey lines acquired in the west Mediterranean may have missed salt structures or created gaps in salt structures. However, reliable structural analysis of a salt basin was possible with the dataset used in this project offering densely spaced sample intervals, in-lines and cross-lines and therefore a full imaging of salt structures and minibasins. A quick arbitrary line with the 3D dataset offers a better control and flexibility in analysing salt structures and minibasins from different angles as oppose to analysis constrained to dip and strike as is detailed in the west Mediterranean project. Interpretations of salt diapir overhangs are at best approximates in 2D but better imaged in 3D. Depositional patterns and structural geometries proximal to diapirs and within minibasins identified in 2D sections may vary in 3D view. 3D data set would allow seismic attribute analysis of depositional sequences such as RMS amplitudes, maximum curvature, coherence etc. (using Paleo Scan for example) and further mapping of geo-bodies and attribute anomalies.

Further work should focus on comparison between 2D and 3D interpretations of structural and depositional patterns around salt structures and in minibasins. Detailed analysis on 3D seismic data would test concepts developed on 2D seismic data and further advance to a fully constrained concept for the 3D and 4D halo-kinematic sequence-stratigraphic analyses.

Overview of applied methodologies: Time vs depth data

Analysis of regional salt tectonic trends (manuscript 1) and minibasin depositional patterns and structural configurations (manuscript 2) formed the core analyses in this project. These analyses are well imaged and have been confidently interpreted on time-migrated seismic data to infer regional salt tectonic evolution and intermittent kinematic phase of salt growth. However it is known that complex seismic velocities in areas with high density of salt intrusions such as in the deepwater Provencal basin raise uncertainties in true positions and thicknesses of stratigraphic depocentres with variations up to hundreds of feet or meters [see Rojo et al. (2016), Jones and Davison (2014)]. Hence depth imaging of salt basins is preferred especially in the oil and gas industry where accurate interpretation of reservoir intervals and the nature of hydrocarbon traps are of utmost importance. Also structurally restored seismic sections employed in this project (manuscript 3) demonstrating formation of the unique depositional patterns and structural configurations developed in this project may show some variations on equivalent depth converted seismic sections.

Overview of applied methodologies: Well data?

Absence of well data used in this study impeded better stratigraphic control of minibasin depositional sequences and inter minibasin correlations. Absolute dating of depositional sequence boundaries and unconformities is possible with well control. Hence relative time scales of halokinetic processes were inferred and correlation of regional chronological successions with minibasin depositional sequences were not possible.

Relevance and future applications

For future applications of this project, the derived work flows, concepts and robust methods; 1. Provide a better understanding of the dynamic tectono-depositional systems around salt structures which could be integrated into an approach for hydrocarbon prospectivity analysis, e.g. reservoir mapping within minibasin sequences and dynamics of trap formation around multi-stage salt structures 2. Could be applied to scaled analogue experiments and contribute to high resolution local-

scale salt tectonic analogue models 3. Could be tested in thick-skinned salt tectonic settings, where distinct basin dynamic pulses influence near diapir and minibasin depositional sequences 4. Could be applied in other depositional environments e.g. fluvio-coastal, to investigate the tectono-depositional patterns and tectono-stratigraphic control factors controlling salt related depocenters.

G. References

Adam, J., Ge, Z. & Sanchez, M. 2011. *Post-rift Salt Tectonic Processes in the Jequitinhonha Basin Implications from Seismic Interpretation & Analogue Experiment.* Royal Holloway, University of London.

Adam, J., Ge, Z. & Sanchez, M. 2012a. Post-rift salt tectonic evolution and key control factors of the Jequitinhonha deepwater fold belt, central Brazil passive margin: Insights from scaled physical experiments. Marine and Petroleum Geology, **37**, 70-100, doi: 10.1016/j.marpetgeo.2012.06.008.

Adam, J., Ge, Z. & Sanchez, M. 2012b. Salt-structural styles and kinematic evolution of the Jequitinhonha deepwater fold belt, central Brazil passive margin. Marine and Petroleum Geology, **37**, 101-120, doi: https://doi.org/10.1016/j.marpetgeo.2012.04.010.

Adam, J., Grujic, D. & Ings, S. 2005. 4-D Physical Modeling of Tectonics and Basin Migration during Salt Mobilization at Passive Margins. *2006 AAPG Annual Convention*, Calgary.

Adam, J. & Krezsek, C. 2012a. Basin-scale salt tectonic processes of the Laurentian Basin, Eastern Canada: insights from integrated regional 2D seismic interpretation and 4D physical experiments. Geological Society, London, Special Publications, **363**, 331-360.

Adam, J. & Krezsek, C. 2012b. Basin-scale salt tectonic processes of the Laurentian Basin, Eastern Canada: insights from integrated regional 2D seismic interpretation and 4D physical experiments. *In*: Alsop, G.I., Archer, S.G., Grant, N.T. & Hodgkinson, R. (eds.) *Salt tectonics, Sediments and Prospectivity*. Geological Society, London, Special Publications, London, 331-360.

Adam, J., Krezsek, C. & Grujic, D. 2006. Thin-skinned extension, salt dynamics and deformation in dynamic depositional systems at passive margins. *8th SEGJ International Symposium Conference Proceedings*,, Kyoto, Japan, 6.

Adam, J., Krezsek, C., MacDonald, C., Campbell, C., Cribb, J., Nedimovic, M., Grujic, D. 2008. Basin-scale salt tectonic processes at the North-Central Scotian Margin: Insights from integrated regional 2D seismic interpretation and 4D physical experiments. *AAPG Annual Convention*, San Antonio, Texas.

Adam, J. & Salt Dynamics Group. 2008. 4D Physical Simulation of Basin-Scale Salt Tectonic Processes and Coupled Depositional Systems from the Rift Basin to Modern Continental Margin. Touch Briefings - Exploration & Production Oil&Gas Review, **6**, 94-97.

Adam, J., Zhiyuan, G. & Sanchez, M. 2012c. Post-rift Basin Evolution and Kinematics of the Salt-detached Deepwater Fold-Belt of the Jequitinhonha Basin, Central East Brazil Passive Margin. *AAPG Annual Conference & Exhibition*, Long Beach, California.

Alsop, G.I., Brown, J.P., Davison, I. & Gibling, M.R. 2000. The geometry of drag zones adjacent to salt diapirs. Journal of the Geological Society of London, **157**, 1019-1029.

Alsop, G.I., Weinberger, R., Levi, T. & Marco, S. 2016. Cycles of passive versus active diapirism recorded along an exposed salt wall. Journal of Structural Geology, **84**, 47-67, doi: 10.1016/j.jsg.2016.01.008.

Andrie, J.R., Giles, K.a., Lawton, T.F. & Rowan, M.G. 2012. Halokinetic-sequence stratigraphy, fluvial sedimentology and structural geometry of the Eocene Carroza Formation along La Popa salt weld, La Popa Basin, Mexico. Geological Society, London, Special Publications, **363**, 59-79, doi: 10.1144/SP363.4.

Aschoff, J.L. & Giles, K.A. 2005. Salt diapir-influenced, shallow-marine sediment dispersal patterns: Insights from outcrop analogs. AAPG Bulletin, **89**, 447-469.

Bache, F., Gargani, J., Suc, J.-P., Gorini, C., Rabineau, M., Popescu, S.-M., Leroux, E., Couto, D.D., Jouannic, G., Rubino, J.-L., Olivet, J.-L., Clauzon, G., Dos Reis, A.T. & Aslanian, D. 2015. Messinian evaporite deposition during sea level rise in the Gulf of Lions (Western Mediterranean). Marine and Petroleum Geology, **66**, 262-277, doi: 10.1016/j.marpetgeo.2014.12.013.

Banham, S.G. & Mountney, N.P. 2013a. Controls on fluvial sedimentary architecture and sediment-fill state in salt-walled mini-basins: Triassic Moenkopi Formation, Salt Anticline Region, SE Utah, USA. Basin Research, **25**, 709-737, doi: 10.1111/bre.12022.

Banham, S.G. & Mountney, N.P. 2013b. Evolution of fluvial systems in salt-walled mini-basins: a review and new insights. Sedimentary Geology, 142-166.
Berné, S. & Gorini, C. 2005. The Gulf of Lions: An overview of recent studies within the French 'Margins' programme. Marine and Petroleum Geology, **22**, 691-693, doi: 10.1016/j.marpetgeo.2005.04.004.
Biju-Duval, B., Letouzey, J. & Montadert, L. 1978. Structure and evolution of the Mediterranean basins. Initial Reports of the Deep Sea Drilling Project, **42**, 951-984, doi: 10.2973/dsdp.proc.42-1.150.1978.
Bourillot, R., Vennin, E., Rouchy, J.M., Blanc-Valleron, M.M., Caruso, A. & Durlet, C. 2010. The end of the Messinian Salinity Crisis in the western Mediterranean: Insights from the carbonate platforms of south-eastern Spain. Sedimentary Geology, **229**, 224-253, doi: 10.1016/j.sedgeo.2010.06.010.
Brandes, C., Pollok, L., Schmidt, C., Wilde, V. & Winsemann, J. 2012. Basin modelling of a lignite-bearing salt rim syncline: insights into rim syncline evolution and salt diapirism in NW Germany. Basin Research, **24**, 699-716, doi: 10.1111/j.1365-2117.2012.00544.x.
Brun, J.-P. & Fort, X. 2011a. Salt tectonics at passive margins: Geology versus models. Marine and Petroleum Geology, **28**, 1123-1145, doi: 10.1016/j.marpetgeo.2011.03.004.
Brun, J. & Fort, X. 2004. Compressional salt tectonics (Angolan margin). Tectonophysics, **382**, 129-150.
Brun, J.P. & Fort, X. 2011b. Salt tectonics at passive margins: Geology versus models. Marine and Petroleum Geology, **28**, 1123-1145, doi: doi:10.1016/j.marpetgeo.2011.03.004.
Brun, J.P. & Fort, X.T. 2010. The analysis of salt tectonic systems. *GSL-SEPM Conference - Salt Tectonics, Sedimentation, and Prospectivity*, London.
Butler, R.W.H., McClelland, E. & Jones, R.E. 1999. Calibrating the duration and timing of the Messinian salinity crisis in the Mediterranean: linked tectonoclimatic signals in thrust-top basins of Sicily. Journal of the Geological Society, London, **156**, 827-835.
Callot, J.-p., Salel, J.-f., Letouzey, J., Daniel, J.-m. & Ringenbach, J.-c. 2016. Three-dimensional evolution of salt-controlled minibasins : Interactions , folding , and mega fl ap development. **9**, 1419-1442, doi: 10.1306/03101614087.
Carminati, E., Doglioni, C., Gelabert, B., Panza, G.F., Raykova, R.B. & Roca, E. 2004. Evolution of the Western Mediterranean. Principles of Phanerozoic Regional Geology, 1-29.
Carminati, E., Lustrino, M. & Doglioni, C. 2012. Geodynamic evolution of the central and western Mediterranean: Tectonics vs. igneous petrology constraints. Tectonophysics, **579**, 173-192, doi: 10.1016/j.tecto.2012.01.026.
Cartwright, J., Jackson, M., Dooley, T. & Higgins, S. 2012. Strain partitioning in gravity-driven shortening of a thick, multilayered evaporite sequence. Geological Society, London, Special Publications, **363**, 449-470, doi: 10.1144/sp363.21.
Cribb, J. 2009. *Analogue modelling of salt tectonic processes beneath the shelf and deepwater slope of the eastern Nova Scotian margin.* B.Sc. Thesis, B.Sc. Thesis, Dalhousie University.
Demercian, S., Szatmari, P. & Cobbold, P.C. 1993. Style and pattern of salt diapirs due to thin-skinned gravitational gliding, Campos and Santos basins, offshore Brazil. Tectonophysics, **228**, 393-433.
Dewey, J., Helman, M., D. Knott, S., Turco, E. & H. W. Hutton, D. 1989. Kinematics of the western Mediterranean. **45**, 265-283.
Diegel, F.A., Karlo, J.F., Schuster, D.C., Shoup, R.C. & Tauvers, P.R. 1995. Cenozoic Structural Evolution and Tectono-Stratigraphic Framework of the Northern Gulf Coast Continental Margin. *In*: Jackson, M.P.A., Roberts, D.G. & Snelson, S. (eds.) *Salt tectonics: a global perspective: AAPG Memoir*. AAPG, 109-151.
Dooley, T.P., Jackson, M. & Hudec, M.R. 2009. Inflation and deflation of deeply buried salt stocks during lateral shortening. Journal of Structural Geology, **31**, 582-600.

dos Reis, A.T., Gorini, C. & Mauffret, A. 2005a. Implications of salt–sediment interactions on the architecture of the Gulf of Lions deep-water sedimentary systems—western Mediterranean Sea. Marine and Petroleum Geology, **22**, 713-746, doi: 10.1016/j.marpetgeo.2005.03.006.
dos Reis, A.T., Gorini, C. & Mauffret, A. 2005b. Implications of salt–sediment interactions on the architecture of the Gulf of Lions deep-water sedimentary systems—western Mediterranean Sea. Marine and Petroleum Geology, **22**, 713-746, doi: 10.1016/j.marpetgeo.2005.03.006.
Driussi, O., Maillard, A., Ochoa, D., Lofi, J., Chanier, F., Gaullier, V., Briais, A., Sage, F., Sierro, F. & Garcia, M. 2015. Messinian Salinity Crisis deposits widespread over the Balearic Promontory: Insights from new high-resolution seismic data. Marine and Petroleum Geology, **66**, 41-54, doi: 10.1016/j.marpetgeo.2014.09.008.
Droz, L., dos Reis, a.T., Rabineau, M., Berné, S. & Bellaiche, G. 2006. Quaternary turbidite systems on the northern margins of the Balearic Basin (Western Mediterranean): A synthesis. Geo-Marine Letters, **26**, 347-359, doi: 10.1007/s00367-006-0044-0.
Duffy, O.B., Fernandez, N., Hudec, M.R., Jackson, M.P.A., Burg, G., Dooley, T.P. & Jackson, C.A.L. 2017. Lateral mobility of minibasins during shortening: Insights from the SE Precaspian Basin, Kazakhstan. Journal of Structural Geology, **97**, doi: 10.1016/j.jsg.2017.02.002.
Duval, B., Cramez, C. & Jackson, M.P.A. 1992. Raft tectonics in the Kwanza Basin, Angola. Marine and Petroleum Geology, **9**, 389-404.
Ferrer, O., Roca, E. & Vendeville, B.C. 2014. The role of salt layers in the hangingwall deformation of kinked-planar extensional faults: Insights from 3D analogue models and comparison with the Parentis Basin. Tectonophysics, **636**, 338-350, doi: http://dx.doi.org/10.1016/j.tecto.2014.09.013.
Fort, X. & Brun, J.P. 2012. Kinematics of regional salt flow in the northern Gulf of Mexico.
Fort, X., Brun, J.P. & Chauvel, F. 2004a. Contraction induced by block rotation above salt (Angolan margin). Marine and Petroleum Geology, **21**, 1281–1294.
Fort, X., Brun, J.P. & Chauvel, F. 2004b. Salt tectonics on the Angolan margin, synsedimentary deformation processes. AAPG Bulletin, **88**, 1523-1544.
Gaullier, V. & Vendeville, B.C. 2005. Salt tectonics driven by sediment progradation: Part II—Radial spreading of sedimentary lobes prograding above salt. AAPG Bulletin, **89**, 1081–1089.
Ge, H., Jackson, M. & Vendeville, B. 1997. Kinematics and dynamics of salt tectonics driven by progradation. AAPG Bulletin, **81**, 398-423.
Ge, Z., Rosenau, M., Warsitzka, M. & Gawthorpe, R.L. 2019. Overprinting translational domains in passive margin salt basins: insights from analogue modelling. Solid Earth, **10**, 1283-1300, doi: 10.5194/se-10-1283-2019.
Gemmer, L., Beaumont, C. & Ings, S.J. 2005. Dynamic modelling of passive margin salt tectonics: effects of water loading, sediment properties and sedimentation patterns. Basin Research, **17**, 382-402, doi: 310.1111/j.1365-2117.2005.00274.x.
Gemmer, L., Ings, S., Medvedev, S. & Beaumont, C. 2004. Salt tectonics driven by differential sediment loading Stability analysis and finite-element experiments.
Giles, K.A. & Lawton, T.F. 2002a. Halokinetic sequence stratigraphy adjacent to the El Papalote diapir, northeastern Mexico. AAPG Bulletin 86, **86**, 823-840.
Giles, K.A. & Lawton, T.F. 2002b. Halokinetic Sequence Stratigraphy Adjacent to the El Papalote Diapir, Northeastern Mexico. American Associacion of Petroleum Geologists Bulletin, **86**, 823-840, doi: 10.1306/61eedbac-173e-11d7-8645000102c1865d.
Giles, K.A., Lawton, T.F. & Rowan, M.G. 2004. Summary of Halokinetic Sequence Chacteristics from Outcrop Studies of La Popa Salt Basin, Northeastern Mexico. *24th Bob F. Perkins Research Conference*, Houston, Texas, 625-634.
Giles, K.A. & Rowan, M.G. 2012. Concepts in halokinetic-sequence deformation and stratigraphy. Geological Society, London, Special Publications, **363**, 7-31, doi: 10.1144/sp363.2.
Gorini, C., Montadert, L. & Rabineau, M. 2015. New imaging of the salinity crisis: Dual Messinian lowstand megasequences recorded in the deep basin of both the eastern and western Mediterranean. Marine and Petroleum Geology, **66**, 278-294, doi: 10.1016/j.marpetgeo.2015.01.009.

Gottschalk, R.R., Anderson, A.V., Walker, J.D. & Da Silva, J.C. 2004. Modes of contractional salt tectonics in Angola Block 33, Lower Congo Basin, West Africa. *Sediment Interactions and Hydrocarbon Prospectivity, Concepts, Applications and Case Studies for the 21st Century*, SEPM, Houston, TX., 705-734.
Granado, P., Urgeles, R., Sàbat, F., Albert-Villanueva, E., Roca, E., Muñoz, J.A., Mazzuca, N. & Gambini, R. 2016. Geodynamical framework and hydrocarbon plays of a salt giant: the NW Mediterranean Basin. Petroleum Geoscience, **22**, 309-321, doi: 10.1144/petgeo2015-084.
Guerra, M.C.M. & Underhill, J.R. 2012. Role of halokinesis in controlling structural styles and sediment dispersal in the Santos Basin, offshore Brazil. Geological Society, London, Special Publications, **363**, 175-206, doi: 10.1144/SP363.9.
Guieu, G.r. & Roussel, J. 1990. Arguments for the pre-rift uplift and rift propagation in the Ligurian-Provencal Basin (northwestern Mediterranean) In the light of Pyrenean Provencal Orogeny. Tectonics, **9**, 1113-1142.
Gunnell, Y., Zeyen, H. & Calvet, M. 2008a. Geophysical evidence of a missing lithospheric root beneath the Eastern Pyrenees: Consequences for post-orogenic uplift and associated geomorphic signatures. Earth and Planetary Science Letters, **276**, 302-313, doi: 10.1016/j.epsl.2008.09.031.
Gunnell, Y., Zeyen, H. & Calvet, M. 2008b. Geophysical evidence of a missing lithospheric root beneath the Eastern Pyrenees: Consequences for post-orogenic uplift and associated geomorphic signatures. Earth and Planetary Science Letters, **276**, 302-313, doi: 10.1016/j.epsl.2008.09.031.
Harding, R. & Huuse, M. 2015. Salt on the move: Multi stage evolution of salt diapirs in the Netherlands North Sea. Marine and Petroleum Geology, **61**, 39--55, doi: 10.1016/j.marpetgeo.2014.12.003.
Hearon IV, T.E., Rowan, M., A., G.K. & H., a.H.W. 2014. Halokinetic deformation adjacent to the deepwater Auger diapir, Garden Banks 470, northern Gulf of Mexico: Testing the applicability of an outcrop-based model using subsurface data. Special section: Salt tectonics and interpretation, **2**, SM57-SM76.
Hearon, T.E., Rowan, M.G., Giles, K.A., Kernen, R.A., Gannaway, C.E., Lawton, T.F. & Fiduk, J.C. 2015. Allochthonous salt initiation and advance in the northern Flinders and eastern Willouran ranges, South Australia: Using outcrops to test subsurface-based models from the northern Gulf of Mexico. AAPG Bulletin, **99**, 293-331.
Heidari, M., Nikolinakou, M.A., Hudec, M.R. & Flemings, P.B. 2016. Geomechanical analysis of a welding salt layer and its effects on adjacent sediments. Tectonophysics, **683**, 172-181, doi: 10.1016/j.tecto.2016.06.027.
Heidbach, O., Reinecker, J., Tingay, M., Müller, B., Sperner, B., Fuchs, K. & Wenzel, F. 2007. Plate boundary forces are not enough: Second- and third-order stress patterns highlighted in the World Stress Map database. Tectonics, **29**, 19, doi: 10.1029/2007TC002133.
Holser, W.T., Clement, G.P., Jansa, L.F. & Wade, J.A., 1988. . In (ed.): . 1988. Evaporite deposits of the North Atlantic rift. *In*: Manspeizer, W. (ed.) *Triassic and Jurassic Rifting, Continental Breakup and the Origin of the Atlantic Ocean and Passive Margins, Dev. Geotecton*, 525-556.
Hudec, M.R. 2003. Quick-look chart for restoration of salt structures in cross section. Bureau of Economic Geology Publication, EM0009, poster + 10-page booklet.
Hudec, M.R. & Jackson, M.P.A. 2002a. Structural segmentation, inversion, and salt tectonics on a passive margin: Evolution of the Inner Kwanza Basin, Angola. Bulletin of the Geological Society of America, **114**, 1222-1244.
Hudec, M.R. & Jackson, M.P.A. 2002b. Structural segmentation, inversion, and salt tectonics on a passive margin: Evolution of the Inner Kwanza Basin, Angola. Geological Society of America Bulletin, **114**, 1222-1244, doi: 10.1130/0016-7606(2002)114<1222:ssiast>2.0.co;2.
Hudec, M.R. & Jackson, M.P.A. 2004. Regional restoration across the Kwanza Basin, Angola: Salt tectonics triggered by repeated uplift of a metastable passive margin. AAPG Bulletin, **88**, 971-990, doi: 10.1306/02050403061.
Hudec, M.R. & Jackson, M.P.A. 2007. Terra infirma: Understanding salt tectonics. Earth-Science Reviews, **82**, 1-28.

Hudec, M.R., Jackson, M.P.A. & Schultz-Ela, D.D. 2009a. The paradox of minibasin subsidence into salt: Clues to the evolution of crustal basins. Bulletin of the Geological Society of America, doi: 10.1130/B26275.1.
Hudec, M.R., Jackson, M.P.A. & Schultz-Ela, D.D. 2009b. The paradox of minibasin subsidence into salt: Clues to the evolution of crustal basins. Geological Society of America Bulletin, **121**, 201-221, doi: 10.1130/b26275.1.
Hughes, M. & Davison, I. 1993. Geometry and growth kinematics of salt pillows in the southern North Sea. Tectonophysics, **228**, 239-254.
Ings, S., Beaumont, C. & Gemmer, L. 2004. Numerical Modeling of Salt Tectonics on Passive Continental Margins: Preliminary Assessment of the Effects of Sediment Loading, Buoyancy, Margin Tilt, and Isostasy. *24th Annual GCSSEPM Foundation Bob F. Perkins Research Conference Proceedings*, 38-68.
Ings, S.J. & Shimeld, J.W. 2006. A new conceptual model for the structural evolution of a regional salt detachment on the northeast Scotian margin, offshore eastern Canada. American Association of Petroleum Geologists Bulletin, **90**, 1407-1423.
Jackson, M., Cloos, M., Hudec, M., Steel, R., Sen, M. & Peel, F. 2010. An Analysis of Salt Welding.
Jackson, M., Vendeville, B. & Schultz-Ela, D. 1994a. Structural dynamics of salt systems. Annual Review of Earth and Planetary Sciences, **22**, 93-117.
Jackson, M., Vendeville, B. & Schultz-Ela, D.D. 1994b. Strutural dynamics of salt diapirs.
Jackson, M.P.A. 1995. Retrospective Salt Tectonics. *In*: Jackson, M.P.A., Roberts, D.G. & Snelson, S. (eds.) *Salt tectonics: a global perspective: AAPG Memoir*. AAPG, 1-28.
Jackson, M.P.a. & Hudec, M.R. 2009. Interplay of Basement Tectonics, Salt Tectonics, and Sedimentation in the Kwanza Basin, Angola. *In*: Town, A.C. (ed.) *Search and Discovery Article*.
Jackson, M.P.A. & Hudec, M.R. 2011. Salt Tectonics: Priciples and Practice
Jackson, M.P.A. & Hudec, M.R. 2017. Salt Tectonics: Principles and Practice. Cambridge University Press.
Jackson, M.P.A., Hudec, M.R. & Jennette, D.C. 2004. Insights from a gravity-driven linked system in deep-water lower Congo Basin, Gabon. *In*: Post, P.J., Olson, D.L., Lyons, K.T., Palmes, S.L., Harrison, P.F. & Rosen, N.C. (eds.) *In: Salt-Sediment Interactions and Hydrocarbon Prospectivity Concepts, Applications, and Case Studies for the 21st Century* SEPM Foundation, 24th Annual Research Conference, 735-752.
Jolivet, L., Augier, R., Robin, C., Suc, J.-P. & Rouchy, J.M. 2006. Lithospheric-scale geodynamic context of the Messinian salinity crisis. Sedimentary Geology, **188**, 9-33.
Jones, I.F. & Davison, I. 2014. Seismic imaging in and around salt bodies. Interpretation, **2**, SL1-SL20, doi: 10.1190/int-2014-0033.1.
Kendell, K. 2005. Nova Scotia's Energy - Fueling the future. *In*: Energy, N.S.D.o. (ed.) *International Forum 2005*.
Kernen, R.A., Giles, K.A., Rowan, M.G., Lawton, T.F. & Hearon, T.E. 2012a. Depositional and halokinetic-sequence stratigraphy of the Neoproterozoic Wonoka Formation adjacent to Patawarta allochthonous salt sheet, Central Flinders Ranges, South Australia. Geological Society, London, Special Publications, **363**, 81-105, doi: 10.1144/sp363.5.
Kernen, R.A., Giles, K.A., Rowan, M.G., Lawton, T.F. & Hearon, T.E. 2012b. Depositional and halokinetic-sequence stratigraphy of the Neoproterozoic Wonoka Formation adjacent to Patawarta allochthonous salt sheet, Central Flinders Ranges, South Australia. *In*: Archer, S.G., Alsop, G.I., Hartley, A.J., Grant, N.T. & Hodgkinson, R. (eds.) *Salt Tectonics, Sediments and Prospectivity*. Geological Society, 81-105.
Kidd, R., Bernoulli, D., Garrison, R.E., Fabricius, F.H. & Mélières, F. 1978. 56. LITHOLOGIC FINDINGS OF DSDP LEG 42A, MEDITERRANEAN SEA.
Kukla, P.A., Urai, J.L., Warren, J.K., Reuning, L., Becker, S., Schoenherr, J. & Mohr, M. 2010. An integrated, multi-scale approach to salt dynamics. *Geological Society - Salt Tectonics, Sediments and Prospectivity*.

Leroux, E., Aslanian, D., Rabineau, M., Moulin, M., Granjeon, D., Gorini, C. & Droz, L. 2015a. Sedimentary markers in the Provençal Basin (western Mediterranean): A window into deep geodynamic processes. Terra Nova, **27**, 122-129, doi: 10.1111/ter.12139.
Leroux, E., Aslanian, D., Rabineau, M., Moulin, M., Granjeon, D., Gorini, C. & Droz, L. 2015b. Sedimentary markers in the Provençal Basin (western Mediterranean): a window into deep geodynamic processes. Terra Nova, **27**, 122-129, doi: 10.1111/ter.12139.
Letouzey, J., Colletta, B., Vially, R. & Chermette, J.C. 1995. Evolution of Salt-Related Structures in Compressional Settings. *In*: Jackson, M.P.A., Roberts, D.G. & Snelson, S. (eds.) *Salt tectonics: a global perspective: AAPG Memoir*. AAPG, 41-60.
Liro, L.M. & Coen, R. 1995. Salt Deformation History and Postsalt Strucutral Trends, Offshore Southern Gabon, West Africa. *In*: Jackson, M.P.A., Roberts, D.G. & Snelson, S. (eds.) *Salt tectonics: a global perspective: AAPG Memoir*. AAPG, 323-331.
MacDonald, C., Campbell, C., Cribb, J., Adam, J., Nedimovic, M., Louden, K. & Krezsek, C. 2008. Salt Tectonics and Basin Evolution of the North-Central Scotian Margin. *Nova Scotia Energy Forum*, Antigonish, Nova Scotia, Canada.
Madof, A.S., Christie-Blick, N. & Anders, M.H. 2009. Stratigraphic controls on a salt-withdrawal intraslope minibasin, north-central Green Canyon, Gulf of Mexico: Implications for misinterpreting sea level change. AAPG Bulletin, **93**, 535-561, doi: 10.1306/12220808082.
Maillard, A., Gaullier, V., Vendeville, B.C. & Odonne, F. 2003. Influence of differential compaction above basement steps on salt tectonics in the Ligurian-Provencal Basin, Northwest Mediterranean. Marine and Petroleum Geology, **20**, 13-27.
Mannie, A.S., Jackson, C.A.L. & Hampson, G.J. 2014. Shallow-marine reservoir development in extensional diaper-collapse minibasins: An integrated subsurface case study from the Upper Jurassic of the Cod terrace, Norwegian North Sea. AAPG Bulletin, **98**, 2019-2055, doi: 10.1306/03201413161.
Maria A. Nikolinakou, M.H., Michael R. Hudec, & Flemings, P.B. 2017. Initiation and growth of salt diapirs in tectonically stable settings: Upbuilding and megaflaps. AAPG Bulletin, **101**, 887-905, doi: 10.1306/09021615245.
Marton, L., Tari, G. & Lehmann, C. 2000. Evolution of the Angolan passive margin, West Africa, with emphasis on post-salt structural styles. Atlantic rifts and continental margins, **115**, 129–149.
Massimi, P., Quarteroni, A., Saleri, F. & Scrofani, G. 2007. Modeling of salt tectonics. Computer Methods in Applied Mechanics and Engineering, **197**, 281-293.
Mauffret, a. & Gorini, C. 1996. Structural style and geodynamic evolution of Camargue and Western Provencal basin, southeastern France. Tectonics, **15**, 356-375, doi: 10.1029/95TC02407.
Mauffret, A., Pascal, G., Maillard, A. & Gorini, C. 1995. Tectonics and deep structure of the north-western Mediterranean Basin. Marine and Petroleum Geology, **12**, 645-666, doi: 10.1016/0264-8172(95)98090-R.
McBride, B.C., Rowan, M.G. & Weimer, P. 1998. The evolution of allochthonous salt systems, northern Green Canyon and Ewing Bank (offshore Louisiana), northern Gulf of Mexico. Aapg Bulletin-American Association of Petroleum Geologists, **82**, 1013-1036.
Mianaekere, V. & Adam, J. In review-a. Convergent contractional salt tectonics in the Western Mediterranean Messinian salt basins: Passive margin salt tectonics. *In*: London, R.H.U.o. (ed.).
Mianaekere, V. & Adam, J. In review-b. 'Halo-kinematic' sequence stratigraphic analysis adjacent to salt diapirs in the deepwater contractional province, Liguro-Provencal Basin, Western Mediterranean. *In*: London, R.H.U.o. (ed.).
Mianaekere, V. & Adam, J. in review-c. 'Halo-kinematic' sequence stratigraphic analysis adjacent to salt diapirs in the deepwater

contractional province, Liguro-Provencal Basin, Western Mediterranean. Geological Society London Special Publications.
Mitchell, N.C., Ligi, M., Ferrante, V., Bonatti, E. & Rutter, E. 2010. Submarine salt flows in the central Red Sea. Geological Society of America Bulletin, **122**, 701-713, doi: 10.1130/B26518.1.

Mohriak, W.U., Macedo, J.M., Castellani, R.T., Rangel, H.D., Barros, A.Z.N. & Latgé, M.A.L. 1995. Salt Tectonics and Structural Styles in the Deep-Water Province of the Cabo Frio Region, Rio de Janeiro, Brazil. *In*: Jackson, M.P.A., Roberts, D.G. & Snelson, S. (eds.) *Salt tectonics: a global perspective: AAPG Memoir*. AAPG, 273-304.
Mohriak, W.U., Nemcok, M. & Enciso, G. 2008. South Atlantic divergent margin evolution: rift-border uplift and salt tectonics in the basins of SE Brazil. *In*: Pankhurst, R.J., Trouw, R.A.J., Brito Neves, B.B. & de Wit, M.J. (eds.) *West Gondwana: Pre-Cenozoic Correlations Across the South Atlantic Region*. Geological Society, London, Special Publications, 365-398.
Montadert, L., Letouzey, J. & Mauffret, A. 1978. MESSINIAN EVENT: SEISMIC EVIDENCE. Initial reports of the deep sea drilling project 42.
Nikolinakou, M.A., Heidari, M., Hudec, M.R. & Flemings, P.B. 2017. Initiation and growth of salt diapirs in tectonically stable settings: Upbuilding and megaflaps. AAPG Bulletin, **101**, 887-905, doi: 10.1306/09021615245.
Obone-Zue-Obame, E.M.M., Gaullier, V., Sage, F.F., Maillard, A., Lofi, J., Vendeville, B.C., Thinon, I. & Rehault, J.-P.P. 2011. The sedimentary markers of the Messinian salinity crisis and their relation with salt tectonics on the Provençal margin (western Mediterranean):: results from the" MAURESC" cruise. Bulletin De La Societe Geologique De France, **182**, 181-196, doi: 10.2113/gssgfbull.182.2.181.
Ohneiser, C., Florindo, F., Stocchi, P., Roberts, A.P., DeConto, R.M. & Pollard, D. 2015. Antarctic glacio-eustatic contributions to late Miocene Mediterranean desiccation and reflooding. Nature Communications, **6**, 8765, doi: 10.1038/ncomms9765.
Patruno, S., Hampson, G.J. & Jackson, C.a.L. 2015. Quantitative characterisation of deltaic and subaqueous clinoforms. Earth-Science Reviews, **142**, 79-119, doi: 10.1016/j.earscirev.2015.01.004.
Peel, F.J. 2014. How do salt withdrawal minibasins form? Insights from forward modelling, and implications for hydrocarbon migration. Tectonophysics, **630**, 222-235, doi: 10.1016/j.tecto.2014.05.027.
Peel, F.J., Travis, C.J. & Hossack, J. 1995. Genetic Structural Provinces and Salt Tectonics of the Cenozoic Offshore U.S. Gulf of Mexico: A Preliminary Analysis. *In*: Jackson, M.P.A., Roberts, D.G. & Snelson, S. (eds.) *Salt tectonics: a global perspective: AAPG Memoir*. AAPG, 153-175.
Quirk, D.G., Schødt, N., Lassen, B., Ings, S.J., Hsu, D., Hirsch, K.K. & Von Nicolai, C. 2012. Salt tectonics on passive margins: examples from Santos, Campos and Kwanza basins. Geological Society, London, Special Publications, **363**, 207-244, doi: 10.1144/sp363.10.
Ratcliff, D.W., Gray, S.H. & Whitmore, N.D. 1992. Seismic imaging of salt structures in the Gulf of Mexico. The Leading Edge, doi: 10.1190/1.1436876.
Ribes, C., Kergaravat, C., Bonnel, C., Crumeyrolle, P., Callot, J.-P., Poisson, A., Temiz, H. & Ringenbach, J.-C. 2015a. Fluvial sedimentation in a salt-controlled mini-basin: stratal patterns and facies assemblages, Sivas Basin, Turkey. Sedimentology, **62**, 1513-1545, doi: 10.1111/sed.12195.
Ribes, C., Kergaravat, C., Bonnel, C., Crumeyrolle, P., Callot, J.P., Poisson, A., Temiz, H. & Ringenbach, J.C. 2015b. Fluvial sedimentation in a salt-controlled mini-basin: stratal patterns and facies assemblages, Sivas Basin, Turkey. Sedimentology, **62**, 1513-1545, doi: 10.1111/sed.12195.
Ribes, C., Kergaravat, C., Crumeyrolle, P., Lopez, M., Bonnel, C., Poisson, A., Kavak, K.S., Callot, J.P. & Ringenbach, J.C. 2017. Factors controlling stratal pattern and facies distribution of fluvio-lacustrine sedimentation in the Sivas mini-basins, Oligocene (Turkey). Basin Research, **29**, 596-621, doi: 10.1111/bre.12171.
Roberts, G. & Christoffersen, T. 2013. The West Mediterranean Salt Basin – A Future Petroleum Producing Province ?*. **50791**.
Rojo, L.A., Escalona, A. & Schulte, L. 2016. The use of seismic attributes to enhance imaging of salt structures in the Barents Sea. First Break, doi: 0.3997/1365-2397.2016014.
Rouchy, J.M. & Caruso, A. 2006. The Messinian salinity crisis in the Mediterranean basin: A reassessment of the data and an integrated scenario. Sedimentary Geology, **188â€“189**, 35-67.

Rowan, M. & Vendeville, B. 2006. Foldbelts with early salt withdrawal and diapirism: Physical model and examples from the northern Gulf of Mexico and the flinders Ranges, Australia. Marine and Petroleum Geology, **23**, 871-891.
Rowan, M.G. 2014a. Passive-margin salt basins: hyperextension, evaporite deposition, and salt tectonics. Basin Research, **26**, 154-182, doi: 10.1111/bre.12043.
Rowan, M.G. 2014b. Passive-margin salt basins: hyperextension, evaporite deposition, and salt tectonics. Basin Research, **26**, 154-182, doi: 10.1111/bre.12043.
Rowan, M.G., Giles, K.a., Hearon IV, T.E. & Fiduk, J.C. 2016a. Megaflaps adjacent to salt diapirs. AAPG Bulletin, **100**, 1723-1747, doi: 10.1306/05241616009.
Rowan, M.G., Giles, K.A., Hearon, T.E. & Fiduk, J.C. 2016b. Megaflaps adjacent to salt diapirs. AAPG Bulletin.
Rowan, M.G., Lawton, T.F. & Giles, K.A. 2012. Anatomy of an exposed vertical salt weld and flanking strata, La Popa Basin, Mexico. Geological Society, London, Special Publications, **363**, 33-57, doi: 10.1144/sp363.3.
Rowan, M.G., Lawton, T.F., Giles, K.A. & Ratliff, R.A. 2003a. Near-salt deformation in La Popa basin, Mexico, and the northern Gulf of Mexico: A general model for passive diapirism. AAPG Bulletin, **87**, 733-756.
Rowan, M.G., Lawton, T.F., Giles, K.A. & Ratliff, R.A. 2003b. Near-salt deformation in La Popa basin, Mexico, and the northern Gulf of Mexico: a general model for passive diapirism. . AAPG Bulletin, **87**, 733-756.
Rowan, M.G., Peel, F.J. & Vendeville, B.C. 2004a. Gravity-driven fold belts on passive margins. *In*: McClay, K.R. (ed.) *Thrust tectonics and hydrocarbon systems*. AAPG Memoir, 157-182.
Rowan, M.G., Peel, F.J. & Vendeville, B.C. 2004b. Gravity-driven fold belts on passive margins. AAPG Memoir, **82**, 157-182.
Rowan, M.G. & Ratliff, R.A. 2012. Cross-section restoration of salt-related deformation: Best practices and potential pitfalls. Journal of Structural Geology, doi: 10.1016/j.jsg.2011.12.012.
Rowan, M.G., Trudgill, B.D. & Fiduk, J.C. 2000. Deepwater, salt-cored fold belts: lessons from the Mississippi Fan and Perdido fold belts, northern Gulf of Mexico. *In*: Mohriak, W. & Talwani, M. (eds.) *Atlantic rifts and continental margins*. American Geophysical Union, Washington, DC, United States, 173-191.
Rowan, M.G. & Weimer, P. 1998. Salt-Sediment Interaction, Northern Green Canyon and Ewing Bank (Offshore Louisiana), Northern Gulf of Mexico.
Saura, E., Ardèvol i Oró, L., Teixell, A. & Vergés, J. 2016. Rising and falling diapirs, shifting depocenters, and flap overturning in the Cretaceous Sopeira and Sant Gervàs subbasins (Ribagorça Basin, southern Pyrenees). Tectonics, **35**, 638-662, doi: 10.1002/2015tc004001.
Schreurs, G., Haenni, R., Panien, M. & Vock, P. 2003. Analysis of analogue models by helical X-ray computed tomography. Geological Society Special Publications, **215**, 213-223.
Schultz-Ela, D.D. 2003. Origin of drag folds bordering salt diapirs. AAPG Bulletin, **87**, 757-780, doi: 10.1306/12200201093.
Schultz-Ela, D.D., Jackson, M. & Vendeville, B. 1993. Mechanics of active salt diapirism.
Schuster, D.C. 1995. Deformation of Allochthonous Salt and Evolution of Related Salt-Structural. *In*: Jackson, M.P.A., Roberts, D.G. & Snelson, S. (eds.) *Salt tectonics: a global perspective: AAPG Memoir*. AAPG, 177-198.
Seni, S.J. 1992. Evolution of salt structures during burial of salt sheets on the slope, northern Gulf of Mexico. Marine and Petroleum Geology, **9**, 452-468.
Shimeld, J. 2004. A comparison of salt tectonic sub-provinces beneath the Scotian Slope and Laurentian Fan. *In*: Post, P.J., Olson, D.L., Lyons, K.T., Palmes, S.L., P., F.H. & Rosen, N.C. (eds.) *Salt-sediment interactions and hydrocarbon prospectivity: Concepts, applications and case studies for the 21st century*. . 24th Annual GCSSEPM Foundation Bob F. Perkins Research Conference proceedings, 291-306.
Storetvedt, K.M. 1973. Genesis of West Mediterranean basins. Earth and Planetary Science Letters., **21**, 22-28, doi: 10.1016/0012-821X(73)90221-5.

Talbot, C.J. 1993. Spreading of salt structures in the Gulf of Mexico. Tectonophysics, **228**, 151-166.
Tari, G. & Molnar, J. 2005. Correlation of Syn-Rift Structures Between Morocco and Nova Scotia, Canada. *25th Annual Bob F. Perkins Research Conference*, 132-150.
Tari, G., Molnar, J. & Ashton, P. 2003a. Examples of salt tectonics from West Africa: a comparative approach. *In*: Arthur, T.J., MacGregor, D.S. & Cameron, N. (eds.) *Petroleum Geology of Africa: New Themes and Developing Technologies*. Geological Society of London, Special Publications, 85-104.
Tari, G., Molnar, J. & Ashton, P. 2003b. Examples of salt tectonics from West Africa: a comparative approach. Geological Society, London, Special Publications, **207**, 85-104, doi: 10.1144/gsl.sp.2003.207.01.05.
Trudgill, B.D. 2011. Evolution of salt structures in the northern Paradox Basin: Controls on evaporite deposition, salt wall growth and supra-salt stratigraphic architecture. Basin Research, **23**, 208-238, doi: 10.1111/j.1365-2117.2010.00478.x.
Unternehr, P. & de Clarens, P. 2004. A Comparison Between the Salt Basins of the Gulf of Mexico and the South Atlantic.
Vendeville, B. 2002. A new Interpretation of Trusheim's Classic Model of Salt-Diapir Growth. Gulf Coast Association of Geological Societies Transactions, **52**.
Vendeville, B. 2005. Salt tectonics driven by sediment progradation: Part I--Mechanics and kinematics. AAPG Bulletin, **89**, 1071-1079.
Vendeville, B.C., Jackson, M.P.A. & Anonymous. 1990. Physical modeling of the growth of extensional and contractional salt tongues on continental slopes. AAPG Bulletin, **74**, 784.
Vendeville, B.C. & Nilsen, K.T. 1995. Episodic growth of salt diapirs driven by horizontal shortening. *In*: Travis, C.J., Harrison, H., Hudec, M.R., Vendeville, B.C., Peel, F.J. & Perkins, B.F. (eds.) *Salt, Sediment and Hydrocarbons*. Gulf Coast Section Society of Exploration Paleontologists and Mineralogists Foundation 16th Annual Research Conference, 285-295.
Wade, J.A. & MacLean, B.C. 1990. The geology of the southeastern margin of Canada. *In*: Keen, M.J. & Williams, G.L. (eds.) *Geology of the Continental Margin of Eastern Canada*, 167-238.
Wade, J.A., MacLean, B.C. & Williams, G.L. 1995. Mesozoic and Cenozoic stratigraphy, eastern Scotian Shelf: new interpretations. Canadian Journal of Earth Sciences = Journal Canadien des Sciences de la Terre, **32**, 1462-1473.
Waltham, D. 1997. Why does salt start to move? *Tectonophysics*, 117-128.
Warren, J.K. 2010a. Earth-Science Reviews Evaporites through time : Tectonic , climatic and eustatic controls in marine and nonmarine deposits. Earth Science Reviews, **98**, 217-268, doi: 10.1016/j.earscirev.2009.11.004.
Warren, J.K. 2010b. Evaporites through time: Tectonic, climatic and eustatic controls in marine and nonmarine deposits. Earth-Science Reviews, **98**, 217-268.
Weijermars, R., Jackson, M. & Vendeville, B. 1993a. Rheological and tectonic modeling of salt provinces.
Weijermars, R., Jackson, M.P.A. & Vendeville, B. 1993b. Rheological and tectonic modeling of salt provinces. Tectonophysics, **217**, 143-174.
Wheeler, H.E. 1958. Time-stratigraphy. AAPG Bulletin, **42**, 1047-1063.
Whipple, K.X.M., B.J. 2004. Controls on the strength of coupling among climate, erosion, and deformation in two-sided, frictional orogenic wedges at steady state. Journal of Geophysical Research, **109**, doi:10.1029/2003JF000019.
Worrall, D.M. & Snelson, S. 1989. Evolution of the northern Gulf of Mexico, with emphasis on Cenozoic growth faulting and the role of salt. *In*: Bally, A. & Palmer, A. (eds.) *The Geology of North America-An Overview*. Geological Society of America, Boulder, Colorado, 97-138.
Wu, S., Bally, A.W. & Cramez, C. 1990. Allochthonous salt, structure and stratigraphy of the north-eastern Gulf of Mexico. Part II: Structure. Marine and Petroleum Geology, **7**, 334-340.
Yohann, P., Christophe, B., Etienne, J., Matthieu, G. & Michel, L. 2016. Halokinetic sequences in carbonate systems: An example from the Middle Albian Bakio Breccias Formation (Basque Country, Spain). Sedimentary Geology, **334**, doi: 10.1016/j.sedgeo.2016.01.013.